

Developing safe and controllable Clustered Regularly Interspaced Short Palindromic
Repeats (CRISPR)-based therapies with design principles of synthetic biology

by

Farzaneh Moghadam

A Dissertation Presented in Partial Fulfillment
of the Requirements for the Degree
Doctor of Philosophy

Approved July 2020 by the
Graduate Supervisory Committee:

Samira Kiani, Chair
Mo Ebrahimkhani
Josh Labaer

ARIZONA STATE UNIVERSITY

August 2020

ABSTRACT

The CRISPR/Cas9 gene-editing tool is currently in clinical trials as the excitement about its therapeutic potential is exponentially growing. However, many of the developed CRISPR based genome engineering methods cannot be broadly translated in clinical settings due to their unintended consequences. These consequences, such as immune reactions to CRISPR, immunogenic adverse events following receiving of adeno-associated virus (AAV) as one of the clinically relevant delivery agents, and CRISPR off-target activity in the genome, reinforces the necessity for improving the safety of CRISPR and the gene therapy vehicles. Research into designing more advanced CRISPR systems will allow for the increased ability of editing efficiency and safety for human applications. This work 1- develops strategies for decreasing the immunogenicity of CRISPR/Cas9 system components and improving the safety of CRISPR-based gene therapies for human subjects, 2- demonstrates the utility of this system *in vivo* for transient repression of components of innate and adaptive immunity, and 3- examines an inducible all-in-one CRISPR-based control switch to pave the way for controllable CRISPR-based therapies.

Aims

Aim 1: Developing strategies for decreasing the immunogenicity of CRISPR/Cas9 system components and improving the safety of CRISPR-based gene therapies for human subjects. Here, the pre-existing immune response to SpCas9 in healthy individuals is characterized and the immunodominant T cell epitopes are identified with the aim of

developing SpCas9 proteins that have diminished capacity to invoke human adaptive response.

Aim 2: Developing synthetic immunomodulation *in vivo* using a CRISPR-based enhanced transcriptional repressor. Here, the principles of transcription modulation of genes *in vivo* are explored and optimized. Then, the utility of this system *in vivo* for transient repression of components of host immune response against AAV-mediated gene therapy is demonstrated.

Aim 3: Employment of CRISPR multi-functionality to engineer an all-in-one inducible safety switch to gain control over CRISPR functionality *in vivo*. It is essential to develop and test CRISPR logic circuits with incorporated safety switches to gain precise control over the CRISPR function in human applications. Here, the development of CRISPR-mediated therapies to temporally control CRISPR activity and prevent its function whenever necessary is discussed.

DEDICATION

To Dr. Poursan Shariat-Razavi, my first teacher who thought me to believe in hard work and that so much could be done with little; my mother who inspired me to be a strong independent woman who achieves her goals through education and believing in herself; my father for teaching me to have big dreams; and my sisters for the effort that they put in me to teach me how to be a leader and showing me their love and support at every step of this journey. I owe my greatest gratitude to my husband, whose love, encouragement, and support sustained me throughout my PhD.

ACKNOWLEDGMENTS

I would like to acknowledge the members of my committee, Dr. Mo Ebrahimkhani, and Dr. Josh LaBaer for their time, and expertise throughout this project. Special thanks to my supervisor, Dr. Samira Kiani, who guided and encouraged me to continue the hard work and be hopeful when the road got tough. Without her persistent help, completion of this work was impossible.

TABLE OF CONTENTS

	Page
LIST OF TABLES.....	xi
LIST OF FIGURES	xii
CHAPTER	
1. ENGINEERED CRISPR SYSTEMS FOR NEXT GENERATION GENE THERAPIES.....	1
1.1. Potential of Clustered Regularly Interspaced Short Palindromic Repeats (CRISPR) as Next Generation Gene Therapy.....	1
1.2. <i>In Vivo</i> Gene Editing Enabled by CRISPR.....	4
1.3. Challenges of CRISPR-based Gene Therapies and Engineering Approaches to Address Them	9
1.3.1. Challenge 1: Diminishing Off-target Activity in the Genome	9
1.3.2. Challenge 2: Enhancing Gene Editing Efficiency <i>In Vivo</i>	11
1.3.3. Challenge 3: Efficient Transcriptional Modulation	14
1.3.4. Challenge 4: Delivery	17
1.3.5. Challenge 5: Immune Response to the Gene Editing Tool	21
1.3.6. Challenge 6: Spatiotemporal Control: Rational Engineering Approaches for Spatiotemporal Control of CRISPR	22
1.4. Opportunities and Future Perspectives.....	27
References	30
2. MULTIFUNCTIONAL CRISPR-CAS9 WITH ENGINEERED IMMUNE-SILENCED HUMAN T CELL EPITOPES.....	51

CHAPTER	Page
2.1. Introduction	53
2.2. Materials and Methods.....	55
2.2.1. Detection of Cas9-specific Serum Antibodies in Healthy Controls.....	55
2.2.2. Cas9 Candidate T-cell Epitope Prediction	56
2.2.3. <i>Ex Vivo</i> Stimulation and Epitope Mapping of Cas9 by ELISpot	57
2.2.4. Autologous APC Generation from Healthy Individual PBMCs	58
2.2.5. T-cell Stimulation by Autologous APCs.....	59
2.2.6. Flow Cytometry Staining for T-cells	60
2.2.7. Pentamer Staining for T-cell Immunophenotyping	60
2.2.8. Vector Design and Construction	61
2.2.9. Cell Culture for Endogenous Target Mutation and Activation	62
2.2.10. Fluorescent Reporter Assay for Quantifying Cas9	62
2.2.11. Quantitative RT-PCR Analysis	63
2.2.12. Endogenous Indel Analysis	63
2.2.13. RNA Sequencing for Quantifying Activator Specificity.....	64
2.3. Results	65
2.3.1. Detection of Cas9-specific Serum Antibodies in Healthy Controls.....	65
2.3.2. Cas9 Candidate T-cell Epitope Prediction	67
2.3.3. T-cell Epitope Mapping of Cas9 and Identification of Two Immunodominant Epitopes	68
2.3.4. Muted Cas9 Proteins Have Lower Immune Recognition and Maintain Their Function and Specificity	70

CHAPTER	Page
2.3.5. Immune Responses to Non-HLA-A*02:01 Cas9 Epitopes	76
2.3.6. Immune Responses to MHC Class II Cas9 Epitopes.....	78
2.4. Discussions.....	79
References	82
3. SYNTHETIC IMMUNOMODULATION WITH A CRISPR SUPER- REPRESSOR <i>IN VIVO</i>	89
3.1. Introduction	89
3.2. Materials and Methods.....	90
3.2.1. Vector Design and Construction	90
3.2.2. AAV Packaging and Purification	91
3.2.3. Cell Culture	91
3.2.4. Transfection of <i>In Vitro</i> Cultured Cells.....	92
3.2.5. Quantitative RT-PCR (qRT-PCR) Analysis	93
3.2.6. Plasma Analysis	93
3.2.7. ELISA-based Chemiluminescent Assay	93
3.2.8. Antibody ELISA.....	94
3.2.9. Lactate Assay	96
3.2.10. Examination of Liver Injury After LPS Injection.....	96
3.2.11. Animals	96
3.2.12. Retro-Orbital Injections	97
3.2.13. Tissue Harvest.....	97
3.2.14. <i>In Vivo</i> LPS Administration	97

CHAPTER	Page
3.2.15. <i>In Vivo</i> Pepjet Administration	97
3.2.16. RNA Sequencing and Data Analysis	98
3.2.17. Statistical Analysis.....	99
3.3. Results	100
3.3.1. CRISPR-mediated Repression with MS2-Hp1aKRAB Is Superior to MS2-KRAB <i>In Vitro</i>	100
3.3.2. CRISPR-mediated Repression of <i>Myd88</i> Locus Can Efficiently be Achieved <i>In Vivo</i> by Recruitment of MS2-HP1aKRAB to gRNA	103
3.3.3. CRISPR-mediated Repression of <i>Myd88</i> Leads to Modulation of Humoral Response Against AAV-mediated Gene Therapy	107
3.3.4. CRISPR-mediated Myd88 Repression Does Not Create Visible Adverse Effect in Long Term	113
3.3.5. CRISPR-mediated Myd88 Repression <i>In Vivo</i> Can Act as a Prophylactic Measure Against Septicemia in Cas9 Transgenic and C57BL/6 Mice ...	114
3.3.6. Nanoparticle-mediated Delivery of <i>Myd88</i> Targeting CRISPR Super-repressors After Exposure to LPS Can Serve as a Therapeutic Modality Against Septicemia	113
3.4. Discussions.....	121
References	123
4. ESTABLISHING TEMPORAL CONTROL OVER CRISPR-BASED TECHNIQUES FOR SAFER GENE THERAPY APPROACHES	130
4.1. Introduction	130

CHAPTER	Page
4.2. Materials and Methods.....	131
4.2.1. Vector Design and Construction	131
4.2.2. AAV Vectors	131
4.2.3. AAV Packaging and Purification	132
4.2.4. Cell Culture	132
4.2.5. Transfection of <i>In Vitro</i> Cultured Cells.....	132
4.2.6. Quantitative RT-PCR (qRT-PCR) Analysis	133
4.2.7. DNA Isolation and Real-time PCR for AAV Genomic Copies	133
4.2.8. Fluorescent Reporter Assay.....	134
4.2.9. Animals	135
4.2.10. Retro-Orbital Injections	135
4.2.11. Tissue Harvest.....	135
4.2.12. <i>In Vivo</i> Tetracycline Delivery.....	136
4.2.13. Statistical Analysis.....	136
4.3. Results	136
4.4. Discussions.....	143
References	143
5. DISCUSSION.....	145
REFERENCES	148
 APPENDIX	
A. SUPPORTING INFORMATION FOR MULTIFUNCTIONAL CRISPR-CAS9 WITH ENGINEERED IMMUNOSILENCED HUMAN T CELL EPITOPES ..166	

APPENDIX	Page
B. SUPPORTING INFORMATION FOR SYNTHETIC IMMUNOMODULATION WITH A CRISPR SUPER-REPRESSOR <i>IN VIVO</i>	184
C. AUTHORSHIP AND CONTRIBUTIONS TO CHAPTERS 1 AND 2	197
BIOGRAPHICAL SKETCH.....	201

LIST OF TABLES

Table	Page
S 2.1. Predicted Cas9 Immunogenic T-cell Epitopes	172
S 2.2. Sequences of Primers Used in This Study.	173
S 2.3. Sequences of gRNAs Uused in This Study	173
S 2.4. Sequence Homology of Epitope α to Amino Acid Sequences from Known Proteins.	174
S 2.5. Sequence Homology of Epitope β to Amino Acid Sequences from Known Proteins	175
S 2.6. Multiple Comparison Results of Mutated Epitope ELISpot Screening.....	176
S 2.7. Sequences of SpCas9 Non-HLA-A*02:01 Class I Epitopes Used to Screen for Pre- existing T-cell Reactivity Against SpCas9 in Healthy Donors.	176
S 2.8. Sequences of Long Peptides that Include Epitopes in the Top 2% of Predicted MHC Class II Binders that Were Used to Screen for SpCas9 Class II Immune Reactivity.	177
S 3.1. Repression Levels of <i>Myd88</i> , <i>Icam-1</i> , and <i>Tnfa</i> Assessed by qRT-PCR in Lung, Blood, and Bone Marrow 3 Weeks Post Retro-orbital Injection of AAV.	194
S 3.2.1. 14nt gRNAs- 5' to 3'	194
S 3.2.2. 20nt gRNAs- 5' to 3'	195
S 3.3.1. Mouse qPCR Primers- 5' to 3'	195
S 3.3.2. Human qPCR Primers- 5' to 3'	196

LIST OF FIGURES

Figure	Page
1.1. Challenges and Answers of CRISPR for <i>In Vivo</i> Gene Therapy.	5
1.2. Modes of Delivery of Cas9 and gRNA for Genome Editing.	19
1.3. Rational Engineering Approaches to Control “When”, “Where”, and “How” CRISPR Functions for Safer <i>In Vivo</i> Gene Therapies.	23
2.1. Detection of Pre-existing B-cell and T-cell Immune Responses to SpCas9 in Healthy Donors and Identification of Two Immunodominant T-cell Epitopes.	66
2.2. SpCas9 Immunodominant Epitope Specific CD8+ T-cell Recognition is Abolished After Anchor Residue Mutation.	71
2.3. Mutated SpCas9 Protein (Cas9-β2) Retains its Function and Specificity.	74
2.4. Immune Responses to Non-HLA-A*02:01 and Class II Epitopes of SpCas9.	77
3.1. Aptamer-mediated CRISPR Repression <i>In Vitro</i>	102
3.2. CRISPR-based Targeted <i>Myd88</i> Repression <i>In Vitro</i> and <i>In Vivo</i> Using MS2 Repressors	105
3.3. Prophylactic Administration of AAV1/MyD88 <i>In Vivo</i> Leads to Modulation of Humoral Immunity Against AAV.	109
3.4. Long-term Efficacy of AAV/Myd88 Repression <i>In Vivo</i>	112
3.5. CRISPR-based Modulation of Host Inflammatory Response Can be a Prophylactic Measure Against LPS-mediated Septicemia in Cas9 Transgenic and WT Mice	115
3.6. Developing Protection Following LPS-mediated Septicemia Using a Dual AAV CRISPR/Cas9 Strategy With AAV1/Cas9 and AAV1 Carrying gRNA-MS2- HP1aKRAB	117

Figure	Page
3.7. Therapeutic Delivery of Nanoparticles Carrying DNA Encoding <i>Myd88</i> -targeting CRISPR Confers Protection Against LPS-mediated Septicemia.....	120
4.1. Build and Test Multifunctional CRISPR-based Control Switches.	138
4.2. Validation of CRISPR Control Switch <i>In Vivo</i>	140
S 2.1. Representative Flow Cytometry Gating for Analysis of Cas9 Function on Synthetic Promoters.	167
S 2.2. Reduced T-cell Response to Epitopes α and β After Mutation of the Anchor Residues.	168
S 2.3. Schematic of the Experiment Assessing Cas9- β 2 Cleavage Capacity at a Synthetic Promoter.....	169
S 2.4. Analysis of Cleavage Capacity of Cas9- α 2 as Compared to WT-Cas9 in a Synthetic Promoter.....	170
S 3.1. Evaluation of Endogenous <i>Myd88</i> Gene Expression Using Different CRISPR-mediated Repressor Circuits.....	185
S 3.2. <i>In Vivo</i> Analysis of AAV1 Tropism Towards Different Tissues.....	186
S 3.3. RNA-seq Analyses of Bone Marrow Samples Collected from Mice Treated With AAV1/ <i>Myd88</i> -MS2-HP1aKrab Versus AAV1/ <i>Myd88</i> -MS2-Krab.....	187
S 3.4. Evaluation of Endogenous <i>Myd88</i> Gene Expression Following Multiple AAV Administration	189
S 3.5. Analysis of a Set of Immune-related Transcripts Following LPS Injury	190
S 3.6. Assessing the Level of a Panel of Immune Related Genes in Lung and Bone Marrow Following LPS Injection.....	191

Figure	Page
S 3.7. Targeted Gene Silencing in Wild-type Mice Using a Dual CRISPR/Cas9 System With AAV1/Cas9 and AAV1 Carrying gRNA-MS2- HP1aKRAB	192
S 3.8. Assessing the Repression Efficiency of AAV1-Myd88 Targeting a Different Region of Myd88 in Liver.....	193

CHAPTER 1

ENGINEERED CRISPR SYSTEMS FOR NEXT GENERATION GENE THERAPIES

Author Contribution: M.P. and F.M. designed and wrote the manuscript and initial sketch of figures. S.K. and MRE edited and wrote the manuscript and figures. This manuscript highlights advancements in engineering CRISPR system that can be directly applicable in safer and more specific genome engineering approaches towards next generation gene therapies. M.P. as the first author of the manuscript did a very good job in going through all the published manuscript focusing on advancements in engineering CRISPR systems specially used for mammalian cells. As the senior graduate student specialized in this field, I supervised his efforts and provided inputs and directions. At the end, I worked on reshaping the manuscript and refining the structure.

1.1. Potential of clustered regularly interspaced short palindromic repeats (CRISPR) as next generation gene therapy

Gene therapy is now a viable therapeutic strategy for a range of clinical conditions. According to the Journal of Gene Medicine Clinical Trials database, in USA alone, about 1532 gene therapy trials have been performed since 1989, with cancer and monogenic diseases being most prevalent indications. With the advent of precision medicine initiative and improvement of gene editing and delivery techniques, it is imperative that the number of gene therapy trials will increase in the next decades to functionally examine and validate genetic information obtained from patients. Despite their tremendous potentials to treat many conditions, gene therapies have classically faced a

number of challenges ranging from economic feasibility to patients' safety. Earlier gene therapies faced push back as patients such as Jesse Gelsinger (1999) died due to complications of the therapies that originated from immune response to the delivery virus. Safety, therefore, became a key concern. Controlling immune response to gene therapy, as well as its spatiotemporal limitation such that target tissue specificity is met, non-target tissues are unaffected and non-specific genetic mutagenesis (such as germline modification) is avoided, are key components of safety for gene therapies. Transgene sizes have also been classically limited by the payload capacity of delivery vectors, making it quite difficult to deliver large piece of genes or multiple transgenes to the same cell *in vivo*.

Clustered regularly interspaced short palindromic repeats (CRISPR) is a unique technology when gene therapies are concerned. CRISPR was first discovered during early sequencing of bacterial genomes when short exogenous viral/phage DNA sequences were found integrated into endogenous genomic DNA.¹⁻² The biology of this artifact was slowly uncovered as an immune-like system for protecting bacteria/archaea from infection.³⁻⁴ If the microorganism survived a pathogenic invader, the CRISPR system could record a piece of the invader's DNA into its genome and use it to protect against repeat infection.⁵⁻⁶ The widely studied CRISPR system from *Streptococcus Pyogenes* (sp) is a type II bacterial defense-system for recognizing, targeting, and eliminating foreign DNA.⁶⁻⁷ In these bacteria, the exogenous DNA is transcribed into a pre-CRISPR RNA (pre-crRNA), which is annealed to trans-activating small RNA (tracr-RNA).⁸ This complex is then processed by RNase III creating a mature CRISPR RNA (crRNA)-tracr RNA capable of guiding Cas9 (ribo)nuclease to foreign DNA for cleavage.⁹ The 20

nucleotides on the 5' end of crRNA are complementary to the target DNA sequence.⁹ After recognizing the three nucleotides of protospacer adjacent motif (PAM) on 3' end of target sequence at foreign DNA, Cas9 binds, unwinds DNA and performs DNA cleavage. This DNA double strand break (DSB) is mediated by the HNH and the RuvC nuclease domains of Cas9, that cleave the target strand and non-target strand of DNA, respectively.⁹ crRNA and tracr-RNA fusions have been synthetically produced, engineered and shortened into guide RNA's (gRNA) for simple, programmable targeting of genomic sequences in virtually any species.⁹⁻¹⁰ As CRISPR technology became more accessible, other engineered CRISPR components began appearing that are based on modifying the Cas9 protein (and its nuclease activity) and gRNAs. Such advancements have started to be used in conjunction with one another, producing strategies for multiplex genome engineering. These products have rapidly enabled gene knock out, homology directed repair driven gene correction, site directed transcriptional activation and repression of genes, single nucleotide substitutions, imaging of genomic loci or synthetic gene circuits in a wide variety of organisms.¹¹⁻¹⁴

CRISPR offers several advantages for gene therapies. It is a cost-effective tool for genomic manipulation with an ease of engineering and programmability superior to prior gene editing tools such as zinc finger nucleases and transcription activator-like effector nucleases (TALENs). Moreover, multiplexing through delivery of small gRNAs enable simultaneous manipulation of multiple endogenous genes using available delivery platforms, an advancement which was not easily achievable before. CRISPR clinical trials have started and will yield new information on how this system works in humans and illuminate its limitations. As CRISPR enters human trials, safety and controllability

of this tool *in vivo* will gain significance. In this review, we focus on challenges of CRISPR-based gene therapies and advancements in engineering CRISPR that can be directly applicable for designing safer and controllable CRISPR as next generation human gene therapies.

1.2. *In vivo* gene editing enabled by CRISPR

Recent *in vivo* studies give insight into the potential of using the CRISPR technology for gene therapies. Most of these studies employ the site-directed DNA endonuclease activity of CRISPR-Cas9 for gene disruption or editing.¹⁵⁻³⁶ For the purpose of this review, we focus only on studies that have examined CRISPR functionality in mice. One prominent application of CRISPR is to correct hereditary conditions that arise following monogenic or polygenic mutations by disrupting dominant mutated genes or deleting the mutated region. Duchenne muscular dystrophy (DMD) caused by mutations in dystrophin was one of the early targets of such CRISPR application *in vivo*. A number of groups tested CRISPR to restore expression of dystrophin and treat DMD by exploiting non-homologous end joining (NHEJ) mediated DNA repair machinery to delete/disrupt the mutated region of dystrophin following DNA DSB induced by CRISPR.^{25, 37-41} In one of the early studies, multiple gRNAs were employed to create a large deletion of 10 exons (45-55), where 62% of mutations of DMD patients lie. This deletion repaired the reading frame for dystrophin and coded a truncated mRNA of the protein.²⁵ This truncation is known to display mild symptoms of dystrophy, an improvement for most patients. In another study, Zhang *et al.* reported the correction of DMD mutations in patient-derived induced pluripotent stem cells (iPSCs) and mouse, by delivery of the newly discovered

Prevotella and Francisella CRISPR (Cpf1) nuclease.⁴¹ They successfully restored dystrophin expression with correction of DMD mutations through both edition of a nonsense mutation or skipping of an out-of-frame DMD exon.⁴¹⁻⁴² CRISPR faces a number of challenges that need to be overcome for safer human translation. These challenges include (A) potential off target cleavage in the genome, (B) requirement of enhanced HDR efficiency for gene editing, (C) efficiency of transcriptional modulation with CRISPR, (D) delivery, (E) immune response and (F) spatiotemporal control. Research in the field of CRISPR design and engineering is unraveling different technologies and CRISPR variants to address these needs. We have summarized some of the solutions under each category in Figure 1.1.

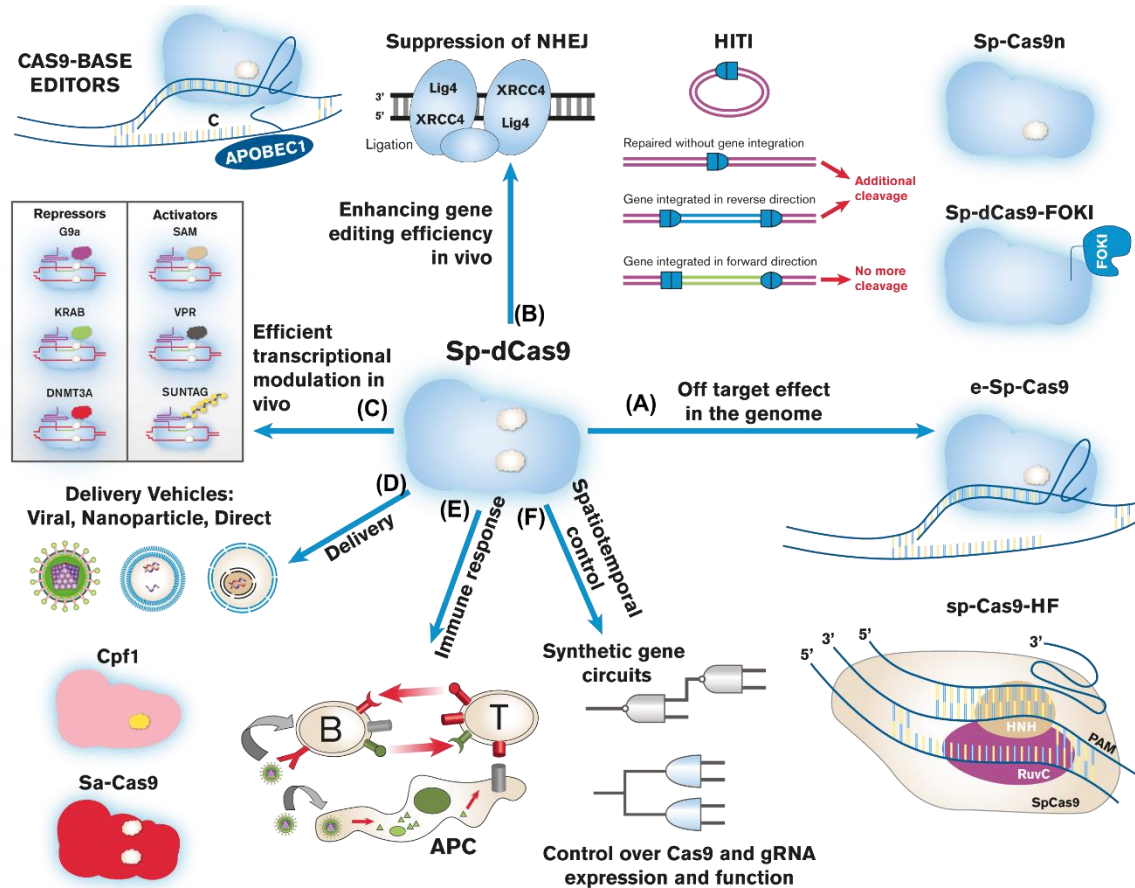


Figure 1.1. Challenges and answers of CRISPR for *in vivo* gene therapy.

CRISPR can be delivered in the form of DNA, RNA, or ribonucleoproteins (RNPs). Each form of delivery has advantages and disadvantages. DNA enables long term expression and spatiotemporal control of Cas9/gRNA expression using cell/context specific transcription factors. In addition, they can be packaged into available viral (such as AAV), non-viral delivery methods or injected directly to the site of interest. However, DNA can integrate into genome and requires transcription and translation machineries for expression of CRISPR, which can further prolong the process. RNA can be also delivered using similar strategies. However, by diminishing the risk of integration in the genome, RNA can present a safer option for gene therapies. RNA is short lived which can be an unfavorable feature in conditions where longer term expression is desired. RNPs bypass transcription and translation and exert their effect with a faster kinetics inside the cells. By being short-lived RNPs can exert less off target effects in the genome. RNPs can be delivered by electroporation or through nanoparticles, however, the efficiency of delivery requires further improvement in this case.

Ruan *et al.* demonstrated that CRISPR/Cas9 system represents a promising therapeutic approach for the treatment of patients with Leber congenital amaurosis (LCA10), which is severe retinal dystrophy caused by generation of a cryptic splice donor site in *CEP290* gene. They achieved effective deletion of the intronic mutation in the *CEP290* and restored the expression of wild-type *CEP290* by delivering CRISPR/Cas9 via adeno associated virus (AAV).⁴³ Later, Yu *et al.* developed a promising treatment for patients with retinitis pigmentosa that causes blindness due to loss of photoreceptors, by performing *in vivo* knockdown of *Nrl* via delivering

CRISPR/Cas9. Nrl gene encodes neural retina-specific leucine zipper protein, a rod fate determinant during photoreceptor development. In this study survival of rods and function of cones were considerably improved by treatment with CRISPR/Cas9 in three different mouse models of retinal degeneration.⁴⁴ In another study, Murlidharan *et al.* engineered an AAV strain that shows high tropism towards neural cells. They used this virus (AAV2g8) to deliver gRNA targeting the schizophrenia risk gene MIR137 (encoding MIR137) in Cas9 knockin mice, which resulted in brain-specific deletion of this gene.⁴⁵ Similar studies using nanoparticles are also being explored. Mianne *et al.* tested local delivery of CRISPR to mouse inner ear hair cells using cationic liposomal reagents.⁴⁶ The study delivered protein Cas9:gRNA complexes which garnered a 20% mutation efficiency in hair cells.⁴⁶ These studies collectively propose CRISPR/Cas9 as a promising gene therapy platform for diseases of nervous system. CRISPR also shows promise as a novel anti-viral therapy. It was recently used for excising of HIV DNA in mouse and rat through tail-vein injection of a recombinant AAV9 virus containing sa-Cas9 and gRNAs. The approach resulted in excision of about 978bp HIV data from different organs including liver, lung, spleen and circulating lymphocytes.⁴⁷

Harnessing homology directed repair (HDR) machinery for precise correction of genetic mutation or insertion of genetic materials in desired loci, has been another highly desirable application of CRISPR. One of the first studies focused on adult, type I tyrosinemia mouse model. The disease phenotype, a fatal mutation characterized by liver damage particularly in hepatocytes, is caused by a mutation in fumarylacetoacetate hydrolase (fah).²⁴ CRISPR and repair template were delivered through hydrodynamic injection and resulted in >.4% gene correction in the hepatocyte population.²⁴ The

corrected cells outcompeted their mutated counterparts thereby replenishing a healthy hepatocyte community and recovering a normal phenotype . Though this study reveals the potential of *in vivo* gene correction, its very low efficiency would limit the therapeutic action in most diseases. A follow up study increased the efficiency to >6% by using gRNA and donor DNA template incorporated within a single AAV along with Cas9 mRNA delivered by a lipid nanoparticle.⁴⁸ Another group used a dual-AAV strategy that enabled the Cas9-mediated correction of a metabolic liver disease in newborn mice with up to ~10% gene correction in hepatocytes.⁴⁹

HDR is also being studied in diseases of the eye and blood. Wu *et al.* attempted to repair mutated *Crygc* to correct cataracts in mice zygotes. They showed that, although HDR-repairs occur less frequently, both the homologous allele and an exogenously delivered oligonucleotide can be used as repair templates.¹⁵ Out of 78 born pups, 13 (17%) were repaired by HDR and 11 (14%) by non-homologous end joining (NHEJ). HDR-mediated repair was shown to completely recover phenotypic characterizations – in this case the loss of cataract symptoms.¹⁵ Guan *et al.* demonstrated correction of over 0.56% of F9 Y371D, which is a mutation that causes severe hemophilia B in adult mice.⁵⁰ Editing of F9 alleles in hepatocytes was done upon receiving naked DNA constructs containing Cas9 components that target the F9 Y371D mutation and restored hemostasis.⁵⁰

While gene editing is a prominent application of CRISPR for gene therapies, transient transcriptional activation or repression of genes is desirable when we consider changing the course of complex diseases such metabolic diseases, or tissue regeneration. However, CRISPR mediated transcriptional modulation seems to be more challenging *in vivo*.

Studies using CRISPR for transcriptional modulation *in vivo* are beginning to emerge. Recently, Chew *et al.* showcased the ability to activate the expression of endogenous genes by delivering Cas9 fused to an activation domain packaged into an AAV system.⁵¹ Although the authors achieved moderate level of activation, challenges, such as an immune response to CRISPR, complicated the analysis of the result. However, this study demonstrates the feasibility of CRISPR for genome modulation and sets the stage for future optimization studies.

1.3. Challenges of CRISPR-based gene therapies and engineering approaches to address them

CRISPR-based therapeutics face several challenges that necessitate further work before clinical applications can be tested. Increasing CRISPR specificity to control genomic off-target effect, improving CRISPR gene editing efficiency, spatiotemporal regulation of the CRISPR activity *in vivo*, controlling possible adverse immune responses to CRISPR, and the appropriate method of delivery are among the challenges that need to be properly addressed for human translation of CRISPR. In the next section, we will describe advances in CRISPR engineering that are beginning to address these challenges (Figure 1.1).

1.3.1. Challenge 1: Diminishing off-target activity in the genome

One requirement to human translation of CRISPR, is to ensure precise on target activity of Cas9 in the genome. Off-target genetic mutations need to be efficiently detected and prevented. To increase the specificity of sp-Cas9 for gene editing, a number

of Cas9 protein variants have been developed (Figure 1.1-A).⁵²⁻⁵⁴ The structurally-guided mutations between the HNH and RuvC of sp-Cas9 nuclease domains, gave way to Cas9 nickase, which is mutated in one of the nuclease domains to produce only single-stranded cleavage. Paired nickase that target sequences in opposite strands of DNA can decrease off-target effects by 50- to 1500-fold without influencing on-target function.⁵⁵ A similar approach relies on the fusion of catalytically inactive Cas9 (dCas9) with a heterodimeric DNA nuclease catalytic domain of FokI, which created RNA-guided FokI-dCas9 nucleases (RFNs).⁵⁴ This complex, requires dimerization of two FokI-dCas9 complexes for DNA cleavage. Hence, it shows a ~140-fold increase in specificity compared to wildtype Cas9 and a four-fold increase compared to paired Cas9 nickases.

Later studies revealed the structure of sp-Cas9 protein charged grooves that mediated the stabilization of non-target DNA strands following sp-Cas9 binding.⁵² The removal of these grooves by mutations in Cas9 protein increased the need for higher strength binding between base pairs thereby increasing the discrimination between matched and mismatched base pairs.⁵² This enhanced sp-Cas9 possesses improved ability to recognize single/double-base mismatches between the target-strand and gRNA, which results in a ~10 fold reduction in off-target cleavage.⁵² Following similar notion, Kleinstiver *et al.* developed a high fidelity sp-Cas9 protein (sp-Cas9-HF1), which demonstrated almost complete loss of off-target cleavage when targeted to standard non-repetitive regions.⁵⁶

Alongside engineering of sp-Cas9 for improved specificity, precise detection of off-target effects on the genomic loci is important. Several approaches have been developed for this purpose. To ensure accurate detection of off-target mutations, deep sequencing of entire genome is a preferred method, especially when human applications are concerned.

Methods such as genome-wide, unbiased identification of DSB enabled by sequencing (GUIDE-seq), which employs double strand oligodeoxynucleotide tags integrated in site of DNA cleavage in the genome, are examples of strategies that can be employed to comprehensively detect CRISPR off-target cleavage and DNA breakpoint hotspots.⁵⁷ Very recently, circularization for *in vitro* reporting of cleavage effects by sequencing (CIRCLE-seq), has been proposed as a superior *in vitro* technique to detect genome-wide off target mutation of CRISPR.⁵⁸ These and similar techniques are enhancing our abilities to detect and examine CRISPR off target functions and set the stage for further engineering strategies to remove unintended effects of CRISPR for human application.

1.3.2. Challenge 2: Enhancing gene editing efficiency *in vivo*

One impediment to therapeutic gene correction is the efficiency and type of DNA repair following the CRISPR induced DNA DSB. The most popular methods of gene editing are taking advantage of two DNA repair pathways, NHEJ and HDR. NHEJ, which can repair a variety of DNA damages including DSBs, is active throughout the cell cycle, and does not require a repair template.⁵⁹ NHEJ is an efficient method of DNA repair that is active in both dividing and non-dividing cells. It mediates ligation of two DNA break ends, is error-prone and can nonspecifically lead to insertions/deletions in genes and disruption of reading frames. HDR, in contrary, takes advantage of a template to repair DNA by copying the exact sequences of the template and pasting it within the DSB site. HDR-mediated gene editing enables precise correction of genetic mutation or insertion of genetic materials in desired genetic loci. However, It mainly occurs during S/G2 phases of the cell cycle, when the sister chromatid is present to act as a repair

template.⁶⁰ As such, HDR-mediated repair of genes is less efficient than NHEJ and in non-dividing cells will prove difficult. This challenge gains even more significance when complications of *in vivo* physiology and delivery are considered. Along this notion, several strategies have been suggested to increase HDR efficiency following CRISPR mediated DNA DSB (Figure 1.1-B).

Yang *et al.* showed increased genetic editing efficiency when stem cells are synchronized into S/G2, providing context for HDR-driven gene correction.⁶¹⁻⁶² HDR has also been shown to be enhanced by using single stranded DNA donors that asymmetrically align with the DSB.⁶³ This particular strategy provided a 60% increase in HDR efficiency taking advantage of the mechanism for DSB creation and DNA strand release during Cas9-mediated edits.⁴⁵ One of these mechanisms is the ordered release of DNA strands, particularly the distal non-target strand which is released from Cas9 first.⁴⁵ This along with the ssDNA donor enhances the chance of HDR-mediated repair, the dynamics of which are examined by Richardson *et al.*⁴⁵ To enhance HDR following CRISPR mediated DNA cleavage, Chu *et al.* employed shRNAs or small molecules that repress NHEJ key molecules KU70, KU80 or DNA ligase IV and showed up to eight-fold improvement of HDR in human and mouse cell lines.⁶⁴ Similarly, Yu *et al.* performed small molecule screening to enhance (L755507 and Brefeldin A) HDR up to nine fold in stem cells.⁶⁵ Paquet *et al.* showed that HDR-mediated mono versus dual-allelic repair can be achieved by choosing a distance between gRNA target sites and the mutation site. If bi-allelic repair is desired, then the proximity of the gRNA to the mutation must be lessened. On the other end, increasing the distance between the

mutation and gRNA target site decreases HDR efficiency, hence the sub-optimum repair leads to single allele correction and heterozygosity for the target gene.⁶⁶

Circumventing the limitations of HDR has also become a major scientific interest. Strategies utilizing NHEJ mechanisms to deliver short-homologous templates have been described.⁶⁷⁻⁶⁹ Homology-independent targeted integration (HITI) is a recently introduced method that uses NHEJ to allow for directed gene alteration.⁶⁹ HITI takes advantage of a rationally designed gRNA that targets the site of interest and recuts the insertion site if the strands reanneal, or if the template is input in an undesired direction. This increases the probability that the DNA template is input in the correction orientation. HITI is more effective than HDR in HEK293 cells – improving efficiency to between 40-60%. HITI also corrected mouse neurons *in vitro* with efficiencies up to 55.9% while HDR had efficiencies between ~1-3%.⁶⁹ HITI's ability to repair non-dividing cell lineages is particularly important for gene therapies *in vivo* while simultaneously being an efficient gene repair mechanism.

Other recent methods attempt gene correction without dependence on NHEJ or HDR repair mechanisms. The use of cytidine deaminases allows for targeted C to T conversions without introducing double stranded breaks using Zinc Fingers, TALE, and Cas9.⁷⁰⁻⁷¹ Kondor *et al.* created base editors (BE), using dCas9 and Cas9 nickase in fusion to either apolipoprotein B mRNA editing enzyme catalytic polypeptide-like family proteins (APOBECs) or other activation induced cytidine deaminases.⁷¹ In their third generation of constructs (Cas9 nickase fused to APOBEC and uracil glycosylase inhibitor) the authors observed up to 37% efficiency of base editing.⁷¹ Later, Yang *et al.* achieved a 2.5% C to T base editing in HEK293 cells using zinc finger and TALEs fused

to similar enzymes. These advancements increase our ability to correct genes without relying on traditional DNA repair machinery. This is particularly important in cases of non-dividing cells and when *in vivo* delivery is concerned. The repertoire of CRISPR base editors and their functionality is now actively being expanded.⁷²

1.3.3. Challenge 3: Efficient transcriptional modulation

Catalytically inactive Cas9 (dCas9) was one of the first variants created where its nuclease activity was removed by two point mutations within the catalytic domains of the protein, preventing DSBs but retaining RNA-guided genomic targeting.⁷³ dCas9 has been repurposed to function as a transcriptional modulator alone or in fusion with known transcriptional modulators. dCas9 does not induce DSB, therefore it can serve as a safer option than Cas9 nuclease for gene therapy and eliminates the risk of permanently altering DNA at unwanted sites (e.g., germline DNA) (Figure 1.1-C). This variant of Cas9 can be exploited in conditions where gene activation or imprinting are the cause of diseases. In addition, transient and multiplexed modulation of endogenous genes, a feature that is enabled by CRISPR technology, can be an attractive cure for acute or chronic response to injury, where inflammatory cascade involving multiple genes becomes dysregulated.

Although dCas9 alone has been shown to decrease transcription from endogenous and synthetic promoters through steric hindrance, protein fusions were developed to enhance the effect. Examples of primary fusion proteins used for CRISPR-based transcriptional modulation include repressors such as the Krüppel-associated box (KRAB) or four concatenated mSin3 interaction domains (SID4X). In case of transcriptional activation,

VP16, VP64, VP160 and p65 activation domains have been tested in fusion with dCas9 protein.⁷⁴⁻⁷⁸ While these strategies achieved significant modulation of endogenous genes, for observing a clinically relevant phenotype *in vivo*, the ability to enhance efficiencies of transcriptional modulations are desired. Along this line, researchers have sought to examine the synergistic effect of multiple of these domains in a single setting. Synergistic activation mediator (SAM) approach uses p65, and the activation domain of HSF1 (P65-HSF1) in fusion with the MS2 bacteriophage coat protein.⁷⁹ This strategy brings these activation domains to CRISPR/DNA complex through MS2 binding to engineered gRNAs carrying Ms2 target sites. SAM has reliably upregulated multiple genes ~90% from basal levels with insignificant off-target gene modulation.⁷⁹ Similarly, Chavez *et al.* generated a tripartite activator, VP64-p65-and Epstein–Barr virus R transactivator Rta (VPR), fused to dCas9, which led to significant improvement for activation of endogenous gene over VP64 alone.⁷⁷ Another method named SunTag recruits multiple copies of fusion proteins (such as VP64 activation domain) to Cas9/gRNA complex. In this approach, Cas9 is tethered to multiple copies of a protein scaffold to which single chain variable fragment antibodies fused to effector domains bind.⁸⁰ In K562 cells, where the target gene CXCR4 is normally expressed lowly, a dCas9-SunTag-VP64 fusion improved mRNA upregulation from a 28% with dCas9-VP64 alone to 330% with SunTag.⁸⁰

Although, improved strategies have been built for transcriptional activation, generation of enhanced repressors has been less explored. Recently, Amabile *et al.* generated synthetic inducible transcriptional repressors by fusing KRAB domain or other known transcriptional repressors such as SETDB1, G9a, HP1 α , DNMT3L, EZH2, and

SUV420H2 to DNA binding proteins including tet and Cas9. Authors showed that triple repressors, DNA methyltransferase (DNMT)3L, KRAB, DNMT3A improved the efficiency of repression as compared to single or double repressors.⁸¹

Epigenetic editing is another method of affecting transcription. dCas9 fusion with DNMT3A silences genes through targeted CpG methylation.⁸²⁻⁸³ Another example is the histone demethylase LSD1, from *Neisseria meningitidis*, which has also been fused to dCas9 and acts on distal enhancers of the genes to mediate the repression of enhancers.⁸⁴ Oppositely, epigenetic upregulation of gene expression can also be accomplished with human acetyltransferase p300 fused to Sp-dCas9 for targeted acetylation of histone H3 (lysine 27) within promoter/enhancer regions.⁸⁵ In addition, Tet1 demethylase catalytic domain has been fused to sp-dCas9 and MS2 coat protein to achieve efficient upregulation of endogenous genes.⁸⁶

In all these cases understanding the design principles for enhanced transcriptional activation or repression has been a subject of active research. N versus C terminal fusions to dCas9 affects transcriptional modulation efficiency. A second consideration for transcriptional activation, especially in cases such as SAM or VPR, has been the initial level of gene expression as well as location of targeting of gRNAs relative to transcriptional start site.⁷⁹ If the baseline expression of a gene is higher, further activation is less efficient. Chavez *et al.* has investigated the robustness and efficiency multiple Cas9 activators in multiple species in depth and has found that VPR, SunTag and SAM system provide superior activation than traditional activation domains in many species.⁸⁷ In terms of repression, the efficiency has been highly dependent on the gRNA targeting site and chromatin structure. It is interesting to note that recent studies have shown that

Cas9 in fusion with activation domains such as VP64 or VPR can be used for transcriptional repression of endogenous genes or synthetic promoters by carefully choosing where gRNA binds relative to TSS.⁸⁸⁻⁸⁹ All these studies, will be fundamental to employ CRISPR for transcriptional modulation in clinic. However, full appreciation of CRISPR activators or repressors as a gene therapy tool, will also rely on advancements of delivery methods to accommodate large size of these protein cargos.

1.3.4. Challenge 4: Delivery

Delivery is a major challenge in most of current gene therapies and CRISPR is not an exception. For *in vivo* gene editing, Cas9 and a gRNA should be packaged and delivered as DNA, mRNA, or as a ribonucleoprotein (translated Cas9 complexed with a gRNA) (Figure 1.1-D). Choice of these forms is educated by downstream application. DNA has the advantage of being placed into vehicles such as a viral vector capable of cellular entrance and promoter-mediated transcription of Cas9 and its gRNA.^{53, 90-91} This method, has the advantage of employing the promoters and transcriptional machinery of cells to spatiotemporally regulate CRISPR expression and function. In addition, it is a method of choice when long term expression is required for cases such as transcriptional modulation. However, potential DNA-integration into mammalian cells are concerning.⁹² This issue is non-existent in mRNA delivery of Cas9/gRNA. Unlike DNA, mRNA must be delivered through electroporation, RNA viruses or nanoparticle encapsulation; all mediating cellular delivery.^{48, 93} This method bypasses transcription while allowing cellular degradation of the mRNA. However, mRNA is short-lived and may not serve as a right mode of transport when long term cellular presence of CRISPR components is required

for downstream effects. Ribonucleoproteins (RNPs) circumvent translation of Cas9, lowering the steps needed for editing while still naturally degrading.³ They also overcome the challenge of competing naturally derived RNAs that may interfere with RNP complexation within a cell if delivered as DNA or mRNA.⁹⁴ Though, RNP's have yet to be successfully encapsulated by nanoparticles, they represent a viable form of delivery.

Once the desired form of CRISPR for delivery is chosen, the parts are incorporated within viral vehicles, lipid or polymer-based nanoparticles or in some cases, directly delivered as naked DNA or RNA (Figure 1.2). Viral delivery enables simple processing/packing as well as long-term expression but can introduce immunogenic responses or integration in unwanted loci in genome. One limiting factor is the amount of genomic information that can be packaged within clinically safe viruses. AAV- is a prevalent type of DNA viruses that is used in clinic but has a small payload with a capacity of ~4.7kb. Size limitations will be a hurdle especially when considering the delivery of accessory components with CRISPR, such as safety genetic switches or protein fusions. RNA viruses such as alphavirus, on the other hand, provide several advantages including larger payload capacity, replication of delivered RNA cargo in host, which amplifies the signal in cells, as well as minimal risk of incorporation in the genome.

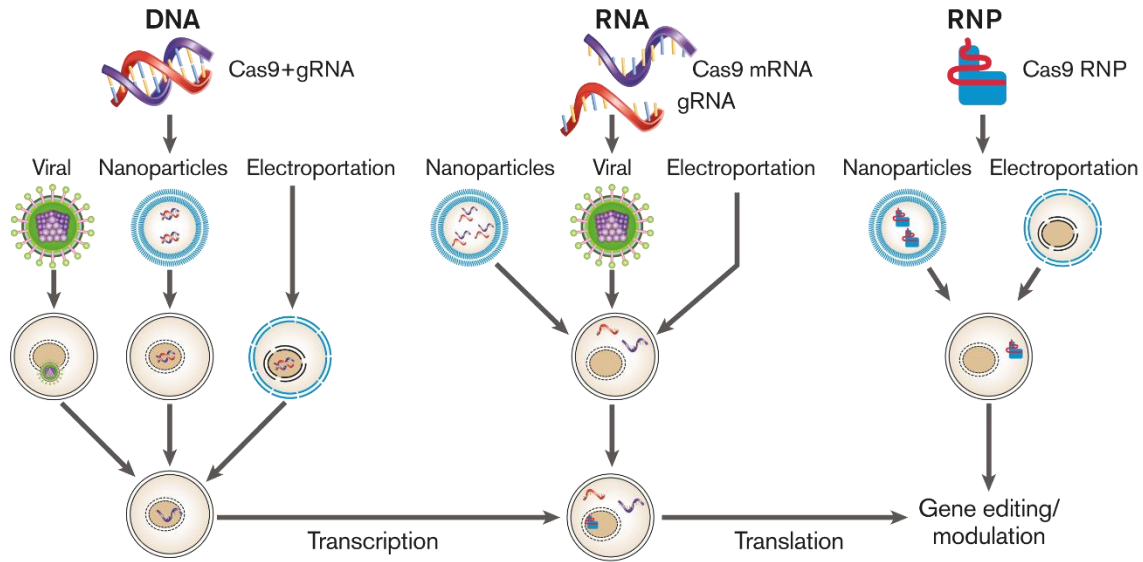


Figure 1.2. Modes of delivery of Cas9 and gRNA for genome editing.

However, alphaviruses and RNA replicons can illicit innate immune response in cells, which hampers their wide applications and limits them mostly to immune-tolerant tissues such as tumors.⁹⁵ It is noteworthy that the field of synthetic virology is generating engineered viruses with special features that enable further control over viruses. By treating viruses such as AAV as programmable and tunable biomolecular devices, researchers are engineering the viruses to control the gene delivery further spatiotemporally. As an example, Gomez *et al.* engineered an AAV virus that can localize to nucleus upon exposure to red light. This was achieved through fusion of its capsid protein with a R light dependent interaction partner phytochrome interacting factor 6, (PIF6) from *Arabidopsis thaliana* that can bind its partner, phytochrome B (PhyB) bearing a nuclear localization signal (NLS), upon exposure to red light.⁹⁶ Thus, combination of synthetic virology with CRISPR engineering can be an attractive avenue for generating safer and controllable gene therapies.

Nanoparticles are a secondary method of delivery that can accommodate larger payloads. Cationic lipid nanoparticles, that encapsulate anionic molecules, is a choice tool for intracellular delivery.^{46, 97} Engineered lipid nanoparticles can accomplish cell-type specific delivery of load through changes in diameter, variations in outer components, changes in the lipid base being used, their hydrophilicity/hydrophobicity, and their charge.^{46, 97} One advancement includes the creation of zwitterionic amino lipid nanoparticles which can deliver long mRNA and gRNAs with great efficiency (~90% expression of target proteins).⁹⁸ Nanoparticles can be made non-immunogenic, are stable for long periods of time, and can deliver proteins like Cas9.^{46, 99} Biocompatibility and clearance is one reason nanoparticles may be a preferred method of delivery.

Lastly, hydrodynamic vascular Injection of plasmid DNA or intramuscular electroporation of DNA or RNA have also been examined to deliver CRISPR component *in vivo*.^{24, 39} An advantage of these approaches is the minimal processing of DNA needed for delivery. However, this strategy demonstrates low efficiency of DNA delivery *in vivo*.

To address some of the delivery challenges, Cas9 from various species with smaller sizes have been exploited. *Staphylococcus aureus* Cas9 (sa-Cas9), is >1kb smaller than sp-Cas9.¹⁰⁰⁻¹⁰¹ This addresses issues of size, especially in vectors where genomic space is constrained such as AAV. CRISPR from Cpf1 is another example. Cpf1 is a class II CRISPR system with no tracrRNA (only a 39nt crRNA), and T-rich PAM sites.¹⁰²⁻¹⁰⁵ This variant of Cas9 gives enhanced ability to target genomic regions of interests, which are not GC rich, with efficiency and specificity. The smaller size of Cpf1 and its crRNA, makes it cheaper for synthesis, easier for engineering and facilitates viral based gene therapies that have packaging limitations. However, more studies are needed to fully

characterize Cpf1 and its functionality similar to sp-Cas9 before its full application for genome engineering can be evaluated.

Other types of CRISPR engineering approaches are focused on rationally splitting Cas9 proteins to two separate fragments of nuclease and α -helical lobes. In this case, the gRNA mediates the recruitment of the two fragments to target DNA and hence creating the complete Cas9-gRNA complex.¹⁰⁶ By decreasing the size of individual Cas9 components, the split Cas9 can be better packaged within viral particles and can be a practical option for AAV-based CRISPR gene therapies.¹⁰⁶ In addition, this approach gives another layer of control to where gene editing happens which is a favorable design for *in vivo* studies.

1.3.5. Challenge 5: Immune response to the gene editing tool

Being a bacterial derived system, patient immune response to CRISPR will be another key concern as clinical trials begin (Figure 1.1-E). However, to date, only limited studies have explored this aspect. Immune response to adenovirus-delivered sp-Cas9 was investigated in mouse models by Wang *et al.* sp-Cas9 specific antibodies were found to be elevated in this setting.¹⁶ More recently, a study led by Chew *et al.* showed that AAV mediated CRISPR delivered *in vivo* elicited both humoral and cellular immune response, however, the study did not detect extensive cellular damage within the two-week timeframe of the study.⁵¹ Further studies are needed to enhance our understanding and ability to control immune response against CRISPR before its human translation can be explored.

1.3.6. Challenge 6: Spatiotemporal control: Rational Engineering approaches for spatiotemporal control of CRISPR

To spatiotemporally control CRISPR function, several rational design approaches have been developed (Figure 1.1-F, Figure 1.3-A to D). One method that has drawn the interest of researchers is light-activated gene editing. A recent example develops light-activated CRISPR/Cas9 effectors (LACE), which utilized light-inducible CRY2 and CIB1 proteins from *Arabidopsis Thaliana* that heterodimerize when exposed to 450nm light. This enables light inducible complexation of two domains, recruiting VP64 to dCas9, and upregulation of gene expression.¹⁰⁷ A second method of light-activated CRISPR uses a caged amino acids strategy. Cas9 is “caged” (unable to bind to gRNAs) before being exposed to light as a lysine essential for its function is photo-caged.¹⁰⁸ After exposure, the lysine is released and Cas9 function restored. A third light-inducible method of Cas9 activation involves the fusing of two split Cas9 fragments with photo-inducible dimerization domains. When irradiated with blue light the domains combine enabling gene editing – if the light is extinguished the domains are dissociated and no further edits occur.¹⁰⁹

Chemically inducible CRISPR-Cas9 has been created to respond to doxycycline, rapamycin, and 4-hydroxytamoxifen.¹¹⁰⁻¹¹² Doxycycline inducible CRISPR-Cas9 system to modulate or knock out multiple genes simultaneously (*in vitro* and *in vivo*) have been used in multiple studies.¹¹³⁻¹¹⁷ Gao *et al.* recently developed orthogonal dCas9 regulators that are fused with chemical or light inducible dimerization domains. They used this strategy to achieve activation/repression of endogenous genes in an orthogonal and inducible manner.¹¹⁸ Examples of promoter specific Cas9 activity have enabled

cell/tissue-specific gene inactivation in multiple species such as zebrafish and human cells.¹¹⁹⁻¹²⁰

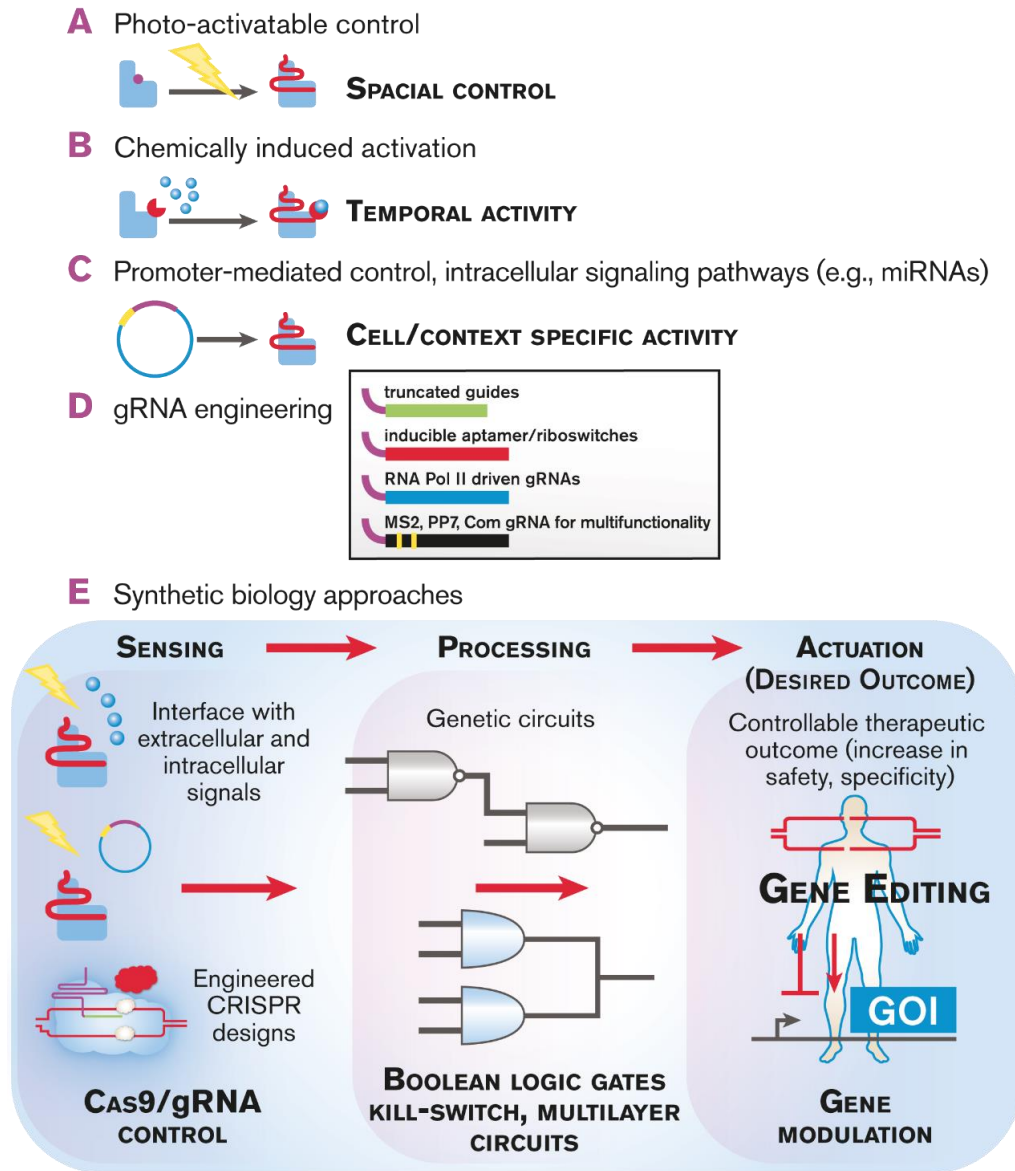


Figure 1.3. Rational engineering approaches to control “when”, “where”, and “how” CRISPR functions for safer *in vivo* gene therapies. (A) Light activated gene editing is a unique tool that enables temporal and spatial control of Cas9 mediated gene editing. Both Cas9, gRNA, and essential heterodimerizing proteins can be engineered to be switched

on or off when exposed to the correct wavelength of light. (B) The induction of gene editing can also be mediated by chemicals, such as 4-hydroxytamoxifen and doxycycline. (C) Promoter-mediated gene expression of CRISPR components is a well-known method of achieving cell-type specific activation of gene modification. (D) gRNA engineering is another strategy to achieve control or customizability of CRISPR. gRNAs can be engineered to be inducible using RNA Pol II promoters, can have aptamers inserted in their sequence that lead to multifunctionality for CRISPR (MS2, PP7 and Com), or can be shortened for increased specificity or ablation of Cas9 nuclease function. (E) Synthetic genetic circuits enable more control over CRISPR therapies. This is achieved through sensing, processing, and actuation steps. The integration of control mechanisms and engineered CRISPR components can increase safety and efficiency of gene therapies.

The study from Liu *et al.* in 2014 shows bladder-cancer specific gene editing dependent on human uroplakin II (bladder specific) and human telomerase reverse transcriptase (cancer-specific) expression, each encoding one component of CRISPR.¹²⁰ The developed AND gate led to CRISPR function only in cells with two specific promoters enabling enhancement of cell/context specificity of CRISPR. Cas9/gRNA functionality and some modifiable. Briner *et al.* demonstrated that gRNA stem loops are amenable to insertion or deletion, a finding that helped future engineering approaches to bring in additional functionality into gRNAs.¹²² By inserting protein binding RNA aptamers (MS2, PP7, Com) within permissive modules in gRNA, researchers have achieved orthogonal functionality such as activation and repression of genes.¹²³ Other approaches modified gRNA length. The complementary base pairs on the gRNA, which is usually around 20nt to the target genomic location, when lessened below 20nt have

been found to increase gene editing specificity.¹²⁴ Interestingly at 14nt or below the Cas9-gRNA binds DNA but does not cleave, demonstrating that shortened gRNAs ablate Cas9 nuclease activity.^{89, 125} This feature was exploited to achieve a multifunctional Cas9 complex that can activate and disrupt genes simultaneously in a single cell. gRNA has also been modified for programmable expression from RNA Polymerase type II (Pol II) promoters for increased tissue/context specific controllability.^{89, 126-130} By including modified riboswitches within gRNA that are responsive to small molecules or endogenous signaling protein, Liu *et al.* recently generated CRISPR–Cas9-based 'signal conductors' that sense external or internal signals (e.g., P53, NF-kb) and subsequently regulate transcription of endogenous genes in response to the input signal.¹⁴ In their designs, binding of protein of interest to riboswitches, creates steric changes in gRNAs and renders them effective to target desired loci.¹⁴ Such strategy is another practical approach to incorporate spatiotemporal control within the CRISPR system. Nowak *et al.* have summarized gRNA engineering strategies in their review and for further studies we refer the readers to their work.¹²¹ Above mentioned engineering approaches leverage multi-component nature and modularity of the CRISPR system. The inherent modularity of CRISPR enables us to link the expression/activity of each component to one small molecule/light inducible or cell/context specific factor and thereby, achieve tight spatiotemporal regulation of this system for future gene therapies.

To exert control over “how” CRISPR modulate genes, we and others developed CRISPR genetic circuits in human and bacterial cells (Figure 1.3-E). We showed that layering gRNAs expressed from RNA polymerase type III or II promoters in human cells can regulate gRNA functionality in stepwise manner.¹²⁶ Such circuits would enable

sequential modulation of endogenous genes, where gRNAs modulates genes one after another. This approach would be applicable specially in complex diseases such as metabolic diseases (e.g., diabetes) or cell-fate reprogramming, where stepwise modulation of genes is needed. Nissim *et al.* combined a similar CRISPR circuit with RNAi system, which enables additional control over CRISPR function, when interfaced with endogenous or cell-specific signals such as miRNAs.¹²⁷ A similar strategy was demonstrated in bacteria by Nielson *et al.* where multi-input and layered Boolean logic gates was developed and tested with CRISPR.¹³¹ Their circuits enabled modulation of one gRNA by another gRNA, which in turn repressed the transcription from an output promoter (NOT or NOR gates). Such genetic logic gates in bacteria can have tangible clinical application for modulation of gene expression in gut microbial, programmable probiotics or antimicrobial resistance as well as cancer therapies.¹³²

Genetic Safety switches incorporated within the CRISPR system can also address safety concerns in situations such as unwanted immune reaction. Along this line, we recently employed a multifunctional CRISPR to generate multi-layered genetic safety circuits in human cells. We generated a truncated gRNA that guides a catalytically active sp-Cas9 fused with VPR domain to a promoter, enabling transcriptional activation or repression of a reporter. A gRNA with 20nt guide length, which induces Cas9 nuclease activity, can then be induced using small molecules to generate Cas9-VPR mediated DNA cleavage, thereby terminating the function of CRISPR.⁸⁹ Another study with similar intent fused *Escherichia coli* dihydrofolate reductase degradation domain to the N terminus of sp-dCas9.¹³³ Trimethoprim (TMP) can then be added to bind and stabilize the degron and blocking degradation. This allows Cas9 enough time to find and edit its

desired target and once the small molecule is removed the Cas9-degron will return to being constitutively degraded.¹³³ Recently, naturally occurring off-switches in bacteria have been described for CRISPR system from *N. meningitidis*. The anti-CRISPR proteins could bind the Cas9 protein in human cells and disable gene editing. Although quite in the beginning of the road, these naturally occurring anti-CRISPRs could also someday be useful in controlling CRISPR functions at the tissue of interest in human therapies.¹³⁴ Although further studies are needed to fully optimize and delineate the clinical implication of these safety switches, they represent ways to generate CRISPR modulating systems with built-in safety switches that are deliverable in therapeutic settings.

1.4. Opportunities and Future Perspectives

With the advent of precision medicine initiative, CRISPR can play a major role in moving this initiative a step forward and translate individual's data into personalized therapies for correction/modulation of genetic abnormalities. Marriage of the field of synthetic biology with the CRISPR technology, the advances of gene delivery technologies, CRISPR design enhancement, and data management need to converge to generate safer and more controllable CRISPR strategies. Whether sp-Cas9 system will continue to be a leading CRISPR system in clinic or it will be replaced with CRISPR from other species, such as Cpf1, is still unclear. However, with the speed of CRISPR movement, it is important to put control mechanisms in place, whether it is at level of genetic elements transferred to human or in a more general term, in society.

Clinical trials using CRISPR technology are in horizon. The first trial intends to investigate the safety of ex-vivo CRISPR mediated immune cell therapy. Recently, the CRISPR-edited cells were injected into patients, led by Sichuan University in China, using this technique to knock out PD-1 (Programmed cell death protein 1) in lymphocytes.¹³⁵ The first expected trial in the United States will enroll approximately 18 participants. Their T-cell's will be edited to better detect tumor cells and to avoid tumor mediated inactivation of T-cell response. More importantly the study should collect data on immunogenic responses and if repaired cells can out-compete unedited cells. About six of the current CRISPR clinical studies shown on clinicaltrials.gov are PD-1-based therapies for cancers (esophageal, bladder, prostate, Renal cell carcinoma, non-small cell lung cancer, and malignancies associated with Epstein-Barr virus. The 7th trial focuses on using CRISPR to treat HPV-related symptoms/neoplasms by disrupting vital genes (HPV16/18) to reduce growth and induce cell death.

Along with the advent of CRISPR-driven therapies - the question of who wins the patent has been in the limelight. The patent battle between the Broad Institute and University of California Berkley/University of Vienna has been the epicenter. One of the main focuses has been on patent US8697359 B1 which was recently awarded to the Broad Institute detailing the use of CRISPR-Cas9 systems in eukaryotic cells. Unrelenting attention has been given to these cases as the potential lucrative nature of the technology will be well into the billions. The biotechnology market spiked in favor of Editas Medicine (who associates closely with the Broad Institute) rapidly after the announcement awarding the Broad patent US8697359 B1. This patent battle is not two-sided, many other groups are vying for their position in earning these patents. It speaks to

the ease of using and bettering CRISPR-Cas technology and the interest it has garnered all over the world.

As CRISPR gene therapies become more prominent and possible, the need to address the ethical and safety concerns grows. One of the first moral lines set, addressed the implications of editing the human germline.¹³⁶⁻¹³⁷ Editing somatic cells, the non-reproducing cell-types that most of the proposed therapies target, provides a way of treating individuals while leaving reproductive cells that will be passed onto future generations, unmodified.¹³⁷ Editing the germline can have unforeseeable consequences on the evolution of species. Genetic enhancement is another ethical concern. Therefore, public, along with scientists, must be educated in the science, ethical and biosafety issues behind gene therapies using CRISPR, so that CRISPR benefits will be appreciated and harms will be avoided.

With the advent of precision medicine initiative, CRISPR can play a major role in moving this initiative a step forward and translate individual's data into personalized therapies for correction/modulation of genetic abnormalities. Marriage of the field of synthetic biology with the CRISPR technology, the advances of gene delivery technologies, CRISPR design enhancement, and data management need to converge to generate safer and more controllable CRISPR strategies. Whether sp-Cas9 system will continue to be a leading CRISPR system in clinic or it will be replaced with CRISPR from other species, such as Cpf1, is still unclear. However, with the speed of CRISPR movement, it is important to put control mechanisms in place, whether it is at level of genetic elements transferred to human or in a more general term, in society. This review focuses on evaluating CRISPR potential as a next generation *in vivo* gene therapy

platform and discusses bioengineering advancements that can address challenges associated with clinical translation of this emerging technology.

References

1. Bolotin, A.; Quinquis, B.; Sorokin, A.; Ehrlich, S. D., Clustered regularly interspaced short palindrome repeats (CRISPRs) have spacers of extrachromosomal origin. *Microbiology* **2005**, *151* (Pt 8), 2551-61.
2. Mojica, F. J.; Diez-Villasenor, C.; Garcia-Martinez, J.; Soria, E., Intervening sequences of regularly spaced prokaryotic repeats derive from foreign genetic elements. *J Mol Evol* **2005**, *60* (2), 174-82.
3. Gasiunas, G.; Barrangou, R.; Horvath, P.; Siksnys, V., Cas9-crRNA ribonucleoprotein complex mediates specific DNA cleavage for adaptive immunity in bacteria. *Proc Natl Acad Sci U S A* **2012**, *109* (39), E2579-86.
4. Sapranaukas, R.; Gasiunas, G.; Fremaux, C.; Barrangou, R.; Horvath, P.; Siksnys, V., The *Streptococcus thermophilus* CRISPR/Cas system provides immunity in *Escherichia coli*. *Nucleic Acids Res* **2011**, *39* (21), 9275-82.
5. Shipman, S. L.; Nivala, J.; Macklis, J. D.; Church, G. M., Molecular recordings by directed CRISPR spacer acquisition. *Science* **2016**, *353* (6298), aaf1175.
6. Garneau, J. E.; Dupuis, M. E.; Villion, M.; Romero, D. A.; Barrangou, R.; Boyaval, P.; Fremaux, C.; Horvath, P.; Magadan, A. H.; Moineau, S., The CRISPR/Cas bacterial immune system cleaves bacteriophage and plasmid DNA. *Nature* **2010**, *468* (7320), 67-71.

7. Shmakov, S.; Abudayyeh, O. O.; Makarova, K. S.; Wolf, Y. I.; Gootenberg, J. S.; Semenova, E.; Minakhin, L.; Joung, J.; Konermann, S.; Severinov, K.; Zhang, F.; Koonin, E. V., Discovery and Functional Characterization of Diverse Class 2 CRISPR-Cas Systems. *Mol Cell* **2015**, *60* (3), 385-97.
8. Deltcheva, E.; Chylinski, K.; Sharma, C. M.; Gonzales, K.; Chao, Y.; Pirzada, Z. A.; Eckert, M. R.; Vogel, J.; Charpentier, E., CRISPR RNA maturation by trans-encoded small RNA and host factor RNase III. *Nature* **2011**, *471* (7340), 602-7.
9. Jinek, M.; Chylinski, K.; Fonfara, I.; Hauer, M.; Doudna, J. A.; Charpentier, E., A programmable dual-RNA-guided DNA endonuclease in adaptive bacterial immunity. *Science* **2012**, *337* (6096), 816-21.
10. Sander, J. D.; Joung, J. K., CRISPR-Cas systems for editing, regulating and targeting genomes. *Nat Biotechnol* **2014**, *32* (4), 347-55.
11. Kapahnke, M.; Banning, A.; Tikkanen, R., Random Splicing of Several Exons Caused by a Single Base Change in the Target Exon of CRISPR/Cas9 Mediated Gene Knockout. *Cells* **2016**, *5* (4).
12. Liang, X.; Potter, J.; Kumar, S.; Ravinder, N.; Chesnut, J. D., Enhanced CRISPR/Cas9-mediated precise genome editing by improved design and delivery of gRNA, Cas9 nuclease, and donor DNA. *J Biotechnol* **2017**, *241*, 136-146.
13. Chen, B.; Gilbert, L. A.; Cimini, B. A.; Schnitzbauer, J.; Zhang, W.; Li, G. W.; Park, J.; Blackburn, E. H.; Weissman, J. S.; Qi, L. S.; Huang, B., Dynamic imaging of genomic loci in living human cells by an optimized CRISPR/Cas system. *Cell* **2013**, *155* (7), 1479-91.

14. Liu, Y.; Zhan, Y.; Chen, Z.; He, A.; Li, J.; Wu, H.; Liu, L.; Zhuang, C.; Lin, J.; Guo, X.; Zhang, Q.; Huang, W.; Cai, Z., Directing cellular information flow via CRISPR signal conductors. *Nat Methods* **2016**, *13* (11), 938-944.
15. Wu, Y.; Liang, D.; Wang, Y.; Bai, M.; Tang, W.; Bao, S.; Yan, Z.; Li, D.; Li, J., Correction of a genetic disease in mouse via use of CRISPR-Cas9. *Cell Stem Cell* **2013**, *13* (6), 659-62.
16. Wang, D.; Mou, H.; Li, S.; Li, Y.; Hough, S.; Tran, K.; Li, J.; Yin, H.; Anderson, D. G.; Sontheimer, E. J.; Weng, Z.; Gao, G.; Xue, W., Adenovirus-Mediated Somatic Genome Editing of Pten by CRISPR/Cas9 in Mouse Liver in Spite of Cas9-Specific Immune Responses. *Hum Gene Ther* **2015**, *26* (7), 432-42.
17. Liang, P.; Xu, Y.; Zhang, X.; Ding, C.; Huang, R.; Zhang, Z.; Lv, J.; Xie, X.; Chen, Y.; Li, Y.; Sun, Y.; Bai, Y.; Songyang, Z.; Ma, W.; Zhou, C.; Huang, J., CRISPR/Cas9-mediated gene editing in human trippronuclear zygotes. *Protein Cell* **2015**, *6* (5), 363-72.
18. Mandal, P. K.; Ferreira, L. M.; Collins, R.; Meissner, T. B.; Boutwell, C. L.; Friesen, M.; Vrbanac, V.; Garrison, B. S.; Stortchevoi, A.; Bryder, D.; Musunuru, K.; Brand, H.; Tager, A. M.; Allen, T. M.; Talkowski, M. E.; Rossi, D. J.; Cowan, C. A., Efficient ablation of genes in human hematopoietic stem and effector cells using CRISPR/Cas9. *Cell Stem Cell* **2014**, *15* (5), 643-52.
19. Schwank, G.; Koo, B. K.; Sasselli, V.; Dekkers, J. F.; Heo, I.; Demircan, T.; Sasaki, N.; Boymans, S.; Cuppen, E.; van der Ent, C. K.; Nieuwenhuis, E. E.; Beekman, J. M.; Clevers, H., Functional repair of CFTR by CRISPR/Cas9 in intestinal stem cell organoids of cystic fibrosis patients. *Cell Stem Cell* **2013**, *13* (6), 653-8.

20. Tebas, P.; Stein, D.; Tang, W. W.; Frank, I.; Wang, S. Q.; Lee, G.; Spratt, S. K.; Surosky, R. T.; Giedlin, M. A.; Nichol, G.; Holmes, M. C.; Gregory, P. D.; Ando, D. G.; Kalos, M.; Collman, R. G.; Binder-Scholl, G.; Plesa, G.; Hwang, W. T.; Levine, B. L.; June, C. H., Gene editing of CCR5 in autologous CD4 T cells of persons infected with HIV. *N Engl J Med* **2014**, *370* (10), 901-10.
21. Hai, T.; Teng, F.; Guo, R.; Li, W.; Zhou, Q., One-step generation of knockout pigs by zygote injection of CRISPR/Cas system. *Cell Res* **2014**, *24* (3), 372-5.
22. Wang, X.; Cao, C.; Huang, J.; Yao, J.; Hai, T.; Zheng, Q.; Wang, X.; Zhang, H.; Qin, G.; Cheng, J.; Wang, Y.; Yuan, Z.; Zhou, Q.; Wang, H.; Zhao, J., One-step generation of triple gene-targeted pigs using CRISPR/Cas9 system. *Sci Rep* **2016**, *6*, 20620.
23. Niu, Y.; Shen, B.; Cui, Y.; Chen, Y.; Wang, J.; Wang, L.; Kang, Y.; Zhao, X.; Si, W.; Li, W.; Xiang, A. P.; Zhou, J.; Guo, X.; Bi, Y.; Si, C.; Hu, B.; Dong, G.; Wang, H.; Zhou, Z.; Li, T.; Tan, T.; Pu, X.; Wang, F.; Ji, S.; Zhou, Q.; Huang, X.; Ji, W.; Sha, J., Generation of gene-modified cynomolgus monkey via Cas9/RNA-mediated gene targeting in one-cell embryos. *Cell* **2014**, *156* (4), 836-43.
24. Yin, H.; Xue, W.; Chen, S.; Bogorad, R. L.; Benedetti, E.; Grompe, M.; Koteliansky, V.; Sharp, P. A.; Jacks, T.; Anderson, D. G., Genome editing with Cas9 in adult mice corrects a disease mutation and phenotype. *Nat Biotechnol* **2014**, *32* (6), 551-3.
25. Ousterout, D. G.; Kabadi, A. M.; Thakore, P. I.; Majoros, W. H.; Reddy, T. E.; Gersbach, C. A., Multiplex CRISPR/Cas9-based genome editing for correction of dystrophin mutations that cause Duchenne muscular dystrophy. *Nat Commun* **2015**, *6*, 6244.

26. Sung, Y. H.; Kim, J. M.; Kim, H. T.; Lee, J.; Jeon, J.; Jin, Y.; Choi, J. H.; Ban, Y. H.; Ha, S. J.; Kim, C. H.; Lee, H. W.; Kim, J. S., Highly efficient gene knockout in mice and zebrafish with RNA-guided endonucleases. *Genome Res* **2014**, *24* (1), 125-31.
27. Wang, H.; Yang, H.; Shivalila, C. S.; Dawlaty, M. M.; Cheng, A. W.; Zhang, F.; Jaenisch, R., One-step generation of mice carrying mutations in multiple genes by CRISPR/Cas-mediated genome engineering. *Cell* **2013**, *153* (4), 910-8.
28. Lin, S. R.; Yang, H. C.; Kuo, Y. T.; Liu, C. J.; Yang, T. Y.; Sung, K. C.; Lin, Y. Y.; Wang, H. Y.; Wang, C. C.; Shen, Y. C.; Wu, F. Y.; Kao, J. H.; Chen, D. S.; Chen, P. J., The CRISPR/Cas9 System Facilitates Clearance of the Intrahepatic HBV Templates In Vivo. *Mol Ther Nucleic Acids* **2014**, *3*, e186.
29. Liao, H. K.; Gu, Y.; Diaz, A.; Marlett, J.; Takahashi, Y.; Li, M.; Suzuki, K.; Xu, R.; Hishida, T.; Chang, C. J.; Esteban, C. R.; Young, J.; Izpisua Belmonte, J. C., Use of the CRISPR/Cas9 system as an intracellular defense against HIV-1 infection in human cells. *Nat Commun* **2015**, *6*, 6413.
30. Nakagawa, Y.; Oikawa, F.; Mizuno, S.; Ohno, H.; Yagishita, Y.; Satoh, A.; Osaki, Y.; Takei, K.; Kikuchi, T.; Han, S. I.; Matsuzaka, T.; Iwasaki, H.; Kobayashi, K.; Yatoh, S.; Yahagi, N.; Isaka, M.; Suzuki, H.; Sone, H.; Takahashi, S.; Yamada, N.; Shimano, H., Hyperlipidemia and hepatitis in liver-specific CREB3L3 knockout mice generated using a one-step CRISPR/Cas9 system. *Sci Rep* **2016**, *6*, 27857.
31. Ruan, J.; Li, H.; Xu, K.; Wu, T.; Wei, J.; Zhou, R.; Liu, Z.; Mu, Y.; Yang, S.; Ouyang, H.; Chen-Tsai, R. Y.; Li, K., Highly efficient CRISPR/Cas9-mediated transgene knockin at the H11 locus in pigs. *Sci Rep* **2015**, *5*, 14253.

32. Long, C.; McAnally, J. R.; Shelton, J. M.; Mireault, A. A.; Bassel-Duby, R.; Olson, E. N., Prevention of muscular dystrophy in mice by CRISPR/Cas9-mediated editing of germline DNA. *Science* **2014**, *345* (6201), 1184-8.
33. Kalebic, N.; Taverna, E.; Tavano, S.; Wong, F. K.; Suchold, D.; Winkler, S.; Huttner, W. B.; Sarov, M., CRISPR/Cas9-induced disruption of gene expression in mouse embryonic brain and single neural stem cells in vivo. *EMBO Rep* **2016**, *17* (3), 338-48.
34. Kim, H. K.; Song, M.; Lee, J.; Menon, A. V.; Jung, S.; Kang, Y. M.; Choi, J. W.; Woo, E.; Koh, H. C.; Nam, J. W.; Kim, H., In vivo high-throughput profiling of CRISPR-Cpf1 activity. *Nat Methods* **2016**.
35. Miller, J. B.; Zhang, S.; Kos, P.; Xiong, H.; Zhou, K.; Perelman, S. S.; Zhu, H.; Siegwart, D. J., Non-Viral CRISPR/Cas Gene Editing In Vitro and In Vivo Enabled by Synthetic Nanoparticle Co-Delivery of Cas9 mRNA and sgRNA. *Angew Chem Int Ed Engl* **2016**.
36. Wei, Y.; Chen, Y.; Qiu, Y.; Zhao, H.; Liu, G.; Zhang, Y.; Meng, Q.; Wu, G.; Chen, Y.; Cai, X.; Wang, H.; Ying, H.; Zhou, B.; Liu, M.; Li, D.; Ding, Q., Prevention of Muscle Wasting by CRISPR/Cas9-mediated Disruption of Myostatin In Vivo. *Mol Ther* **2016**, *24* (11), 1889-1891.
37. Xu, L.; Park, K. H.; Zhao, L.; Xu, J.; El Refaey, M.; Gao, Y.; Zhu, H.; Ma, J.; Han, R., CRISPR-mediated Genome Editing Restores Dystrophin Expression and Function in mdx Mice. *Mol Ther* **2016**, *24* (3), 564-9.
38. Nelson, C. E.; Hakim, C. H.; Ousterout, D. G.; Thakore, P. I.; Moreb, E. A.; Castellanos Rivera, R. M.; Madhavan, S.; Pan, X.; Ran, F. A.; Yan, W. X.; Asokan,

- A.; Zhang, F.; Duan, D.; Gersbach, C. A., In vivo genome editing improves muscle function in a mouse model of Duchenne muscular dystrophy. *Science* **2016**, *351* (6271), 403-7.
39. Long, C.; Amoasii, L.; Mireault, A. A.; McAnally, J. R.; Li, H.; Sanchez-Ortiz, E.; Bhattacharyya, S.; Shelton, J. M.; Bassel-Duby, R.; Olson, E. N., Postnatal genome editing partially restores dystrophin expression in a mouse model of muscular dystrophy. *Science* **2016**, *351* (6271), 400-3.
40. Bengtsson, N. E.; Hall, J. K.; Odom, G. L.; Phelps, M. P.; Andrus, C. R.; Hawkins, R. D.; Hauschka, S. D.; Chamberlain, J. R.; Chamberlain, J. S., Muscle-specific CRISPR/Cas9 dystrophin gene editing ameliorates pathophysiology in a mouse model for Duchenne muscular dystrophy. *Nat Commun* **2017**, *8*, 14454.
41. Zhang, Y.; Long, C.; Li, H.; McAnally, J. R.; Baskin, K. K.; Shelton, J. M.; Bassel-Duby, R.; Olson, E. N., CRISPR-Cpf1 correction of muscular dystrophy mutations in human cardiomyocytes and mice. *Sci Adv* **2017**, *3* (4), e1602814.
42. Xu, L.; Zhao, L.; Gao, Y.; Xu, J.; Han, R., Empower multiplex cell and tissue-specific CRISPR-mediated gene manipulation with self-cleaving ribozymes and tRNA. *Nucleic Acids Res* **2017**, *45* (5), e28.
43. Ruan, G. X.; Barry, E.; Yu, D.; Lukason, M.; Cheng, S. H.; Scaria, A., CRISPR/Cas9-Mediated Genome Editing as a Therapeutic Approach for Leber Congenital Amaurosis 10. *Mol Ther* **2017**, *25* (2), 331-341.
44. Yu, W.; Mookherjee, S.; Chaitankar, V.; Hiriyanna, S.; Kim, J. W.; Brooks, M.; Ataeijannati, Y.; Sun, X.; Dong, L.; Li, T.; Swaroop, A.; Wu, Z., Nrl knockdown by

- AAV-delivered CRISPR/Cas9 prevents retinal degeneration in mice. *Nat Commun* **2017**, *8*, 14716.
45. Murlidharan, G.; Sakamoto, K.; Rao, L.; Corriher, T.; Wang, D.; Gao, G.; Sullivan, P.; Asokan, A., CNS-restricted Transduction and CRISPR/Cas9-mediated Gene Deletion with an Engineered AAV Vector. *Mol Ther Nucleic Acids* **2016**, *5* (7), e338.
46. Zuris, J. A.; Thompson, D. B.; Shu, Y.; Guilinger, J. P.; Bessen, J. L.; Hu, J. H.; Maeder, M. L.; Joung, J. K.; Chen, Z. Y.; Liu, D. R., Cationic lipid-mediated delivery of proteins enables efficient protein-based genome editing in vitro and in vivo. *Nat Biotechnol* **2015**, *33* (1), 73-80.
47. Kaminski, R.; Bella, R.; Yin, C.; Otte, J.; Ferrante, P.; Gendelman, H. E.; Li, H.; Booze, R.; Gordon, J.; Hu, W.; Khalili, K., Excision of HIV-1 DNA by gene editing: a proof-of-concept in vivo study. *Gene Ther* **2016**, *23* (8-9), 690-5.
48. Yin, H.; Song, C. Q.; Dorkin, J. R.; Zhu, L. J.; Li, Y.; Wu, Q.; Park, A.; Yang, J.; Suresh, S.; Bizhanova, A.; Gupta, A.; Bolukbasi, M. F.; Walsh, S.; Bogorad, R. L.; Gao, G.; Weng, Z.; Dong, Y.; Koteliansky, V.; Wolfe, S. A.; Langer, R.; Xue, W.; Anderson, D. G., Therapeutic genome editing by combined viral and non-viral delivery of CRISPR system components in vivo. *Nat Biotechnol* **2016**, *34* (3), 328-33.
49. Yang, Y.; Wang, L.; Bell, P.; McMenamin, D.; He, Z.; White, J.; Yu, H.; Xu, C.; Morizono, H.; Musunuru, K.; Batshaw, M. L.; Wilson, J. M., A dual AAV system enables the Cas9-mediated correction of a metabolic liver disease in newborn mice. *Nat Biotechnol* **2016**, *34* (3), 334-8.
50. Guan, Y.; Ma, Y.; Li, Q.; Sun, Z.; Ma, L.; Wu, L.; Wang, L.; Zeng, L.; Shao, Y.; Chen, Y.; Ma, N.; Lu, W.; Hu, K.; Han, H.; Yu, Y.; Huang, Y.; Liu, M.; Li, D.,

CRISPR/Cas9-mediated somatic correction of a novel coagulator factor IX gene mutation ameliorates hemophilia in mouse. *EMBO Mol Med* **2016**, 8 (5), 477-88.

51. Chew, W. L.; Tabebordbar, M.; Cheng, J. K.; Mali, P.; Wu, E. Y.; Ng, A. H.; Zhu, K.; Wagers, A. J.; Church, G. M., A multifunctional AAV-CRISPR-Cas9 and its host response. *Nat Methods* **2016**, 13 (10), 868-74.
52. Slaymaker, I. M.; Gao, L.; Zetsche, B.; Scott, D. A.; Yan, W. X.; Zhang, F., Rationally engineered Cas9 nucleases with improved specificity. *Science* **2016**, 351 (6268), 84-8.
53. Cong, L.; Ran, F. A.; Cox, D.; Lin, S.; Barretto, R.; Habib, N.; Hsu, P. D.; Wu, X.; Jiang, W.; Marraffini, L. A.; Zhang, F., Multiplex genome engineering using CRISPR/Cas systems. *Science* **2013**, 339 (6121), 819-23.
54. Wyvekens, N.; Topkar, V. V.; Khayter, C.; Joung, J. K.; Tsai, S. Q., Dimeric CRISPR RNA-Guided FokI-dCas9 Nucleases Directed by Truncated gRNAs for Highly Specific Genome Editing. *Hum Gene Ther* **2015**, 26 (7), 425-31.
55. Ran, F. A.; Hsu, P. D.; Lin, C. Y.; Gootenberg, J. S.; Konermann, S.; Trevino, A. E.; Scott, D. A.; Inoue, A.; Matoba, S.; Zhang, Y.; Zhang, F., Double nicking by RNA-guided CRISPR Cas9 for enhanced genome editing specificity. *Cell* **2013**, 154 (6), 1380-9.
56. Kleinstiver, B. P.; Pattanayak, V.; Prew, M. S.; Tsai, S. Q.; Nguyen, N. T.; Zheng, Z.; Joung, J. K., High-fidelity CRISPR-Cas9 nucleases with no detectable genome-wide off-target effects. *Nature* **2016**, 529 (7587), 490-5.
57. Tsai, S. Q.; Zheng, Z.; Nguyen, N. T.; Liebers, M.; Topkar, V. V.; Thapar, V.; Wyvekens, N.; Khayter, C.; Iafrate, A. J.; Le, L. P.; Aryee, M. J.; Joung, J. K.,

- GUIDE-seq enables genome-wide profiling of off-target cleavage by CRISPR-Cas nucleases. *Nat Biotechnol* **2015**, *33* (2), 187-97.
58. Tsai, S. Q.; Nguyen, N. T.; Malagon-Lopez, J.; Topkar, V. V.; Aryee, M. J.; Joung, J. K., CIRCLE-seq: a highly sensitive in vitro screen for genome-wide CRISPR-Cas9 nuclease off-targets. *Nat Methods* **2017**.
59. Davis, A. J.; Chen, D. J., DNA double strand break repair via non-homologous end-joining. *Transl Cancer Res* **2013**, *2* (3), 130-143.
60. Pardo, B.; Gomez-Gonzalez, B.; Aguilera, A., DNA repair in mammalian cells: DNA double-strand break repair: how to fix a broken relationship. *Cell Mol Life Sci* **2009**, *66* (6), 1039-56.
61. Lin, S.; Staahl, B. T.; Alla, R. K.; Doudna, J. A., Enhanced homology-directed human genome engineering by controlled timing of CRISPR/Cas9 delivery. *Elife* **2014**, *3*, e04766.
62. Gutschner, T.; Haemmerle, M.; Genovese, G.; Draetta, G. F.; Chin, L., Post-translational Regulation of Cas9 during G1 Enhances Homology-Directed Repair. *Cell Rep* **2016**, *14* (6), 1555-66.
63. Richardson, C. D.; Ray, G. J.; DeWitt, M. A.; Curie, G. L.; Corn, J. E., Enhancing homology-directed genome editing by catalytically active and inactive CRISPR-Cas9 using asymmetric donor DNA. *Nat Biotechnol* **2016**, *34* (3), 339-44.
64. Chu, V. T.; Weber, T.; Wefers, B.; Wurst, W.; Sander, S.; Rajewsky, K.; Kuhn, R., Increasing the efficiency of homology-directed repair for CRISPR-Cas9-induced precise gene editing in mammalian cells. *Nat Biotechnol* **2015**, *33* (5), 543-8.

65. Yu, C.; Liu, Y.; Ma, T.; Liu, K.; Xu, S.; Zhang, Y.; Liu, H.; La Russa, M.; Xie, M.; Ding, S.; Qi, L. S., Small molecules enhance CRISPR genome editing in pluripotent stem cells. *Cell Stem Cell* **2015**, *16* (2), 142-7.
66. Paquet, D.; Kwart, D.; Chen, A.; Sproul, A.; Jacob, S.; Teo, S.; Olsen, K. M.; Gregg, A.; Noggle, S.; Tessier-Lavigne, M., Efficient introduction of specific homozygous and heterozygous mutations using CRISPR/Cas9. *Nature* **2016**, *533* (7601), 125-9.
67. Auer, T. O.; Duroure, K.; De Cian, A.; Concordet, J. P.; Del Bene, F., Highly efficient CRISPR/Cas9-mediated knock-in in zebrafish by homology-independent DNA repair. *Genome Res* **2014**, *24* (1), 142-53.
68. Maresca, M.; Lin, V. G.; Guo, N.; Yang, Y., Obligate ligation-gated recombination (ObLiGaRe): custom-designed nuclease-mediated targeted integration through nonhomologous end joining. *Genome Res* **2013**, *23* (3), 539-46.
69. Suzuki, K.; Tsunekawa, Y.; Hernandez-Benitez, R.; Wu, J.; Zhu, J.; Kim, E. J.; Hatanaka, F.; Yamamoto, M.; Araoka, T.; Li, Z.; Kurita, M.; Hishida, T.; Li, M.; Aizawa, E.; Guo, S.; Chen, S.; Goebel, A.; Soligalla, R. D.; Qu, J.; Jiang, T.; Fu, X.; Jafari, M.; Esteban, C. R.; Berggren, W. T.; Lajara, J.; Nunez-Delicado, E.; Guillen, P.; Campistol, J. M.; Matsuzaki, F.; Liu, G. H.; Magistretti, P.; Zhang, K.; Callaway, E. M.; Zhang, K.; Belmonte, J. C., In vivo genome editing via CRISPR/Cas9 mediated homology-independent targeted integration. *Nature* **2016**, *540* (7631), 144-149.
70. Yang, L.; Briggs, A. W.; Chew, W. L.; Mali, P.; Guell, M.; Aach, J.; Goodman, D. B.; Cox, D.; Kan, Y.; Lesha, E.; Soundararajan, V.; Zhang, F.; Church, G.,

- Engineering and optimising deaminase fusions for genome editing. *Nat Commun* **2016**, 7, 13330.
71. Komor, A. C.; Kim, Y. B.; Packer, M. S.; Zuris, J. A.; Liu, D. R., Programmable editing of a target base in genomic DNA without double-stranded DNA cleavage. *Nature* **2016**, 533 (7603), 420-4.
72. Kim, Y. B.; Komor, A. C.; Levy, J. M.; Packer, M. S.; Zhao, K. T.; Liu, D. R., Increasing the genome-targeting scope and precision of base editing with engineered Cas9-cytidine deaminase fusions. *Nat Biotechnol* **2017**, 35 (4), 371-376.
73. Qi, L. S.; Larson, M. H.; Gilbert, L. A.; Doudna, J. A.; Weissman, J. S.; Arkin, A. P.; Lim, W. A., Repurposing CRISPR as an RNA-guided platform for sequence-specific control of gene expression. *Cell* **2013**, 152 (5), 1173-83.
74. Thakore, P. I.; D'Ippolito, A. M.; Song, L.; Safi, A.; Shivakumar, N. K.; Kabadi, A. M.; Reddy, T. E.; Crawford, G. E.; Gersbach, C. A., Highly specific epigenome editing by CRISPR-Cas9 repressors for silencing of distal regulatory elements. *Nat Methods* **2015**, 12 (12), 1143-9.
75. Agne, M.; Blank, I.; Emhardt, A. J.; Gabelein, C. G.; Gawlas, F.; Gillich, N.; Gonschorek, P.; Juretschke, T. J.; Kramer, S. D.; Louis, N.; Muller, A.; Rudorf, A.; Schafer, L. M.; Scheidmann, M. C.; Schmunk, L. J.; Schwenk, P. M.; Stammnitz, M. R.; Warmer, P. M.; Weber, W.; Fischer, A.; Kaufmann, B.; Wagner, H. J.; Radziwill, G., Modularized CRISPR/dCas9 effector toolkit for target-specific gene regulation. *ACS Synth Biol* **2014**, 3 (12), 986-9.

76. Gimenez, C. A.; Ielpi, M.; Mutto, A.; Grosembacher, L.; Argibay, P.; Pereyra-Bonnet, F., CRISPR-on system for the activation of the endogenous human INS gene. *Gene Ther* **2016**, *23* (6), 543-7.
77. Chavez, A.; Scheiman, J.; Vora, S.; Pruitt, B. W.; Tuttle, M.; E, P. R. I.; Lin, S.; Kiani, S.; Guzman, C. D.; Wiegand, D. J.; Ter-Ovanesyan, D.; Braff, J. L.; Davidsohn, N.; Housden, B. E.; Perrimon, N.; Weiss, R.; Aach, J.; Collins, J. J.; Church, G. M., Highly efficient Cas9-mediated transcriptional programming. *Nat Methods* **2015**, *12* (4), 326-8.
78. Balboa, D.; Weltner, J.; Euroola, S.; Trokovic, R.; Wartiovaara, K.; Otonkoski, T., Conditionally Stabilized dCas9 Activator for Controlling Gene Expression in Human Cell Reprogramming and Differentiation. *Stem Cell Reports* **2015**, *5* (3), 448-59.
79. Konermann, S.; Brigham, M. D.; Trevino, A. E.; Joung, J.; Abudayyeh, O. O.; Barcena, C.; Hsu, P. D.; Habib, N.; Gootenberg, J. S.; Nishimasu, H.; Nureki, O.; Zhang, F., Genome-scale transcriptional activation by an engineered CRISPR-Cas9 complex. *Nature* **2015**, *517* (7536), 583-8.
80. Tanenbaum, M. E.; Gilbert, L. A.; Qi, L. S.; Weissman, J. S.; Vale, R. D., A protein-tagging system for signal amplification in gene expression and fluorescence imaging. *Cell* **2014**, *159* (3), 635-46.
81. Amabile, A.; Migliara, A.; Capasso, P.; Biffi, M.; Cittaro, D.; Naldini, L.; Lombardo, A., Inheritable Silencing of Endogenous Genes by Hit-and-Run Targeted Epigenetic Editing. *Cell* **2016**, *167* (1), 219-232 e14.
82. McDonald, J. I.; Celik, H.; Rois, L. E.; Fishberger, G.; Fowler, T.; Rees, R.; Kramer, A.; Martens, A.; Edwards, J. R.; Challen, G. A., Reprogrammable CRISPR/Cas9-

- based system for inducing site-specific DNA methylation. *Biol Open* **2016**, *5* (6), 866-74.
83. Vojta, A.; Dobrinic, P.; Tadic, V.; Bockor, L.; Korac, P.; Julg, B.; Klasic, M.; Zoldos, V., Repurposing the CRISPR-Cas9 system for targeted DNA methylation. *Nucleic Acids Res* **2016**, *44* (12), 5615-28.
84. Kearns, N. A.; Pham, H.; Tabak, B.; Genga, R. M.; Silverstein, N. J.; Garber, M.; Maehr, R., Functional annotation of native enhancers with a Cas9-histone demethylase fusion. *Nat Methods* **2015**, *12* (5), 401-3.
85. Hilton, I. B.; D'Ippolito, A. M.; Vockley, C. M.; Thakore, P. I.; Crawford, G. E.; Reddy, T. E.; Gersbach, C. A., Epigenome editing by a CRISPR-Cas9-based acetyltransferase activates genes from promoters and enhancers. *Nat Biotechnol* **2015**, *33* (5), 510-7.
86. Xu, X.; Tao, Y.; Gao, X.; Zhang, L.; Li, X.; Zou, W.; Ruan, K.; Wang, F.; Xu, G. L.; Hu, R., A CRISPR-based approach for targeted DNA demethylation. *Cell Discov* **2016**, *2*, 16009.
87. Chavez, A.; Tuttle, M.; Pruitt, B. W.; Ewen-Campen, B.; Chari, R.; Ter-Ovanesyan, D.; Haque, S. J.; Cecchi, R. J.; Kowal, E. J.; Buchthal, J.; Housden, B. E.; Perrimon, N.; Collins, J. J.; Church, G., Comparison of Cas9 activators in multiple species. *Nat Methods* **2016**, *13* (7), 563-7.
88. Braun, C. J.; Bruno, P. M.; Horlbeck, M. A.; Gilbert, L. A.; Weissman, J. S.; Hemann, M. T., Versatile in vivo regulation of tumor phenotypes by dCas9-mediated transcriptional perturbation. *Proc Natl Acad Sci U S A* **2016**, *113* (27), E3892-900.

89. Kiani, S.; Chavez, A.; Tuttle, M.; Hall, R. N.; Chari, R.; Ter-Ovanesyan, D.; Qian, J.; Pruitt, B. W.; Beal, J.; Vora, S.; Buchthal, J.; Kowal, E. J.; Ebrahimkhani, M. R.; Collins, J. J.; Weiss, R.; Church, G., Cas9 gRNA engineering for genome editing, activation and repression. *Nat Methods* **2015**, *12* (11), 1051-4.
90. Cho, S. W.; Kim, S.; Kim, J. M.; Kim, J. S., Targeted genome engineering in human cells with the Cas9 RNA-guided endonuclease. *Nat Biotechnol* **2013**, *31* (3), 230-2.
91. Mali, P.; Yang, L.; Esvelt, K. M.; Aach, J.; Guell, M.; DiCarlo, J. E.; Norville, J. E.; Church, G. M., RNA-guided human genome engineering via Cas9. *Science* **2013**, *339* (6121), 823-6.
92. Wang, Z.; Troilo, P. J.; Wang, X.; Griffiths, T. G.; Pacchione, S. J.; Barnum, A. B.; Harper, L. B.; Pauley, C. J.; Niu, Z.; Denisova, L.; Follmer, T. T.; Rizzuto, G.; Ciliberto, G.; Fattori, E.; Monica, N. L.; Manam, S.; Ledwith, B. J., Detection of integration of plasmid DNA into host genomic DNA following intramuscular injection and electroporation. *Gene Ther* **2004**, *11* (8), 711-21.
93. Hashimoto, M.; Takemoto, T., Electroporation enables the efficient mRNA delivery into the mouse zygotes and facilitates CRISPR/Cas9-based genome editing. *Sci Rep* **2015**, *5*, 11315.
94. Mekler, V.; Minakhin, L.; Semenova, E.; Kuznedelov, K.; Severinov, K., Kinetics of the CRISPR-Cas9 effector complex assembly and the role of 3'-terminal segment of guide RNA. *Nucleic Acids Res* **2016**, *44* (6), 2837-45.
95. Lundstrom, K., Alphaviruses in gene therapy. *Viruses* **2015**, *7* (5), 2321-33.
96. Gomez, E. J.; Gerhardt, K.; Judd, J.; Tabor, J. J.; Suh, J., Light-Activated Nuclear Translocation of Adeno-Associated Virus Nanoparticles Using Phytochrome B for

- Enhanced, Tunable, and Spatially Programmable Gene Delivery. *ACS Nano* **2016**, *10* (1), 225-37.
97. Wang, M.; Zuris, J. A.; Meng, F.; Rees, H.; Sun, S.; Deng, P.; Han, Y.; Gao, X.; Pouli, D.; Wu, Q.; Georgakoudi, I.; Liu, D. R.; Xu, Q., Efficient delivery of genome-editing proteins using bioreducible lipid nanoparticles. *Proc Natl Acad Sci U S A* **2016**, *113* (11), 2868-73.
98. Miller, J. B.; Zhang, S.; Kos, P.; Xiong, H.; Zhou, K.; Perelman, S. S.; Zhu, H.; Siegwart, D. J., Non-Viral CRISPR/Cas Gene Editing In Vitro and In Vivo Enabled by Synthetic Nanoparticle Co-Delivery of Cas9 mRNA and sgRNA. *Angew Chem Int Ed Engl* **2017**, *56* (4), 1059-1063.
99. Zolnik, B. S.; Gonzalez-Fernandez, A.; Sadrieh, N.; Dobrovolskaia, M. A., Nanoparticles and the immune system. *Endocrinology* **2010**, *151* (2), 458-65.
100. Ran, F. A.; Cong, L.; Yan, W. X.; Scott, D. A.; Gootenberg, J. S.; Kriz, A. J.; Zetsche, B.; Shalem, O.; Wu, X.; Makarova, K. S.; Koonin, E. V.; Sharp, P. A.; Zhang, F., In vivo genome editing using *Staphylococcus aureus* Cas9. *Nature* **2015**, *520* (7546), 186-91.
101. Friedland, A. E.; Baral, R.; Singhal, P.; Loveluck, K.; Shen, S.; Sanchez, M.; Marco, E.; Gotta, G. M.; Maeder, M. L.; Kennedy, E. M.; Kornepati, A. V.; Sousa, A.; Collins, M. A.; Jayaram, H.; Cullen, B. R.; Bumcrot, D., Characterization of *Staphylococcus aureus* Cas9: a smaller Cas9 for all-in-one adeno-associated virus delivery and paired nickase applications. *Genome Biol* **2015**, *16*, 257.
102. Zetsche, B.; Gootenberg, J. S.; Abudayyeh, O. O.; Slaymaker, I. M.; Makarova, K. S.; Essletzbichler, P.; Volz, S. E.; Joung, J.; van der Oost, J.; Regev, A.; Koonin,

- E. V.; Zhang, F., Cpf1 is a single RNA-guided endonuclease of a class 2 CRISPR-Cas system. *Cell* **2015**, *163* (3), 759-71.
103. Kim, D.; Kim, J.; Hur, J. K.; Been, K. W.; Yoon, S. H.; Kim, J. S., Genome-wide analysis reveals specificities of Cpf1 endonucleases in human cells. *Nat Biotechnol* **2016**, *34* (8), 863-8.
104. Toth, E.; Weinhardt, N.; Bencsura, P.; Huszar, K.; Kulcsar, P. I.; Talas, A.; Fodor, E.; Welker, E., Cpf1 nucleases demonstrate robust activity to induce DNA modification by exploiting homology directed repair pathways in mammalian cells. *Biol Direct* **2016**, *11*, 46.
105. Abudayyeh, O. O.; Gootenberg, J. S.; Konermann, S.; Joung, J.; Slaymaker, I. M.; Cox, D. B.; Shmakov, S.; Makarova, K. S.; Semenova, E.; Minakhin, L.; Severinov, K.; Regev, A.; Lander, E. S.; Koonin, E. V.; Zhang, F., C2c2 is a single-component programmable RNA-guided RNA-targeting CRISPR effector. *Science* **2016**, *353* (6299), aaf5573.
106. Wright, A. V.; Sternberg, S. H.; Taylor, D. W.; Staahl, B. T.; Bardales, J. A.; Kornfeld, J. E.; Doudna, J. A., Rational design of a split-Cas9 enzyme complex. *Proc Natl Acad Sci U S A* **2015**, *112* (10), 2984-9.
107. Polstein, L. R.; Gersbach, C. A., A light-inducible CRISPR-Cas9 system for control of endogenous gene activation. *Nat Chem Biol* **2015**, *11* (3), 198-200.
108. Hemphill, J.; Borchardt, E. K.; Brown, K.; Asokan, A.; Deiters, A., Optical Control of CRISPR/Cas9 Gene Editing. *J Am Chem Soc* **2015**, *137* (17), 5642-5.
109. Nihongaki, Y.; Kawano, F.; Nakajima, T.; Sato, M., Photoactivatable CRISPR-Cas9 for optogenetic genome editing. *Nat Biotechnol* **2015**, *33* (7), 755-60.

110. Dow, L. E.; Fisher, J.; O'Rourke, K. P.; Muley, A.; Kasthuber, E. R.; Livshits, G.; Tschaharganeh, D. F.; Socci, N. D.; Lowe, S. W., Inducible in vivo genome editing with CRISPR-Cas9. *Nat Biotechnol* **2015**, *33* (4), 390-4.
111. Zetsche, B.; Volz, S. E.; Zhang, F., A split-Cas9 architecture for inducible genome editing and transcription modulation. *Nat Biotechnol* **2015**, *33* (2), 139-42.
112. Liu, K. I.; Ramli, M. N.; Woo, C. W.; Wang, Y.; Zhao, T.; Zhang, X.; Yim, G. R.; Chong, B. Y.; Gowher, A.; Chua, M. Z.; Jung, J.; Lee, J. H.; Tan, M. H., A chemical-inducible CRISPR-Cas9 system for rapid control of genome editing. *Nat Chem Biol* **2016**, *12* (11), 980-987.
113. Cao, J.; Wu, L.; Zhang, S. M.; Lu, M.; Cheung, W. K.; Cai, W.; Gale, M.; Xu, Q.; Yan, Q., An easy and efficient inducible CRISPR/Cas9 platform with improved specificity for multiple gene targeting. *Nucleic Acids Res* **2016**, *44* (19), e149.
114. Sim, X.; Cardenas-Diaz, F. L.; French, D. L.; Gadue, P., A Doxycycline-Inducible System for Genetic Correction of iPSC Disease Models. *Methods Mol Biol* **2016**, *1353*, 13-23.
115. de Solis, C. A.; Ho, A.; Holehonnur, R.; Ploski, J. E., The Development of a Viral Mediated CRISPR/Cas9 System with Doxycycline Dependent gRNA Expression for Inducible In vitro and In vivo Genome Editing. *Front Mol Neurosci* **2016**, *9*, 70.
116. Bisht, K.; Grill, S.; Graniel, J.; Nandakumar, J., A lentivirus-free inducible CRISPR-Cas9 system for efficient targeting of human genes. *Anal Biochem* **2017**, *530*, 40-49.

117. Guo, J.; Ma, D.; Huang, R.; Ming, J.; Ye, M.; Kee, K.; Xie, Z.; Na, J., An inducible CRISPR-ON system for controllable gene activation in human pluripotent stem cells. *Protein Cell* **2017**, *8* (5), 379-393.
118. Gao, Y.; Xiong, X.; Wong, S.; Charles, E. J.; Lim, W. A.; Qi, L. S., Complex transcriptional modulation with orthogonal and inducible dCas9 regulators. *Nat Methods* **2016**, *13* (12), 1043-1049.
119. Ablain, J.; Durand, E. M.; Yang, S.; Zhou, Y.; Zon, L. I., A CRISPR/Cas9 vector system for tissue-specific gene disruption in zebrafish. *Dev Cell* **2015**, *32* (6), 756-64.
120. Liu, Y.; Zeng, Y.; Liu, L.; Zhuang, C.; Fu, X.; Huang, W.; Cai, Z., Synthesizing AND gate genetic circuits based on CRISPR-Cas9 for identification of bladder cancer cells. *Nat Commun* **2014**, *5*, 5393.
121. Nowak, C. M.; Lawson, S.; Zerez, M.; Bleris, L., Guide RNA engineering for versatile Cas9 functionality. *Nucleic Acids Res* **2016**, *44* (20), 9555-9564.
122. Briner, A. E.; Donohoue, P. D.; Goma, A. A.; Selle, K.; Slorach, E. M.; Nye, C. H.; Haurwitz, R. E.; Beisel, C. L.; May, A. P.; Barrangou, R., Guide RNA functional modules direct Cas9 activity and orthogonality. *Mol Cell* **2014**, *56* (2), 333-9.
123. Zalatan, J. G.; Lee, M. E.; Almeida, R.; Gilbert, L. A.; Whitehead, E. H.; La Russa, M.; Tsai, J. C.; Weissman, J. S.; Dueber, J. E.; Qi, L. S.; Lim, W. A., Engineering complex synthetic transcriptional programs with CRISPR RNA scaffolds. *Cell* **2015**, *160* (1-2), 339-50.
124. Doench, J. G.; Fusi, N.; Sullender, M.; Hegde, M.; Vaimberg, E. W.; Donovan, K. F.; Smith, I.; Tothova, Z.; Wilen, C.; Orchard, R.; Virgin, H. W.; Listgarten, J.; Root,

- D. E., Optimized sgRNA design to maximize activity and minimize off-target effects of CRISPR-Cas9. *Nat Biotechnol* **2016**, *34* (2), 184-91.
125. Dahlman, J. E.; Abudayyeh, O. O.; Joung, J.; Gootenberg, J. S.; Zhang, F.; Konermann, S., Orthogonal gene knockout and activation with a catalytically active Cas9 nuclease. *Nat Biotechnol* **2015**, *33* (11), 1159-61.
126. Kiani, S.; Beal, J.; Ebrahimkhani, M. R.; Huh, J.; Hall, R. N.; Xie, Z.; Li, Y.; Weiss, R., CRISPR transcriptional repression devices and layered circuits in mammalian cells. *Nat Methods* **2014**, *11* (7), 723-6.
127. Nissim, L.; Perli, S. D.; Fridkin, A.; Perez-Pinera, P.; Lu, T. K., Multiplexed and programmable regulation of gene networks with an integrated RNA and CRISPR/Cas toolkit in human cells. *Mol Cell* **2014**, *54* (4), 698-710.
128. Shechner, D. M.; Hacisuleyman, E.; Younger, S. T.; Rinn, J. L., Multiplexable, locus-specific targeting of long RNAs with CRISPR-Display. *Nat Methods* **2015**, *12* (7), 664-70.
129. Yoshioka, S.; Fujii, W.; Ogawa, T.; Sugiura, K.; Naito, K., Development of a mono-promoter-driven CRISPR/Cas9 system in mammalian cells. *Sci Rep* **2015**, *5*, 18341.
130. Didovyk, A.; Borek, B.; Tsimring, L.; Hasty, J., Transcriptional regulation with CRISPR-Cas9: principles, advances, and applications. *Curr Opin Biotechnol* **2016**, *40*, 177-84.
131. Nielsen, A. A.; Voigt, C. A., Multi-input CRISPR/Cas genetic circuits that interface host regulatory networks. *Mol Syst Biol* **2014**, *10*, 763.

132. Mimee, M.; Tucker, A. C.; Voigt, C. A.; Lu, T. K., Programming a Human Commensal Bacterium, *Bacteroides thetaiotaomicron*, to Sense and Respond to Stimuli in the Murine Gut Microbiota. *Cell Syst* **2015**, *1* (1), 62-71.
133. Maji, B.; Moore, C. L.; Zetsche, B.; Volz, S. E.; Zhang, F.; Shoulders, M. D.; Choudhary, A., Multidimensional chemical control of CRISPR-Cas9. *Nat Chem Biol* **2017**, *13* (1), 9-11.
134. Pawluk, A.; Amrani, N.; Zhang, Y.; Garcia, B.; Hidalgo-Reyes, Y.; Lee, J.; Edraki, A.; Shah, M.; Sontheimer, E. J.; Maxwell, K. L.; Davidson, A. R., Naturally Occurring Off-Switches for CRISPR-Cas9. *Cell* **2016**, *167* (7), 1829-1838 e9.
135. Paglialunga, L.; Salih, Z.; Ricciuti, B.; Califano, R., Immune checkpoint blockade in small cell lung cancer: is there a light at the end of the tunnel? *ESMO Open* **2016**, *1* (4), e000022.
136. Cyranoski, D., Ethics of embryo editing divides scientists. *Nature* **2015**, *519* (7543), 272.
137. Lanphier, E.; Urnov, F.; Haecker, S. E.; Werner, M.; Smolenski, J., Don't edit the human germ line. *Nature* **2015**, *519* (7544), 410-1.

CHAPTER 2

MULTIFUNCTIONAL CRISPR-CAS9 WITH ENGINEERED IMMUNOSILENCED HUMAN T CELL EPITOPES

Authors of the published manuscript: S.R.F. and R.E. designed experiments, performed experiments, and analyzed data. F.M. generated Cas9 variant constructs, performed Cas9 functional analysis experiments, and analyzed data. S.Kr. generated predicted Cas9 epitopes and designed and assisted with the T cell experiments. F.M. and S.Kr. contributed equally. J.G.P. analyzed RNA seq data. M.R.E. helped with the design of experiments and interpretation of data. S.K. and K.S.A. supervised this study. R.E. took the lead in writing the manuscript with input from S.R.F., S.K., and K.S.A. and support of all the other authors. I generated Cas9 variant constructs using highly advanced cloning methods such as golden gate assembly method and Gateway recombination cloning. The typical cloning workflow, such as traditional restriction enzyme cloning, involves many steps and can limit your cloning success. This takes considerable time and effort, and success is not guaranteed. In contrast, Gateway recombination cloning technology circumvents these cloning limitations, enabling you to access virtually any expression system. Since I have a lot of experience and have a deep understanding of these methods I was able to generate these constructs in a successful and reliable manner and provide them to my co-authors in order to test them in their established ELISA methods to investigate immune recognition of these mutated Cas9 variants. The results demonstrate that mutating the anchor amino acid of a highly immunogenic epitope can influence the overall immunogenicity of Cas9. Next, I performed Cas9 functional analysis experiments, and analyzed data.

To assess Cas9 functionality and off-target effects after modification, nuclease activity of genetically modified Cas9 variants is measured. Cells were transfected with Cas9 mutants and gRNA targeting endogenous or exogenous genes, and on-target CRISPR/Cas9 mutations in cultured cells caused by nuclease function of Cas9 were identified using deep sequencing. In other assays, Cas9 target recognition and binding function was achieved by transfecting cells with Modified Cas9s and gRNA targeting endogenous or exogenous genes and activation/repression mediators (e.g., SAM) and measuring the expression of genes. In some cases, off-target activity of WT and modified Cas9 proteins were assessed using next generation sequencing. Performing these assays need deep understanding of cell culture techniques, CRISPR technology and being able to design good experiments. I was able to contribute to this part of the project by performing all the Cas9 functional assays successfully. Our data demonstrate that these variants retain nuclease capacity in the locus we studied and demonstrated no significant increase in undesired off-target activity to WT-Cas9.

The CRISPR-Cas9 system has raised hopes for developing personalized gene therapies for complex diseases. Its application for genetic and epigenetic therapies in humans raises concerns over immunogenicity of the bacterially derived Cas9 protein. We detect antibodies to *Streptococcus pyogenes* Cas9 (SpCas9) in at least 5% of 143 healthy individuals. We also report pre-existing human CD8+ T cell immunity in the majority of healthy individuals screened. We identify two immunodominant SpCas9 T cell epitopes for HLA-A*02:01 using an enhanced prediction algorithm that incorporates T cell receptor contact residue hydrophobicity and HLA binding and evaluated them by T cell assays using healthy donor PBMCs. In a proof-of-principle study, we demonstrate that

Cas9 protein can be modified to eliminate immunodominant epitopes through targeted mutation while preserving its function and specificity. Our study highlights the problem of pre-existing immunity against CRISPR-associated nucleases and offers a potential solution to mitigate the T cell immune response.

2.1. Introduction

The Clustered Regularly Interspaced Short Palindromic Repeat (CRISPR)-Cas9 technology has raised hopes for developing personalized gene therapies for complex diseases such as cancer as well as genetic disorders, and is currently entering clinical trials^{1,2}. The history of gene therapy has included both impressive success stories and serious immunologic adverse events³⁻⁸. The expression of *Streptococcus pyogenes* Cas9 protein (SpCas9) in mice has evoked both cellular and humoral immune responses^{9,10}, which raises concerns regarding its safety and efficacy as a gene or epi-gene therapy in humans. These pre-clinical models and host immune reactions to other exogenous gene delivery systems¹¹⁻¹³ suggest that the pathogenic, non-self-origin of Cas9 may be immunogenic in humans.

Both B cell and T cell host responses specific to either the transgene or the viral components of adenoviral^{14,15} and adeno-associated viral (AAV)^{11,12} vectors have been detected, despite relatively low immunogenicity of AAV vectors. In the case of AAV, specific neutralizing antibodies (Abs) and T cells are frequently detected in healthy donors¹⁶⁻¹⁹ and specific CD8+ T cells have been shown to expand following gene delivery¹⁸. There has been recent progress in developing strategies to overcome this problem, such as capsid engineering and transient immunosuppression²⁰⁻²². The potential

consequences of immune responses to expressed proteins from viral vectors or transgenes include neutralization of the gene product; destruction of the cells expressing it, leading to loss of therapeutic activity or tissue destruction; induction of immune memory that prevents re-administration; and fulminant innate inflammatory responses^{23,24}. More potent immune responses to gene therapies have been observed in humans and non-human primate models compared to mice^{8,25}.

Of the Cas9 orthologs derived from bacterial species, the SpCas9 is the best characterized. *S. pyogenes* is a ubiquitous pathogen, with an annual incidence of 700 million worldwide²⁶, but the field is only now beginning to explore potential immunity to SpCas9 in humans^{27,28}. CRISPR application for human therapies will span its use both for gene editing (through DNA double-strand breaks) or epigenetic therapies (without DNA double-strand breaks). In fact, recent reports shed light on CRISPR's ability to activate or repress gene expression in mice²⁹⁻³¹, which opens the door to a variety of new therapeutic applications such as activating silent genes, compensating for disrupted genes, cell fate reprogramming, or silencing disrupted genes, without the concern over permanent change in DNA sequence. However, unlike the use of Cas9 for gene editing, which may only require Cas9 presence in cells for a few hours, current techniques for CRISPR-based epigenetic therapies require longer term expression of Cas9 *in vivo*, possibly for weeks and months^{30,31}, which poses the challenge of combating pre-existing immune response towards Cas9. This challenge will need to be addressed before CRISPR application for human therapies, especially for epigenetic therapies, can be fully implemented. Delivery of CRISPR *in vivo* by incorporating its expression cassette in adeno-associated virus (AAV), will most likely shape many of the initial clinical trials as AAV-based gene

delivery is one of the safest and most prevalent forms of gene therapies in human. AAV will enable longer term expression of Cas9, desirable for epigenetic therapies. Therefore, it is highly likely that CRISPR delivery through AAV and its expression within target cells will engage CD8+ T cell immunity.

Here, we seek to characterize the pre-existing immune response to SpCas9 in healthy individuals and to identify the immunodominant T cell epitopes with the aim of developing SpCas9 proteins that have diminished capacity to invoke human adaptive response. We identify two immunodominant SpCas9 T cell epitopes for HLA-A*02:01 by an improved prediction algorithm and T cell assays using healthy donor PBMCs. We demonstrate that Cas9 protein can be modified to eliminate immunodominant epitopes through targeted mutation while preserving its function and specificity.

2.2. Materials and methods

2.2.1. Detection of Cas9-specific serum antibodies in healthy controls

Healthy control sera (n = 143) used in this study, and previously described⁴⁷, are a subset of a molecular epidemiology study of head and neck cancer at the MD Anderson Cancer Center, collected between January 2006 and September 2008. Samples were collected using a standardized sample collection protocol and stored at -80°C until use. All relevant ethical regulations for work with human participants were followed and written informed consent was obtained from all participants under the Arizona State University institutional review board approval. Participants were ethnically diverse. Sample size was determined based on prior experience and similar experiments in the literature. There was no group allocation and the investigators were blinded to participants' information. *S. pyogenes* lysate was prepared by sonication of bacterial

pellets from overnight cultures of *S. pyogenes* ATCC 19615 in the presence of 1 pill of complete Protease Inhibitor (Sigma-Aldrich) after 3 cycles of freezing and thawing. Serum antibody detection was performed using ELISA. 96-well plates were coated with 20 µg/mL of recombinant *S. pyogenes* Cas9 nuclease (Takara Bio USA, Mountain View, CA), recombinant Epstein-Barr virus nuclear antigen 1 (EBNA; Advanced Biotechnologies Inc., Eldersburg, MD), human hemoglobin (Sigma-Aldrich) or *S. pyogenes* lysate. Sera were diluted 1:50 in 10% *E. coli* lysate prepared in 5% milk-PBST (0.2% tween)⁴⁸, incubated with shaking for 2 hrs at room temperature, and added to the specified wells in duplicate. Horseradish peroxidase (HRP) anti-human IgG Abs (Jackson ImmunoResearch Laboratories, West Grove, PA) were added at 1:10,000, and detected using Supersignal ELISA Femto Chemiluminescent substrate (Thermo Fisher Scientific, Waltham, MA). Luminescence was detected as relative light units (RLU) on a Glomax 96 Microplate Luminometer (Promega, Madison, WI) at 425 nm. The cutoff value was defined as any reactivity higher than the top 99% of RLU values for human hemoglobin (Figure 2.1-A, dotted line).

2.2.2. Cas9 candidate T cell epitope prediction

We predicted MHC class I restricted 9-mer and 10-mer candidate epitopes derived from the Cas9 protein (Uniprot - Q99ZW2) for HLA A*02:01. The protein reference sequence was entered into 5 different prediction algorithms; 3 MHC-binding: IEDB-consensus binding⁴⁹, NetMHCpan binding⁵⁰, Syfpeithi⁵¹ and two antigen-processing algorithms: IEDB-consensus processing, ANN processing⁵². The individual scores from each of the prediction algorithms were then normalized within the pool of predicted

peptides after exclusion of poor binders, and the average normalized binding scores were used to re-rank the candidate peptides. The top 38 candidate peptides (Supplementary Table 2.1) were selected for experimental testing. The IEDB consensus MHC-binding prediction algorithm (<http://www.iedb.org/>) was applied to obtain a list of high binding Cas9 peptides, each of which was assigned a normalized binding score (S_b). The immunogenicity score (S_i) was calculated for each peptide based on its amino acid hydrophobicity (ANN-Hydro)³². MHC class II epitopes were predicted using the recommended setting on IEDB. We used the Visual Molecular Dynamics software⁵³ (<http://www.ks.uiuc.edu/Research/vmd/>) to generate the Cas9 protein structure (PDB ID: 4CMP, Figure 2.2-E).

2.2.3. *Ex vivo* stimulation and epitope mapping of Cas9 by ELISpot

All peripheral blood mononuclear cells (PBMCs) were obtained from healthy individuals with written informed consent under the Arizona State University institutional review board and all relevant ethical regulations for work with human participants were followed. Participants were ethnically diverse. Sample size was determined based on prior experience and similar experiments in the literature. There was no group allocation and the investigators were blinded to participants' information. If PBMCs from a given donor were not reactive to the positive control, the donor was excluded from the study. PBMCs were isolated from fresh heparinized blood by Ficoll–Hypaque (GE Healthcare, UK) density gradient centrifugation and stimulated. Briefly, predicted Cas9 peptides with $S_b < 0.148$ ($n=38$) were synthesized ($> 80\%$ purity) by Proimmune, UK. Each peptide was reconstituted at 1mg/mL in sterile PBS and pools were created by mixing 3-4

candidate peptides. Sterile multiscreen ELISpot plates (Merck Millipore, Billerica, MA, USA) were coated overnight with 5µg/well of anti-IFN-γ capture antibody (clone D1K, # 3420-3-250, Mabtech, USA) diluted in sterile PBS. Frozen PBMCs were thawed rapidly and recombinant human IL-2 (20U/mL, R&D Systems) was added. They were then stimulated in triplicates with 10 µg/mL Cas9 peptide pools (or individual peptides), pre-mixed CEF pool as a positive control (ProImmune, UK), or DMSO as a negative control in the anti-IFN-γ-coated ELISpot plates, (Merck Millipore, Billerica, MA, USA) and incubated in a 37°C, 5% CO₂ incubator for 48 hrs. Plates were washed three times for 5 min each with ELISpot buffer (PBS + 0.5% FBS) and incubated with 1µg/mL anti-IFN-γ secondary detection antibody (clone 7-B6-1, #3420-6-250, Mabtech, USA) for 2 hrs at room temperature, washed and incubated with 1µg/mL Streptavidin ALP conjugate for 1 hr at room temperature. The wells were washed again with ELISpot buffer and spots were developed by incubating for 8-10 min with detection buffer (33 µL NBT, 16.5 µL BCIP, in 100mM Tris-HCl pH 9, 1mM MgCl₂, 150mM NaCl). Plates were left to dry for 2 days and spots were read using the AID ELISpot reader (Autoimmun Diagnostika GmbH, Germany). The average number of spot-forming units for each triplicate was calculated for each test peptide or peptide pool and subtracted from the background signal.

2.2.4. Autologous APC generation from healthy individual PBMCs

Autologous CD40L-activated B cell APCs were generated from healthy donors by incubating whole PBMCs with irradiated (32 Gy) K562-cell line expressing human CD40L (KCD40L) at a ratio of 4:1 (800,000 PBMCs to 200,000 irradiated KCD40Ls) in

each well. The cells were maintained in B cell media (BCM) consisting of IMDM (Gibco, USA), 10% heat-inactivated human serum (Gemini Bio Products, CA, USA), and Antibiotic-Antimycotic (Anti-Anti, Gibco, USA). BCM was supplemented with 10 ng/mL recombinant human IL-4 (R&D Systems, MN, USA), 2 µg/mL Cyclosporin A (Sigma-Aldrich, CA, USA), and insulin transferrin supplement (ITES, Lonza, MD, USA). APCs were re-stimulated with fresh irradiated KCD40Ls on days 5 and 10, after washing with PBS and expanding into a whole 24-well plate. After two weeks, APC purity was assessed by CD19⁺ CD86⁺ expressing cells using flow cytometry and were used for T cell stimulation after >90% purity. APCs were either re-stimulated up to 4 weeks or cryopreserved for re-expansion as necessary.

2.2.5. T cell stimulation by autologous APCs

Antigen-specific T cells were detected by stimulating healthy donor B cell APCs by either peptide pulsing of specific Cas9 epitopes, or by transfecting with mRNA encoding the whole WT or modified Cas9 proteins. Peptide pulsing of APCs was done under BCM 5% human serum, with recombinant IL-4. Transfection of APCs was done with primary P3 buffer in a Lonza 4D Nucleofector and program EO117 (Lonza, MD, USA) and incubated in BCM-10% human serum and IL-4. Twenty-four hrs later, on day 1, APCs were washed and incubated with thawed whole PBMCs at a ratio of 1:2 (200,000 APCs : 400,000 PBMCs) in a 24-well plate in BCM supplemented with 20U/mL recombinant human IL-2 (R&D Systems, MN, USA) and 5ng/mL IL-7 (R&D Systems, MN, USA). On day 5, partial media exchange was performed by replacing half the well with fresh BCM and IL-2. On day 10, fresh APCs were peptide pulsed in a new 24-well plate. On

day 11, expanded T cells were re-stimulated with peptide-pulsed APCs similar to day 1. T cells were used for T cell assays or immunophenotyped after day 18.

2.2.6. Flow cytometry staining for T cells

Cells were washed once in MACS buffer (containing PBS, 1% BSA, 0.5mM EDTA), centrifuged at 550 g for 5 min and re-suspended in 200 μ L MACS buffer. Cells were stained in 100 μ L of staining buffer containing anti-CD137, conjugated with phycoerythrin (PE, clone 4B4-1; BD Biosciences, USA), anti-CD8-PC5 (clone B9.11; Beckman Coulter 1:100), anti-CD4 (clone SK3; BioLegend, 1:200), anti-CD14 (clone 63D3; BioLegend, 1:200), and anti-CD19 (clone HIB19; BioLegend,1:200), all conjugated to Fluorescein isothiocyanate (FITC) for exclusion gates, for 30 min on ice. Samples were covered and incubated for 30 min on ice, washed twice in PBS, and resuspended in 1mL PBS prior to analysis.

2.2.7. Pentamer staining for T cell immunophenotyping

The following HLA-A*02:01 PE-conjugated Cas9 pentamers were obtained from ProImmune: F2A-D-CUS-A*02:01-ILEDIVLTL-Pentamer, 007-Influenza A MP 58-66-GILGFVFTL-Pentamer. T cells were washed twice in MACS buffer with 5% human serum and centrifuged at 550g for 5 min each time. They were then re-suspended in 100 μ L staining buffer (MACS buffer, with 5% human serum and 1mM Dasatanib (ThermoFisher Scientific, MA, USA). Each of the pentamers was added to resuspended T cells, stimulated with the respective peptide or APCs at a concentration of 1:100.

Samples were incubated at room temperature for 30 min in the dark, then washed twice in MACS buffer. Cells were stained in 100 μ L MACS buffer with anti-CD8-PC5, anti-CD4-FITC, anti-CD14-FITC, and anti-CD19-FITC for exclusion gates. Samples were then washed twice with PBS and analyzed by flow cytometry. For flow cytometric analysis, all samples were acquired with Attune flow cytometer (ThermoFisher Scientific, MA, USA) and analyzed using the Attune software. Gates for expression of different markers and pentamers were determined based on flow minus one (FMO) samples for each color after doublet discrimination (Supplementary Figure 2.1). Percentages from each of the gated populations were used for the analysis.

2.2.8. Vector design and construction

Modified Cas9 plasmids: Human codon-optimized *Streptococcus pyogenes* Cas9 sequence was amplified from pSpCas9 (pX330; Addgene plasmid ID: 42230), using forward and reverse primers and inserted within gateway entry vectors using golden gate reaction. Desired mutations were designed within gBlocks (Integrated DNA Technologies). The gBlocks and amplicons were then cloned into gateway entry vectors using golden gate reaction. All the primer sequences are listed in the supplementary table 9 and all the gBlocks sequences are listed in (Supplementary Note 2.1). Next, the Cas9 vectors and CAG promoter cassettes were cloned into an appropriate gateway destination vector via LR reaction (Invitrogen).

U6-sgRNA-MS2 plasmids: These plasmids were constructed by inserting either 14bp or 20bp spacers of gRNAs into sgRNA (MS2) cloning backbone (Addgene plasmid ID: 61424) at BbsI site. All the gRNA sequences are listed in Supplementary Table 2.2.

2.2.9. Cell culture for endogenous target mutation and activation

HEK293FT cell line was purchased from ATCC and maintained in Dulbecco's modified Eagle's medium (DMEM - Life Technologies) containing 10% fetal bovine serum (FBS - Life Technologies), 2mM glutamine, 1mM sodium pyruvate (Life Technologies) and 1% penicillin-streptomycin (Life Technologies) in incubators at 37°C and 5% CO₂. Polyethylenimine (PEI) was used to transfect HEK293FT cells seeded into 24-well plates. Transfection complexes were prepared according to manufacturer's instructions (Polysciences).

2.2.10. Fluorescent reporter assay for quantifying Cas9 function

For the experiment assessing Cas9 cleavage capacity at a synthetic promoter, HEK293FT cells were co-transfected with 200ng gRNA, 200ng Cas9 constructs, 50ng reporter plasmid and 25ng enhanced blue fluorescent protein (EBFP) expressing plasmid as the transfection control. For the experiment assessing Cas9 transcriptional activation capacity at a synthetic promoter, HEK293FT cells were co-transfected with 50ng gRNA, 70ng Cas9 constructs, 100ng MS2-P65-HSF1-GFP (Addgene plasmid ID: 61423), 200ng reporter plasmid.

Fluorescent reporter experiments were performed 48 hrs after transfection. Nonviable cells were excluded from the analysis using 7-AAD (7-amino-actinomycin D) conjugated with PerCP. Next, we selected cells expressing EBFP > 2x10² A.U. or GFP > 2x10² A.U. (transfection markers) in the cleavage and activation experiments, respectively to exclude un-transfected cells (Supplementary Figure 2.1). Flow cytometry was performed using a FACSCelesta flow cytometer (Becton Dickson) with HTS. Flow cytometry data were

analyzed using FlowJo software. Un-transfected controls were included in each experiment. Experiments underwent initial validation in duplicate and then were repeated in triplicate for the final manuscript.

2.2.11. Quantitative RT-PCR analysis

HEK293FT cells were co-transfected with 10 ng gRNA, 200 ng Cas9 constructs, 100 ng MS2-P65-HSF1 (Addgene plasmid ID: 61423) and 25 ng EBFP plasmid as the transfection control. Cells were lysed, and RNA was extracted using RNeasy Plus mini kit (Qiagen) 72 hrs post transfection, followed by cDNA synthesis using the High-Capacity RNA-to-cDNA Kit (Thermo Fisher). qRT-PCR was performed using SYBR Green PCR Master Mix (Thermo Fisher). All analyses were normalized to 18S rRNA (ΔCt) and fold changes were calculated against un-transfected controls ($2^{-\Delta\Delta\text{Ct}}$). Primer sequences for qPCR are listed in Supplementary Table 2.3.

2.2.12. Endogenous indel analysis

HEK293FT cells were co-transfected with 200ng of Cas9 plasmids, 10ng of gRNA coding cassette and 25ng EBFP plasmid as the transfection control. 72 hrs later, transfected cells were dissociated and spun down at 200 g for 5 min at room temperature. Genomic DNA was extracted using 50 μl of QuickExtract DNA extraction solution (Epicentre) according to the manufacturer's instructions. Genomic DNA was amplified by PCR using primers flanking the targeted region. Illumina Tru-Seq library was created by ligating partial adaptors and a unique barcode to the DNA samples.

Next, a small number of PCR cycles was performed to complete the partial adaptors.

Equal amounts of each sample were then pooled and sequenced on Illumina Tru-Seq platform with 2x150 run parameters, which yielded approximately 80,000 reads per sample. Sequencing was performed using a 2x150 paired end (PE) configuration by CCIB DNA Core Facility at Massachusetts General Hospital (Cambridge, MA, USA). The reads were aligned to the target gene reference in *Mus musculus* genome using Geneious software, 9-1-5. To detect the indels (insertions and deletions of nucleic acid sequence at the site of double-strand break), each mutation was evaluated carefully in order to exclude the ones that are caused by sequencing error or any off-target mutation.

The variant frequencies (percentage to total) assigned to each read containing indels were summed up. i.e. indel percentage = total number of indel containing reads/ total number of reads. The minimum number of analyzed reads per sample was 70,000.

2.2.13. RNA sequencing for quantifying activator specificity

HEK293FT cells were co-transfected with 10 ng gRNA targeting *MIAT* locus, 200 ng Cas9 constructs, 100 ng MS2-P65-HSF1 (Addgene plasmid ID: 61423) and 25 ng transfection control. Total RNA was extracted 72 hrs post transfection using RNeasy Plus mini kit (Qiagen) and sent to UCLA TCGB core on dry ice.

Ribosomal RNA depletion, and single read library preparation were performed at UCLA core followed by RNA sequencing using NextSeq500. Coverage was 14 million reads per sample. FASTQ files with single-ended 75bp reads were then aligned to the human GRCh38 reference genome sequence (Ensembl release 90) with STAR⁵⁴, and uniquely-mapped read counts (an average of 14.8 million reads per sample) were obtained with Cufflink⁵⁵. The read counts for each sample were then normalized for the

library size to CPM (counts per million reads) with edgeR⁵⁶. Custom R scripts were then used to generate plots.

2.3. Results

2.3.1. Detection of Cas9-specific serum antibodies in healthy controls

We first determined whether healthy individuals have detectable IgG Abs to SpCas9. Of 143 healthy control sera screened, 82 (57.3%) had detectable Abs against *S. pyogenes* lysate using ELISA (Figure 2.1-A).

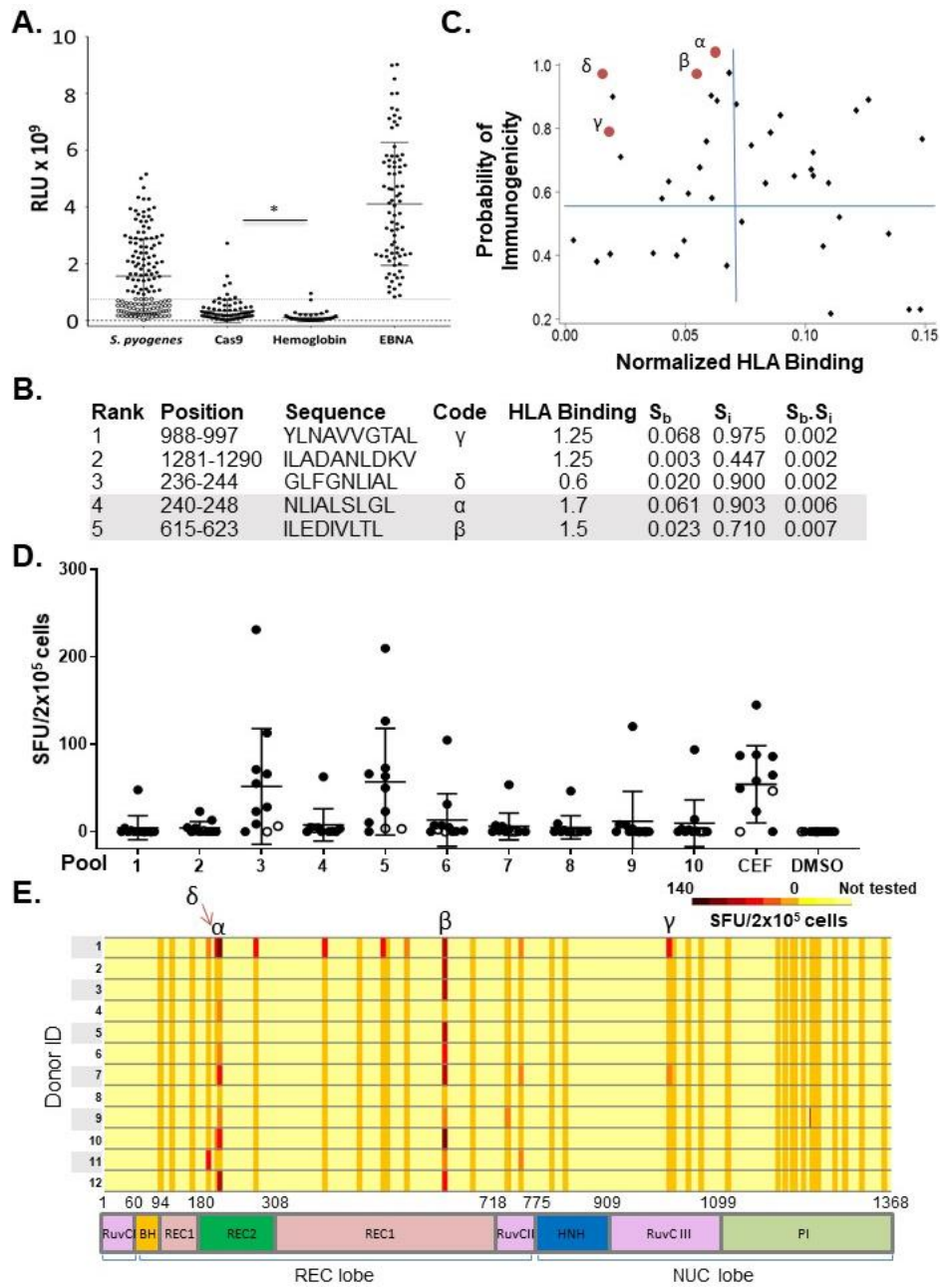


Figure 2.1. Detection of pre-existing B cell and T cell immune responses to SpCas9 in healthy donors and identification of two immunodominant T cell epitopes. **A.** Specific serum Abs were detected against *S. pyogenes* lysate in 57.3% (n=82) of 143 healthy controls. Sera with the highest reactivity to *S. pyogenes* lysate (n=80, black circles) were screened for Abs against recombinant SpCas9, recombinant EBNA-1 protein (positive

control), and human hemoglobin (negative control), of which 7 (8.8%) were positive for SpCas9 (above the dotted line; * $p < 0.0001$). **B.** The top 5 predicted SpCas9 T cell epitopes and their predicted S_b and S_i scores and ranking (based on the $S_b.S_i$ value) ³². These top 5 peptides include the identified immunodominant (α and β ; gray) and subdominant (γ and δ) epitopes that were shown to be immunogenic by IFN- γ ELISpot. **C.** Plot of S_b and S_i of predicted HLA-A*02:01 epitopes for the SpCas9 protein. Red dots represent the immunodominant and subdominant epitopes. **D.** IFN- γ ELISpot assay of T cell reactivity of 12 healthy donors (the two non- HLA-A*02:01 are shown as open circles) to 38 predicted epitopes grouped in 10 pools, CEF (positive control peptide pool), and DMSO (negative control). Peptides α and δ were in pool 5 while β and γ were in pool 3. **E.** IFN- γ ELISpot reactivity of healthy donor T cells (n=12) to epitopes across the different domains of the Cas9 protein. Donors 1-10 were HLA-A*02:01, while 11 and 12 were not. Peptides α and δ overlap in 5 amino acid residues. Data represent mean \pm SD. EBNA-1, Epstein-Barr virus nuclear antigen-1; S_b , normalized binding score; S_i , normalized immunogenicity score. Statistical analysis was performed post hoc and results are exploratory. Sera with the highest reactivity to *S. pyogenes* lysate (n=80) were screened for Abs against recombinant SpCas9, of which 7 (8.8%) were positive ($p < 0.0001$, two-tailed t-test). At least 5.0% of healthy individuals screened in this study had Cas9-specific Abs (Figure 2.1-A).

2.3.2. Cas9 candidate T cell epitope prediction

Whether Cas9-specific antibodies impact the efficacy or safety of CRISPR application in human remains to be seen. However, cellular immunity is expected to have

a more significant impact in case of CRISPR delivery through viruses. The Cas9 expression cassette, delivered by a viral vector, leads to intracellular expression of this protein in target cells, which could evoke a cellular immune response. We thus focused on investigating the T cell immune response against SpCas9. We predicted HLA-A*02:01-restricted T cell epitopes derived from SpCas9 using a model that uses both MHC binding affinity and biochemical properties of immunogenicity³² (Supplementary Table 2.1; the top 5 are shown in Figure 2.1-B). This model incorporates T cell receptor contact residue hydrophobicity and HLA binding prediction, which enhances the efficiency of epitope identification, as we previously reported³². We plotted the calculated normalized binding (S_b) and immunogenicity (S_i) scores for each peptide (Figure 2.1-C) to predict the more immunogenic epitopes, which are expected to have both high HLA binding (low S_b) and more hydrophobicity (high S_i). We chose HLA-A*02:01 because it is the most common HLA type in European/North American Caucasians.

2.3.3. T cell epitope mapping of Cas9 and identification of two immunodominant epitopes

We then investigated whether peripheral blood mononuclear cells (PBMCs) derived from healthy individuals had measurable T cell reactivity against the predicted SpCas9 MHC class I epitopes. We synthesized 38 peptides (Supplementary Table 2.1) and grouped them into 10 pools of 3-4 peptides each. We measured peptide-specific T cell immunity using IFN- γ secretion ELISpot assays with PBMCs derived from 12 healthy individuals (HLA-A*02:01, n=10; non-HLA-A*02:01, n=2) and identified

immunoreactive epitopes within pools 3 or 5 in 83.0% of the donors tested (90% of the HLA-A*02:01 donors; Figure 2.1-D). The seven individual peptides from pools 3 and 5 were evaluated by IFN- γ ELISpot and the dominant immunogenic epitopes were SpCas9_240-248 and SpCas9_615-623, designated peptides α and β , from pools 5 and 3, respectively. The subdominant epitopes were found to be γ and δ from pools 3 and 5, respectively. Both peptides α and β are located in the REC lobe of the Cas9 protein (Figure 2.1-E) that binds the sgRNA and the target DNA heteroduplex³³. The individual peptides within pools that were positive for any donor were evaluated for this donor by IFN- γ ELISpot. The immunoreactivity and position of the 38 predicted peptides (a few of which are overlapping) within the Cas9 protein are shown in Figure 2.1-E.

Peptides α and β are shown as red dots on the epitope prediction plot (Figure 2.1-C) and their sequences and predicted ranking are shown in Figure 2.1-B and Supplementary Table 2.1. As predicted, these peptides had low S_b and high S_i values. Both the immunodominant (α and β) and subdominant (γ and δ) T cell epitopes identified by IFN- γ ELISpot were within the top 5 most immunogenic epitopes predicted by our immunogenicity model³². Their ranking as predicted by the consensus method hosted on the IEDB server using default settings was 14, 5, 18, and 4, respectively. Sequence similarity of peptides α and β to amino acid sequences in known proteins was investigated using Protein BLAST and the IEDB epitope database³⁴. This was done to investigate whether there is any chance that the T cell immune response that we are detecting in healthy individuals could be due to previous exposure to another protein of similar sequence. A peptide was considered ‘similar’ to α or β if no more than 2 of 9 amino acid residues (that are not the second or ninth) were not matching (78% similarity).

None of these two peptides resembled known epitopes in the IEDB database, but similarity to other Cas9 orthologs and other bacterial proteins was detected (Supplementary Tables 2.4 and 2.5). Epitope β has sequence similarity to a peptide derived from the *Neisseria meningitidis* peptide chain release factor 2 protein (ILEDIVLTL versus ILEGIVLTL). Antigen-specific T cells were expanded for 18 days *in vitro* by coculturing healthy donor PBMCs with peptide β -pulsed autologous antigen presenting cells (APCs). Cas9-specific CD8⁺ T cell responses were assessed by flow cytometry. CD8⁺ T cells specific for the HLA-A*0201/ β pentamer were detected after stimulation (3.09%; Figure 2.2-A).

2.3.4. Mutated Cas9 proteins have lower immune recognition and maintain their function and specificity

We next hypothesized that mutation of the MHC-binding anchor residues of the identified immunogenic epitopes would abolish specific T cell recognition (Figure 2.2-A). The epitope anchor residues (2nd and 9th) are not only necessary for peptide binding to the MHC groove, but are also crucial for recognition by the T cell receptor ³². The percentage of CD8⁺ β pentamer⁺ T cells decreased to 0.3% when APCs were pulsed with the mutated peptide (β 2; Figure 2.2-B) compared with 3.09% with the wild type peptide (β ; Figure 2.2-A).

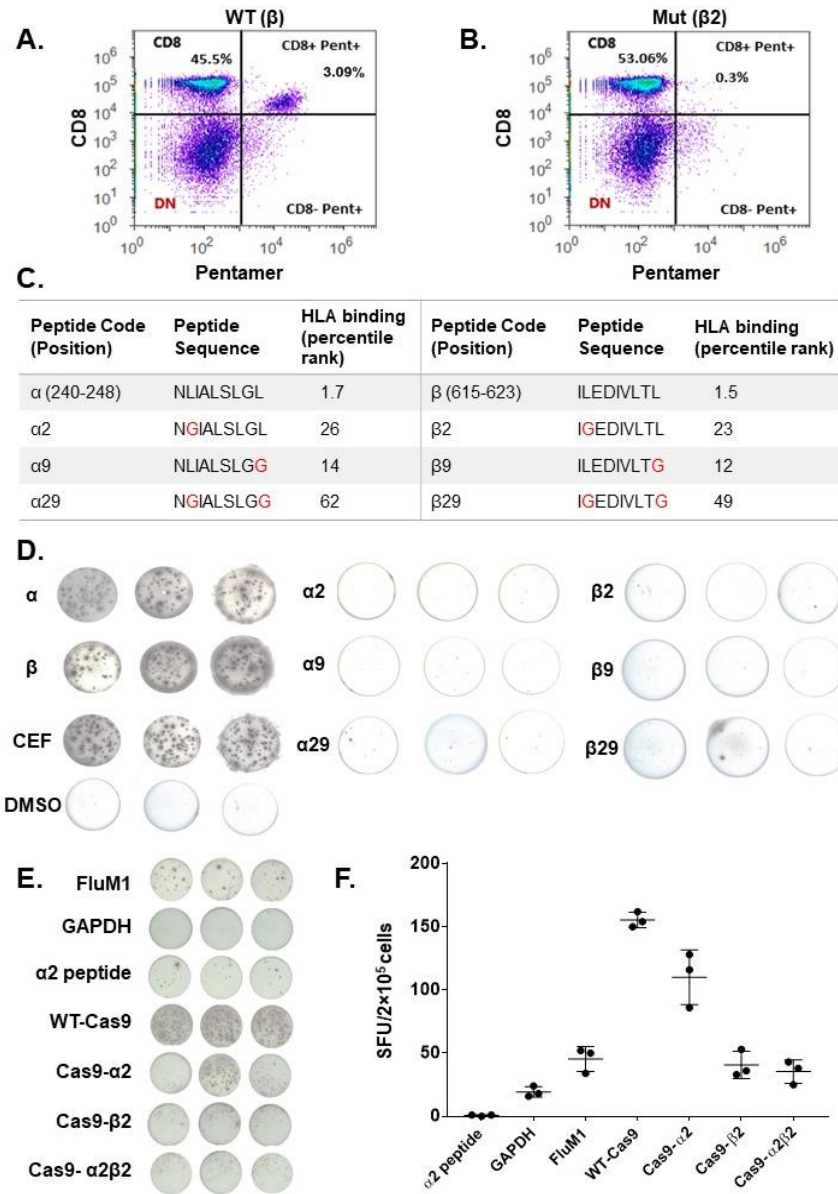


Figure 2.2. SpCas9 immunodominant epitope specific CD8⁺ T cell recognition is abolished after anchor residue mutation. **A.** Epitope β -specific CD8⁺ T cell response detected using β -specific pentamer in PBMCs stimulated with peptide β -pulsed antigen presenting cells. **B.** The percentage of CD8⁺ pentamer β ⁺ T cells was reduced to 0.3% when healthy donor B cell APCs were pulsed with the mutated peptide β 2. **C.** Positions, sequences and IEDB HLA binding percentile rank of epitopes α and β before and after

mutation of the anchor (2nd and/or 9th) residues. S_b , normalized binding score; S_i , normalized immunogenicity score. **D.** Representative IFN- γ ELISpot assay in triplicate wells comparing T cell reactivity to wild type or mutated epitopes α and β . These results are representative of 12 donors and two independent replicates (data from all 12 donors are shown in Supplementary Figure 2.2). **E, F.** IFN- γ ELISpot comparing T cell reactivity to APCs expressing WT or modified Cas9 proteins. APCs expressing FluM1 were used as a positive control. APCs expressing GAPDH or spiked with peptide $\alpha 2$ were used as negative controls. Data represent mean \pm SEM of 5 replicates (right). Statistical analysis was performed post hoc and results are exploratory.

We then examined the reactivity of healthy donor T cells to modified peptides α or β with mutations in residues 2, 9, or both (sequences are shown in Figure 2.2-C) using IFN- γ ELISpot assay. The epitope-specific T cell reactivity was markedly reduced with the mutant peptides (Supplementary Figure 2.2; representative ELISPOT well images are shown in Figure 2.2-D). The average reduction for the responsive HLA-A*02:01 donors was 25-fold from α to $\alpha 29$ (n=7; p<0.03) and 30-fold from β to $\beta 29$ (n=8; p<0.03; Benjamini-Hochberg; Supplementary Figure 2.2; Supplementary Table 2.6). The predicted binding affinity to MHC class II was also decreased for $\alpha 2$ and $\beta 2$ epitopes, although the experimental significance of this alteration is unknown.

We then generated modified Cas9 constructs by mutating the second residue of peptide α (L241G; Cas9- $\alpha 2$), peptide β (L616G; Cas9- $\beta 2$), or both (Cas9- $\alpha 2\beta 2$). To measure the effect of mutating the anchor residue of the immunogenic epitopes on T cell recognition of the Cas9 protein, we transiently transfected healthy donor B cell APCs with mRNA encoding wild type Cas9 (WT-Cas9), Cas9- $\alpha 2$, Cas9- $\beta 2$, or Cas9- $\alpha 2\beta 2$. The

T cell response measured by IFN- γ ELISpot after coculturing of Cas9 transfected APCs with autologous PBMCs was significantly decreased for the modified Cas9 proteins (Figure 2.2-E and F). Introduction of the β 2 mutation was the most effective in reducing T cell immunogenicity (5.5-fold, $p < 0.0001$, two-tailed t-test). This mutation in the REC1 domain (Figure 2.1E and 2.3A) is not located in any of the two regions that are absolutely essential for DNA cleavage, the repeat-interacting (97–150) and the anti-repeat-interacting (312–409) regions³³. These results demonstrate that mutating the anchor amino acid of a highly immunogenic epitope can influence the overall immunogenicity of Cas9. Thus, engineering Cas9 variants with reduced immunogenicity potential can be used in conjunction with other strategies for safer CRISPR therapies and even possibly reduce the dosage of systemic immunosuppression needed for patients.

We therefore tested the function of Cas9- β 2 in comparison with WT-Cas9 in the context of DNA cleavage and transcriptional modulation. To examine the nuclease activity of Cas9- β 2 and compare with WT-Cas9, we targeted Cas9- β 2 or WT-Cas9 to an endogenous locus (*EMX-1*) and measured percent indel formation (Figure 2.3-B and C). Our data demonstrate that Cas9- β 2 retains nuclease capacity in the locus we studied as well as on a synthetic promoter (Figure 2.3-C, Supplementary Figure 2.3-A and B).

Next, we determined whether Cas9- β 2 can successfully recognize and bind its target DNA leading to transcriptional modulation. We first tested this in the context of enhanced transgene expression from a synthetic CRISPR responsive promoter in HEK293 cells using 14nt gRNAs and aptamer-mediated recruitment of transcriptional modulators similar to what we had shown before (Supplementary Figure 2.3-C and D).

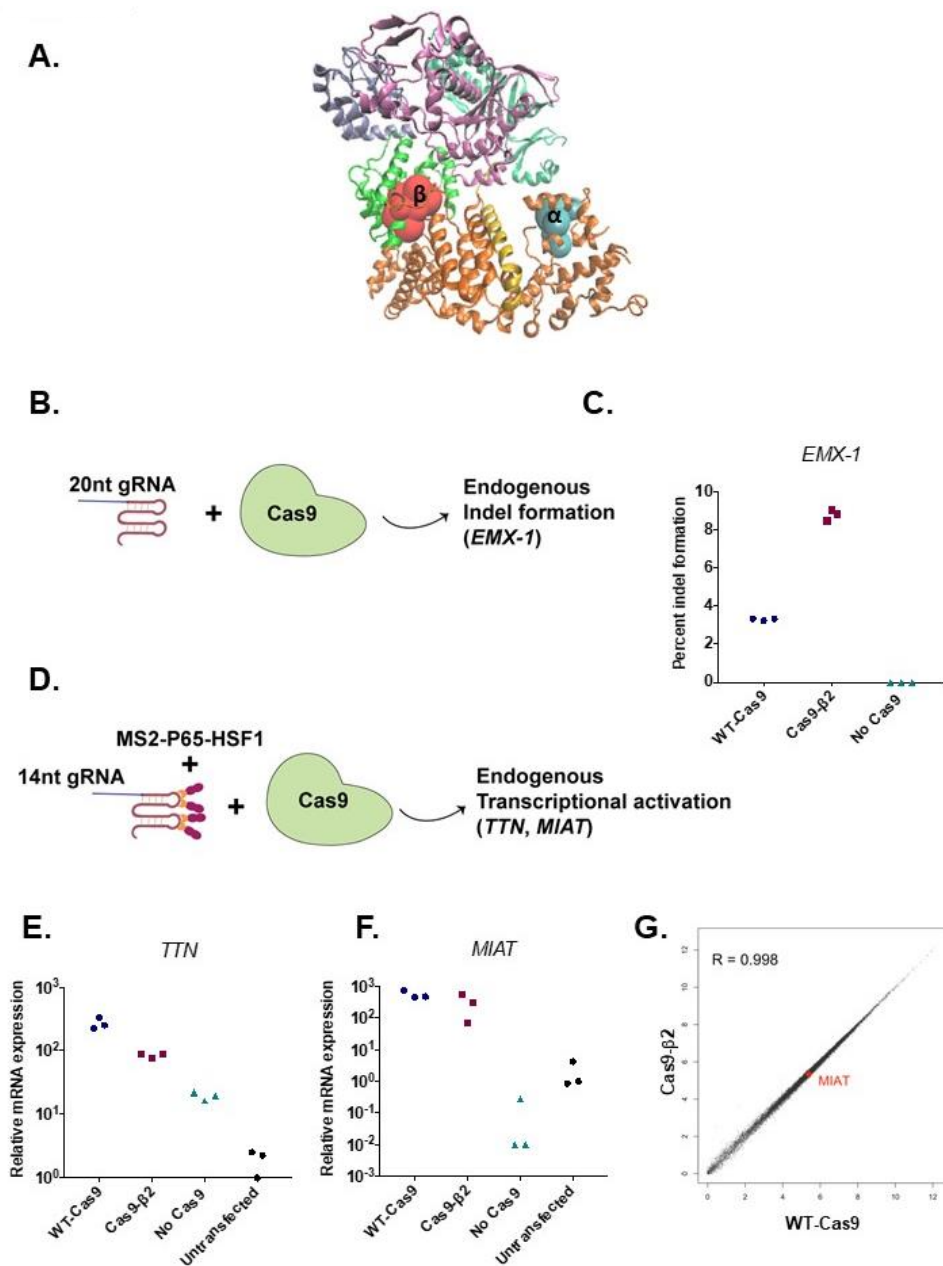


Figure 2.3. Mutated SpCas9 protein (Cas9- β 2) retains its function and specificity. **A.** 3D structure of the SpCas9 protein, showing the location of the identified immunodominant epitopes α and β . **B.** Schematic of the experiment assessing mutagenesis capacity of Cas9- β 2. Cells were transfected with either WT-Cas9, Cas9- β 2, or an empty plasmid as well as 20nt gRNA targeting *EMX-1* locus. 72 hrs after

transfection, percent cleavage was assessed by DNA extraction and illumina sequencing. **C.** Percentage of indel formation in *EMX-1* locus. Data represent mean +/-SD of three individual transfections. **D.** Schematic of the experiment assessing gRNA binding, DNA targeting and transcriptional modulation with Cas9- β 2. Cells were transfected with either WT-Cas9, Cas9- β 2, or an empty plasmid as well as 14nt gRNA targeting *TTN* or *MIAT* in the presence of MS2-P65-HSF1 (transcriptional modulation). 72 hrs after transfection, mRNA was assessed by qRT-PCR. **E** and **F.** Shown is the mRNA level relative to an untransfected control experiment (n=3 independent technical replicaes). **G.** Mean expression levels of 24,078 protein-coding and non-coding RNA genes for WT-Cas9 and Cas9- β 2 (each in duplicate) are shown. For visualization purposes, the values were transformed to a $\log_2(\text{CPM}+1)$ scale. *MIAT*, the gRNA target gene, is highlighted in red, and R denotes Pearson correlation coefficient between two groups.

Having shown successful transgene activation, we then investigated whether this variant retains such capacity within the chromosomal contexts of endogenous genes. We transfected the cells with plasmids encoding Cas9- β 2 or WT-Cas9 and 14nt gRNAs against two different endogenous genes (*TTN* and *MIAT*). qRT-PCR analysis showed that this variant successfully led to target gene expression (Figure 2.3-D and F). To further characterize Cas9- β 2 specificity, we performed genome-wide RNA sequencing after targeting Cas9- β 2 or WT-Cas9 to the *MIAT* locus for transcriptional activation. The results demonstrated no significant increase in undesired off-target activity by Cas9- β 2 as compared to WT-Cas9 (Figure 2.3-G).

To show the extensibility of our approach, we tested the function of Cas9- α 2, that has a mutation located in the REC2 domain (Figure 2.1-E and 2.3-A). Cas9- α 2 also

demonstrated DNA cleavage and transcriptional modulation functionality comparable with WT-Cas9 (Supplementary Figure 2.4 A to E). This is consistent with a previous study which showed that Cas9 with a deleted REC2 domain retains its nuclease activity³³. When T cells were stimulated with APCs spiked with peptide $\alpha 2$, the percentage of CD8⁺ CD137⁺ T cells (a marker of T cell activation³⁵) was decreased by 2.3-fold as compared to WT peptide α stimulation (Supplementary Figure 2.4-F).

2.3.5. Immune responses to non-HLA-A*02:01 Cas9 epitopes

We next predicted T cell epitopes derived from SpCas9 for non-HLA-A*02:01 alleles using the IEDB analysis tool. We selected and synthesized 5-6 epitopes (sequences shown in Supplementary Table 2.7) for each of 7 common alleles (A*01:01, A*03:01, A*11:01, A*24:02, B*08:01, B*44:01, B*55:01) and used them to stimulate PBMCs derived from 6 healthy donors with the corresponding HLA alleles. Of the peptides and alleles screened, we detected peptide-specific T cell immune response (in more than one donor) against peptide 25 in two HLA-A*24:02 donors ($p < 0.05$; results for HLA-A*24:02 are shown as an example in Figure 2.4-A).

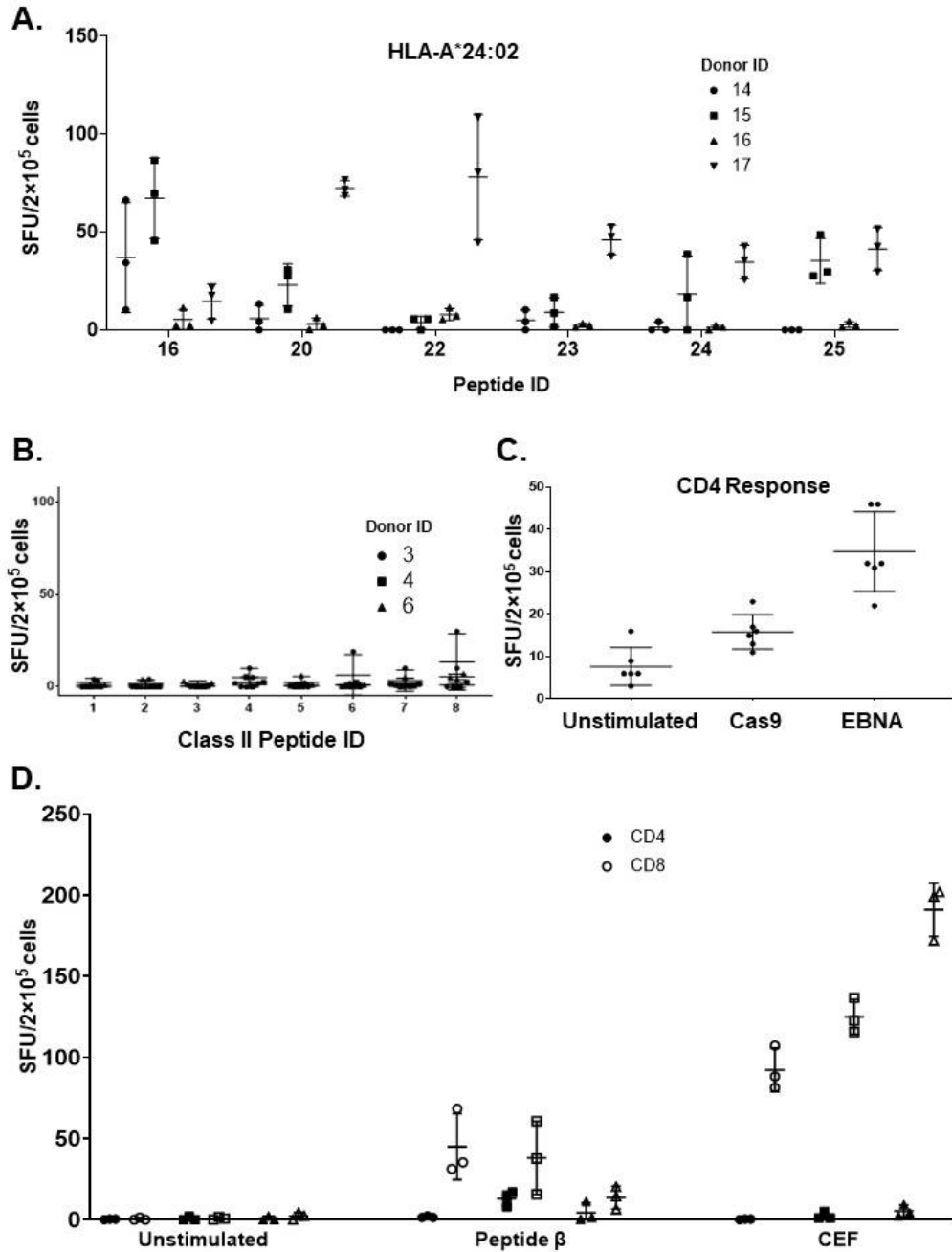


Figure 2.4. Immune responses to non-HLA-A*02:01 and class II epitopes of SpCas9. **A.** Representative IFN- γ ELISpot reactivity of healthy donor T cells to non-HLA-A*02:01 SpCas9 class I epitopes (HLA-A*024:02 is shown as an example). **B.** IFN- γ ELISpot reactivity of healthy donor MACS-sorted CD4⁺ T cells to SpCas9 long peptides that include epitopes in the top 2% of predicted MHC class II binders. **C.** IFN- γ ELISpot

reactivity of healthy donor CD8-depleted PBMCs stimulated with recombinant SpCas9 or EBNA proteins for 10 days. **D.** IFN- γ ELISpot reactivity of MACS sorted CD4⁺ (black dots) or CD8⁺ (open dots) T cells isolated from PBMCs from 3 healthy donors unstimulated or stimulated with peptide β or CEF. Data represent mean +/- SD.

2.3.6. Immune responses to MHC Class II Cas9 epitopes

We also predicted MHC class II binding epitopes for the SpCas9 protein to HLA-DRB1 (10 alleles), HLA-DQ (5 alleles), and HLA-DP (8 alleles) using the IEDB analysis tool. For MHC class II, epitope α is predicted to be a top binder to HLA-DRB1*01:02 and epitope β a top binder to HLA-DPA1*01:03 and DPB1*02:01. We selected and synthesized SpCas9 long peptides that include epitopes in the top 2% of predicted MHC class II binders (sequences and alleles shown in Supplementary Table 2.8) and measured peptide-specific CD4⁺ T cell immunity using IFN- γ secretion ELISpot assays with CD8-depleted PBMCs derived from 3 healthy individuals. We detected limited CD4⁺ immune responses against the peptides tested (Figure 2.4-B). This prompted us to evaluate the CD4⁺ T cell immune response against the whole Cas9 protein compared with a positive control protein. We stimulated healthy donor CD8-depleted PBMCs with recombinant SpCas9 or EBNA proteins for 10 days and detected a modest response (less than twofold of that of unstimulated cells; Figure 2.4-C). We then sought to investigate whether the immune response that we detected against peptide β was primarily derived by CD4⁺ or CD8⁺ T lymphocytes. We stimulated MACS sorted CD4⁺ or CD8⁺ T cells isolated from PBMCs from 3 donors with peptide β and detected a primarily CD8⁺ response in all 3 donors (Figure 2.4-D).

2.4. Discussion

The detection of pre-existing B cell and T cell immunity to the most widely used nuclease ortholog of the CRISPR-Cas9 tool in a significant proportion of healthy humans confirms previous studies in mice^{9,10} and a recent study in humans²⁷ and sheds light on the need for more studies of the immunological risks of this system. A recent study reported SpCas9-specific T-cell-mediated killing of autologous CRISPR-treated APCs *in vitro*²⁸. However, the consequences of Cas9-specific immunity *in vivo* remain to be seen. The CD8+ T cell immunity we observed is likely memory responses, as they are observed without *ex vivo* stimulation. However, following 18 days of T cell stimulation by peptides α or β , expansion of naïve T cells is not precluded. This suggests that even in the absence of a pre-existing immune response, the expression of Cas9 in naïve individuals may trigger a T cell response that could prevent subsequent administration. This could be avoided by switching to Cas9 orthologs from other bacterial species, but can be difficult given the epitope conservation across Cas9 proteins from multiple *Streptococcus* species and resemblance to sequences from other bacterial proteins such as the common pathogen *N. meningitidis*, that asymptotically colonizes the nasopharynx in 10% of the population³⁶. Therefore, selective deimmunization (immune-silencing) of Cas9 can represent an attractive alternative, particularly in patients where high-dose systemic immune-suppression is contraindicated, such as in patients with chronic infectious diseases. This strategy can be important in particular when longer term expression of Cas9 will be desired.

Using IFN- γ ELISpot, we detected a modest CD4⁺ immune response against recombinant SpCas9 protein and no response to any of the class II SpCas9 peptides that

we used. This is consistent with a recent study that found the majority of the CD4⁺ response against SpCas9 to be restricted to the Treg compartment with minimum IFN- γ and TNF- α secretion²⁸. While a more comprehensive epitope mapping study is needed, we did not experimentally detect immunodominant epitopes among the top binders of the non-HLA-A*02:01 alleles. We show here that silencing one epitope for an HLA-A*02:01 donor (who was also positive for A*11:01, B*39:01, and B*46:01) was sufficient to significantly reduce the Cas9 immunogenicity. However, whether other mutations need to be introduced to the protein for complete silencing in HLA-A*02:01 negative individuals, needs further investigation. Conventional methods of deimmunizing non-human therapeutic proteins rely on trial-and-error mutagenesis or machine learning and often includes deletion of whole regions of the protein³⁷⁻⁴¹. Here, as a general principle, we show that alteration of one of the anchor residues of an immunodominant epitope abolished specific T cell recognition. However, HLA allotype diversity and the existence of numerous epitopes in the large Cas9 protein may complicate the process of complete deimmunization. The overall impact of removal of select immunodominant epitopes remains to be seen; both reduction⁴² and enhancement⁴³ of the immunogenicity of subdominant epitopes have been reported with similar approaches for other proteins.

The top binding T cell epitopes within Cas9 that are most promiscuous for common HLA class I and class II alleles have been recently predicted *in silico* using IEDB⁴⁴. However, this is the first study that experimentally validates predicted immunodominant epitopes. None of the HLA-A*02:01 epitopes that we report overlap with the peptides previously predicted⁴⁴. This is not surprising since our prediction model is optimized for HLA-A*02:01. Thus, improved algorithms are needed to predict epitopes that hold up in

experimental validation, as we show here. The use of CRISPR-Cas9 in humans may eventually necessitate creating HLA type-specific Cas9 variants, particularly for applications that require long-term Cas9 expression.

Non-specific localized immune suppressive approaches, such as those used by tumor cells and some viruses may complement these strategies for complete deimmunization. Antigen presentation can be blocked by viral proteins interfering with antigen presentation (VIPRs), such as the adenoviral E319K or US2 and US11 from the human cytomegalovirus⁴⁵ or molecules that inhibit proteasomal antigen processing such as the Epstein-Barr virus Gly-Ala repeat⁴⁶. Deimmunized Cas9 may be useful in reduction of the dosage of other immunomodulatory measures needed to be co-administered in patients, thus facilitating therapeutic CRISPR applications as we develop better understanding of the immunological consequences of this system.

Conventional methods of deimmunizing non-human therapeutic proteins rely on trial-and-error mutagenesis, machine learning, and often includes deletion of whole regions of the protein. Here, as a general principle, we show that alteration of one of the anchor residues of an immunodominant epitope abolished specific T cell recognition. However, HLA allotype diversity and the existence of numerous epitopes in the large Cas9 protein complicate the process of complete deimmunization. The overall impact of removal of select immunodominant epitopes remains to be seen; similar approaches for other proteins have resulted in reduction and enhancement of the immunogenicity of subdominant epitopes. Non-specific immune suppressive approaches may complement these strategies for complete deimmunization. One attractive strategy is the co-expression of Cas9 with gRNAs targeting immune modulatory molecules such as programmed

death-ligand 1 (PD-L1) or Indoleamine 2,3-Dioxygenase 1 (IDO1) to further boost immune-silencing. We anticipate that deimmunized Cas9 will be useful for therapeutic CRISPR applications

References

- 1 Cyranoski, D. Chinese scientists to pioneer first human CRISPR trial. *Nature News* **535**, 476, (2016).
- 2 Reardon, S. First CRISPR clinical trial gets green light from US panel. *Nature* **531**, (2016).
- 3 Cavazzana-Calvo, M. *et al.* Gene therapy of human severe combined immunodeficiency (SCID)-X1 disease. *Science* **288**, 669-672, (2000).
- 4 Gaspar, H. B. *et al.* Gene therapy of X-linked severe combined immunodeficiency by use of a pseudotyped gammaretroviral vector. *Lancet* **364**, 2181-2187, (2004).
- 5 Howe, S. J. *et al.* Insertional mutagenesis combined with acquired somatic mutations causes leukemogenesis following gene therapy of SCID-X1 patients. *J Clin Invest* **118**, 3143-3150, (2008).
- 6 Marshall, E. Gene Therapy Death Prompts Review of Adenovirus Vector. *Science* **286**, 2244-2245, (1999).
- 7 Hacein-Bey-Abina, S. *et al.* Sustained correction of X-linked severe combined immunodeficiency by ex vivo gene therapy. *N Engl J Med* **346**, 1185-1193, (2002).
- 8 Manno, C. S. *et al.* Successful transduction of liver in hemophilia by AAV-Factor IX and limitations imposed by the host immune response. *Nat Med* **12**, 342-347, (2006).

- 9 Chew, W. L. *et al.* A multifunctional AAV-CRISPR-Cas9 and its host response. *Nat Methods* **13**, 868-874, (2016).
- 10 Wang, D. *et al.* Adenovirus-Mediated Somatic Genome Editing of Pten by CRISPR/Cas9 in Mouse Liver in Spite of Cas9-Specific Immune Responses. *Hum Gene Ther* **26**, 432-442, (2015).
- 11 Mays, L. E. & Wilson, J. M. The complex and evolving story of T cell activation to AAV vector-encoded transgene products. *Mol Ther* **19**, 16-27, (2011).
- 12 Mingozzi, F. & High, K. A. Immune responses to AAV vectors: overcoming barriers to successful gene therapy. *Blood* **122**, 23-36, (2013).
- 13 Yin, H. *et al.* Non-viral vectors for gene-based therapy. *Nat Rev Genet* **15**, 541-555, (2014).
- 14 Ahi, Y. S., Bangari, D. S. & Mittal, S. K. Adenoviral Vector Immunity: Its Implications and circumvention strategies. *Current gene therapy* **11**, 307-320, (2011).
- 15 Aldhamen, Y. A. & Amalfitano, A. in *Adenoviral Vectors for Gene Therapy (Second Edition)* 391-422 (Academic Press, 2016).
- 16 Thwaite, R., Pages, G., Chillon, M. & Bosch, A. AAVrh.10 immunogenicity in mice and humans. Relevance of antibody cross-reactivity in human gene therapy. *Gene Ther* **22**, 196-201, (2015).
- 17 Boutin, S. *et al.* Prevalence of serum IgG and neutralizing factors against adeno-associated virus (AAV) types 1, 2, 5, 6, 8, and 9 in the healthy population: implications for gene therapy using AAV vectors. *Hum Gene Ther* **21**, 704-712, (2010).

- 18 Mingozzi, F. *et al.* CD8(+) T-cell responses to adeno-associated virus capsid in humans. *Nat Med* **13**, 419-422, (2007).
- 19 Scallan, C. D. *et al.* Human immunoglobulin inhibits liver transduction by AAV vectors at low AAV2 neutralizing titers in SCID mice. *Blood* **107**, 1810-1817, (2006).
- 20 Bartel, M., Schaffer, D. & Buning, H. Enhancing the Clinical Potential of AAV Vectors by Capsid Engineering to Evade Pre-Existing Immunity. *Front Microbiol* **2**, 204, (2011).
- 21 Martino, A. T. *et al.* Engineered AAV vector minimizes in vivo targeting of transduced hepatocytes by capsid-specific CD8+ T cells. *Blood* **121**, 2224-2233, (2013).
- 22 Mingozzi, F. *et al.* Overcoming preexisting humoral immunity to AAV using capsid decoys. *Sci Transl Med* **5**, 194ra192, (2013).
- 23 Jiang, H. *et al.* Effects of transient immunosuppression on adenoassociated, virus-mediated, liver-directed gene transfer in rhesus macaques and implications for human gene therapy. *Blood* **108**, 3321-3328, (2006).
- 24 Kay, M. A. State-of-the-art gene-based therapies: the road ahead. *Nat Rev Genet* **12**, 316-328, (2011).
- 25 Gao, G. *et al.* Adeno-associated virus-mediated gene transfer to nonhuman primate liver can elicit destructive transgene-specific T cell responses. *Hum Gene Ther* **20**, 930-942, (2009).
- 26 Carapetis, J. R., Steer, A. C., Mulholland, E. K. & Weber, M. The global burden of group A streptococcal diseases. *Lancet Infect Dis* **5**, 685-694, (2005).

- 27 Simhadri, V. L. *et al.* Prevalence of Pre-existing Antibodies to CRISPR-Associated Nuclease Cas9 in the USA Population. *Molecular therapy. Methods & clinical development* **10**, 105-112, (2018).
- 28 Wagner, D. L. *et al.* High prevalence of Streptococcus pyogenes Cas9-reactive T cells within the adult human population. *Nature Medicine*, (2018).
- 29 Ibrahim, S. H. & Robertson, K. D. Use of the CRISPR/Cas9-Based Epigenetic Gene Activation System in Vivo: a New Potential Therapeutic Modality. *Hepatology*, (2018).
- 30 Liao, H. K. *et al.* In Vivo Target Gene Activation via CRISPR/Cas9-Mediated Trans-epigenetic Modulation. *Cell* **171**, 1495-1507 e1415, (2017).
- 31 Zheng, Y. *et al.* CRISPR interference-based specific and efficient gene inactivation in the brain. *Nat Neurosci* **21**, 447-454, (2018).
- 32 Chowell, D. *et al.* TCR contact residue hydrophobicity is a hallmark of immunogenic CD8+ T cell epitopes. *Proc Natl Acad Sci U S A* **112**, E1754-1762, (2015).
- 33 Nishimasu, H. *et al.* Crystal Structure of Cas9 in Complex with Guide RNA and Target DNA. *Cell* **156**, 935-949, (2014).
- 34 Vita, R. *et al.* The immune epitope database (IEDB) 3.0. *Nucleic Acids Res* **43**, D405-412, (2015).
- 35 Wolf, M. *et al.* Activation-induced expression of CD137 permits detection, isolation, and expansion of the full repertoire of CD8+ T cells responding to antigen without requiring knowledge of epitope specificities. *Blood* **110**, 201-210, (2007).
- 36 Pollard, A. J. & Maiden, M. C. J. *Meningococcal Vaccines*. (Humana Press, 2001).

- 37 King, C. *et al.* Removing T-cell epitopes with computational protein design. *Proc Natl Acad Sci U S A* **111**, 8577-8582, (2014).
- 38 Mazor, R. *et al.* Rational design of low immunogenic anti CD25 recombinant immunotoxin for T cell malignancies by elimination of T cell epitopes in PE38. *Cell Immunol* **313**, 59-66, (2017).
- 39 Salvat, R. S. *et al.* Computationally optimized deimmunization libraries yield highly mutated enzymes with low immunogenicity and enhanced activity. *Proc Natl Acad Sci U S A* **114**, E5085-E5093, (2017).
- 40 Cantor, J. R. *et al.* Therapeutic enzyme deimmunization by combinatorial T-cell epitope removal using neutral drift. *Proc Natl Acad Sci U S A* **108**, 1272-1277, (2011).
- 41 Tangri, S. *et al.* Rationally engineered therapeutic proteins with reduced immunogenicity. *J Immunol* **174**, 3187-3196, (2005).
- 42 Yeung, V. P. *et al.* Elimination of an Immunodominant CD4⁺ T Cell Epitope in Human IFN- β Does Not Result in an In Vivo Response Directed at the Subdominant Epitope. *The Journal of Immunology* **172**, 6658-6665, (2004).
- 43 Mok, H., Lee, S., Wright, D. W. & Crowe, J. E. Enhancement of the CD8⁺ T cell response to a subdominant epitope of respiratory syncytial virus by deletion of an immunodominant epitope. *Vaccine* **26**, 4775-4782, (2008).
- 44 Chew, W. L. Immunity to CRISPR Cas9 and Cas12a therapeutics. *Wiley Interdiscip Rev Syst Biol Med* **10**, (2018).
- 45 Yewdell, J. W. & Hill, A. B. Viral interference with antigen presentation. *Nature Immunology* **3**, 1019, (2002).

- 46 Levitskaya, J. *et al.* Inhibition of antigen processing by the internal repeat region of the Epstein-Barr virus nuclear antigen-1. *Nature* **375**, 685-688, (1995).
- 47 Anderson, K. S. *et al.* HPV16 antibodies as risk factors for oropharyngeal cancer and their association with tumor HPV and smoking status. *Oral oncology* **51**, 662-667, (2015).
- 48 Wang, J. *et al.* A versatile protein microarray platform enabling antibody profiling against denatured proteins. *Proteomics Clin Appl* **7**, 378-383, (2013).
- 49 Moutaftsi, M. *et al.* A consensus epitope prediction approach identifies the breadth of murine TCD8⁺-cell responses to vaccinia virus. *Nature biotechnology* **24**, 817, (2006).
- 50 Hoof, I. *et al.* NetMHCpan, a method for MHC class I binding prediction beyond humans. *Immunogenetics* **61**, 1, (2009).
- 51 Rammensee, H.-G., Bachmann, J., Emmerich, N. P. N., Bachor, O. A. & Stevanović, S. SYFPEITHI: database for MHC ligands and peptide motifs. *Immunogenetics* **50**, 213-219, (1999).
- 52 Tenzer, S. *et al.* Modeling the MHC class I pathway by combining predictions of proteasomal cleavage, TAP transport and MHC class I binding. *Cellular and Molecular Life Sciences* **62**, 1025-1037, (2005).
- 53 Humphrey, W., Dalke, A. & Schulten, K. VMD: Visual molecular dynamics. *Journal of Molecular Graphics* **14**, 33-38, (1996).
- 54 Dobin, A. *et al.* STAR: ultrafast universal RNA-seq aligner. *Bioinformatics* **29**, 15-21, (2013).

- 55 Trapnell, C. *et al.* Differential gene and transcript expression analysis of RNA-seq experiments with TopHat and Cufflinks. *Nature Protocols* **7**, 562-578, (2012).
- 56 Robinson, M. D., McCarthy, D. J. & Smyth, G. K. edgeR: a Bioconductor package for differential expression analysis of digital gene expression data. *Bioinformatics* **26**, 139-140, (2010).

CHAPTER 3
SYNTHETIC IMMUNOMODULATION WITH A
CRISPR SUPER-REPRESSOR *IN VIVO*

3.1. Introduction

Recent repurposing of the Clustered Regularly Interspaced Short Palindromic Repeats (CRISPR) system for transcriptional modulation is now opening a myriad of therapeutic opportunities at the level of transcription, which was once considered as “undruggable”. Transcriptional control over genes involved in immunity can generate a universal therapeutic modality for a broad range of acute or chronic inflammatory conditions in humans as well infectious diseases at the time of pandemics. In addition, such control provides a powerful means for biological discoveries. However, despite the great potential, there have been limited studies that have translated CRISPR transcriptional tools *in vivo*, with far fewer that explore the utility of the system for transcriptional repression¹⁻⁹. Prior CRISPR-based transcriptional repressors *in vivo* operated based on catalytically “dead” Cas9 protein (dCas9) fused to Kruppel-associated box domain (KRAB) domain, the current gold standard for dCas9-based repression studies¹⁰⁻¹⁷. But yet it is not entirely clear where a KRAB-based *in vivo* repressor stands in comparison with recently reported “enhanced” CRISPR repressors¹⁸.

Additionally, a useful genetic engineering platform should employ both transcriptional control and gene editing on demand to allow a high level of control at both the DNA and RNA level (e.g. to simultaneously modulate immune responses), a goal achievable through changing the length of guide RNAs (gRNAs) from the 5’ end when

using Cas9 nuclease¹⁹. Yet, it is not known if truncated gRNAs can provide effective means for synthetic repression of transcription *in vivo*, giving rise to physiologically relevant phenotypes.

Here, we set out to determine whether we can achieve synthetic immunomodulation *in vivo* using a CRISPR-based enhanced transcriptional repressor. Myeloid differentiation primary response 88 (MyD88) is a key node in innate and adaptive immune responses, acting as an essential adaptor molecule for a number of signaling pathways including Toll-like receptor (TLR), response to septicemia, and formation of adaptive immunity against viruses such as Adeno-associated virus (AAV)²⁰⁻²³. *MYD88* activating mutations are implicated in a number of lymphoid malignancies, in particular Waldenström macroglobulinemia and activated B-cell diffuse large B-cell lymphomas²⁴. However, it is not clear whether we can achieve control over its transcription *in vivo*. Given the central role of MyD88 signaling in innate and adaptive immunity²¹ we sought to examine synthetic transcriptional modulation over this locus *in vivo*.

3.2. Materials and methods

3.2.1. Vector Design and Construction

MS2 Fusion constructs: To construct the MS2-fused transcriptional repressors, the specific domains of interest were amplified from vectors previously published in our group and subsequently cloned into the pcDNA3-MS2-VP64 backbone (Addgene plasmid ID: 79371). The pcDNA3-MS2-VP64 vector was digested with NotI and AgeI to remove the VP64 domain and then the amplified repressors were cloned into this backbone via the Gibson Assembly method. All the repressor sequences are listed in in supplementary information note

U6-gRNA-MS2 plasmids: To generate these plasmids, 14bp or 20bp guide sequences were inserted into sgRNA-MS2 cloning backbone (Addgene plasmid ID: 61424) at the BbsI site via golden gate-based reaction. All the gRNA sequences are listed in the Table 2 in supplementary information.

AAV vectors: Following cloning of the gRNAs into a U6-sgRNA-MS2 backbone, the U6-gRNA encoding region was amplified from this vector and inserted within gateway entry vectors using golden gate reaction. Using the same method, the repressor or activator domain and a truncated human EF1a promoter (Gift from Dr. Noah Davidsohn, Dr. Church lab) were cloned into gateway entry vectors. Further sub-cloning of all these components into AAV backbone via gateway reaction (Invitrogen) generated final AAV vectors. Cas9 plasmids were purchased from Addgene (AAV-CMVc-Cas9 #106431 and pAAV-RSV-SpCas9 #85450).

3.2.2. AAV packaging and purification

AAV vectors were digested by SmaI digest to test the integrity of ITR regions before virus production. Verified AAV vectors were used to generate AAV2/1-Myd88, AAV2/1 MockgRNA and AAV2/1 GFP and AAV2/9-Pcsk9 by PackGene® Biotech, LLC. The virus titers were quantified via Real-time SYBR Green PCR at 1.5E+13 GC/ml against standard curves using linearized parental AAV vectors.

3.2.3. Cell culture

HEK293FT and Neuro-2a cell lines (purchased from ATCC) were maintained in Dulbecco's modified Eagle's medium (DMEM - Life Technologies) with 10% fetal

bovine serum (FBS - Life Technologies), 2mM glutamine, 1.0 mM sodium pyruvate (Life Technologies) and 1% streptomycin– penicillin mix (Gibco) in incubators at 37 °C and 5% CO₂.

3.2.4. Transfection of *in vitro* cultured cells

HEK293FT cells were seeded approximately 50,000 cells per well in 24-well plates and transfected the next day. HEK293FT cells were co-transfected with plasmids encoding gRNA (10 ng), dCas9 or dCas9-H1aKRAB (200 ng), MS2-fused repressor (100 ng), puromycin resistant gene (50 ng), and Enhanced Blue Fluorescent Protein (EBFP) as a transfection control (25 ng). Polyethylenimine (PEI) (Polysciences) was used to transfect HEK293FT cells. Transfection complexes were prepared according to manufacturer's instructions. Cells were treated with 0.5ug/ml puromycin (Gibco-life tech) at 24 hours post-transfection. Cells were collected 72 hours post-transfection and total RNA was collected from cells using RNAeasy Plus Mini Kit (Qiagen).

Neuro-2a cells were seeded approximately 50,000 cells per well in 24-well plates and transfected the next day. Cells were co-transfected with plasmids encoding gRNA (10-100 ng), Cas9 nuclease (70 ng), dCas9 or dCas9-H1aKRAB (200 ng), and EBFP as a transfection control (25 ng), and a Puromycin resistance gene (50ng). Plasmids were delivered to Neuro-2a cells with Lipofectamine LTX. Cells were treated with 0.5ug/ml puromycin (Gibco-life tech) at 24 hours post-transfection. For the experiment shown in Figure 1F, 3 days later, cells were treated with LPS at the concentration of 10ug/ml (LPS was added to induce *Myd88* expression) and after 5 hours total RNA was collected from cells using RNEasy Plus Mini Kit (Qiagen).

3.2.5. Quantitative RT-PCR (qRT-PCR) Analysis

Cells or tissues were lysed, and RNA was extracted using RNEasy Plus Mini Kit (Qiagen) or Trizol (Life Technologies) followed by cDNA synthesis using the High-Capacity RNA-to-cDNA Kit (Thermo Fisher). qRT-PCR was performed using SYBR Green PCR Master Mix (Thermo Fisher). All analyses were normalized to 18S rRNA and fold-changes were calculated against No gRNA control groups for *in vitro* transfection experiments and a universal control for *in vivo* experiments ($2^{-\Delta\Delta Ct}$). Universal control is a blood sample collected from an uninjected Cas9 transgenic mouse, which did not receive any AAV injection and was kept as the reference throughout all analyses for comparison of values among different organs. Primer sequences for qPCR are listed in Table 3 in supplementary information.

3.2.6. Plasma analysis

After harvesting mice, plasma samples were aliquoted and stored at -80 °C. Plasma levels of cholesterol were measured via a colorimetric assay according to the manufacturer's instructions (Thermo- Scientific Total Cholesterol Reagents #TR13421). Plasma Pcsk9 protein levels were quantified by ELISA according to the manufacturer's instructions (R&D Systems #MPC900).

3.2.7. ELISA-based chemiluminescent assay

Lung samples were lysed using 1x cell lysis buffer (Cell Signaling) (ratio of 100 mg of tissue to 1 ml of buffer) followed by homogenization and sonication of the lysed tissue. The assay was performed using the Q-Plex™ Mouse Cytokine – Screen (16-Plex) kit

(Quansys Biosciences) following the manufacturer's protocol. Briefly, samples or calibrators were added into wells of a 96 well plate arrayed with analyte specific antibodies that capture GMCSF, IL-1 α , IL-1 β , IL-4, IL-5, IL-6, IL-12p70, IL-17, MCP-1, MIP-1 α , RANTES, and TNF α . Plates were washed and biotinylated analyte specific antibodies were added. After washing, streptavidin-horseradish peroxidase (SHRP) was added. Following an additional wash, the amount of SHRP remaining on each location of the array was measured with the addition of a chemiluminescent substrate.

3.2.8. Antibody ELISA

Anti-AAV antibody assay

Fifty microliters of AAV particles diluted in 1x coating buffer (13 mM sodium carbonate, 35 mM sodium bicarbonate buffer, pH 9.2) containing 2×10^9 per viral particles were added to each well in a Microlon® high protein binding 96-well plate (Greiner) and incubated overnight. Wells were washed three times with 1x Tris Buffered Saline + Tween-20 (TBST, Bethyl) and blocked with 1x Tris Buffered Saline + 1% BSA (Bethyl) for 1 hour at RT. Wells were washed three times with TBST. The standard curve for Figure 2B was generated using purified mouse antibody (Mouse host IgG2a anti-AAV1 (Fitzgerald-MBS830111), Mouse IgG1 unlabeled - Southern Biotech clone 15H6, Mouse IgG2a unlabeled) in twofold dilutions in TBST + 1% BSA + 1:500 negative control mouse plasma, beginning from a concentration of 10,000 ng/ml AAV1 antibody. The standards were added to the plate followed by diluting the plasma samples (samples were diluted 1:500 for Figure 2B and no dilution for Figure 2D and 2F) and incubated for 1 hour at RT. Wells were washed four times with TBST and then goat anti-mouse HRP

antibody was added at a concentration of 1:500 and incubated for 1 hour at RT. Wells were washed four times with wash buffer and TMB substrate was added to the wells. Reactions were terminated by adding 0.18 M H₂SO₄ after development of the standard curve (15 minutes). Finally, absorbance was measured at 450 wavelengths using a plate reader (BioTek). Absorbance results were exported and analyzed in Excel.

Anti SaCas9 antibody assay

Microplates were coated with 50 µl per well at 1 µg/ml Sacas9 protein diluted in 50mM carbonate buffer at pH 9.0. Plates were incubated overnight at 4° C. Wells were washed three times with 1× Tris Buffered Saline + Tween-20 (TBST, Bethyl). Wells were blocked with 200 µl/well of blocking buffer (PBS containing 1% BSA and 0.02% azide) and incubated overnight at 4° C. Wells were washed three times with 1× PBS+0.02% azide. Plasma samples and control were added to the wells at 50 µl/well diluted in blocking buffer and incubated 1 hour at room temperature. Antibodies may be serially diluted for determining titer or diluted to previously determined working concentration for screening assays or antigen quantitation. Wells were washed three times with PBS containing 0.05% Tween-20. Goat anti-mouse HRP antibody was added at a concentration of 1:500 and incubated for 1 hour at RT. Wells were washed. Reactions were terminated by adding 0.18 M H₂SO₄ after 15 minutes. Finally, absorbance was measured at 450 wavelengths using a plate reader (BioTek). Absorbance results were exported and analyzed in Excel.

3.2.9. Lactate assay

Blood samples were collected using EDTA coated tubes. Samples were centrifuged at 1,000 x g for 10 minutes. Plasma was collected and stored at -80°C. Lactate assay was performed following the manufacturer's protocol (L-Lactate Assay Kit, Cayman Chemicals). Briefly, samples were deproteinated by adding 0.5 M MPA. After pelleting the protein, supernatant was added to Potassium Carbonate and centrifuged at 10,000 x g for five minutes at 4° C. Samples were diluted four-fold and added to the designated wells. Next, assay buffer cofactor mixture, Fluorometric Substrate, and Enzyme Mixture were added to each well. Plate was incubated for 20 minutes at RT and the fluorescence was measured using an excitation wavelength of 530-540 nm and an emission wavelength of 585-595 nm. Absorbance results were exported and analyzed in Excel according to the manufacturer's protocol.

3.2.10. Examination of liver injury after LPS injection

Plasma samples were sent to IDEXX Laboratories to measure a panel of tissue injury markers including ALT, Cholesterol, LDL, HDL, BUN, Albumin, LDH, and Lipase.

3.2.11. Animals

All the experiments with animals were approved by the Institutional Animal Care and Use Committee (IACUC) at Arizona State University and have been performed according to institutional guidelines. All the experiments were performed on at least 3 mice of 6-8 weeks old per group. Both male and female were included in experiments. The sample size in each group is indicated in each figure legend.

Both male and female Rosa26-Cas9 knockin mice (JAX Stock number 026179) and male C57BL/6 mice (JAX Stock number: 000664) were used for AAV/CRISPR repression experiments.

3.2.12. Retro-Orbital injections

AAV particles were delivered to mice through retro-orbital injection of the venous sinus. Animals were anesthetized with 3% isoflurane and virus particles were injected to the left eye with 100 microliters of AAV solution (1E+11 to 1E+12 genome copy per mouse).

3.2.13. Tissue harvest

Mice were euthanized via CO₂ inhalation. Tissue samples taken from liver, lung, bone marrow and blood were collected in RLT Plus buffer (Qiagen) and frozen or snap frozen for RNA analysis.

3.2.14. *In vivo* LPS administration

Mice were given intraperitoneal (i.p.) injection of lipopolysaccharides (from *Escherichia coli* 0127:B8 (Sigma-Aldrich, St. Louis, MO, USA) dissolved in phosphate-buffered saline (PBS) at a concentration of 2-5 mg/ml. Mice were euthanized 6-72 hours post LPS injection (timeline is included in schematics) via CO₂ inhalation.

3.2.15. *In vivo* Pepjet administration

Mice received 60 µg of DNA containing 10 µg Cas9 and 50 µg Myd88-HP1aKRAB or Mock-HP1aKRAB via retro-orbital injection. PepJet™ reagent (SignaGen

Laboratories, Catalog #: SL100501) was used for *in vivo* transfection. DNA was mixed with PepJet at the ratio of PepJet™ (μL): DNA (μg) 2:1 and prepared according to the manufacturer's protocol.

3.2.16. RNA Sequencing and Data Analysis

In vitro experiments

N2A cells were co-transfected with 10ng gRNA targeting *Myd88* loci, respectively. 200ng dCas9 constructs, 100ng MS2-HP1aKRAB, 50ng puromycin resistant gene, and 25ng transfection control. Cells were treated with 0.5ug/ml puromycin (Gibco-life tech) at 24 hours post-transfection. Total RNA was extracted 72 hours post transfection using RNeasy Plus Mini Kit (Qiagen) and sent to UCLA TCGB core on dry ice. Ribosomal RNA depletion and paired end read library preparation were performed at UCLA core followed by RNA sequencing using NextSeq500. Coverage was 20 million reads per sample. FASTQ files with pair-ended 75bp reads were then aligned to the mouse GRCm38 reference genome sequence (Ensembl release 90) with STAR, and uniquely mapped read counts (an average of 14.8 million reads per sample) were obtained with Cufflink. The read counts for each sample were then normalized for the library size to CPM (counts per million reads) with edgeR. Custom R scripts were then used to generate plots.

In vivo experiments

RNA was extracted from mice bone marrow samples using RNeasy Plus Mini Kit (Qiagen) followed by globin mRNA depletion using GLOBINclear™ Kit, mouse/rat kit (Thermofisher). None-directional library preparation was performed at Novogene

Corporation Inc. followed by RNA sequencing using Illumina Nova Platform with paired-end 150 run (2×150 bases). Coverage was minimum 25 million reads per sample. FASTQ files were then aligned to mouse genome sequence using STAR software and uniquely mapped read counts were visualized with Integrative Genomics Viewer (IGV). Gene expression level was calculated by the number of mapped reads. According to all gene expression level (RPKM or FPKM) of each sample, correlation coefficient of sample between groups was calculated. Read counts obtained from Gene Expression Analysis were used for differential expression analysis and differential expression analysis of different groups was performed using the DESeq2 R package. Hierarchical clustering analysis was carried out of log₁₀ (FPKM+1) of union differential expression genes, within all comparison groups. ClusterProfiler software was used for enrichment analysis, including GO Enrichment, DO Enrichment, KEGG Enrichment and Reactome Enrichment.

3.2.17. Statistical analysis

All *in vitro* experiments shown were done in triplicates with similar results obtained. All *in vivo* experiments were repeated in at least three biological replicates with similar results obtained. Mice were randomly allocated to control or experimental conditions. Experimenters were not blinded to conditions during data collection or analyses. Statistical analyses are included in the figure legends. Data are presented as the mean + SEM. N = number of individual transfections for *in vitro* experiments and N = number of animals for *in vivo* experiments. Statistical analyses were performed using GraphPad Software (GraphPad) using the non-parametric one-tailed Mann-Whitney U test. p value

≤ 0.05 was considered significant (* $p \leq 0.05$, ** $p \leq 0.01$, *** $p \leq 0.001$, **** $p \leq 0.0001$).

3.3. Results

3.3.1. CRISPR-mediated repression with MS2-Hp1aKRAB is superior to MS2-KRAB *in vitro*

We previously reported “enhanced” CRISPR-based transcriptional repressors *in vitro* developed by direct fusion of a set of modulators to catalytically dead Cas9 protein (MeCP2, MBD2 or HP1a)¹⁸. We first devised an experiment to determine which transcriptional repression domain from our previously published candidates can lead to efficient transcriptional repression when fused to the MS2 coat protein (referred here to as MS2) and recruited to the CRISPR complex by gRNA aptamer binding (Fig. 1A)¹⁸. Quantitative real time polymerase chain reaction (qRT-PCR) analysis of a set of target genes in Human Embryonic Kidney 293 (HEK293FT) cells established that MS2-HP1aKRAB [heterochromatin protein 1 (HP1a)- Krüppel associated box (KRAB)] enabled efficient repression across the genes we tested (Fig. 1B).

To translate these findings *in vivo*, we set out to utilize nuclease competent *Streptococcus Pyogenes* (Sp) -Cas9 transgenic mice as they enable us to eliminate potential confounding effects associated with delivery of Cas9. Therefore, we devised a pair of truncated gRNAs that target Cas9 nuclease and MS2-HP1aKRAB to the *Myd88* promoter (Fig. 1C). This strategy allows Cas9 nuclease to be repurposed to a nuclease null protein for transcriptional repression¹⁹. We first compared the functionality of the truncated gRNA compared to the full-length gRNA in Mouse neuroblastoma (N2A) cells (Fig. 1C). RNA sequencing showed that transcriptional repression using truncated gRNA

is as efficient and specific as traditional 20nt gRNA-based repression *in vitro* (Fig. 1D-E). Moreover, this strategy yielded similar efficiency in repressing the *Myd88* locus as when a dCas9-Hp1aKRAB fusion protein is used with comparable levels of dCas9 and Hp1aKRAB (Extended Data Fig. 1A-B). Next, we set out to examine MS2-HP1aKRAB-mediated repression of endogenous mouse *Myd88* levels *in vitro* and compared the efficiency with commonly used KRAB-based transcriptional repression. We used a previously reported non-targeting mock gRNA as a control²⁵. qRT-PCR for *Myd88* demonstrated the *in vitro* functionality of the gRNAs and superiority of MS2-HP1aKRAB in repression of endogenous *Myd88* (Fig. 1F).

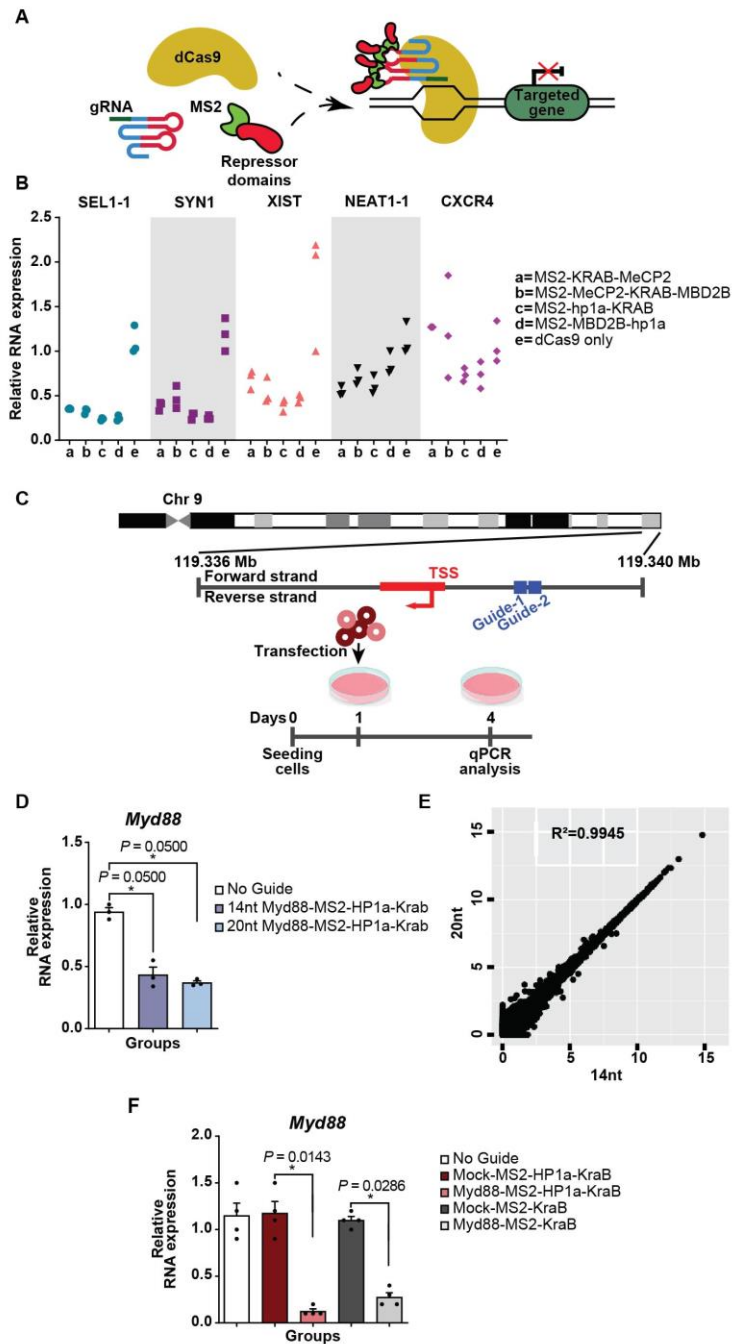


Figure 3.1. Aptamer-mediated CRISPR repression *in vitro*. (A) Schematic of aptamer-mediated recruitment of repressor domains to CRISPR complex. (B) mRNA expression of targeted genes following aptamer-mediated recruitment of repressor

domains to CRISPR complex in HEK293FT cells. Fold changes were quantified relative to dCas9 only control group (N=3 biologically independent samples). (C) Top: Schematic representation of the gRNA binding sites targeted to the promoter of *Myd88*; Bottom: Schematic of experiment design. Mouse neuroblastoma (N2A) cells were transfected with either 14 nucleotide or 20 nucleotide *Myd88* gRNA pairs together with dCas9 plasmid and MS2-HP1aKRAB cassette. Expression levels of *Myd88* mRNA were analyzed using qRT-PCR three days post transfection. (D) Fold changes of mRNA of *Myd88* were quantified relative to the No Guide group (N = 3 biologically independent samples). The bars represent the mean + S.E.M. (E) Mean expression levels of 24476 protein-coding and 16648 non-coding RNA genes following targeting *Myd88* gene are shown. For visualization purposes, the values were transformed to a $\log_2(\text{TPM}+1)$ scale. R denotes the Pearson correlation coefficient between two groups (N = 3 biologically independent samples). The bars represent the mean + S.E.M. (F) qRT-PCR analysis of *Myd88* mRNA expression levels post LPS treatment in N2A cells. Fold changes were quantified relative to the expression level of cells receiving non-targeting Mock gRNA (N = 4 biologically independent samples). The bars represent the mean + S.E.M. Statistical analysis was performed using the non-parametric one-tailed Mann-Whitney U test. p value ≤ 0.05 was considered significant (*p ≤ 0.05).

3.3.2. CRISPR-mediated repression of *Myd88* locus can efficiently be achieved *in vivo* by recruitment of MS2-HP1aKRAB to gRNA

To test this repressor *in vivo*, we pursued delivery through packaging gRNAs and MS2-repression cassettes within Adeno-Associated Viruses (AAVs). Different AAV serotypes have been used to deliver CRISPR *in vivo*. The most common serotype has

been AAV9, which has high affinity to parenchymal cell populations^{26,27}. Here, we employed a hybrid AAV2/1 serotype, which is a recombinant AAV consisting of AAV2 inverted terminal repeats, and AAV1 *Rep* and *Cap* genes (here on referred to only as AAV1 for simplicity). AAV1 has been shown to be effective in transduction of components of the immune system and non-parenchymal cells such as dendritic and endothelial cells²⁸⁻³⁰. Moreover, AAV1 capsid can induce MyD88 signaling as part of the pathways of immunity against AAVs in the host^{31,32}. Our assessment of AAV1 tissue affinity revealed the highest expression in blood, lung, and bone marrow (Extended Data Fig. 2). Subsequently, we performed systemic delivery of AAV1/Myd88 gRNA or control AAV1/Mock gRNA with MS2-HP1aKRAB or MS2-KRAB cassettes to Cas9 nuclease transgenic mice (Fig. 2A). Three weeks after injections, blood, lung, and bone marrow were harvested and *Myd88* expression was assessed by qRT-PCR (Fig. 2B). Compared to uninjected controls, AAV delivery led to an increase in *Myd88* across different tissues we tested. Treatment with CRISPR to repress endogenous *Myd88* with HP1aKRAB led to a significant reduction in the level of *Myd88* in blood (~84%), lung (~75%), and bone marrow (~63%) as compared to the mock gRNA-treated group, in agreement with high affinity of AAV1 for these tissues. Administration of the KRAB domain alone led to a less pronounced repression of *Myd88* in lung (~52%), blood (~59%), and bone marrow (~34%), with slightly higher variation among the animals tested (Fig.2B).

To assess the potency of repression in rewiring the downstream gene regulatory network, we evaluated the levels of tumor necrosis factor- α (TNF- α) and intercellular adhesion molecule-1 (ICAM-1), two signaling elements directly modulated by the

MyD88 signaling pathway³³⁻³⁵. *Myd88* targeting with MS2-HP1aKRAB led to a significant reduction in *Icam-1* and *Tnfa* expression across multiple tissues, whereas targeting with MS2-KRAB did not lead to a similar consistent effect (Fig. 2C-D and Supplementary information Table1).

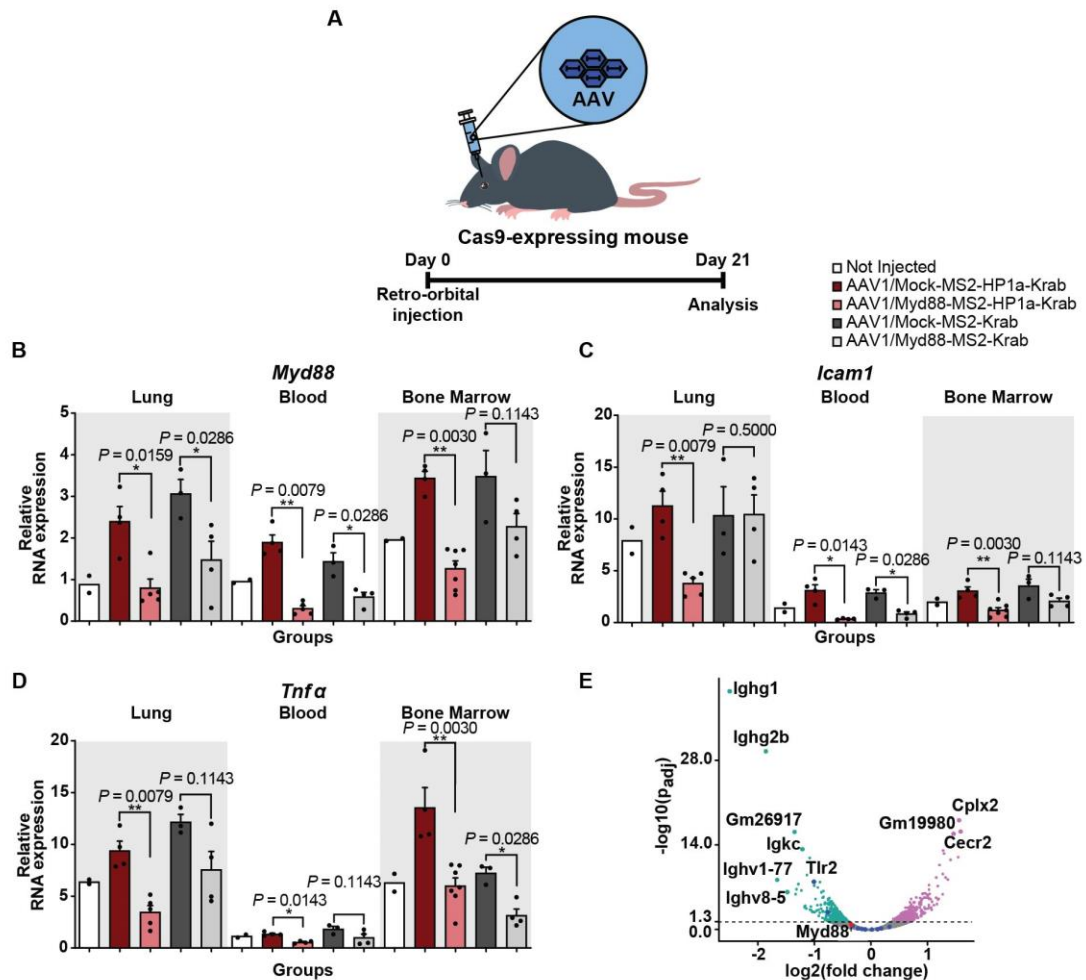


Figure 3.2. CRISPR-based targeted *Myd88* repression *in vitro* and *in vivo* using MS2 repressors. (A) Schematic of experiments demonstrating retro-orbital injection of AAV1/Myd88 or Mock repressors to Cas9 nuclease transgenic mice. (B) qRT-PCR

analysis of *Myd88* expression levels in lung, blood, and bone marrow of Cas9 transgenic mice 3 weeks post retro-orbital injections of $1E+12$ GC of AAV1/*Myd88* or AAV1/Mock vectors carrying MS2- HP1a -KRAB or MS2-KRAB (N = 4 mice for injected groups except for the following: Mock/MS2-KRAB group N=3 mice, *Myd88*/MS2-HP1aKRAB in bone marrow N=7 mice, *Myd88*/MS2-HP1aKRAB in blood and lung N= 5 mice, and N = 2 mice for not injected group). Fold changes are relative to universal control. The bars represent the mean + S.E.M. (C and D) Fold-change in the expression level of *Icam-1* (C), and *Tnfa* (D) mRNA relative to the universal control. (N = 4 mice for injected groups except for the following: Mock/MS2-KRAB group N=3 mice, *Myd88*/MS2-HP1aKRAB in bone marrow N=7 mice, *Myd88*/MS2-HP1aKRAB in lung N=5 mice, and N = 2 mice for not injected group). The bars represent the mean + S.E.M. (E) Volcano plot showing significance versus expression of differentially expressed genes between bone marrow samples collected from mice treated with *Myd88*-MS2-HP1aKRAB versus *Myd88*-MS2-KRAB. Points above the dotted line represent genes significantly (adj. p-value <0.05) up and down regulated. Highly downregulated genes in the presence of MS2-HP1aKRAB are a family of immunoglobulin heavy and light chains (N=2 mice). Statistical analysis was performed using the two-tailed t test and Benjamini-Hochberg multiple comparisons adjustment. Universal control is a blood sample collected from an uninjected Cas9 transgenic mouse. Statistical analysis for panel A-E was performed using the non-parametric one-tailed Mann-Whitney U test. A p value ≤ 0.05 was considered significant (*p ≤ 0.05 , **p ≤ 0.01).

To perform a systematic assessment of the repression efficiency of MS2- HP1aKRAB system as compared to MS2-KRAB, we performed next generation RNA sequencing on

the bone marrow of mice treated with these constructs. MS2-HP1aKRAB-treated mice expressed lower *Myd88* levels compared to MS2-KRAB-treated ones (Extended Data Fig. 3A), which was accompanied with changes in downstream signaling pathways such as *Illβ*. Of note, GO Enrichment analysis revealed that Myd88-MS2-HP1aKRAB-treated mice had significant downregulation of signaling pathways implicated in the immune and defense response against foreign organisms and bacteria, which are pathways associated with MyD88 function (Extended Data Fig. 3B). Similarly, the Reactome database revealed the TLR pathway as one of the highly significant downregulated pathways in the presence of MS2-HP1aKRAB (Extended Data Fig. 3C). This evidence suggests that modulation of *Myd88* and its downstream immune pathways is most effective with the MS2- HP1a KRAB repressor *in vivo*.

Interestingly, volcano plotting of differentially expressed genes revealed the constant region of heavy chain of immunoglobulin G1 and G2 (*Ighg1* and *Ighg2b*) and other immunoglobulin-related heavy and light chain genes as most downregulated with HP1a KRAB relative to KRAB (Fig. 2E). This is interesting finding in light of the mouse genetic background (C57BL/6), which has been shown to produce high level of IgGs³⁶.

3.3.3. CRISPR-mediated repression of *Myd88* leads to modulation of humoral response against AAV-mediated gene therapy and the efficacy of its function

Prior studies demonstrate that viral DNA stimulates TLR (i.e. TLR9), which in turn activates MyD88 and initiates downstream signaling events leading to adaptive immunity and antibody production against AAVs^{8,16}. In light of prior evidence and the observed repression of the immunoglobulin pathway, we asked whether there was a decrease in the AAV-specific humoral response following treatment with AAV1 carrying *Myd88*-

targeting gRNAs and MS2-HP1aKRAB cassettes (here on referred to as AAV1/Myd88 for simplicity) as compared to control viruses carrying mock gRNAs (AAV1/Mock). Three weeks after injection, we measured immunoglobulin G (IgG) response against the AAV1 capsid. We detected a 50% decrease in plasma IgG2a levels against AAV1 in AAV1/Myd88 group compared to AAV1/Mock-treated animals. (Fig. 3A).

Antibody formation against the AAV capsid is an important barrier to re-administration of AAV-based gene therapies, often leading to rapid clearance of the virus and other deleterious effects related to destruction of the virus or transduced cells by immune system. To further probe the prophylactic effect of *Myd88* repression on modulating humoral immunity upon AAV1 re-administration, we asked whether pre-treatment with AAV1/Myd88 can influence IgG level against AAV1 upon re-administration of AAV1/Mock. Analysis of IgG1 and IgG2A in the plasma demonstrated lower levels after initial *Myd88* repression, hinting to the potential of this strategy in modulating humoral response to AAV1 re-administration (Fig. 3B and Extended Data Fig. 4A-B).

To examine the extensibility of this strategy to modulate response against other AAV serotypes, we pre-treated mice with AAV1/Myd88 or AAV1/Mock and, 7 days later, systemically injected them with AAV9 that carried a *LacZ* or *Staphylococcus aureus* Cas9 (Sa-Cas9) cassette. In both instances, analysis of total IgG levels against AAV9 demonstrated that *Myd88* repression led to a lower antibody response against AAV9. Moreover, this was accompanied by significantly lower antibodies against Sa-Cas9 and higher transcript levels of *LacZ* in the blood (Fig. 3C-D). These data demonstrate that modulation of immunoglobulin production through *Myd88* repression can influence the

humoral response against more than one AAV serotype and its cargo. Higher LacZ expression in blood in this context hints to potentially higher efficiency of the gene therapy using this approach.

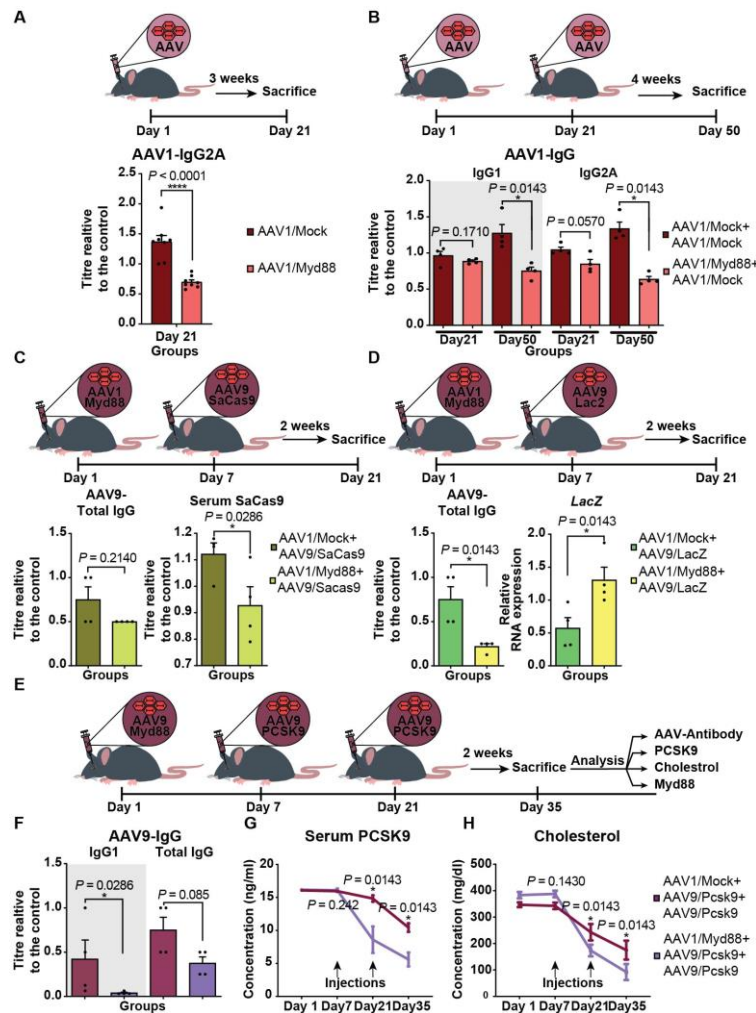


Figure 3.3. Prophylactic administration of AAV1/MyD88 *in vivo* leads to modulation of humoral immunity against AAV. (A) Top: Schematic of experiments demonstrating involving retro-orbital injection of AAV-Myd88 or Mock repressors to Cas9 nuclease transgenic mice; Bottom: Analysis of anti-AAV1 IgG2A antibody measured by ELISA.

Relative optical density (OD) values are quantified relative to the AAV1/Mock group (N=8 mice). (B) Top: Schematic of experiments demonstrating Cas9 transgenic mice treated with AAV1/Myd88 or AAV1/Mock at day 1, followed by a second administration of AAV1/Mock on day 21; Bottom: Anti-AAV1 IgG1 and total IgG antibody measured by ELISA at different time points. Relative optical density values are quantified relative to a value of AAV1/Mock+AAV1/Mock group (N=4 mice). (C) Top: Schematic of experiments demonstrating Cas9 transgenic mice treated with AAV1/Myd88 or AAV1/Mock at day 1, followed by a second administration of AAV9/SaCas9 on day 21; Bottom: Analysis of Anti-AAV9 IgG and Anti Sa-Cas9 levels in mice sera. Relative optical density values are quantified relative to the AAV1/Mock+AAV9/SaCas9 group (N=4 mice). (D) Top: Schematic of experiments demonstrating Cas9 transgenic mice treated with AAV1/Myd88 or AAV1/Mock at day 1, followed by a second administration of AAV9/LacZ on day 21; Bottom: Analysis of Anti-AAV9 IgG in mice sera and LacZ mRNA levels in blood. Relative optical density values are quantified relative to the AAV1/Mock+AAV9/LacZ group (N=4 mice). (E) Top: Schematic of the experiment. Cas9 nuclease transgenic mice were treated with AAV1-Myd88 or AAV1-Mock vectors via retro-orbital injection followed by a second and third injection of AAV9-Pcsk9 vectors on day 7 and 21. The legend represents the summary of the treatment groups. (F) Analysis of anti-AAV9 IgG and total IgG antibody measured by ELISA. Relative optical density values are quantified relative to the AAV1/Mock+AAV9/PCSK9+AAV9/PCSK9 group (N=4 mice). (G and H) Plasma samples collected from treated animals were assayed for (G) PCSK9 and (H) Cholesterol at days 0, 7, 21, and 30 (N=4 mice). Panel A-H data are expressed as mean + S.E.M. (Mock= Mock-HP1aKRAB, Myd88= Myd88-

HP1aKRAB, PCSK9= PCSK9-HP1aKRAB). Statistical analyses were performed using the non-parametric one-tailed Mann-Whitney U test. A p value ≤ 0.05 was considered significant (*p ≤ 0.05 , and ****p ≤ 0.0001).

To further explore this notion in the context of CRISPR therapies, we pre-treated the mice with AAV1/Myd88 or AAV1/Mock and then subjected them to two rounds of AAV9-based gene therapies 7 and 14 days apart (Fig. 3E). In this case, AAV9 carries a cassette for CRISPR-mediated repression of Proprotein convertase subtilisin/kexin type 9 (PCSK9), similar to the strategy we employed for *Myd88* repression. PCSK9 is an enzyme encoded by the *PCSK9* gene. This enzyme binds to the low-density lipoprotein (LDL) receptor at the surface of hepatocytes and initiates ingestion of the LDL receptor. Therefore, when PCSK9 is blocked or repressed, more LDL receptors are present to remove LDL from blood which, lowers blood LDL-cholesterol levels. This enzyme has been the target of previous *in vivo* CRISPR applications³⁷⁻³⁹.

Our data show that the AAV1/Myd88 pre-treated group has decreased *Myd88* expression (Extended Data Fig. 4C-D) as well as lower IgG1 and total IgG levels against AAV9 compared to the control (Fig. 3F). This observation was accompanied by better PCSK9 repression and lower plasma cholesterol levels, suggesting increased efficiency of the gene therapies (Fig. 3G-H). Altogether, these data present an exciting opportunity to modulate humoral immunity against AAV, possibly through prophylactic repression of *Myd88* with a tool inherently suited to perform both gene editing and epigenetic modulation (nuclease competent CRISPR).

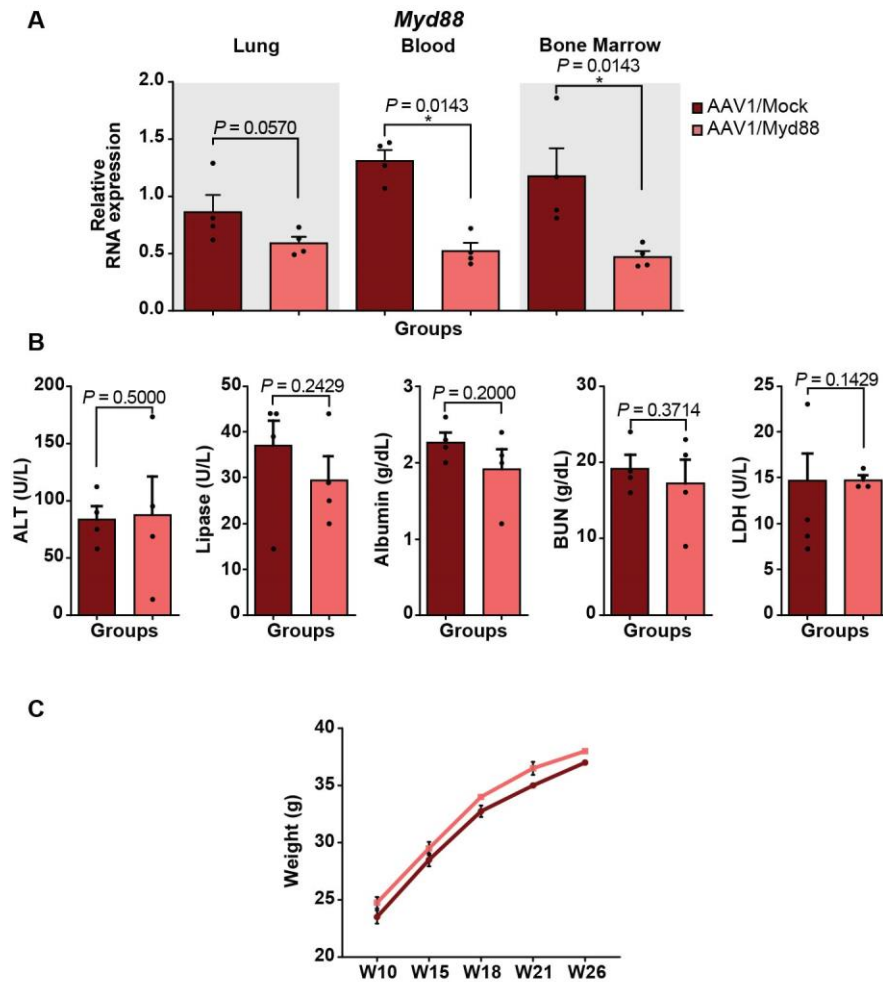


Figure 3.4. Long-term efficacy of AAV/Myd88 repression *in vivo*. (A) qRT-PCR analysis of *in vivo Myd88* expression level in lung, blood, and bone marrow of Cas9 transgenic mice five months post retro-orbital injections of 1E+12 GC of AAV/Myd88 or AAV/Mock vectors (N = 4 mice). The bars represent the mean + S.E.M. (B) Assessing the expression of a panel of general health markers in plasma samples collected from mice. About 5 months after AAV delivery, plasma samples were collected from mice and the concentration of ALT, Lipase, Albumin, BUN, and LDH were assessed in different groups. The bars represent the mean + S.E.M. (C) Body weight measurements of mice

injected with 1E+12 GC of AAV/Myd88 or AAV/Mock vectors carrying MS2-HP1a-KRAB showing similar growth condition (N = 4 mice). The bars represent the mean \pm S.E.M. (Mock= Mock-HP1a-KRAB, Myd88= Myd88-HP1a-KRAB). Fold change expression levels were quantified relative to the universal control. Universal control is a blood sample collected from an unjected mouse. Statistical analysis was performed using the non-parametric one-tailed Mann-Whitney U test. A p value ≤ 0.05 was considered significant (*P ≤ 0.05).

3.3.4. CRISPR mediated Myd88 repression does not create visible adverse effect in long term.

Next, we probed the long-term efficacy of AAV1/Myd88 repression *in vivo* to further assess its durability and possible negative consequences. Analysis of *Myd88* transcripts in lung, blood, and bone marrow twenty-three weeks after injection showed *Myd88* repression in the AAV1/Myd88 group (Fig. 4A). To assess possible negative consequences of long-term reduction of MyD88 level, we analyzed some key indicators of major internal organ functions including Blood Urea Nitrogen (BUN) for Kidney, Alanine Transaminase (ALT) and Albumin for liver, Lipase for pancreas, and Lactic Acid Dehydrogenase (LDH) as a marker of tissue damage. None of these markers were significantly different than mock-treated groups (Fig. 4B). Moreover, tracking the weight of the mice suggested that there were not any detectable deleterious effects on the general health and well-being as all animals demonstrated comparable weights (Fig. 4C).

3.3.5. CRISPR mediated Myd88 repression *in vivo* can act as a prophylactic measure against septicemia in Cas9 transgenic and C57BL/6 mice

We then asked whether this strategy could act as a prophylactic modality during septicemia, when there is an augmented systemic immune response. Septicemia is a pressing medical issue due to the emergence of antibiotic-resistance and rising longevity of patients suffering from chronic diseases⁴⁰. Moreover, high mortality rates due to septicemia still remain a medical challenge following trauma in the battlefield, highlighting the need for novel prevention strategies⁴¹.

We pre-treated Cas9 mice with AAV1/Myd88 or AAV1/Mock and three weeks later subjected them to systemic lipopolysaccharides (LPS) (from *Escherichia coli* 0127:B8) treatment. Six hours following LPS, we harvested lung, blood, and bone marrow and assessed the transcript levels of *Myd88* and major inflammatory cytokines (Fig. 5A). We observed significant repression of *Myd88* in lung (61%), blood (80%), and bone marrow (76%) compared to AAV1/Mock-treated mice (Fig. 5B). In response to LPS, plasma lactate level, a systemic marker associated with septicemia and tissue damage⁴², was significantly lower when mice were pre-treated with the AAV1/Myd88 repression cassette before LPS exposure, indicating a reduced systemic injury (Fig. 5C). Additionally, *Myd88* repression prevented upregulation of a wide range of inflammatory and immune-related cytokines that are directly or indirectly downstream of Myd88 signaling such as *Icam-1*, *Tnfa*, *Ncf*, *Il6*, *Ifn- α* , *Ifn- β* , *Ifn- γ* , and *Stat4* (Fig. 5D and Extended Data Fig. 5-6). Analysis of plasma and lung cytokine levels using a quantitative ELISA-based chemiluminescent assay revealed lower level of cytokines in *Myd88*-repressed mice (Fig. 5E).

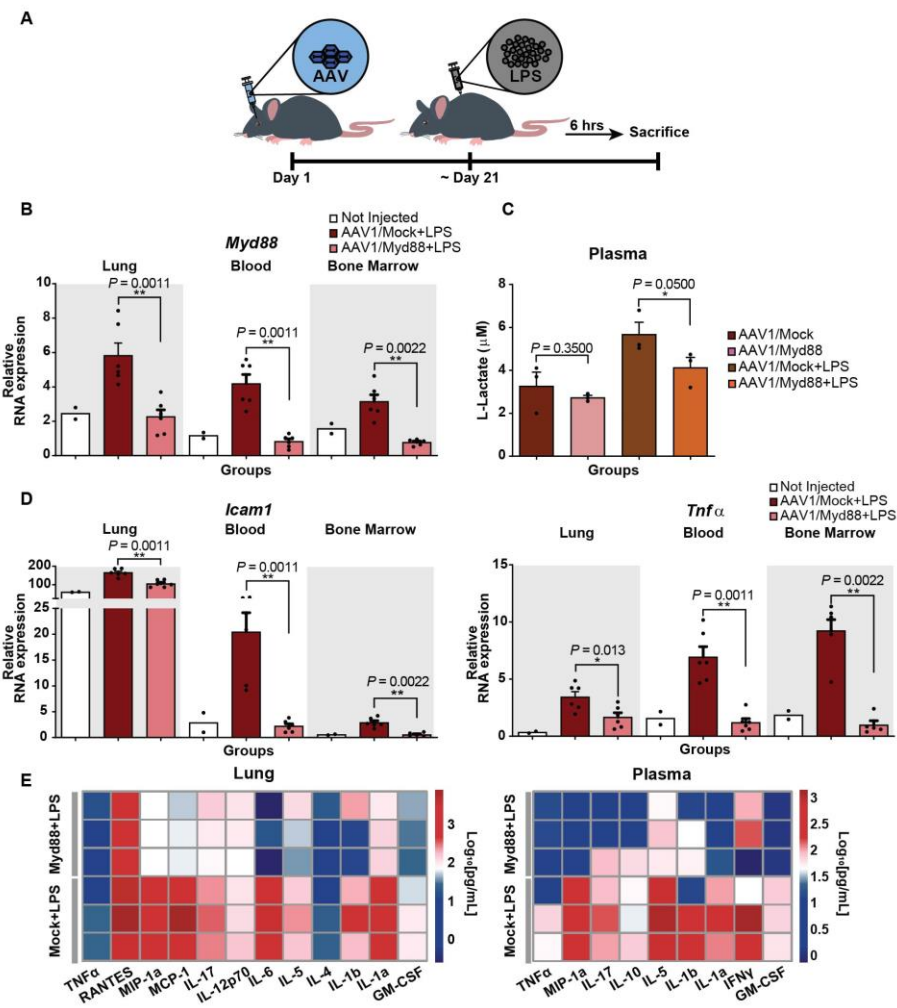


Figure 3.5. CRISPR-based modulation of host inflammatory response can be a prophylactic measure against LPS-mediated septicemia in Cas9 transgenic and WT mice. (A) Schematic of the experimental design to assess the protective effect of CRISPR-mediated MyD88 repression in septicemia. $1\text{E}+12$ GC of AAV vectors were injected to Cas9-expressing mice via retro-orbital injection and approx. 3 weeks later they were treated i.p. with LPS (5mg/kg). 6 hours post LPS injection mice were sacrificed. (B) qRT-PCR analysis of *in vivo* Myd88 expression relative to the universal control following LPS injection (N = 6 mice for injected groups, except Bone Marrow of Myd88 group

which is N=5 mice, and N = 2 mice for Not Injected group). The bars represent the mean + S.E.M. (C) Circulating L-lactate in plasma samples collected from mice 6 hours post LPS injection (N=3 mice). The bars represent the mean + S.E.M. (D) qRT-PCR analysis of *Icam-1*, and *Tnfa* mRNA expression in lung, blood, and bone marrow quantified relative to the universal control following LPS injection (N = 6 mice for injected groups, except Bone Marrow of Myd88 group which is N=5 mice ,and N = 2 mice for Not Injected group). The bars represent the mean + S.E.M. (E) Measurement of a panel of inflammatory cytokines in lung and plasma using multiplex-ELISA assay; values are displayed in the heatmaps as log base 10 of the measured concentration (N=3 mice). Statistical analysis was performed using the non-parametric one-tailed Mann-Whitney U test. A p value ≤ 0.05 was considered significant (*p ≤ 0.05 , **p ≤ 0.01).

To explore whether we can achieve similar outcomes by simultaneous delivery of Cas9 and gRNA-MS2-Hp1aKRAB cassettes to wild-type animals, we examined a dual AAV1 system in which a second virus carries a Sp-Cas9 nuclease cassette (Fig.6A). This strategy was capable of decreasing *Myd88* transcripts in C57BL/6 mice, both in the presence and absence of septicemia, leading to phenotypically relevant response similar to what we observed in Cas9 transgenic animals (Fig. 6B-D and Extended Data Fig. 7).

+ S.E.M. (C) Six hours post LPS injection plasma samples were collected from mice and the concentration of L-Lactate was assessed in different groups (N=3). The bars represent the mean + S.E.M. (D) qRT-PCR analysis of *Icam-1*, *Tnfa*, *Ncf*, *Il6*, and *Il1β* mRNA expression in blood, bone marrow, and lung. Fold change expression levels were quantified relative to the universal control (N = 4 mice). The bars represent the mean + S.E.M. (Mock= Mock-HP1aKRAB, Myd88= Myd88-HP1aKRAB). Universal control is a blood sample collected from an uninjected Cas9 transgenic mouse. Statistical analysis was performed using the non-parametric one-tailed Mann-Whitney U test. A p value ≤ 0.05 was considered significant (*p ≤ 0.05).

3.3.6. Nanoparticle mediated delivery of *Myd88* targeting CRISPR super-repressors after exposure to LPS can serve as a therapeutic modality against septicemia

To examine the therapeutic potential of this approach after exposure to LPS, we sought to deliver CRISPR plasmids to C57BL/6 through a nanoparticle-based approach, as they enable faster and more feasible delivery for CRISPR-based gene modulation as compared to the AAV-based system. Given the significance of liver damage after intra-peritoneal LPS exposure and the notion that majority of the nanoparticles delivered systematically accumulate in the liver and lungs, we focused on studying the liver. We first examined whether AAV1/Myd88 can repress *Myd88* expression in liver. Having difficulty repressing *Myd88* in the liver with our current pair of gRNAs, we designed another pair targeting a different region of the *Myd88* promoter. The new gRNAs led to *Myd88* repression in the liver upon AAV mediated delivery to Cas9 transgenic mice. This was also observed following LPS injury (Extended Data Fig. 8A-B). Next, we set out to examine the therapeutic effect of this system in C57BL/6 mice 2 hours post exposure to

LPS. We injected the mice with nanoparticles carrying Cas9, gRNAs, and MS2-HP1aKRAB cassettes and examined the systemic inflammatory response against LPS (Fig 7A). 72 hours post CRISPR delivery, blood, lung, liver, and bone marrow were harvested and *Myd88* expression was assessed by qRT-PCR. Treatment led to a reduction in the levels of *Myd88* in the blood, lung, bone marrow, and liver as compared to the Mock treated group (Fig. 7B). This *Myd88* repression prevented upregulation of a wide range of inflammatory markers followed by LPS exposure (Fig. 7C). Analysis of plasma markers of tissue damage of the liver showed that we could modulate the detrimental effects of LPS injection (Fig. 7D). In particular, high density lipoproteins (HDL) have been shown to increase following LPS treatment to eliminate systemic LPS in order to protect tissues from damage⁴³ and has been associated with MyD88 signaling⁴⁴. In accordance with this, we found *Myd88* repression decreased HDL, low density lipoproteins (LDL), and cholesterol as compared to Mock-treated groups. In addition, *Myd88* repression decreased ALT and Aspartate Aminotransferase (AST), two markers of hepatocyte damage, which further suggests that this approach can be effective therapeutically (Fig. 7D).

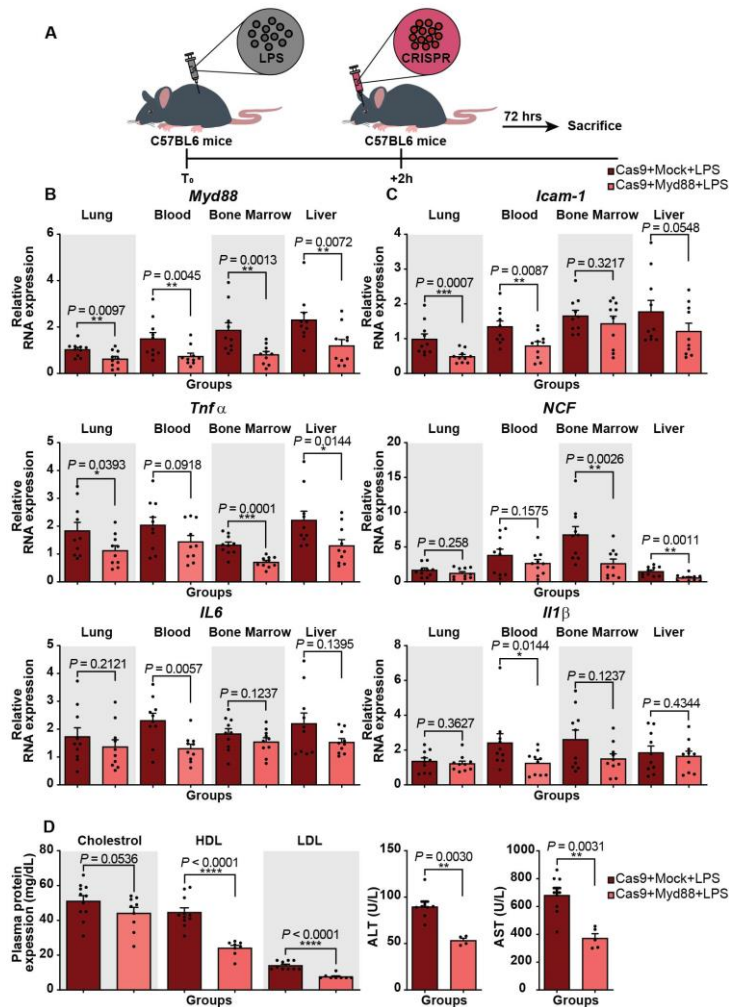


Figure 3.7. Therapeutic delivery of nanoparticles carrying DNA encoding *Myd88*-targeting CRISPR confers protection against LPS-mediated septicemia. (A) Schematic of the experiment. C57BL/6 mice were treated i.p. with LPS(2.5mg/kg). 2 hours later, mice received Cas9 and *Myd88* or Mock vectors via retro-orbital injection using nanoparticles. 72 hours post retro-orbital injection mice were sacrificed. (B-C) Lung, blood, and bone marrow samples were collected from mice. The expression levels of *Myd88* and a panel of immune-related genes were assessed by qRT-PCR. (B) qRT-PCR analysis of *Myd88*

repression following LPS injection and CRISPR-mediated therapy. (N=10 mice). The bars represent the mean + S.E.M. (C) qRT-PCR analysis of *Icam-1*, *Tnfa*, *Ncf*, *Il6*, and *Il1β* mRNA expression in different tissues. Fold changes were quantified relative to the universal control. (N=10 mice). The bars represent the mean + S.E.M. (D) Plasma concentration of Cholesterol (N = 11 mice for Cas9+Mock+LPS, N = 9 mice for Cas9+Myd88+LPS), plasma concentration of HDL (N = 11 mice for Cas9+Mock+LPS, N = 8 mice for Cas9+Myd88+LPS), plasma concentration of LDL (N = 10 mice for Cas9+Mock+LPS, N = 8 mice for Cas9+Myd88+LPS), plasma concentration of ALT (N = 7 mice for Cas9+Mock+LPS, N = 4 mice for Cas9+Myd88+LPS), and plasma concentration of AST (N = 8 mice for Cas9+Mock+LPS, N = 5 mice for Cas9+Myd88+LPS). The bars represent the mean + S.E.M. (Mock=Mock-HP1aKRAB, Myd88= Myd88-HP1aKRAB). Universal control is a blood sample collected from an uninjected Cas9 transgenic mouse. Statistical analysis was performed using the non-parametric one-tailed Mann-Whitney U test. A p value ≤ 0.05 was considered significant (*p ≤ 0.05 , **p ≤ 0.01 , ***p ≤ 0.001 , ****p ≤ 0.0001).

3.4. Discussion

In summary, we provide a potent transcriptional therapeutic modality for synthetic control of immune response *in vivo* using a newly developed CRISPR-based transcriptional super-repressor against endogenous *Myd88*. We show that this system is effective in modulating downstream immune signaling and can create a visible protective phenotype *in vivo*. This notion is especially attractive in the case of delivery using a less common AAV serotype (AAV2/1) known to target smaller cellular populations *in vivo* (e.g. non-parenchymal cells).

We demonstrate that targeting the *Myd88* locus with AAV1/CRISPR generates less immunoglobulin against AAV1 and AAV9 and modulates general immunoglobulin expression patterns, consistent with prior reports on the failure of generation of an antigen-specific *IgG2a* response in *MyD88*^{-/-} animals⁴⁵. The ability to control *Myd88* transcript levels using a CRISPR-based synthetic repressor is of significance in light of the common challenges involved with AAV-based clinical gene therapies, as this pathway has been shown to be a key node in induction of humoral immunity against many AAV serotypes and not just AAV2/1 *in vivo*. Moreover, we argue that this method can be a powerful tool to dissect biological questions at the level of *Myd88* transcription. Here, we demonstrate that a prophylactic regime that represses *Myd88* can be used to increase efficiency of subsequent viral-based gene delivery by preventing a surge in humoral response.

This strategy was also effective in modulating the systemic inflammatory response against (LPS)-induced endotoxemia both prophylactically and therapeutically. CRISPR-mediated endogenous repression of *Myd88* prevented upregulation of a wide range of inflammatory markers and conferred a protective phenotype. Further studies are needed to address the extensibility of CRISPR super repressors to other endogenous genes of the immune system and to define target tissues and cellular players, as well as to characterize the applicability to other infectious diseases. However, the ability to modulate host immune response using this strategy is a promising step towards generating a universal yet targeted tool to prevent exaggerated inflammatory response and severe tissue damage in the context of emerging infectious diseases.

HP1a protein is composed of a chromodomain (CD), which confers specific binding to methylated H3 lysine 9 and a chromoshadow domain (CSD), and can directly interact with H3K9-specific histone methylases, including SetDB1 and Suv39h1/2^{46,47}. In this study to minimize the potential nonspecific effects of ectopic HP1a expression, we used a truncated form of HP1a containing only the CSD. Several questions remain about how and if this truncated version still leads to the spread of chromatin repression marks beyond the targeted loci. While HP1 proteins can dimerize via the CSD, such homodimerization alone appears insufficient to explain the ability of these proteins to spread along chromatin⁴⁸⁻⁵⁰. Further analysis is needed to look at the genome wide effects of using truncated HP1a protein.

Taken together, we demonstrate the promise of CRISPR-based transcriptional regulation as a readily programmable tool for modulating inflammatory conditions and protecting against an infectious condition. Employment of a nuclease competent Cas9 and a truncated gRNA in this study opens up an opportunity for simultaneous application of CRISPR for targeted gene editing while modulating the immune response, which makes CRISPR-mediated gene repression superior to other systems such as shRNA-mediated repression.

References

- 1 Moreno, A. M. *et al.* In Situ Gene Therapy via AAV-CRISPR-Cas9-Mediated Targeted Gene Regulation. *Mol Ther* **26**, 1818-1827, doi:10.1016/j.ymthe.2018.04.017 (2018).

- 2 Thakore, P. I. *et al.* RNA-guided transcriptional silencing in vivo with *S. aureus* CRISPR-Cas9 repressors. *Nat Commun* **9**, 1674, doi:10.1038/s41467-018-04048-4 (2018).
- 3 Zheng, Y. *et al.* CRISPR interference-based specific and efficient gene inactivation in the brain. *Nat Neurosci* **21**, 447-454, doi:10.1038/s41593-018-0077-5 (2018).
- 4 Zhou, H. *et al.* In vivo simultaneous transcriptional activation of multiple genes in the brain using CRISPR-dCas9-activator transgenic mice. *Nat Neurosci* **21**, 440-446, doi:10.1038/s41593-017-0060-6 (2018).
- 5 Liao, H. K. *et al.* In Vivo Target Gene Activation via CRISPR/Cas9-Mediated Trans-epigenetic Modulation. *Cell* **171**, 1495-1507 e1415, doi:10.1016/j.cell.2017.10.025 (2017).
- 6 Breinig, M. *et al.* Multiplexed orthogonal genome editing and transcriptional activation by Cas12a. *Nature methods* **16**, 51-54 (2019).
- 7 Matharu, N. *et al.* CRISPR-mediated activation of a promoter or enhancer rescues obesity caused by haploinsufficiency. *Science* **363**, eaau0629 (2019).
- 8 Xu, L., Zhao, L., Gao, Y., Xu, J. & Han, R. Empower multiplex cell and tissue-specific CRISPR-mediated gene manipulation with self-cleaving ribozymes and tRNA. *Nucleic acids research* **45**, e28-e28 (2017).
- 9 Xu, X. *et al.* High-fidelity CRISPR/Cas9-based gene-specific hydroxymethylation rescues gene expression and attenuates renal fibrosis. *Nature communications* **9**, 1-15 (2018).
- 10 Gilbert, L. A. *et al.* CRISPR-mediated modular RNA-guided regulation of transcription in eukaryotes. *Cell* **154**, 442-451 (2013).

- 11 Gilbert, L. A. *et al.* Genome-scale CRISPR-mediated control of gene repression and activation. *Cell* **159**, 647-661 (2014).
- 12 Kearns, N. A. *et al.* Functional annotation of native enhancers with a Cas9–histone demethylase fusion. *Nature methods* **12**, 401-403 (2015).
- 13 Thakore, P. I. *et al.* Highly specific epigenome editing by CRISPR-Cas9 repressors for silencing of distal regulatory elements. *Nature methods* **12**, 1143 (2015).
- 14 Thakore, P. I., Black, J. B., Hilton, I. B. & Gersbach, C. A. Editing the epigenome: technologies for programmable transcription and epigenetic modulation. *Nature methods* **13**, 127 (2016).
- 15 Konermann, S. *et al.* Optical control of mammalian endogenous transcription and epigenetic states. *Nature* **500**, 472-476 (2013).
- 16 La Russa, M. F. & Qi, L. S. The new state of the art: Cas9 for gene activation and repression. *Molecular and cellular biology* **35**, 3800-3809 (2015).
- 17 Evers, B. *et al.* CRISPR knockout screening outperforms shRNA and CRISPRi in identifying essential genes. *Nature biotechnology* **34**, 631 (2016).
- 18 Yeo, N. C. *et al.* An enhanced CRISPR repressor for targeted mammalian gene regulation. *Nature methods* **15**, 611 (2018).
- 19 Kiani, S. *et al.* Cas9 gRNA engineering for genome editing, activation and repression. *Nat Methods* **12**, 1051-1054, doi:10.1038/nmeth.3580 (2015).
- 20 Huang, X. & Yang, Y. Targeting the TLR9-MyD88 pathway in the regulation of adaptive immune responses. *Expert Opin Ther Targets* **14**, 787-796, doi:10.1517/14728222.2010.501333 (2010).

- 21 Janssens, S. & Beyaert, R. A universal role for MyD88 in TLR/IL-1R-mediated signaling. *Trends Biochem Sci* **27**, 474-482 (2002).
- 22 Warner, N. & Nunez, G. MyD88: a critical adaptor protein in innate immunity signal transduction. *J Immunol* **190**, 3-4, doi:10.4049/jimmunol.1203103 (2013).
- 23 Plant, L., Wan, H. & Jonsson, A.-B. MyD88-dependent signaling affects the development of meningococcal sepsis by nonlipooligosaccharide ligands. *Infection and immunity* **74**, 3538-3546 (2006).
- 24 Yu, X. *et al.* MYD88 L265P mutation in lymphoid malignancies. *Cancer research* **78**, 2457-2462 (2018).
- 25 Liao, H.-K. *et al.* Use of the CRISPR/Cas9 system as an intracellular defense against HIV-1 infection in human cells. *Nature communications* **6**, 6413 (2015).
- 26 Castle, M. J., Turunen, H. T., Vandenberghe, L. H. & Wolfe, J. H. in *Gene Therapy for Neurological Disorders* 133-149 (Springer, 2016).
- 27 Merkel, S. F. *et al.* Trafficking of adeno-associated virus vectors across a model of the blood–brain barrier; a comparative study of transcytosis and transduction using primary human brain endothelial cells. *Journal of neurochemistry* **140**, 216-230 (2017).
- 28 Chen, S. *et al.* Efficient transduction of vascular endothelial cells with recombinant adeno-associated virus serotype 1 and 5 vectors. *Human gene therapy* **16**, 235-247 (2005).
- 29 Veron, P. *et al.* Major subsets of human dendritic cells are efficiently transduced by self-complementary adeno-associated virus vectors 1 and 2. *J Virol* **81**, 5385-5394, doi:10.1128/JVI.02516-06 (2007).

- 30 Lu, Y. & Song, S. Distinct immune responses to transgene products from rAAV1 and rAAV8 vectors. *Proc Natl Acad Sci U S A* **106**, 17158-17162, doi:10.1073/pnas.0909520106 (2009).
- 31 Sudres, M. *et al.* MyD88 signaling in B cells regulates the production of Th1-dependent antibodies to AAV. *Mol Ther* **20**, 1571-1581, doi:10.1038/mt.2012.101 (2012).
- 32 Zhu, J., Huang, X. & Yang, Y. The TLR9-MyD88 pathway is critical for adaptive immune responses to adeno-associated virus gene therapy vectors in mice. *J Clin Invest* **119**, 2388-2398, doi:10.1172/JCI37607 (2009).
- 33 Lin, X., Kong, J., Wu, Q., Yang, Y. & Ji, P. Effect of TLR4/MyD88 signaling pathway on expression of IL-1beta and TNF-alpha in synovial fibroblasts from temporomandibular joint exposed to lipopolysaccharide. *Mediators Inflamm* **2015**, 329405, doi:10.1155/2015/329405 (2015).
- 34 Park, G. S. & Kim, J. H. LPS Up-Regulates ICAM-1 Expression in Breast Cancer Cells by Stimulating a MyD88-BLT2-ERK-Linked Cascade, Which Promotes Adhesion to Monocytes. *Mol Cells* **38**, 821-828, doi:10.14348/molcells.2015.0174 (2015).
- 35 Yu, M. *et al.* MyD88-dependent interplay between myeloid and endothelial cells in the initiation and progression of obesity-associated inflammatory diseases. *J Exp Med* **211**, 887-907, doi:10.1084/jem.20131314 (2014).
- 36 Van den Akker, T. W., de Glopper-van der Veer, E., Radl, J. & Benner, R. The influence of genetic factors associated with the immunoglobulin heavy chain locus on

- the development of benign monoclonal gammopathy in ageing IgH-congenic mice. *Immunology* **65**, 31 (1988).
- 37 Thakore, P. I. *et al.* RNA-guided transcriptional silencing in vivo with *S. aureus* CRISPR-Cas9 repressors. *Nature communications* **9**, 1-9 (2018).
- 38 Abifadel, M. *et al.* Mutations in PCSK9 cause autosomal dominant hypercholesterolemia. *Nature genetics* **34**, 154 (2003).
- 39 Maxwell, K. N. & Breslow, J. L. Adenoviral-mediated expression of Pcsk9 in mice results in a low-density lipoprotein receptor knockout phenotype. *Proceedings of the National Academy of Sciences* **101**, 7100-7105 (2004).
- 40 Zhang, H. *et al.* Sepsis induces hematopoietic stem cell exhaustion and myelosuppression through distinct contributions of TRIF and MYD88. *Stem cell reports* **6**, 940-956 (2016).
- 41 Ma, X.-Y., Tian, L.-X. & Liang, H.-P. Early prevention of trauma-related infection/sepsis. *Military Medical Research* **3**, 33 (2016).
- 42 Cho, S.-Y. & Choi, J.-H. Biomarkers of sepsis. *Infection & chemotherapy* **46**, 1-12 (2014).
- 43 Yao, Z. *et al.* Blood-borne lipopolysaccharide is rapidly eliminated by liver sinusoidal endothelial cells via high-density lipoprotein. *The Journal of Immunology* **197**, 2390-2399 (2016).
- 44 Dandekar, A. *et al.* Toll-like receptor (TLR) signaling interacts with CREBH to modulate high-density lipoprotein (HDL) in response to bacterial endotoxin. *Journal of Biological Chemistry* **291**, 23149-23158 (2016).

- 45 Schnare, M. *et al.* Toll-like receptors control activation of adaptive immune responses. *Nat Immunol* **2**, 947-950, doi:10.1038/ni712 (2001).
- 46 Hiragami, K. & Festenstein, R. Heterochromatin protein 1: a pervasive controlling influence. *Cellular and molecular life sciences CMLS* **62**, 2711-2726 (2005).
- 47 Schultz, D. C., Ayyanathan, K., Negorev, D., Maul, G. G. & Rauscher, F. J. SETDB1: a novel KAP-1-associated histone H3, lysine 9-specific methyltransferase that contributes to HP1-mediated silencing of euchromatic genes by KRAB zinc-finger proteins. *Genes & development* **16**, 919-932 (2002).
- 48 Canzio, D. *et al.* Chromodomain-mediated oligomerization of HP1 suggests a nucleosome-bridging mechanism for heterochromatin assembly. *Molecular cell* **41**, 67-81 (2011).
- 49 Meehan, R. R., Kao, C. F. & Pennings, S. HP1 binding to native chromatin in vitro is determined by the hinge region and not by the chromodomain. *The EMBO journal* **22**, 3164-3174 (2003).
- 50 Canzio, D., Larson, A. & Narlikar, G. J. Mechanisms of functional promiscuity by HP1 proteins. *Trends in cell biology* **24**, 377-386 (2014).

CHAPTER 4

ESTABLISHING TEMPORAL CONTROL OVER CRISPR-BASED TECHNIQUES FOR SAFER GENE THERAPY APPROACHES

4.1. Introduction

The potential of CRISPR for *in vivo* gene editing is being unraveled in many recent publications. For human use, the safety of CRISPR and gene therapy vehicles must be carefully addressed. While much CRISPR research has focused on site-specific genome editing/disruption *in vitro* and *in vivo*, only a fraction of studies has focused on application of catalytically inactive Cas9 proteins for transcriptional modulation. For many clinical applications, transient transcriptional repression of a gene can provide a safer alternative to permanent gene disruption, which may alter germline DNA or create unintended genome mutations. Efforts to improve regulatory control over CRISPR, such as engineering spatiotemporally controlled CRISPR, have been very limited. Here we demonstrate developing and testing CRISPR logic circuits that carry internal safety regulatory controls AAV viruses reside in cells for long time, or even integrate in genome. Incorporation of a safety genetic switch to modulate CRISPR and AAV virus titer after therapy will be important for human translation. Also, by reducing the duration of CRISPR expression from viral vector, the genetic safety switches can reduce the CRISPR off-target effect in the genome. For safe clinical translation, it is essential to expand CRISPR toolkits to fine-tune gene therapies should an adverse reaction happens. Therefore, we next set out to address this notion by harnessing CRISPR multi-

functionality to develop control switches that can regulate both the function of CRISPR and the dosage of delivered carrier viruses.

4.2. Materials and methods

4.2.1. Vector Design and Construction

MS2 Fusion constructs: The MS2 fused transcriptional activator plasmid was purchased from addgene (Addgene plasmid ID: 61423). The MS2-P65-HSF1-GFP was amplified from this vector and sub-cloned into a gateway entry vector for further cloning into AAV backbone.

U6-gRNA-MS2 plasmids: To generate these plasmids, 14bp or 20bp guide sequences were inserted into sgRNA-MS2 cloning backbone (Addgene plasmid ID: 61424) at BbsI site via golden gate-based reaction. All the gRNA sequences are listed in the table 1 in supplementary note.

4.2.2. AAV vectors

Following cloning of the gRNAs into a U6-sgRNA-MS2 backbone, the U6-gRNA encoding region was amplified from this vector and inserted within gateway entry vectors using golden gate reaction. Using the same method, the activator domain and a short EF1a promoter were cloned into gateway entry vectors. The designed safety switch sgRNA sequence was synthesized as gBlocks (Integrated DNA Technologies) and inserted into a gateway entry vector (Addgene plasmid ID: 62084) digested with HindIII and SphI. Further sub-cloning of all these components into AAV backbone via LR

reaction (Invitrogen) generated final AAV vectors. All the primer sequences are listed in table 2 in supplementary note.

4.2.3. AAV packaging and purification

Constructed AAV vectors were digested by SmaI digest to test the integrity of ITR regions before virus production. Verified AAV vectors were used to generate AAV2/DJ-TTN, AAV2/DJ-Cas9, and AAV2/1-Cas9 by PackGene® Biotech, LLC. The virus titers were quantified via Real-time SYBR Green PCR at $1.5E+13$ GC/ml against standard curves using linearized parental AAV vectors.

4.2.4. Cell culture

HEK293FT, and Neuro-2a, cell lines (purchased from ATCC) were maintained in Dulbecco's modified Eagle's medium (DMEM - Life Technologies) with 10% fetal bovine serum (FBS - Life Technologies), 2mM glutamine, 1.0 mM sodium pyruvate (Life Technologies) and 1% streptomycin– penicillin mix (Gibco) in incubators at 37 °C and 5% CO₂.

4.2.5. Transfection of *in vitro* cultured cells

For control switch experiments targeting human genes HEK293FT cells were co-transfected with plasmid DNA encoding gRNA circuits (400 ng), Cas9 nuclease (100 ng), and EBFP as a transfection control (25 ng). For the control switch experiment targeting GFP expression to validate the safety gRNA function, HEK293FT cells were co-transfected with plasmid DNA encoding gRNA circuits (250 ng), Cas9 nuclease (25 ng),

and EBFP as a transfection control (50 ng). Polyethylenimine (PEI) (Polysciences) was used to transfect HEK293FT cells. Transfection complexes were prepared according to manufacturer's instructions.

For control switch experiments targeting mouse genes, Neuro-2a cells were co-transfected with plasmids encoding gRNA circuits (400 ng), Cas9 nuclease (100 ng), and EBFP as a transfection control (25 ng). Plasmids were delivered to Neuro-2a cells with Lipofectamine LTX (Life Technologies). Two hours post-transfection, cells were treated with tetracycline 50uM (Sigma). Cells were collected 48-72 hours post-transfection and total RNA was collected from cells using RNeasy Plus mini kit (Qiagen) following manufacturer's instruction.

4.2.6. Quantitative RT-PCR (qRT-PCR) Analysis

Cells or tissues were lysed, and RNA was extracted using RNeasy Plus mini kit (Qiagen) or trizol (Life Technologies) followed by cDNA synthesis using the High-Capacity RNA-to-cDNA Kit (Thermo Fisher) or iScript cDNA synthesis kit (Bio-Rad). qRT-PCR was performed using SYBR Green PCR Master Mix (Thermo Fisher). All analyses were normalized to 18s rRNA and fold-changes were calculated against Cas9 only control groups for *in vitro* transfection experiments and AAV-GFP group for *in vitro* transduction or *in vivo* experiments ($2^{-\Delta\Delta Ct}$). Primer sequences for qPCR are listed in table 2 in supplementary notes.

4.2.7. DNA isolation and real-time PCR for AAV genomic copies in tissues

DNA isolation from tissues was performed using DNeasy blood and tissue kit

(Qiagen) according to the manufacturer's protocol. qPCR reactions consist of 100 ng template DNA from each sample and primers and probes for viral inverted terminal repeats (ITRs) using Probe Based qPCR Master Mix (IDT) according to the manufacturer's protocol. Data was normalized to mouse *Acvr2b* control gene.

4.2.8. Fluorescent Reporter Assay

HEK293T cells were transfected with the built-in safety circuit along with a Cas9 expression cassette. 48 hours after transfection, cells were assayed by flow cytometry to measure GFP signal. Cells were trypsinized with trypsin (Gibco) and then inactivated using Hanks Balanced Salt Solution (HBSS-/-; Corning Life Sciences) supplemented with 10% FBS. Next, cells were transferred to a 96- well plate and pelleted at 300g for 2 min at 4 °C. Cells were resuspended in 200 μ L of phosphate-buffered saline (PBS; Corning Life Sciences) with 10% FBS after aspiration of the supernatant. 7-AAD (7-amino-actinomycin D) conjugated with PerCP was used for the exclusion of nonviable cells in analysis. We selected live cells (PerCP negative population) expressing blue fluorescence $>2 \times 10^2$ A.U as our transfection marker to exclude the un-transfected cells from the analysis and quantified the percentage of cells expressing GFP $>10^3$ A.U. Flow cytometry was performed using a FACSCelesta flow cytometer (Becton Dickson) with HTS. EBFP was measured with violet laser (405 nm) and a 450/50 filter; GFP, measured with a 488-nm laser and a 530/30 filter. We gathered at least 300,000 flow cytometer events per sample.

4.2.9. Animals

All the experiments with animals were approved by the Institutional Animal Care and Use Committee (IACUC) at Arizona State University and have been performed according to institutional guidelines. All the experiments were performed on at least 3 mice of 6-8 weeks old per group. Both male and female were included in experiments. The sample size in each group is indicated in each figure legend.

Male C57BL/6 mice (JAX Stock number: 000664) were used for studying AAV2/1-GFP, tropism towards different organs and AAV-CRISPR control switch experiments. Both male and female Rosa26-Cas9 knockin mice (JAX Stock number 026179) were used for AAV-CRISPR repression experiments.

4.2.10. Retro-Orbital injections

AAV particles were delivered to mice through retro-orbital injection of the venous sinus. Animals were anesthetized with 3% isoflurane and virus particles were injected to the left eye with 100 microliters of AAV solution (1E11 to 1E12 genome copy per mouse for a total of 1.01E+12 GC AAV-TTN and AAV-Cas9 (100:1 ratio).

4.2.11. Tissue harvest

Mice were euthanized via CO₂ inhalation. Tissue samples taken from liver, spleen, lung, testis, bone marrow and blood were collected in RLT (Life Technologies) or snap frozen for RNA analysis.

4.2.12. *In vivo* tetracycline delivery

Mice were given intraperitoneal (i.p.) injection of tetracycline (Sigma) at a concentration of 20 mg/kg three consecutive days prior to the harvest. Mice were euthanized 24 hours post the last tetracycline injection via CO₂ inhalation.

4.2.13. Statistical analysis

Statistical analyses are included in the figure legends. Data are presented as the mean \pm SEM or mean \pm SD. N = number of individual transfections for *in vitro* experiments and N = number of animals for *in vivo* experiments. Statistical analyses were performed using prim 7 Software (GraphPad). We performed One-tailed Student's t-test. P < 0.05 was considered significant and represented as * (p < 0.05), ** (p < 0.01), *** (p < 0.001).

4.3. Results

For safe clinical translation, it is essential to expand CRISPR toolkits to fine-tune gene therapies should an adverse reaction happens. Therefore, we next set out to address this notion by harnessing CRISPR multi-functionality to develop control switches that can regulate both the function of CRISPR and the dosage of delivered carrier viruses.

We focused on generating CRISPR genetic control switches with a size suitable for the limited payload capacity of one or two AAV viruses. Our previously reported multifunctional CRISPR-Cas9 with the ability of switching between nuclease-dependent and -independent functions through gRNA engineering enables us to perform simultaneous genetic and epigenetic modulations¹. Based on this notion, we engineered an inducible safety gRNA by incorporating a previously reported tetracycline responsive

riboswitches within a full length (20nt) gRNA, which renders the inactive gRNA to an active form in the presence of the tetracycline². Subsequently, we designed a genetic circuit within one AAV transfer vector containing three transcription units: 1) A “worker” gRNA, defined as a truncated gRNA responsible for transcriptional modulation of a desired endogenous genes through recruitment of Cas9 nuclease and an MS2-effector complex, 2) a full length “safety” gRNA, carrying a tetracycline responsive aptamer, which is also orthogonal to mouse genome, 3) and an MS2-activator complex (MS2-HSF1-P65-GFP)³ (Figure 4.1-A).

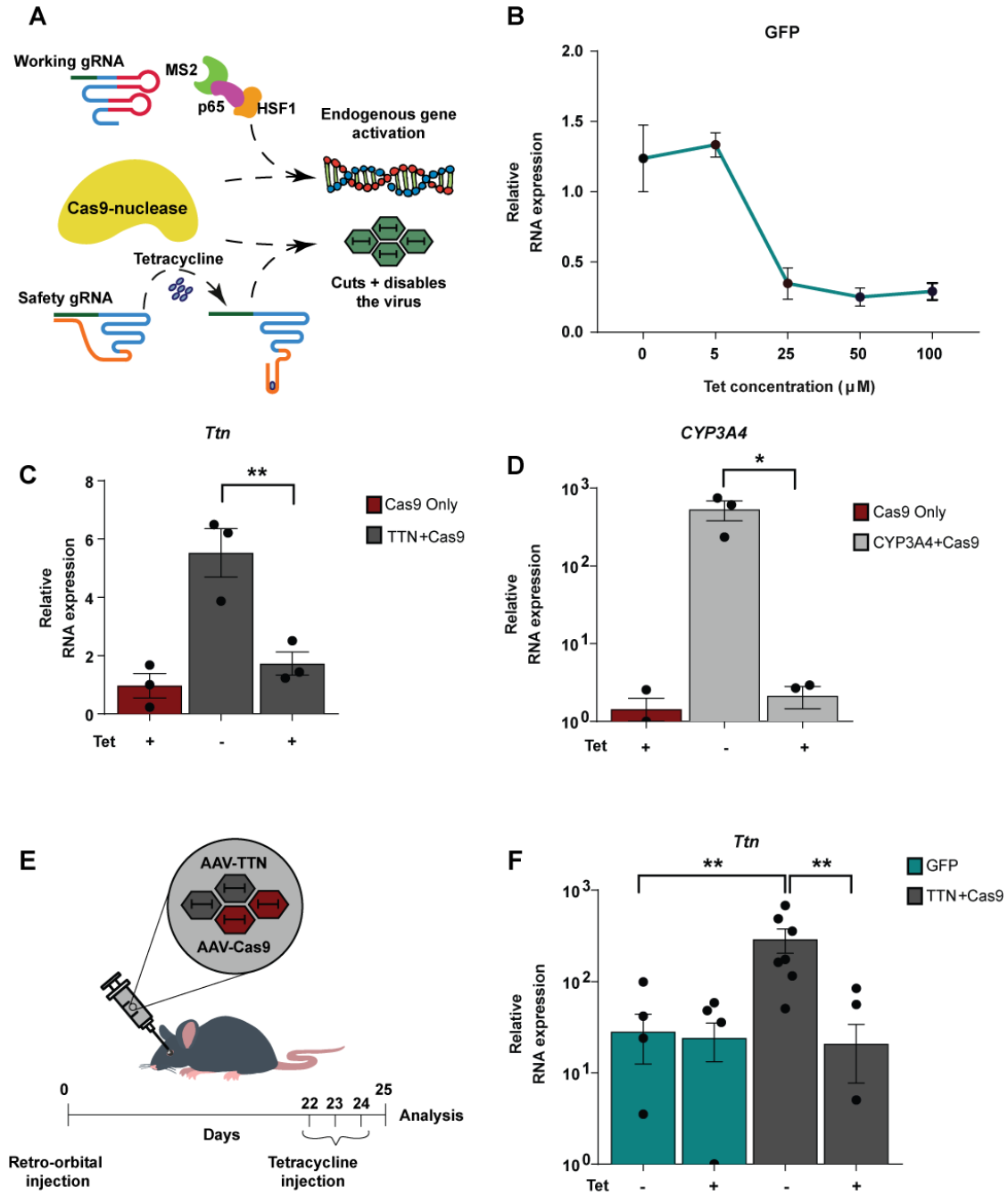


Figure 4.1. Build and test Multifunctional CRISPR-based control switches (A) Schematic illustrates the design of CRISPR-based control switch. Cas9 nuclease acts as a transcriptional activator through recruitment of the worker (14nt) gRNA and an activator complex to the desired endogenous locus. Cas9 retains its nuclease activity when binds

the safety (20nt) gRNA which targets orthogonal sites located within the AAV vector. Safety gRNA is activated upon receiving tetracycline. (B) Data shows GFP expression as a surrogate for the integrity of the AAV vector 24 hours after transfection of HEK293FT cells. Fold changes were calculated relative to the GFP expression level of cells cultured in the absence of tetracycline. (N = 3 biologically independent samples). (C and D) Validation of control switch *in vitro* through qRT-PCR measurement of *Ttn* mRNA level in Neuro 2A (C) and *CYP3A4* mRNA level in HEK293FT (D) upon addition of tetracycline (Tet). Cells were transfected with AAV-Cyp3a4 or AAV-TTN vector along with AAV-Cas9 vector. Levels of targeted gene activation were quantified by qPCR 72 hours post-transfection. Fold changes were quantified relative to Cas9 only control group. (N = 3 independent transfections). (E) Schematic of Co-administration of AAV-TTN and AAV-Cas9 to mice via retro-orbital injection. (F) qRT-PCR analysis of TTN mRNA in spleen samples after AAV-TTN and AAV-Cas9 co-injections. Gene expression fold changes were quantified relative to AAV-GFP control mice treated with tetracycline (N = 7 for AAV-TTN groups and N = 6 for AAV-GFP groups) **P <0.01 indicates statistical significance measured by Students' t-test. Tet = tetracycline.

Building upon our previously published CRISPR responsive promoters⁴, we designed the AAV transfer vector to contain minimum seven safety gRNA target sites in locations that do not interfere with expression of transgenes from AAV. More precisely, we inserted two safety gRNA target sites upstream and downstream of TATA box in U6 promoter driving working gRNAU6 promoter, four target sites within the promoter region of the activation domains and one immediately upstream of the Poly (A) (Figure 4.2-A).

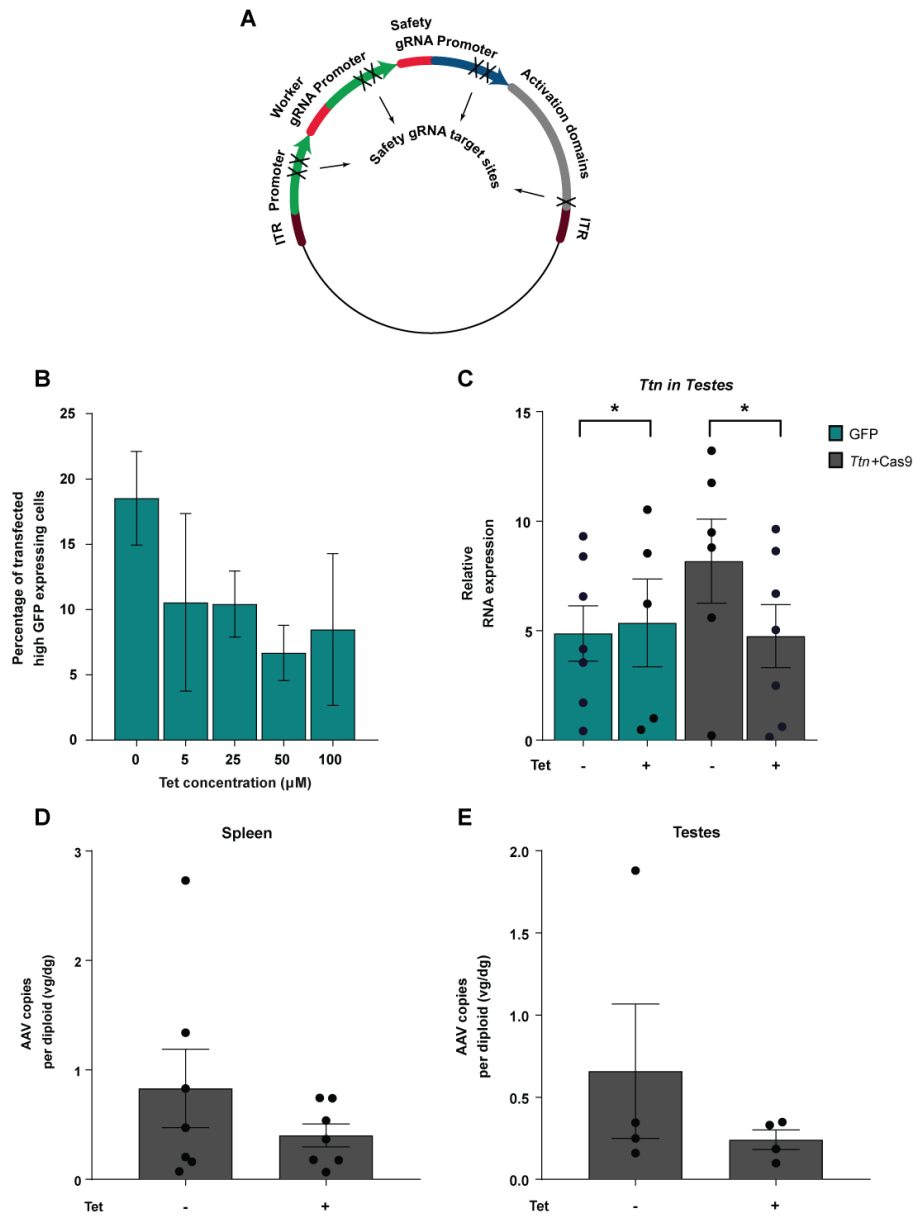


Figure 4.2. Validation of CRISPR control switch *in vivo*. (A) Schematic representation of the AAV transfer vector encoding all-in-one CRISPR based control switch. (B) Data shows mean \pm SD of geometric mean of GFP expression 48 hours after transfection of HEK293FT cells. Percentage of high GFP expressing cells was assessed by flow cytometry in cells expressing $>2 \times 10^2$ A.U of a transfection marker. (N = 3

biologically independent samples). (C) qRT-PCR analysis of *Ttn* mRNA level in testes 3 weeks post co-administration of AAV-TTN and AAV-Cas9 to C57BL/6 mice. Fold changes were quantified relative to AAV-GFP control with tetracycline treatment (N = 5-7) **P* <0.05. (D and E) qPCR analysis of AAV genome copy number in spleen (D) and testes (E) in mice receiving AAV-TTN and AAV-Cas9 with and without tetracycline treatment. AAV genomic copies per mouse diploid genome were calculated against standard curves for both viral inverted terminal repeats (ITRs) and the mouse *Acvr2b* sequence (N = 4-7). Tet = tetracycline.

To determine whether the safety gRNA is responsive to tetracycline, we first co-delivered the circuit into HEK293 cells together with Cas9 expression cassette. We cultured the cells in the presence and absence of different tetracycline concentrations and performed qRT-PCR and flow cytometry to measure GFP expression, as a surrogate for the integrity of the AAV vector. As demonstrated in Figure 4.1-B and Figure 4.2-B, we observed a stepwise reduction in GFP expressing cells following the addition of tetracycline both by qPCR and flow cytometry, which hint to the activation of the safety 20nt gRNA and disruption of the circuit after addition of Tetracycline. To further evaluate the function of entire control switch *in vitro*, we designed “worker” gRNA to target titin (*Ttn*) promoter, which encodes one of the largest proteins in mouse and human with crucial functional and structural roles in muscles and similar tissues. We transfected mouse Neuroblastoma cell line (Neuro-2A cells) with Cas9 expression cassette as well as an AAV transfer vector containing 14nt “worker” gRNA targeting *Ttn*, 20nt “safety” gRNA and MS2-activator (MS2-HSF1-P65) cassette and examined the circuit function 72 hours later (Figure 4.1-C). Our data demonstrate activation of *Ttn*, and near complete

turn-off of the *Ttn* expression upon addition of tetracycline. Next, we extended our approach to human HEK 293FT cell line targeting endogenous *CYP3A4* (a key member of the cytochrome P450 family of metabolizing enzymes). We showed around 600-fold activation using 14nt gRNA and Cas9 nuclease competent protein. We could dramatically reduce such expression via activation of a 20nt safety gRNA subsequent to addition of tetracycline (Figure 4.1-D). Having demonstrated the efficient functionality of this safety switch *in vitro*, we tested the functionality of this engineered system *in vivo*. We packaged the engineered genetic circuit in AAVDJ capsid, a synthetic AAV serotype, able to efficiently transduce a broad range of cell types⁵. The AAV2/DJ viruses harboring our engineered genetic circuit and Cas9 nuclease were delivered systemically into 6 to 8-week-old C57Bl/6 mice. Three weeks post injections, subgroups of mice were treated with tetracycline for three consecutive days prior to harvesting tissues. Following tissue harvest, we detected high *Ttn* activation in spleen (Figure 4.1-F). Furthermore, *Ttn* expression was significantly reduced in mice receiving tetracycline treatment. In agreement with previous reports, we also detected CRISPR activity in reproductive organs (Testes) following systemic delivery⁶. We observed modest activation of *Ttn* in testes, which was further reduced by tetracycline treatment and induction of safety gRNA (Figure 4.2-C). The detection of CRISPR activity in testes was particularly intriguing, considering the biosafety concerns of CRISPR therapies. Measurement of AAV virus titer in spleen and testes further demonstrates that tetracycline leads to a decrease in the AAV titer in CRISPR treated mice as compared to GFP treated mice that did not receive tetracycline. (Figure 4.2-D and E). Collectively, these results provide proof of concept for

the utility of multifunctional CRISPR/Cas9 in the generation of control switches that regulate both CRISPR action and the virus titer for *in vivo* gene therapies.

4.4. Discussions

Employment of a nuclease competent Cas9 and a truncated gRNA in this study opens an opportunity for simultaneous application of CRISPR for targeted gene editing while modulating the inflammatory response in the targeted tissue. AAV vectors reside in cells for a long time and this prolonged expression of CRISPR in tissues raises the concern that the possible unwanted effects could be exacerbated, specifically when a longer-term expression is desired to achieve durable epigenetic modulation. Therefore, built-in control switches will provide a layer of safety and control for CRISPR epigenetic and genetic therapies. Our proposed approach provides proof of concept that CRISPR multifunctionality can be exploited to mitigate safety concerns and induce controllability for both CRISPR and its delivery platform. This can be a strategy that mandates less complicated FDA regulations for clinical trials compared to incorporating other exogenous protein regulators as it is based on only one operational system, here CRISPR itself.

References

- 1 Kiani, S. *et al.* Cas9 gRNA engineering for genome editing, activation and repression. *Nature methods* **12**, 1051 (2015).
- 2 Liu, Y. *et al.* Directing cellular information flow via CRISPR signal conductors. *Nature methods* **13**, 938 (2016).

- 3 Konermann, S. *et al.* Genome-scale transcriptional activation by an engineered CRISPR-Cas9 complex. *Nature* **517**, 583 (2015).
- 4 Kiani, S. *et al.* CRISPR transcriptional repression devices and layered circuits in mammalian cells. *Nature methods* **11**, 723 (2014).
- 5 Grimm, D. *et al.* In vitro and in vivo gene therapy vector evolution via multispecies interbreeding and retargeting of adeno-associated viruses. *Journal of virology* **82**, 5887-5911 (2008).
- 6 Chew, W. L. *et al.* A multifunctional AAV-CRISPR-Cas9 and its host response. *Nature methods* **13**, 868 (2016).

CHAPTER 5

DISCUSSION

CRISPR-based therapeutics face several challenges that necessitate further work before clinical applications can be tested. Increasing CRISPR specificity to minimize genomic off-target effect, improving CRISPR gene editing efficiency, spatiotemporal regulation of the CRISPR activity *in vivo*, controlling possible adverse immune responses to CRISPR, and the appropriate method of delivery are among the biggest challenges that need to be properly addressed before translating CRISPR technologies to clinic.

Among these challenges, I have addressed three major barriers for human applications of CRISPR genetic/epigenetic therapies. Being a bacterial derived system, patient immune response to CRISPR is a key concern as clinical trials begin. However, to date, only limited studies have explored this aspect. In chapter 2, we detected antibodies to *Streptococcus pyogenes* Cas9 (SpCas9) in at least 5% of 143 healthy individuals. We also reported pre-existing human CD8⁺ T cell immunity in the majority of healthy individuals screened. We identified two immunodominant SpCas9 T cell epitopes for HLA-A*02:01 using an enhanced prediction algorithm that incorporates T cell receptor contact residue hydrophobicity and HLA binding and evaluated them by T cell assays using healthy donor PBMCs. In a proof-of-principle study, we demonstrated that Cas9 protein can be modified to eliminate immunodominant epitopes through targeted mutation while preserving its function and specificity. Our study highlighted the problem of pre-existing immunity against CRISPR-associated nucleases and offers a potential solution to mitigate the T cell immune response. Further studies are needed to enhance

our understanding and ability to control immune response against CRISPR before its human translation can be explored.

CRISPR-based modulation of gene expression will be beneficial for a variety of complex diseases such as inflammatory and autoimmune diseases, in which expression of multiple genes is dysregulated. Clinical implementation of CRISPR–Cas9 requires comprehensive evaluation of its *in vivo* profile. In chapter 3, we established platforms for CRISPR-mediated transcriptional modulators of endogenous genes and showed modulation of potential host responses to CRISPR-based therapies. We provided the first proof of concept study to modulate “therapy induced inflammatory response” by CRISPR-mediated transient repression of endogenous genes *in vivo*. Although further studies are needed to decode exact repression dynamics and design principles of this approach, the findings set the stage to use CRISPR to reprogram body’s own protective mechanisms in combating inflammation, e.g. subsequent to viral exposure. We showed that this system is effective *in* modulating layers of downstream signaling and can create a visible protective phenotype *in vivo*.

To spatiotemporally control CRISPR function, several rational design approaches have been developed. such as developing light-activated CRISPR/Cas9 effectors (LACE), Doxycycline inducible CRISPR-Cas9 system promoter specific Cas9 activity. Recently, naturally occurring off-switches in bacteria have been described for CRISPR system from *N. meningitidis*. The anti-CRISPR proteins could bind the Cas9 protein in human cells and disable gene editing, although quite in the beginning of the road, these naturally occurring anti-CRISPRs could also someday be useful in controlling CRISPR functions at the tissue of interest in human therapies. gRNA engineering is another component of

CRISPR that is capable of augmenting CRISPR customizability and controllability. By including modified riboswitches within gRNA that are responsive to small molecules or endogenous signaling protein, above mentioned engineering approaches leverage multi-component nature and modularity of the CRISPR system. Employment of a nuclease competent Cas9 and a truncated gRNA in my work enabled simultaneous application of CRISPR for targeted gene editing. Although administration of immunosuppressive drugs can be used to control adverse reactions, their application may be contraindicated in certain patient populations with conditions such as chronic infectious diseases and poses systemic side effects. Concomitant control of immune response against AAV and Cas9 in tissues that pick up CRISPR therapies can be employed in conjunction with immunosuppression to facilitate therapies and reduce unintended side effects. AAV vectors reside in cells for a long time and this prolonged expression of CRISPR in tissues raises the concern that the possible untoward effects could be exacerbated, specifically when a longer-term expression is desired to achieve durable epigenetic modulation. Therefore, built-in control switches will provide a layer of safety and control for CRISPR epigenetic/genetic therapies. Our proposed approach provided proof of concept that CRISPR multifunctionality can be exploited to mitigate safety concerns and induce controllability. This can be a strategy that mandates less complicated FDA regulations for clinical trials compared to incorporating other exogenous protein regulators as it is based on only one operational system, here CRISPR itself.

REFERENCES

- Abifadel, M., et al. (2003). "Mutations in PCSK9 cause autosomal dominant hypercholesterolemia." *Nature genetics* 34(2): 154.
- Ablain, J., et al. (2015). "A CRISPR/Cas9 vector system for tissue-specific gene disruption in zebrafish." *Dev Cell* 32(6): 756-764.
- Abudayyeh, O. O., et al. (2016). "C2c2 is a single-component programmable RNA-guided RNA-targeting CRISPR effector." *Science* 353(6299): aaf5573.
- Agne, M., et al. (2014). "Modularized CRISPR/dCas9 effector toolkit for target-specific gene regulation." *ACS Synth Biol* 3(12): 986-989.
- Ahi, Y. S., et al. (2011). "Adenoviral Vector Immunity: Its Implications and circumvention strategies." *Current gene therapy* 11(4): 307-320.
- Aldhamen, Y. A. and A. Amalfitano (2016). 16 - Methods to Mitigate Immune Responses to Adenoviral Vectors A2 - Curiel, David T. *Adenoviral Vectors for Gene Therapy (Second Edition)*. San Diego, Academic Press: 391-422.
- Amabile, A., et al. (2016). "Inheritable Silencing of Endogenous Genes by Hit-and-Run Targeted Epigenetic Editing." *Cell* 167(1): 219-232 e214.
- Anderson, K. S., et al. (2015). "HPV16 antibodies as risk factors for oropharyngeal cancer and their association with tumor HPV and smoking status." *Oral Oncol* 51(7): 662-667.
- Auer, T. O., et al. (2014). "Highly efficient CRISPR/Cas9-mediated knock-in in zebrafish by homology-independent DNA repair." *Genome Res* 24(1): 142-153.
- Balboa, D., et al. (2015). "Conditionally Stabilized dCas9 Activator for Controlling Gene Expression in Human Cell Reprogramming and Differentiation." *Stem Cell Reports* 5(3): 448-459.
- Bartel, M., et al. (2011). "Enhancing the Clinical Potential of AAV Vectors by Capsid Engineering to Evade Pre-Existing Immunity." *Front Microbiol* 2: 204.
- Bengtsson, N. E., et al. (2017). "Muscle-specific CRISPR/Cas9 dystrophin gene editing ameliorates pathophysiology in a mouse model for Duchenne muscular dystrophy." *Nat Commun* 8: 14454.
- Bisht, K., et al. (2017). "A lentivirus-free inducible CRISPR-Cas9 system for efficient targeting of human genes." *Anal Biochem* 530: 40-49.

Bolotin, A., et al. (2005). "Clustered regularly interspaced short palindrome repeats (CRISPRs) have spacers of extrachromosomal origin." *Microbiology* 151(Pt 8): 2551-2561.

Boutin, S., et al. (2010). "Prevalence of serum IgG and neutralizing factors against adeno-associated virus (AAV) types 1, 2, 5, 6, 8, and 9 in the healthy population: implications for gene therapy using AAV vectors." *Hum Gene Ther* 21(6): 704-712.

Braun, C. J., et al. (2016). "Versatile in vivo regulation of tumor phenotypes by dCas9-mediated transcriptional perturbation." *Proc Natl Acad Sci U S A* 113(27): E3892-3900.

Breinig, M., et al. (2019). "Multiplexed orthogonal genome editing and transcriptional activation by Cas12a." *Nature methods* 16(1): 51-54.

Briner, A. E., et al. (2014). "Guide RNA functional modules direct Cas9 activity and orthogonality." *Mol Cell* 56(2): 333-339.

Cantor, J. R., et al. (2011). "Therapeutic enzyme deimmunization by combinatorial T-cell epitope removal using neutral drift." *Proc Natl Acad Sci U S A* 108(4): 1272-1277.

Canzio, D., et al. (2011). "Chromodomain-mediated oligomerization of HP1 suggests a nucleosome-bridging mechanism for heterochromatin assembly." *Molecular cell* 41(1): 67-81.

Canzio, D., et al. (2014). "Mechanisms of functional promiscuity by HP1 proteins." *Trends in cell biology* 24(6): 377-386.

Cao, J., et al. (2016). "An easy and efficient inducible CRISPR/Cas9 platform with improved specificity for multiple gene targeting." *Nucleic Acids Res* 44(19): e149.

Carapetis, J. R., et al. (2005). "The global burden of group A streptococcal diseases." *Lancet Infect Dis* 5(11): 685-694.

Castle, M. J., et al. (2016). *Controlling AAV tropism in the nervous system with natural and engineered capsids. Gene Therapy for Neurological Disorders, Springer: 133-149.*

Cavazzana-Calvo, M., et al. (2000). "Gene therapy of human severe combined immunodeficiency (SCID)-X1 disease." *Science* 288(5466): 669-672.

Chavez, A., et al. (2015). "Highly efficient Cas9-mediated transcriptional programming." *Nat Methods* 12(4): 326-328.

Chavez, A., et al. (2016). "Comparison of Cas9 activators in multiple species." *Nat Methods* 13(7): 563-567.

Chen, B., et al. (2013). "Dynamic imaging of genomic loci in living human cells by an optimized CRISPR/Cas system." *Cell* 155(7): 1479-1491.

Chen, S., et al. (2005). "Efficient transduction of vascular endothelial cells with recombinant adeno-associated virus serotype 1 and 5 vectors." *Human gene therapy* 16(2): 235-247.

Chew, W. L. (2018). "Immunity to CRISPR Cas9 and Cas12a therapeutics." *Wiley Interdiscip Rev Syst Biol Med* 10(1).

Chew, W. L., et al. (2016). "A multifunctional AAV-CRISPR-Cas9 and its host response." *Nat Methods* 13(10): 868-874.

Chew, W. L., et al. (2016). "A multifunctional AAV-CRISPR-Cas9 and its host response." *Nature methods* 13(10): 868.

Cho, S.-Y. and J.-H. Choi (2014). "Biomarkers of sepsis." *Infection & chemotherapy* 46(1): 1-12.

Cho, S. W., et al. (2013). "Targeted genome engineering in human cells with the Cas9 RNA-guided endonuclease." *Nat Biotechnol* 31(3): 230-232.

Chowell, D., et al. (2015). "TCR contact residue hydrophobicity is a hallmark of immunogenic CD8+ T cell epitopes." *Proc Natl Acad Sci U S A* 112(14): E1754-1762.

Chu, V. T., et al. (2015). "Increasing the efficiency of homology-directed repair for CRISPR-Cas9-induced precise gene editing in mammalian cells." *Nat Biotechnol* 33(5): 543-548.

Cong, L., et al. (2013). "Multiplex genome engineering using CRISPR/Cas systems." *Science* 339(6121): 819-823.

Cyranoski, D. (2015). "Ethics of embryo editing divides scientists." *Nature* 519(7543): 272.

Cyranoski, D. (2016). "Chinese scientists to pioneer first human CRISPR trial." *Nature News* 535(7613): 476.

Dahlman, J. E., et al. (2015). "Orthogonal gene knockout and activation with a catalytically active Cas9 nuclease." *Nat Biotechnol* 33(11): 1159-1161.

Dandekar, A., et al. (2016). "Toll-like receptor (TLR) signaling interacts with CREBH to modulate high-density lipoprotein (HDL) in response to bacterial endotoxin." *Journal of Biological Chemistry* 291(44): 23149-23158.

Davis, A. J. and D. J. Chen (2013). "DNA double strand break repair via non-homologous end-joining." *Transl Cancer Res* 2(3): 130-143.

de Solis, C. A., et al. (2016). "The Development of a Viral Mediated CRISPR/Cas9 System with Doxycycline Dependent gRNA Expression for Inducible In vitro and In vivo Genome Editing." *Front Mol Neurosci* 9: 70.

Deltcheva, E., et al. (2011). "CRISPR RNA maturation by trans-encoded small RNA and host factor RNase III." *Nature* 471(7340): 602-607.

Didovyk, A., et al. (2016). "Transcriptional regulation with CRISPR-Cas9: principles, advances, and applications." *Curr Opin Biotechnol* 40: 177-184.

Dobin, A., et al. (2013). "STAR: ultrafast universal RNA-seq aligner." *Bioinformatics* 29(1): 15-21.

Doench, J. G., et al. (2016). "Optimized sgRNA design to maximize activity and minimize off-target effects of CRISPR-Cas9." *Nat Biotechnol* 34(2): 184-191.

Dow, L. E., et al. (2015). "Inducible in vivo genome editing with CRISPR-Cas9." *Nat Biotechnol* 33(4): 390-394.

Evers, B., et al. (2016). "CRISPR knockout screening outperforms shRNA and CRISPRi in identifying essential genes." *Nature biotechnology* 34(6): 631.

Friedland, A. E., et al. (2015). "Characterization of *Staphylococcus aureus* Cas9: a smaller Cas9 for all-in-one adeno-associated virus delivery and paired nickase applications." *Genome Biol* 16: 257.

Gao, G., et al. (2009). "Adeno-associated virus-mediated gene transfer to nonhuman primate liver can elicit destructive transgene-specific T cell responses." *Hum Gene Ther* 20(9): 930-942.

Gao, Y., et al. (2016). "Complex transcriptional modulation with orthogonal and inducible dCas9 regulators." *Nat Methods* 13(12): 1043-1049.

Garneau, J. E., et al. (2010). "The CRISPR/Cas bacterial immune system cleaves bacteriophage and plasmid DNA." *Nature* 468(7320): 67-71.

Gasiunas, G., et al. (2012). "Cas9-crRNA ribonucleoprotein complex mediates specific DNA cleavage for adaptive immunity in bacteria." *Proc Natl Acad Sci U S A* 109(39): E2579-2586.

Gaspar, H. B., et al. (2004). "Gene therapy of X-linked severe combined immunodeficiency by use of a pseudotyped gammaretroviral vector." *Lancet* 364(9452): 2181-2187.

Gilbert, L. A., et al. (2014). "Genome-scale CRISPR-mediated control of gene repression and activation." *Cell* 159(3): 647-661.

Gilbert, L. A., et al. (2013). "CRISPR-mediated modular RNA-guided regulation of transcription in eukaryotes." *Cell* 154(2): 442-451.

Gimenez, C. A., et al. (2016). "CRISPR-on system for the activation of the endogenous human INS gene." *Gene Ther* 23(6): 543-547.

Gomez, E. J., et al. (2016). "Light-Activated Nuclear Translocation of Adeno-Associated Virus Nanoparticles Using Phytochrome B for Enhanced, Tunable, and Spatially Programmable Gene Delivery." *ACS Nano* 10(1): 225-237.

Grimm, D., et al. (2008). "In vitro and in vivo gene therapy vector evolution via multispecies interbreeding and retargeting of adeno-associated viruses." *Journal of virology* 82(12): 5887-5911.

Guan, Y., et al. (2016). "CRISPR/Cas9-mediated somatic correction of a novel coagulator factor IX gene mutation ameliorates hemophilia in mouse." *EMBO Mol Med* 8(5): 477-488.

Guo, J., et al. (2017). "An inducible CRISPR-ON system for controllable gene activation in human pluripotent stem cells." *Protein Cell* 8(5): 379-393.

Gutschner, T., et al. (2016). "Post-translational Regulation of Cas9 during G1 Enhances Homology-Directed Repair." *Cell Rep* 14(6): 1555-1566.

Hacein-Bey-Abina, S., et al. (2002). "Sustained correction of X-linked severe combined immunodeficiency by ex vivo gene therapy." *N Engl J Med* 346(16): 1185-1193.

Hai, T., et al. (2014). "One-step generation of knockout pigs by zygote injection of CRISPR/Cas system." *Cell Res* 24(3): 372-375.

Hashimoto, M. and T. Takemoto (2015). "Electroporation enables the efficient mRNA delivery into the mouse zygotes and facilitates CRISPR/Cas9-based genome editing." *Sci Rep* 5: 11315.

Hemphill, J., et al. (2015). "Optical Control of CRISPR/Cas9 Gene Editing." *J Am Chem Soc* 137(17): 5642-5645.

Hilton, I. B., et al. (2015). "Epigenome editing by a CRISPR-Cas9-based acetyltransferase activates genes from promoters and enhancers." *Nat Biotechnol* 33(5): 510-517.

Hiragami, K. and R. Festenstein (2005). "Heterochromatin protein 1: a pervasive controlling influence." *Cellular and molecular life sciences CMLS* 62(23): 2711-2726.

Hoof, I., et al. (2009). "NetMHCpan, a method for MHC class I binding prediction beyond humans." *Immunogenetics* 61(1): 1.

Howe, S. J., et al. (2008). "Insertional mutagenesis combined with acquired somatic mutations causes leukemogenesis following gene therapy of SCID-X1 patients." *J Clin Invest* 118(9): 3143-3150.

Huang, X. and Y. Yang (2010). "Targeting the TLR9-MyD88 pathway in the regulation of adaptive immune responses." *Expert Opin Ther Targets* 14(8): 787-796.

Humphrey, W., et al. (1996). "VMD: Visual molecular dynamics." *Journal of Molecular Graphics* 14(1): 33-38.

Ibrahim, S. H. and K. D. Robertson (2018). "Use of the CRISPR/Cas9-Based Epigenetic Gene Activation System in Vivo: a New Potential Therapeutic Modality." *Hepatology*.

Janssens, S. and R. Beyaert (2002). "A universal role for MyD88 in TLR/IL-1R-mediated signaling." *Trends Biochem Sci* 27(9): 474-482.

Jiang, H., et al. (2006). "Effects of transient immunosuppression on adenoassociated, virus-mediated, liver-directed gene transfer in rhesus macaques and implications for human gene therapy." *Blood* 108(10): 3321-3328.

Jinek, M., et al. (2012). "A programmable dual-RNA-guided DNA endonuclease in adaptive bacterial immunity." *Science* 337(6096): 816-821.

Kalebic, N., et al. (2016). "CRISPR/Cas9-induced disruption of gene expression in mouse embryonic brain and single neural stem cells in vivo." *EMBO Rep* 17(3): 338-348.

Kaminski, R., et al. (2016). "Excision of HIV-1 DNA by gene editing: a proof-of-concept in vivo study." *Gene Ther* 23(8-9): 690-695.

Kapahnke, M., et al. (2016). "Random Splicing of Several Exons Caused by a Single Base Change in the Target Exon of CRISPR/Cas9 Mediated Gene Knockout." *Cells* 5(4).

Kay, M. A. (2011). "State-of-the-art gene-based therapies: the road ahead." *Nat Rev Genet* 12(5): 316-328.

Kearns, N. A., et al. (2015). "Functional annotation of native enhancers with a Cas9-histone demethylase fusion." *Nat Methods* 12(5): 401-403.

Kearns, N. A., et al. (2015). "Functional annotation of native enhancers with a Cas9-histone demethylase fusion." *Nature methods* 12(5): 401-403.

Kiani, S., et al. (2014). "CRISPR transcriptional repression devices and layered circuits in mammalian cells." *Nat Methods* 11(7): 723-726.

Kiani, S., et al. (2014). "CRISPR transcriptional repression devices and layered circuits in mammalian cells." *Nature methods* 11(7): 723.

Kiani, S., et al. (2015). "Cas9 gRNA engineering for genome editing, activation and repression." *Nature methods* 12(11): 1051.

Kiani, S., et al. (2015). "Cas9 gRNA engineering for genome editing, activation and repression." *Nat Methods* 12(11): 1051-1054.

Kim, D., et al. (2016). "Genome-wide analysis reveals specificities of Cpf1 endonucleases in human cells." *Nat Biotechnol* 34(8): 863-868.

Kim, H. K., et al. (2016). "In vivo high-throughput profiling of CRISPR-Cpf1 activity." *Nat Methods*.

Kim, Y. B., et al. (2017). "Increasing the genome-targeting scope and precision of base editing with engineered Cas9-cytidine deaminase fusions." *Nat Biotechnol* 35(4): 371-376.

King, C., et al. (2014). "Removing T-cell epitopes with computational protein design." *Proc Natl Acad Sci U S A* 111(23): 8577-8582.

Kleinstiver, B. P., et al. (2016). "High-fidelity CRISPR-Cas9 nucleases with no detectable genome-wide off-target effects." *Nature* 529(7587): 490-495.

Komor, A. C., et al. (2016). "Programmable editing of a target base in genomic DNA without double-stranded DNA cleavage." *Nature* 533(7603): 420-424.

Konermann, S., et al. (2013). "Optical control of mammalian endogenous transcription and epigenetic states." *Nature* 500(7463): 472-476.

Konermann, S., et al. (2015). "Genome-scale transcriptional activation by an engineered CRISPR-Cas9 complex." *Nature* 517(7536): 583.

Konermann, S., et al. (2015). "Genome-scale transcriptional activation by an engineered CRISPR-Cas9 complex." *Nature* 517(7536): 583-588.

- La Russa, M. F. and L. S. Qi (2015). "The new state of the art: Cas9 for gene activation and repression." *Molecular and cellular biology* 35(22): 3800-3809.
- Lanphier, E., et al. (2015). "Don't edit the human germ line." *Nature* 519(7544): 410-411.
- Levitskaya, J., et al. (1995). "Inhibition of antigen processing by the internal repeat region of the Epstein-Barr virus nuclear antigen-1." *Nature* 375(6533): 685-688.
- Liang, P., et al. (2015). "CRISPR/Cas9-mediated gene editing in human tripronuclear zygotes." *Protein Cell* 6(5): 363-372.
- Liang, X., et al. (2017). "Enhanced CRISPR/Cas9-mediated precise genome editing by improved design and delivery of gRNA, Cas9 nuclease, and donor DNA." *J Biotechnol* 241: 136-146.
- Liao, H.-K., et al. (2015). "Use of the CRISPR/Cas9 system as an intracellular defense against HIV-1 infection in human cells." *Nature communications* 6: 6413.
- Liao, H. K., et al. (2015). "Use of the CRISPR/Cas9 system as an intracellular defense against HIV-1 infection in human cells." *Nat Commun* 6: 6413.
- Liao, H. K., et al. (2017). "In Vivo Target Gene Activation via CRISPR/Cas9-Mediated Trans-epigenetic Modulation." *Cell* 171(7): 1495-1507 e1415.
- Lin, S., et al. (2014). "Enhanced homology-directed human genome engineering by controlled timing of CRISPR/Cas9 delivery." *Elife* 3: e04766.
- Lin, S. R., et al. (2014). "The CRISPR/Cas9 System Facilitates Clearance of the Intrahepatic HBV Templates In Vivo." *Mol Ther Nucleic Acids* 3: e186.
- Lin, X., et al. (2015). "Effect of TLR4/MyD88 signaling pathway on expression of IL-1beta and TNF-alpha in synovial fibroblasts from temporomandibular joint exposed to lipopolysaccharide." *Mediators Inflamm* 2015: 329405.
- Liu, K. I., et al. (2016). "A chemical-inducible CRISPR-Cas9 system for rapid control of genome editing." *Nat Chem Biol* 12(11): 980-987.
- Liu, Y., et al. (2014). "Synthesizing AND gate genetic circuits based on CRISPR-Cas9 for identification of bladder cancer cells." *Nat Commun* 5: 5393.
- Liu, Y., et al. (2016). "Directing cellular information flow via CRISPR signal conductors." *Nature methods* 13(11): 938.

Liu, Y., et al. (2016). "Directing cellular information flow via CRISPR signal conductors." *Nat Methods* 13(11): 938-944.

Long, C., et al. (2016). "Postnatal genome editing partially restores dystrophin expression in a mouse model of muscular dystrophy." *Science* 351(6271): 400-403.

Long, C., et al. (2014). "Prevention of muscular dystrophy in mice by CRISPR/Cas9-mediated editing of germline DNA." *Science* 345(6201): 1184-1188.

Lu, Y. and S. Song (2009). "Distinct immune responses to transgene products from rAAV1 and rAAV8 vectors." *Proc Natl Acad Sci U S A* 106(40): 17158-17162.

Lundstrom, K. (2015). "Alphaviruses in gene therapy." *Viruses* 7(5): 2321-2333.

Ma, X.-Y., et al. (2016). "Early prevention of trauma-related infection/sepsis." *Military Medical Research* 3(1): 33.

Maji, B., et al. (2017). "Multidimensional chemical control of CRISPR-Cas9." *Nat Chem Biol* 13(1): 9-11.

Mali, P., et al. (2013). "RNA-guided human genome engineering via Cas9." *Science* 339(6121): 823-826.

Mandal, P. K., et al. (2014). "Efficient ablation of genes in human hematopoietic stem and effector cells using CRISPR/Cas9." *Cell Stem Cell* 15(5): 643-652.

Manno, C. S., et al. (2006). "Successful transduction of liver in hemophilia by AAV-Factor IX and limitations imposed by the host immune response." *Nat Med* 12(3): 342-347.

Maresca, M., et al. (2013). "Obligate ligation-gated recombination (ObLiGaRe): custom-designed nuclease-mediated targeted integration through nonhomologous end joining." *Genome Res* 23(3): 539-546.

Marshall, E. (1999). "Gene Therapy Death Prompts Review of Adenovirus Vector." *Science* 286(5448): 2244-2245.

Martino, A. T., et al. (2013). "Engineered AAV vector minimizes in vivo targeting of transduced hepatocytes by capsid-specific CD8+ T cells." *Blood* 121(12): 2224-2233.

Matharu, N., et al. (2019). "CRISPR-mediated activation of a promoter or enhancer rescues obesity caused by haploinsufficiency." *Science* 363(6424): eaau0629.

Maxwell, K. N. and J. L. Breslow (2004). "Adenoviral-mediated expression of Pcsk9 in mice results in a low-density lipoprotein receptor knockout phenotype." *Proceedings of the National Academy of Sciences* 101(18): 7100-7105.

Mays, L. E. and J. M. Wilson (2011). "The complex and evolving story of T cell activation to AAV vector-encoded transgene products." *Mol Ther* 19(1): 16-27.

Mazor, R., et al. (2017). "Rational design of low immunogenic anti CD25 recombinant immunotoxin for T cell malignancies by elimination of T cell epitopes in PE38." *Cell Immunol* 313: 59-66.

McDonald, J. I., et al. (2016). "Reprogrammable CRISPR/Cas9-based system for inducing site-specific DNA methylation." *Biol Open* 5(6): 866-874.

Meehan, R. R., et al. (2003). "HP1 binding to native chromatin in vitro is determined by the hinge region and not by the chromodomain." *The EMBO journal* 22(12): 3164-3174.

Mekler, V., et al. (2016). "Kinetics of the CRISPR-Cas9 effector complex assembly and the role of 3'-terminal segment of guide RNA." *Nucleic Acids Res* 44(6): 2837-2845.

Merkel, S. F., et al. (2017). "Trafficking of adeno-associated virus vectors across a model of the blood-brain barrier; a comparative study of transcytosis and transduction using primary human brain endothelial cells." *Journal of neurochemistry* 140(2): 216-230.

Miller, J. B., et al. (2016). "Non-Viral CRISPR/Cas Gene Editing In Vitro and In Vivo Enabled by Synthetic Nanoparticle Co-Delivery of Cas9 mRNA and sgRNA." *Angew Chem Int Ed Engl*.

Miller, J. B., et al. (2017). "Non-Viral CRISPR/Cas Gene Editing In Vitro and In Vivo Enabled by Synthetic Nanoparticle Co-Delivery of Cas9 mRNA and sgRNA." *Angew Chem Int Ed Engl* 56(4): 1059-1063.

Mimee, M., et al. (2015). "Programming a Human Commensal Bacterium, *Bacteroides thetaiotaomicron*, to Sense and Respond to Stimuli in the Murine Gut Microbiota." *Cell Syst* 1(1): 62-71.

Mingozzi, F., et al. (2013). "Overcoming preexisting humoral immunity to AAV using capsid decoys." *Sci Transl Med* 5(194): 194ra192.

Mingozzi, F. and K. A. High (2013). "Immune responses to AAV vectors: overcoming barriers to successful gene therapy." *Blood* 122(1): 23-36.

Mingozzi, F., et al. (2007). "CD8(+) T-cell responses to adeno-associated virus capsid in humans." *Nat Med* 13(4): 419-422.

- Mojica, F. J., et al. (2005). "Intervening sequences of regularly spaced prokaryotic repeats derive from foreign genetic elements." *J Mol Evol* 60(2): 174-182.
- Mok, H., et al. (2008). "Enhancement of the CD8+ T cell response to a subdominant epitope of respiratory syncytial virus by deletion of an immunodominant epitope." *Vaccine* 26(37): 4775-4782.
- Moreno, A. M., et al. (2018). "In Situ Gene Therapy via AAV-CRISPR-Cas9-Mediated Targeted Gene Regulation." *Mol Ther* 26(7): 1818-1827.
- Moutaftsi, M., et al. (2006). "A consensus epitope prediction approach identifies the breadth of murine TCD8+-cell responses to vaccinia virus." *Nat Biotechnol* 24(7): 817.
- Murlidharan, G., et al. (2016). "CNS-restricted Transduction and CRISPR/Cas9-mediated Gene Deletion with an Engineered AAV Vector." *Mol Ther Nucleic Acids* 5(7): e338.
- Nakagawa, Y., et al. (2016). "Hyperlipidemia and hepatitis in liver-specific CREB3L3 knockout mice generated using a one-step CRISPR/Cas9 system." *Sci Rep* 6: 27857.
- Nelson, C. E., et al. (2016). "In vivo genome editing improves muscle function in a mouse model of Duchenne muscular dystrophy." *Science* 351(6271): 403-407.
- Nielsen, A. A. and C. A. Voigt (2014). "Multi-input CRISPR/Cas genetic circuits that interface host regulatory networks." *Mol Syst Biol* 10: 763.
- Nihongaki, Y., et al. (2015). "Photoactivatable CRISPR-Cas9 for optogenetic genome editing." *Nat Biotechnol* 33(7): 755-760.
- Nishimasu, H., et al. (2014). "Crystal Structure of Cas9 in Complex with Guide RNA and Target DNA." *Cell* 156(5): 935-949.
- Nissim, L., et al. (2014). "Multiplexed and programmable regulation of gene networks with an integrated RNA and CRISPR/Cas toolkit in human cells." *Mol Cell* 54(4): 698-710.
- Niu, Y., et al. (2014). "Generation of gene-modified cynomolgus monkey via Cas9/RNA-mediated gene targeting in one-cell embryos." *Cell* 156(4): 836-843.
- Nowak, C. M., et al. (2016). "Guide RNA engineering for versatile Cas9 functionality." *Nucleic Acids Res* 44(20): 9555-9564.
- Ousterout, D. G., et al. (2015). "Multiplex CRISPR/Cas9-based genome editing for correction of dystrophin mutations that cause Duchenne muscular dystrophy." *Nat Commun* 6: 6244.

Paglialunga, L., et al. (2016). "Immune checkpoint blockade in small cell lung cancer: is there a light at the end of the tunnel?" *ESMO Open* 1(4): e000022.

Paquet, D., et al. (2016). "Efficient introduction of specific homozygous and heterozygous mutations using CRISPR/Cas9." *Nature* 533(7601): 125-129.

Pardo, B., et al. (2009). "DNA repair in mammalian cells: DNA double-strand break repair: how to fix a broken relationship." *Cell Mol Life Sci* 66(6): 1039-1056.

Park, G. S. and J. H. Kim (2015). "LPS Up-Regulates ICAM-1 Expression in Breast Cancer Cells by Stimulating a MyD88-BLT2-ERK-Linked Cascade, Which Promotes Adhesion to Monocytes." *Mol Cells* 38(9): 821-828.

Pawluk, A., et al. (2016). "Naturally Occurring Off-Switches for CRISPR-Cas9." *Cell* 167(7): 1829-1838 e1829.

Plant, L., et al. (2006). "MyD88-dependent signaling affects the development of meningococcal sepsis by nonlipooligosaccharide ligands." *Infection and immunity* 74(6): 3538-3546.

Pollard, A. J. and M. C. J. Maiden (2001). *Meningococcal Vaccines*, Humana Press.

Polstein, L. R. and C. A. Gersbach (2015). "A light-inducible CRISPR-Cas9 system for control of endogenous gene activation." *Nat Chem Biol* 11(3): 198-200.

Qi, L. S., et al. (2013). "Repurposing CRISPR as an RNA-guided platform for sequence-specific control of gene expression." *Cell* 152(5): 1173-1183.

Rammensee, H.-G., et al. (1999). "SYFPEITHI: database for MHC ligands and peptide motifs." *Immunogenetics* 50(3-4): 213-219.

Ran, F. A., et al. (2015). "In vivo genome editing using *Staphylococcus aureus* Cas9." *Nature* 520(7546): 186-191.

Ran, F. A., et al. (2013). "Double nicking by RNA-guided CRISPR Cas9 for enhanced genome editing specificity." *Cell* 154(6): 1380-1389.

Reardon, S. (2016). "First CRISPR clinical trial gets green light from US panel." *Nature* 531.

Richardson, C. D., et al. (2016). "Enhancing homology-directed genome editing by catalytically active and inactive CRISPR-Cas9 using asymmetric donor DNA." *Nat Biotechnol* 34(3): 339-344.

Robinson, M. D., et al. (2010). "edgeR: a Bioconductor package for differential expression analysis of digital gene expression data." *Bioinformatics* 26(1): 139-140.

Ruan, G. X., et al. (2017). "CRISPR/Cas9-Mediated Genome Editing as a Therapeutic Approach for Leber Congenital Amaurosis 10." *Mol Ther* 25(2): 331-341.

Ruan, J., et al. (2015). "Highly efficient CRISPR/Cas9-mediated transgene knockin at the H11 locus in pigs." *Sci Rep* 5: 14253.

Salvat, R. S., et al. (2017). "Computationally optimized deimmunization libraries yield highly mutated enzymes with low immunogenicity and enhanced activity." *Proc Natl Acad Sci U S A* 114(26): E5085-E5093.

Sander, J. D. and J. K. Joung (2014). "CRISPR-Cas systems for editing, regulating and targeting genomes." *Nat Biotechnol* 32(4): 347-355.

Sapranauskas, R., et al. (2011). "The *Streptococcus thermophilus* CRISPR/Cas system provides immunity in *Escherichia coli*." *Nucleic Acids Res* 39(21): 9275-9282.

Scallan, C. D., et al. (2006). "Human immunoglobulin inhibits liver transduction by AAV vectors at low AAV2 neutralizing titers in SCID mice." *Blood* 107(5): 1810-1817.

Schnare, M., et al. (2001). "Toll-like receptors control activation of adaptive immune responses." *Nat Immunol* 2(10): 947-950.

Schultz, D. C., et al. (2002). "SETDB1: a novel KAP-1-associated histone H3, lysine 9-specific methyltransferase that contributes to HP1-mediated silencing of euchromatic genes by KRAB zinc-finger proteins." *Genes & development* 16(8): 919-932.

Schwank, G., et al. (2013). "Functional repair of CFTR by CRISPR/Cas9 in intestinal stem cell organoids of cystic fibrosis patients." *Cell Stem Cell* 13(6): 653-658.

Shechner, D. M., et al. (2015). "Multiplexable, locus-specific targeting of long RNAs with CRISPR-Display." *Nat Methods* 12(7): 664-670.

Shipman, S. L., et al. (2016). "Molecular recordings by directed CRISPR spacer acquisition." *Science* 353(6298): aaf1175.

Shmakov, S., et al. (2015). "Discovery and Functional Characterization of Diverse Class 2 CRISPR-Cas Systems." *Mol Cell* 60(3): 385-397.

Sim, X., et al. (2016). "A Doxycycline-Inducible System for Genetic Correction of iPSC Disease Models." *Methods Mol Biol* 1353: 13-23.

Simhadri, V. L., et al. (2018). "Prevalence of Pre-existing Antibodies to CRISPR-Associated Nuclease Cas9 in the USA Population." *Molecular therapy. Methods & clinical development* 10: 105-112.

Slymaker, I. M., et al. (2016). "Rationally engineered Cas9 nucleases with improved specificity." *Science* 351(6268): 84-88.

Sudres, M., et al. (2012). "MyD88 signaling in B cells regulates the production of Th1-dependent antibodies to AAV." *Mol Ther* 20(8): 1571-1581.

Sung, Y. H., et al. (2014). "Highly efficient gene knockout in mice and zebrafish with RNA-guided endonucleases." *Genome Res* 24(1): 125-131.

Suzuki, K., et al. (2016). "In vivo genome editing via CRISPR/Cas9 mediated homology-independent targeted integration." *Nature* 540(7631): 144-149.

Tanenbaum, M. E., et al. (2014). "A protein-tagging system for signal amplification in gene expression and fluorescence imaging." *Cell* 159(3): 635-646.

Tangri, S., et al. (2005). "Rationally engineered therapeutic proteins with reduced immunogenicity." *J Immunol* 174(6): 3187-3196.

Tebas, P., et al. (2014). "Gene editing of CCR5 in autologous CD4 T cells of persons infected with HIV." *N Engl J Med* 370(10): 901-910.

Tenzer, S., et al. (2005). "Modeling the MHC class I pathway by combining predictions of proteasomal cleavage, TAP transport and MHC class I binding." *Cellular and Molecular Life Sciences* 62(9): 1025-1037.

Thakore, P. I., et al. (2016). "Editing the epigenome: technologies for programmable transcription and epigenetic modulation." *Nature methods* 13(2): 127.

Thakore, P. I., et al. (2015). "Highly specific epigenome editing by CRISPR-Cas9 repressors for silencing of distal regulatory elements." *Nat Methods* 12(12): 1143-1149.

Thakore, P. I., et al. (2015). "Highly specific epigenome editing by CRISPR-Cas9 repressors for silencing of distal regulatory elements." *Nature methods* 12(12): 1143.

Thakore, P. I., et al. (2018). "RNA-guided transcriptional silencing in vivo with *S. aureus* CRISPR-Cas9 repressors." *Nat Commun* 9(1): 1674.

Thakore, P. I., et al. (2018). "RNA-guided transcriptional silencing in vivo with *S. aureus* CRISPR-Cas9 repressors." *Nature communications* 9(1): 1-9.

Thwaite, R., et al. (2015). "AAVrh.10 immunogenicity in mice and humans. Relevance of antibody cross-reactivity in human gene therapy." *Gene Ther* 22(2): 196-201.

Toth, E., et al. (2016). "Cpf1 nucleases demonstrate robust activity to induce DNA modification by exploiting homology directed repair pathways in mammalian cells." *Biol Direct* 11: 46.

Trapnell, C., et al. (2012). "Differential gene and transcript expression analysis of RNA-seq experiments with TopHat and Cufflinks." *Nature Protocols* 7(3): 562-578.

Tsai, S. Q., et al. (2017). "CIRCLE-seq: a highly sensitive in vitro screen for genome-wide CRISPR-Cas9 nuclease off-targets." *Nat Methods*.

Tsai, S. Q., et al. (2015). "GUIDE-seq enables genome-wide profiling of off-target cleavage by CRISPR-Cas nucleases." *Nat Biotechnol* 33(2): 187-197.

Van den Akker, T. W., et al. (1988). "The influence of genetic factors associated with the immunoglobulin heavy chain locus on the development of benign monoclonal gammopathy in ageing IgH-congenic mice." *Immunology* 65(1): 31.

Veron, P., et al. (2007). "Major subsets of human dendritic cells are efficiently transduced by self-complementary adeno-associated virus vectors 1 and 2." *J Virol* 81(10): 5385-5394.

Vita, R., et al. (2015). "The immune epitope database (IEDB) 3.0." *Nucleic Acids Res* 43(Database issue): D405-412.

Vojta, A., et al. (2016). "Repurposing the CRISPR-Cas9 system for targeted DNA methylation." *Nucleic Acids Res* 44(12): 5615-5628.

Wagner, D. L., et al. (2018). "High prevalence of *Streptococcus pyogenes* Cas9-reactive T cells within the adult human population." *Nature Medicine*.

Wang, D., et al. (2015). "Adenovirus-Mediated Somatic Genome Editing of Pten by CRISPR/Cas9 in Mouse Liver in Spite of Cas9-Specific Immune Responses." *Hum Gene Ther* 26(7): 432-442.

Wang, H., et al. (2013). "One-step generation of mice carrying mutations in multiple genes by CRISPR/Cas-mediated genome engineering." *Cell* 153(4): 910-918.

Wang, J., et al. (2013). "A versatile protein microarray platform enabling antibody profiling against denatured proteins." *Proteomics Clin Appl* 7(5-6): 378-383.

Wang, M., et al. (2016). "Efficient delivery of genome-editing proteins using bio-reducible lipid nanoparticles." *Proc Natl Acad Sci U S A* 113(11): 2868-2873.

Wang, X., et al. (2016). "One-step generation of triple gene-targeted pigs using CRISPR/Cas9 system." *Sci Rep* 6: 20620.

Wang, Z., et al. (2004). "Detection of integration of plasmid DNA into host genomic DNA following intramuscular injection and electroporation." *Gene Ther* 11(8): 711-721.

Warner, N. and G. Nunez (2013). "MyD88: a critical adaptor protein in innate immunity signal transduction." *J Immunol* 190(1): 3-4.

Wei, Y., et al. (2016). "Prevention of Muscle Wasting by CRISPR/Cas9-mediated Disruption of Myostatin In Vivo." *Mol Ther* 24(11): 1889-1891.

Wofl, M., et al. (2007). "Activation-induced expression of CD137 permits detection, isolation, and expansion of the full repertoire of CD8+ T cells responding to antigen without requiring knowledge of epitope specificities." *Blood* 110(1): 201-210.

Wright, A. V., et al. (2015). "Rational design of a split-Cas9 enzyme complex." *Proc Natl Acad Sci U S A* 112(10): 2984-2989.

Wu, Y., et al. (2013). "Correction of a genetic disease in mouse via use of CRISPR-Cas9." *Cell Stem Cell* 13(6): 659-662.

Wyvekens, N., et al. (2015). "Dimeric CRISPR RNA-Guided FokI-dCas9 Nucleases Directed by Truncated gRNAs for Highly Specific Genome Editing." *Hum Gene Ther* 26(7): 425-431.

Xu, L., et al. (2016). "CRISPR-mediated Genome Editing Restores Dystrophin Expression and Function in mdx Mice." *Mol Ther* 24(3): 564-569.

Xu, L., et al. (2017). "Empower multiplex cell and tissue-specific CRISPR-mediated gene manipulation with self-cleaving ribozymes and tRNA." *Nucleic acids research* 45(5): e28-e28.

Xu, L., et al. (2017). "Empower multiplex cell and tissue-specific CRISPR-mediated gene manipulation with self-cleaving ribozymes and tRNA." *Nucleic Acids Res* 45(5): e28.

Xu, X., et al. (2018). "High-fidelity CRISPR/Cas9-based gene-specific hydroxymethylation rescues gene expression and attenuates renal fibrosis." *Nature communications* 9(1): 1-15.

Xu, X., et al. (2016). "A CRISPR-based approach for targeted DNA demethylation." *Cell Discov* 2: 16009.

Yang, L., et al. (2016). "Engineering and optimising deaminase fusions for genome editing." *Nat Commun* 7: 13330.

Yang, Y., et al. (2016). "A dual AAV system enables the Cas9-mediated correction of a metabolic liver disease in newborn mice." *Nat Biotechnol* 34(3): 334-338.

Yao, Z., et al. (2016). "Blood-borne lipopolysaccharide is rapidly eliminated by liver sinusoidal endothelial cells via high-density lipoprotein." *The Journal of Immunology* 197(6): 2390-2399.

Yeo, N. C., et al. (2018). "An enhanced CRISPR repressor for targeted mammalian gene regulation." *Nature methods* 15(8): 611.

Yeung, V. P., et al. (2004). "Elimination of an Immunodominant CD4⁺ T Cell Epitope in Human IFN- β Does Not Result in an In Vivo Response Directed at the Subdominant Epitope." *The Journal of Immunology* 172(11): 6658-6665.

Yewdell, J. W. and A. B. Hill (2002). "Viral interference with antigen presentation." *Nature Immunology* 3: 1019.

Yin, H., et al. (2014). "Non-viral vectors for gene-based therapy." *Nat Rev Genet* 15(8): 541-555.

Yin, H., et al. (2016). "Therapeutic genome editing by combined viral and non-viral delivery of CRISPR system components in vivo." *Nat Biotechnol* 34(3): 328-333.

Yin, H., et al. (2014). "Genome editing with Cas9 in adult mice corrects a disease mutation and phenotype." *Nat Biotechnol* 32(6): 551-553.

Yoshioka, S., et al. (2015). "Development of a mono-promoter-driven CRISPR/Cas9 system in mammalian cells." *Sci Rep* 5: 18341.

Yu, C., et al. (2015). "Small molecules enhance CRISPR genome editing in pluripotent stem cells." *Cell Stem Cell* 16(2): 142-147.

Yu, M., et al. (2014). "MyD88-dependent interplay between myeloid and endothelial cells in the initiation and progression of obesity-associated inflammatory diseases." *J Exp Med* 211(5): 887-907.

Yu, W., et al. (2017). "Nrl knockdown by AAV-delivered CRISPR/Cas9 prevents retinal degeneration in mice." *Nat Commun* 8: 14716.

Yu, X., et al. (2018). "MYD88 L265P mutation in lymphoid malignancies." *Cancer research* 78(10): 2457-2462.

Zalatan, J. G., et al. (2015). "Engineering complex synthetic transcriptional programs with CRISPR RNA scaffolds." *Cell* 160(1-2): 339-350.

Zetsche, B., et al. (2015). "Cpf1 is a single RNA-guided endonuclease of a class 2 CRISPR-Cas system." *Cell* 163(3): 759-771.

Zetsche, B., et al. (2015). "A split-Cas9 architecture for inducible genome editing and transcription modulation." *Nat Biotechnol* 33(2): 139-142.

Zhang, H., et al. (2016). "Sepsis induces hematopoietic stem cell exhaustion and myelosuppression through distinct contributions of TRIF and MYD88." *Stem cell reports* 6(6): 940-956.

Zhang, Y., et al. (2017). "CRISPR-Cpf1 correction of muscular dystrophy mutations in human cardiomyocytes and mice." *Sci Adv* 3(4): e1602814.

Zheng, Y., et al. (2018). "CRISPR interference-based specific and efficient gene inactivation in the brain." *Nat Neurosci* 21(3): 447-454.

Zhou, H., et al. (2018). "In vivo simultaneous transcriptional activation of multiple genes in the brain using CRISPR-dCas9-activator transgenic mice." *Nat Neurosci* 21(3): 440-446.

Zhu, J., et al. (2009). "The TLR9-MyD88 pathway is critical for adaptive immune responses to adeno-associated virus gene therapy vectors in mice." *J Clin Invest* 119(8): 2388-2398.

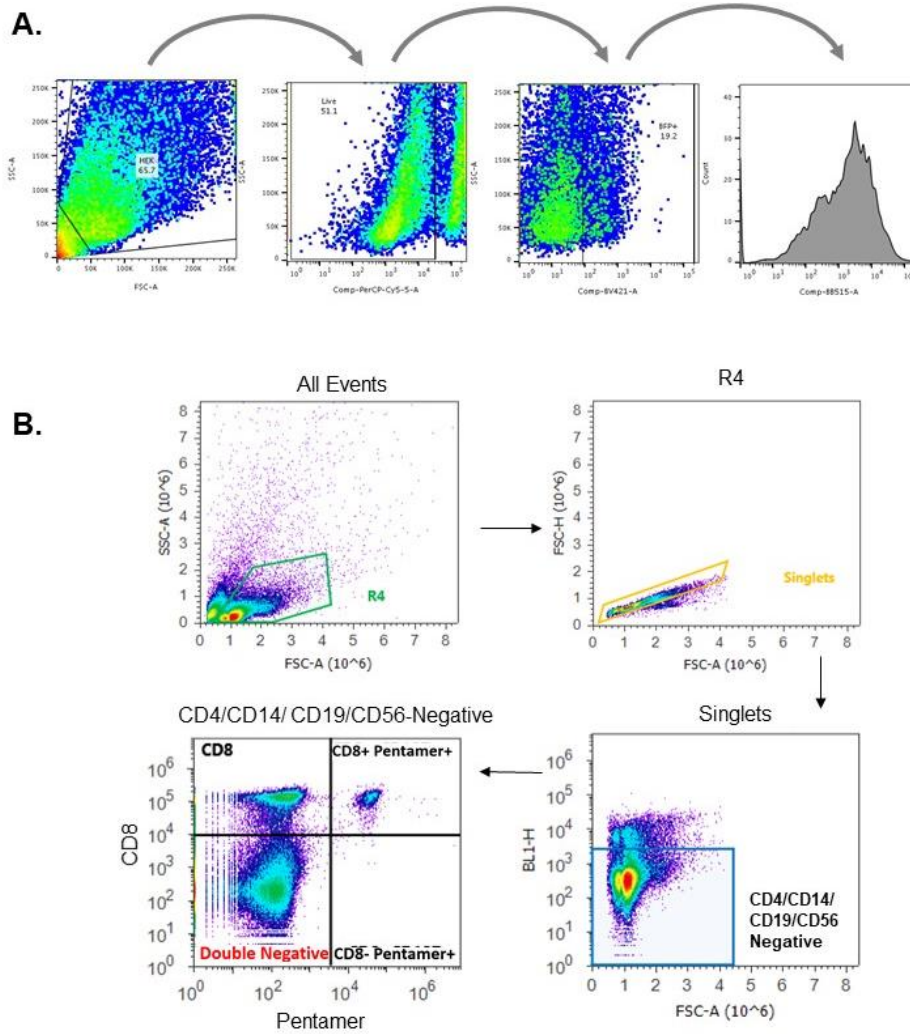
Zolnik, B. S., et al. (2010). "Nanoparticles and the immune system." *Endocrinology* 151(2): 458-465.

Zuris, J. A., et al. (2015). "Cationic lipid-mediated delivery of proteins enables efficient protein-based genome editing in vitro and in vivo." *Nat Biotechnol* 33(1): 73-80.

APPENDIX A

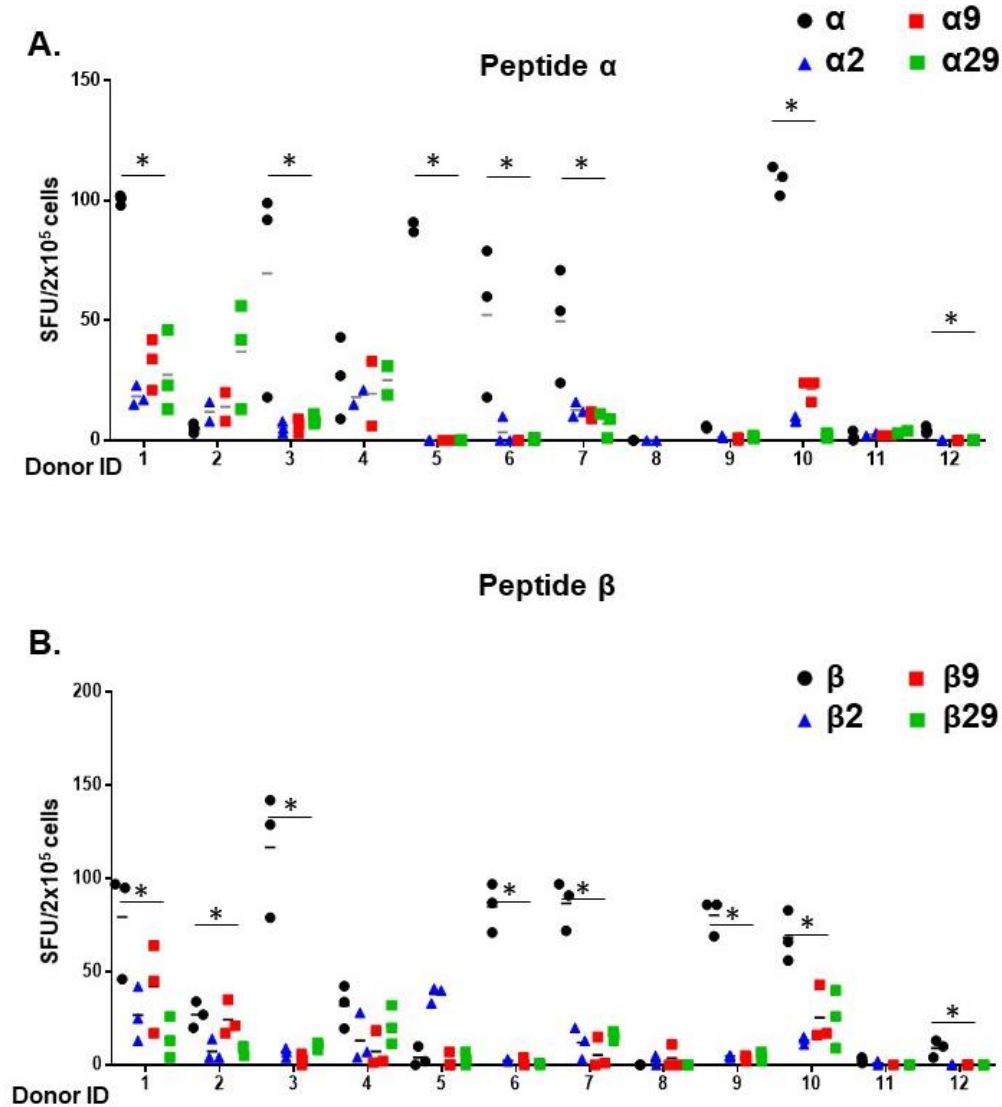
SUPPORTING INFORMATION FOR MULTIFUNCTIONAL CRISPR-CAS9 WITH ENGINEERED IMMUNOSILENCED HUMAN T CELL EPITOPES

Supplementary Figures

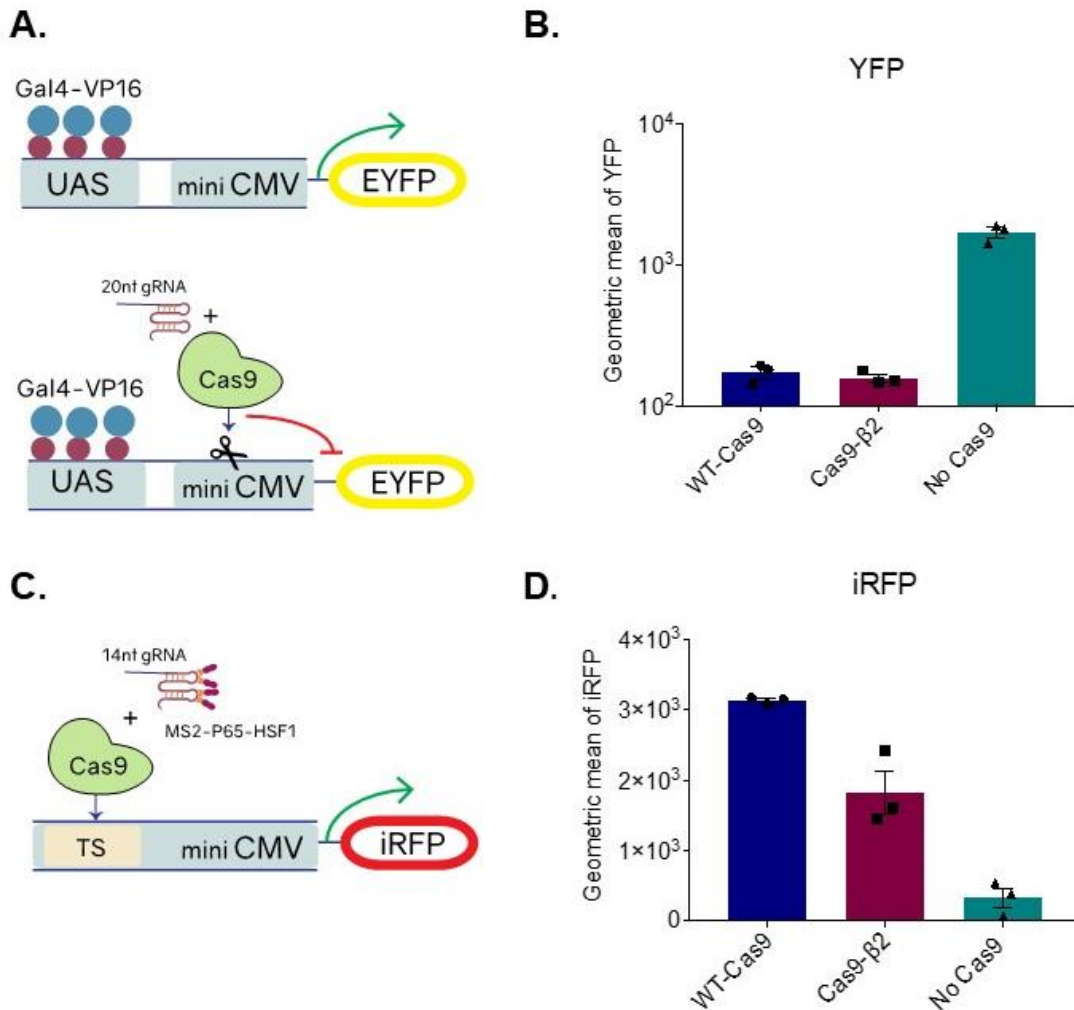


Supplementary Figure 2.1. A. Representative flow cytometry gating for analysis of Cas9 function on synthetic promoters. Cells are gated based on Forward (FSC) and Side Scatter (SSCs). Live cells (PerCP negative population) are selected and then the transfected population is gated based on the expression of a transfection control (here BFP-BV421) more than 2×10^2 A.U. The geometric mean of the output (here YFP-BB515) is determined in this population. B. Flow cytometry gating for analysis of Cas9 pentamer+ CD8+ T lymphocytes (Fig. 2A, B). Cells are gated based on FSC and SSC

and negatively gated on CD4/CD14/CD19/CD56. The CD8-, CD8+, and Cas9 pentamer+ population are shown (bottom right).

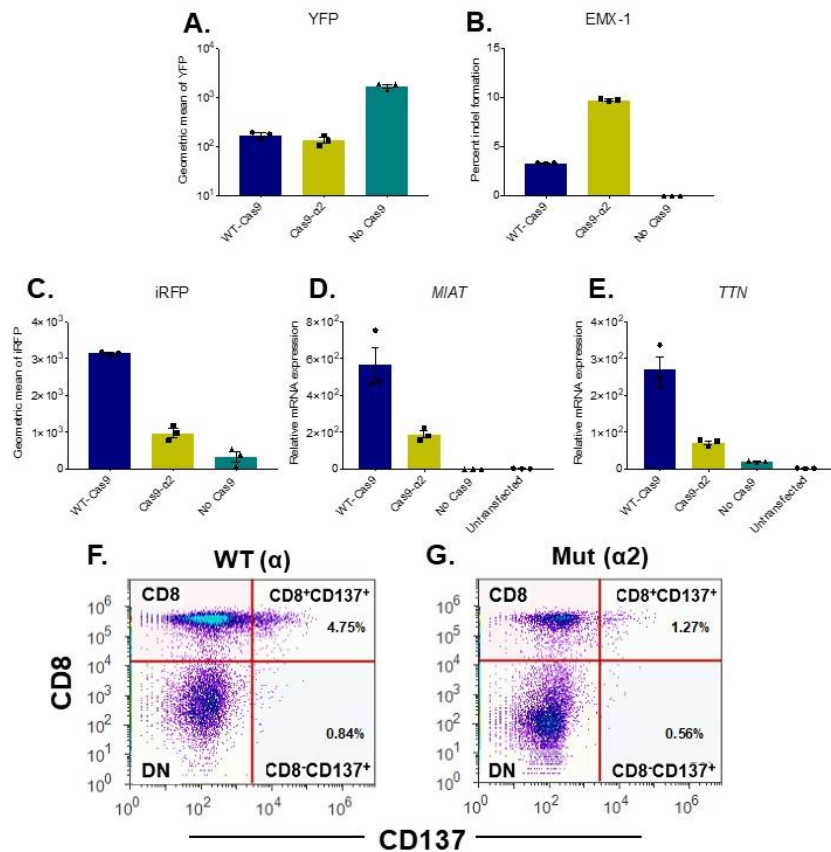


Supplementary Figure 2.2. Reduced T cell response to epitopes α and β after mutation of the anchor residues. (A) and (B). IFN- γ ELISpot for 12 healthy donor PBMCs stimulated with wild type or mutated peptide α (A) or β (B). *Significant SFU change (corrected p value<0.03, 5% FDR; see Supplementary Table 4). Statistical analysis was performed post hoc and results are exploratory.



Supplementary Figure 2.3. A. Schematic of the experiment assessing Cas9-β2 cleavage capacity at a synthetic promoter. Cells were transfected with either WT-Cas9, Cas9-β2 or an empty plasmid as well as 20nt gRNA targeting a synthetic CRISPR promoter that harbors two gRNA target sites flanking a mini-CMV promoter. The targeting and cleavage at the promoter should disrupt the promoter and decrease EYFP expression. B. Each individual dot represents EYFP expression 48 hours after transfection in cells expressing $>2 \times 10^2$ A.U. of a transfection marker (BFP) measured by flow cytometry ($n=3$ independent technical replicates). C. Schematic of the experiment assessing Cas9-β2 transcriptional activation capacity at a synthetic promoter. Cells were transfected with

either WT-Cas9, Cas9- $\beta 2$ or an empty plasmid as well as aptamer binding transcriptional activation domains, and a 14nt gRNA targeting a synthetic CRISPR promoter that harbors multiple target sites upstream of a mini-CMV promoter. Targeting the promoter should enable iRFP expression. D. Each individual dot shows iRFP expression 48 hours after transfection in cells expressing $>2 \times 10^2$ A.U. of a transfection marker (GFP) measured by flow cytometry (n=3 independent technical replicates). Data are presented as mean \pm S.E.M.



Supplementary Figure 2.4. A. Analysis of cleavage capacity of Cas9- $\alpha 2$ as compared to WT-Cas9 in a synthetic promoter. Each individual dot shows EYFP expression 48 hours after transfection in cells expressing $>2 \times 10^2$ A.U. of a transfection marker measured by flow cytometry (n=3 independent technical replicates). B. Percentage of indel formation

in *EMX-1* locus (n=3 independent technical replicates). C. Transcriptional modulation by Cas9- $\alpha 2$ at a synthetic promoter. Each individual dot shows iRFP expression 48 hours after transfection in cells expressing $>2 \times 10^2$ A.U. of a transfection marker measured by flow cytometry (n=3 independent technical replicates). D, E. Data represent the mRNA level relative to an untransfected control experiment. Note for A and C: WT-Cas9 and no Cas9 data are also reported in Supplementary Figure 2. For B-E: WT-Cas9 and no Cas9 data are also reported in Fig.3. (n=3 independent technical replicates). Data represent mean \pm S.E.M. F. Activated CD8+CD137+ T cells detected in PBMCs stimulated with peptide α were reduced in PBMCs stimulated with peptide $\alpha 2$ (data representative of 3 individual stimulations).

Supplementary Tables

Rank	Position	Sequence	Code	Binding			Protein Processing			S _b	S _i	S _b .S _i
				IEDB	NetMHC	SyFpeithi	IEDB	ANN				
1	988-997	YLNAVVG TAL	γ	1.25	21.5	24	0.27	0.02	0.068	0.975	0.002	
2	1281-1290	ILADANLDKV		1.25	11.37	31	-0.06	-0.49	0.003	0.447	0.002	
3	236-244	GLFGNLI AL	δ	0.6	10.12	29	1.15	1.04	0.020	0.900	0.002	
4	240-248	NLI ALSGL	α	1.7	61.18	25	0.15	0.22	0.061	0.903	0.006	
5	615-623	ILEDIVL TL	β	1.5	53.29	29	0.28	0.56	0.023	0.710	0.007	
6	614-623	DILEDIVL TL		4.6	3105.79	28	-1.53	-1.02	0.063	0.888	0.007	
7	719-727	SLHEHIANL		1.4	9.14	30	0.93	0.82	0.013	0.380	0.008	
8	415-423	HLGELHAIL		4.4	276.73	25	-0.75	-0.81	0.071	0.876	0.009	
9	300-308	ILLSDILRV		0.3	6.51	29	0.67	0.7	0.019	0.404	0.011	
10	1086-1095	VLSMPQVNIV		3.65	178.87	26	-1.05	-1.43	0.059	0.758	0.014	
11	719-728	SLHEHIANLA		4.7	60.17	19	-0.98	-1.74	0.126	0.890	0.014	
12	1194-1203	LIILKPKYSL		8.5	966.31	25	-0.97	-1.04	0.090	0.841	0.014	
13	1346-1355	TLIHQSITGL		1.95	57.8	27	0.12	-0.06	0.043	0.632	0.016	
14	1197-1207	KLPKYSLFEL		1.2	10.93	27	0.9	0.5	0.040	0.579	0.017	
15	1041-1050	NIMNFFKTEI		2.65	314.8	19	-1.03	-0.9	0.121	0.857	0.017	
16	512-520	SLLYEYFTV		0.4	4.56	25	0.67	0.55	0.056	0.678	0.018	
17	1309-1318	IIHFLTNL		4.25	1083.6	24	-1.04	-0.78	0.085	0.787	0.018	
18	661-670	RLSRKLINGI		3.5	278.03	24	-0.82	-1.05	0.078	0.746	0.020	
19	1227-1236	ALPSKYVNFL		4.3	111.14	27	0.05	-0.26	0.051	0.594	0.021	
20	996-1004	ALIKKYPKL		2.6	154.09	28	-0.27	0	0.037	0.407	0.022	
21	221-229	RLENLIAQL		4.2	242.87	26	-0.46	-0.46	0.061	0.581	0.026	
22	1237-1245	YLASHYEKL		1.2	10.3	26	0.9	0.84	0.050	0.446	0.027	
23	1265-1273	YLDEIIEQI		0.3	4.8	26	0.62	0.6	0.046	0.399	0.028	
24	1042-1050	IMNFFKTEI		3.2	131.4	21	-0.69	-0.87	0.103	0.724	0.028	
25	815-824	YLQNGRDMYV		0.25	13.01	22	-0.18	-0.07	0.083	0.627	0.031	
26	1212-1220	RMLASAGEL		3.2	333.2	22	-0.64	-0.51	0.095	0.650	0.033	
27	1020-1029	KMI AKSEQEI		3.1	64.01	21	-0.36	-0.9	0.103	0.671	0.034	
28	793-801	SQILKEHPV		2.8	191.23	16	-1.4	-1.36	0.149	0.766	0.035	
29	742-750	KVVDELVKV		2.8	44.75	24	-0.06	-0.26	0.074	0.505	0.036	
30	1181-1190	FLEAKGYKEV		3.25	105.27	21	-1.08	-1.42	0.103	0.651	0.036	
31	160-169	HMIKFRGHFL		4.75	324.13	21	-0.59	-0.73	0.110	0.628	0.041	
32	551-559	LLFKTNRKV		3	381.3	25	-1.52	-1.25	0.067	0.368	0.043	
33	141-149	KLVDSTDKA		3.4	274.05	20	-1.48	-1.17	0.114	0.520	0.055	
34	472-481	TITPWNFEV		4.45	124.55	21	-0.84	-1.21	0.107	0.429	0.061	
35	194-203	QLFEENPINA		1.65	67.94	17	-0.71	-0.79	0.135	0.469	0.072	
36	518-527	FTVYNELTKV		2.55	169.93	20	-1.12	-1.15	0.111	0.216	0.087	
37	473-481	ITPWNFEV		6.4	351.14	18	-1.25	-1.65	0.143	0.229	0.110	
38	970-978	FQFYK VREI		2.7	135.61	16	-0.66	-0.39	0.148	0.229	0.114	

Supplementary Table 2.1. Predicted Cas9 immunogenic T cell epitopes - The table shows Cas9 HLA-A*02:01 epitopes predicted using an integrative prediction model and ranked according to their S_b.S_i score (the lower the more immunogenic). The immunodominant and subdominant epitopes as confirmed by ELISpot are highlighted in dark gray and light gray, respectively. S_b, binding score; S_i, immunogenicity score.

Cas9 fragment1- FW	tttGGTCTCTAGGTCCACCATGGACTATAAGGACCACGA
Cas9 fragment1- RV	tttggctctcaGAACAGCTGGTTGTAGGTCTGCA
Cas9 fragment2-FW	tttGGTCTCTACCAACCGGAAAGTGACCGTGAAG
Cas9 fragment2-RV	tttGGTCTCAAAGCTTACTTTTTCTTTTTGCC
qPCRMIAT-FW	TGGCTGGGGTTTGAACCTT
qPCR-MIAT RV	AGGAAGCTGTTCCAGACTGC
qPCR TTN FW	TGTTGCCACTGGTGCTAAAG
qPCR-TTN-RV	ACAGCAGTCTTCTCCGCTTC
PCR-EMX1-FW	CCATCCCCTTCTGTGAATGT
PCR-EMX1-RV	GGAGATTGGAGACACGGAGA

Supplementary Table 2.2. Sequences of primers used in this study.

MIAT-14bp gRNA	GAGGCTGAGCGCAC
TTN-14bp gRNA	GGAAGTCTCCTTGG
Reporter2-20bp gRNA	GTCCCCTCCACCCCACAGTG
CR10-14bp-gRNA	GCATCAGGAACATGT
EMX1- 20bp gRNA	CACC GAGTCCGAGCAGAAGAAGAA

Supplementary Table 2.3. Sequences of gRNAs used in this study

	<i>Sequence</i>	<i>Similarity (%)</i>	<i>Protein</i>	<i>Sequence ID</i>	<i>Source</i>
1	NLI A SLGL	9/9 (100%)	type II CRISPR RNA-guided endonuclease Cas9	WP_014612333.1	<i>Streptococcus dysgalactiae</i>
2	NLI A SLGL	9/9 (100%)	type II CRISPR RNA-guided endonuclease Cas9	WP_054279288.1	<i>Streptococcus phocae</i>
3	NLI A SLGL	9/9 (100%)	type II CRISPR RNA-guided endonuclease Cas9	WP_067062573.1	<i>Streptococcus pantholopis</i>
4	NLI A SLGL	9/9 (100%)	type II CRISPR RNA-guided endonuclease Cas9	WP_048800889.1	<i>Streptococcus constellatus</i>
5	NLI A SLGL	9/9 (100%)	type II CRISPR RNA-guided endonuclease Cas9	WP_002304487.1	<i>Streptococcus mutans</i>
6	NLI A SLGL	9/9 (100%)	type II CRISPR RNA-guided endonuclease Cas9	WP_049516684.1	<i>Streptococcus anginosus</i>
7	NLI A SLGL	9/9 (100%)	type II CRISPR RNA-guided endonuclease Cas9	WP_003079701.1	<i>Streptococcus macacae</i>
8	NLI A SLGL	9/9 (100%)	type II CRISPR RNA-guided endonuclease Cas9	GAD40915.1	<i>Streptococcus intermedius</i> SK54
9	NLI A ESLGL	8/9 (89%)	Full=RNA polymerase-associated protein RapA; AltName: Full=ATP-dependent helicase HepA	Q6LV34.1	<i>Photobacterium profundum</i> SS9
10	NLI S SLGL	8/9 (89%)	type II CRISPR RNA-guided endonuclease Cas9	WP_096633625.1	<i>Streptococcus parauberis</i>
11	NLI A <u>A</u> LGL	8/9 (89%)	type II CRISPR RNA-guided endonuclease Cas9	WP_075103982.1	<i>Streptococcus cuniculi</i>
12	NLI A <u>A</u> LGL	8/9 (89%)	type II CRISPR RNA-guided endonuclease Cas9	WP_058692367.1	<i>Streptococcus gallolyticus</i>
13	NLI A <u>A</u> LGL	8/9 (89%)	type II CRISPR RNA-guided endonuclease Cas9	WP_061100419.1	<i>Streptococcus pasteurianus</i>
14	NLI A <u>A</u> LGL	8/9 (89%)	type II CRISPR RNA-guided endonuclease Cas9	WP_018363470.1	<i>Streptococcus caballi</i>
15	NLI A <u>A</u> LGL	8/9 (89%)	type II CRISPR RNA-guided endonuclease Cas9	WP_099412266.1	<i>Streptococcus macedonicus</i>
16	NLI A <u>A</u> LGL	8/9 (89%)	type II CRISPR RNA-guided endonuclease Cas9	WP_014334983.1	<i>Streptococcus infantarius</i>
17	<u>D</u> LIALYLGL	7/9 (78%)	Full=NADH-quinone oxidoreductase subunit N; AltName: Full=NADH dehydrogenase I subunit N; AltName: Full=NDH-1 subunit N	A8I421.1	<i>Azorhizobium caulinodans</i> ORS 571
18	NL L <u>A</u> LGL	7/9 (78%)	type II CRISPR RNA-guided endonuclease Cas9	WP_007896501.1	<i>Streptococcus pseudoporcinus</i>
19	NLI G <u>L</u> LGL	7/9 (78%)	type II CRISPR RNA-guided endonuclease Cas9	WP_061587801.1	<i>Streptococcus oralis</i>
20	NL V <u>A</u> LGL	7/9 (78%)	type II CRISPR RNA-guided endonuclease Cas9	WP_074862269.1	<i>Streptococcus equinus</i>
21	NL V <u>A</u> <u>V</u> LGL	7/9 (78%)	type II CRISPR RNA-guided endonuclease Cas9	WP_020917064.1	<i>Streptococcus lutetiensis</i>
22	<u>S</u> LIA F SLGL	7/9 (78%)	ectoine/hydroxyectoine ABC transporter permease subunit EhuD	WP_086160327.1	<i>Streptomyces</i> sp. SCSIO 03032
23	<u>Y</u> LIAL <u>A</u> LGL	7/9 (78%)	ectoine/hydroxyectoine ABC transporter permease subunit EhuD	WP_026413155.1	<i>Actinomadura oligospora</i>

Supplementary Table 2.4. Sequence homology of epitope α to amino acid sequences from known proteins.

	Sequence	Similarity (%)	Protein	Sequence ID	Source
1	ILEDIVLTL	9/9 (100%)	type II CRISPR RNA-guided endonuclease Cas9	WP_084916602.1	<i>Streptococcus dysgalactiae</i>
2	ILEDIVLTL	9/9 (100%)	type II CRISPR RNA-guided endonuclease Cas9	WP_074484960.1	<i>Streptococcus henryi</i>
3	ILEDIVLTL	9/9 (100%)	type II CRISPR RNA-guided endonuclease Cas9	WP_003088697.1	<i>Streptococcus rattii</i>
4	ILEDIVLTL	9/9 (100%)	type II CRISPR RNA-guided endonuclease Cas9	WP_044681799.1	<i>Streptococcus suis</i>
5	ILEDIVLTL	9/9 (100%)	type II CRISPR RNA-guided endonuclease Cas9	WP_024786433.1	<i>Streptococcus mutans</i>
6	ILEDIVLTL	9/9 (100%)	type II CRISPR RNA-guided endonuclease Cas9	WP_057491067.1	<i>Streptococcus orisasini</i>
7	ILEDIVLTL	9/9 (100%)	type II CRISPR RNA-guided endonuclease Cas9	WP_082312238.1	<i>Streptococcus intermedius</i>
8	I E GIVLTL	8/9 (89%)	peptide chain release factor 2	NP_275123.1	<i>Neisseria meningitidis</i> MC58
9	ILEDIVQTL	8/9 (89%)	type II CRISPR RNA-guided endonuclease Cas9	EAO61901.1	<i>Streptococcus agalactiae</i>
10	ILEDIVQTL	8/9 (89%)	type II CRISPR RNA-guided endonuclease Cas9	WP_070454905.1	<i>Streptococcus</i> sp. HMSC063D10
11	VLEDIVLTL	8/9 (89%)	type II CRISPR RNA-guided endonuclease Cas9	WP_075346866.1	<i>Streptococcus</i> sp. 'caviae'
12	VLEDIVLSL	7/9 (78%)	type II CRISPR RNA-guided endonuclease Cas9	WP_093650272.1	<i>Streptococcus varani</i>
13	I E NIVHTL	7/9 (78%)	type II CRISPR RNA-guided endonuclease Cas9	KYF37509.1	<i>Streptococcus mitis</i>
14	I E NIVHTL	7/9 (78%)	type II CRISPR RNA-guided endonuclease Cas9	WP_084972088.1	<i>Streptococcus oralis</i>
15	I E NIVHTL	7/9 (78%)	type II CRISPR RNA-guided endonuclease Cas9	WP_045635197.1	<i>Streptococcus gordonii</i>

Supplementary Table 2.5. Sequence homology of epitope β to amino acid sequences from known proteins.

Donor ID	p value	Corrected p value
Peptide α		
5	0.0000003	0.000001
10	0.0000075	0.0000124
9	0.0007779	0.0008557
1	0.0017641	0.0014554
12	0.0079662	0.0052577
7	0.0387297	0.0213013
6	0.045632	0.0215122
2	0.0655837	0.0270533
3	0.0783807	0.0287396
Peptide β		
9	0.0002026	0.0005757
6	0.0003655	0.0005757
7	0.0007587	0.0007967
3	0.005237	0.0041241
2	0.0096527	0.0060812
1	0.0219659	0.0099651
10	0.0221447	0.0099651
12	0.0272351	0.0107238

Supplementary Table 2.6. Multiple comparison results of mutated epitope ELISpot screening. Uncorrected and corrected p values for donors with a significant reduction in T cell response after mutating epitope α or β by the Benjamini-Hochberg method (5% FDR) are shown for Supplementary Figure 1.

Peptide ID	Peptide Sequence	HLA Allele(s)
15	KTYAHLFDDK	A*03:01 & 11:01
16	FLYLASHYEK	A*03:01 & 24:02 & B55:01 & B08:01
17	KTNRKVTVK	A*03:01
18	KVLPKHSLLY	A*03:01
19	AILSARLSK	A*03:01 & 11:01
20	LSMPQVNIVK	A*11:01 & 24:02 & B44:02 & B44:03
21	TIMERSSEFEK	A*11:01 & B08:01 & B55:01
22	YSNIMNFFK	A*11:01 & 24:02
23	KYPKLESEF	A*24:02 & B08:01
24	RYTRRKNRI	A*24:02
25	YFFYSNIMNF	A*24:02
26	ELDINRLSDY	A*01:01
27	NLDKVLSAY	A*01:01
28	ESEFVYGDY	A*01:01
29	ILDSRMNTKY	A*01:01 & B08:01
30	NTQLQNEKLY	A*01:01
31	NELALPSKY	B*44:02 & B44:03
32	NEMAKVDDSF	B*44:02 & B55:01 & B08:01 & B44:03
33	SEETIPWNF	B*44:02 & B44:03
34	EETIPWNF	B*44:02 & B08:01 & B44:03
35	IANLAGSPA	B*55:01 & B44:03

Supplementary Table 2.7. Sequences of SpCas9 non-HLA-A*02:01 class I epitopes used to screen for pre-existing T cell reactivity against SpCas9 in healthy donors.

Peptide ID	Peptide Sequence	HLA
1	ILEDIVLTLTLFEDR	DPA1/DPB2
2	KNGLFGNLIALSGLTPNF	DRB1
3	RLSDYDVAAIIPQSFLK	DQA1
4	ERHPIFGNIVDEVAYHY	DQA1-2
5	VLPKHSLLEYFTVYNELT	DPA1
6	ATAKYFFYSNIMNFFK	DPA1-2
7	DLRLIYLALAHMIKFR	DRB1-2
8	MKNYWRQLLNAKLITQ	DRB1-3

Sequences of peptides α and β are highlighted.

Supplementary Table 2.8. Sequences of long peptides that include epitopes in the top 2% of predicted MHC class II binders that were used to screen for SpCas9 class II immune reactivity.

Supplementary Note 2.1

Sequences of modified Cas9 genes. Cas9- $\alpha 2$
ATGGACTATAAGGACCACGACGGAGACTACAAGGATCATGATATTGATTACA
AAGACGATGACGATAAGATGGCCCCAAAGAAGAAGCGGAAGGTCGGTATCC
ACGGAGTCCCAGCAGCCGACAAGAAGTACAGCATCGGCCTGGACATCGGCA
CCAACTCTGTGGGCTGGGCCGTGATCACCGACGAGTACAAGGTGCCAGCAA
GAAATTCAAGGTGCTGGGCAACACCGACCGGCACAGCATCAAGAAGAACCT
GATCGGAGCCCTGCTGTTTCGACAGCGGCGAAACAGCCGAGGCCACCCGGCTG
AAGAGAACCGCCAGAAGAAGATACACCAGACGGAAGAACCGGATCTGCTAT
CTGCAAGAGATCTTCAGCAACGAGATGGCCAAGGTGGACGACAGCTTCTTCC
ACAGACTGGAAGAGTCCTTCCCTGGTGGAAAGAGGATAAGAAGCACGAGCGGC
ACCCCATCTTCGGCAACATCGTGGACGAGGTGGCCTACCACGAGAAGTACCC
CACCATCTACCACCTGAGAAAGAACTGGTGGACAGCACCGACAAGGCCGA
CCTGCGGCTGATCTATCTGGCCCTGGCCACATGATCAAGTCCGGGGCCACT
TCCTGATCGAGGGCGACCTGAACCCCGACAACAGCGACGTGGACAAGCTGTT
CATCCAGCTGGTGCAGACCTACAACCAGCTGTTTCGAGGAAAACCCCATCAAC
GCCAGCGGCGTGGACGCCAAGGCCATCCTGTCTGCCAGACTGAGCAAGAGCA
GACGGCTGGAAAATCTGATCGCCAGCTGCCCGGCGAGAAGAAGAATGGCC

TGTTTCGGAAACGGTATTGCCCTGAGCCTGGGCCTGACCCCCAACTTCAAGAG
CAACTTCGACCTGGCCGAGGATGCCAACTGCAGCTGAGCAAGGACACCTAC
GACGACGACCTGGACAACCTGCTGGCCAGATCGGCGACCAGTACGCCGACC
TGTTTCTGGCCGCCAAGAACCTGTCCGACGCCATCCTGCTGAGCGACATCCTG
AGAGTGAACACCGAGATACCAAGGCCCCCCCTGAGCGCCTCTATGATCAAGA
GATACGACGAGCACCACCAGGACCTGACCCTGCTGAAAGCTCTCGTGCGGCA
GCAGCTGCCTGAGAAGTACAAAGAGATTTTCTTCGACCAGAGCAAGAACGGC
TACGCCGGCTACATTGACGGCGGAGCCAGCCAGGAAGAGTTCTACAAGTTCA
TCAAGCCCATCCTGGAAAAGATGGACGGCACCGAGGAACTGCTCGTGAAGCT
GAACAGAGAGGACCTGCTGCGGAAGCAGCGGACCTTCGACAACGGCAGCAT
CCCCACCAGATCCACCTGGGAGAGCTGCACGCCATTCTGCGGCGGCAGGAA
GATTTTACCCATTCTGAAGGACAACCGGGAAAAGATCGAGAAGATCCTGA
CCTTCCGCATCCCCTACTACGTGGGCCCTCTGGCCAGGGGAAACAGCAGATT
CGCCTGGATGACCAGAAAAGAGCGAGGAAAACCATCACCCCCTGGAACCTCGA
GGAAGTGGTGGACAAGGGCGCTTCCGCCAGAGCTTCATCGAGCGGATGACC
AACTTCGATAAGAACCTGCCAACGAGAAGGTGCTGCCAAGCACAGCCTGC
TGTACGAGTACTTCACCGTGTATAACGAGCTGACCAAAGTGAAATACGTGAC
CGAGGGAATGAGAAAAGCCCGCCTTCTGAGCGGCGAGCAGAAAAAGGCCAT
CGTGGACCTGCTGTTCAAGACCAACCGGAAAAGTGACCGTGAAGCAGCTGAAA
GAGGACTACTTCAAGAAAATCGAGTGCTTCGACTCCGTGGAAATCTCCGGCG
TGGAAGATCGGTTCAACGCCTCCCTGGGCACATACCACGATCTGCTGAAAAT
TATCAAGGACAAGGACTTCTGGACAATGAGGAAAACGAGGACATTCTTGAA
GATATCGTGCTGACCCTGACACTGTTTGAGGACAGAGAGATGATCGAGGAAC
GGCTGAAAACCTATGCCACCTGTTTCGACGACAAAGTGATGAAGCAGCTGAA
GCGGCGGAGATACACCGGCTGGGGCAGGCTGAGCCGGAAGCTGATCAACGG
CATCCGGGACAAGCAGTCCGGCAAGACAATCCTGGATTTCTGAAGTCCGAC
GGCTTCGCCAACAGAACTTCATGCAGCTGATCCACGACGACAGCCTGACCT
TTAAAGAGGACATCCAGAAAGCCCAGGTGTCCGGCCAGGGCGATAGCCTGC
ACGAGCACATTGCCAATCTGGCCGGCAGCCCCGCCATTAAGAAGGGCCTCCT
GCAGACAGTGAAGGTGGTGGACGAGCTCGTGAAAGTGATGGGCCGGCACAA
GCCCCGAGAACATCGTGATCGAAATGGCCAGAGAGAACCAGACCACCAGAA
GGGACAGAAGAACAGCCGCGAGAGAATGAAGCGGATCGAAGAGGGGCATCAA
AGAGCTGGGCAGCCAGATCCTGAAAGAACACCCCCTGGAAAACACCCAGCT
GCAGAACGAGAAGCTGTACCTGTACTACCTGCAGAATGGGCGGGATATGTAC
GTGGACCAGGAACTGGACATCAACCGGCTGTCCGACTACGATGTGGACCATA
TCGTGCCTCAGAGCTTTCTGAAGGACGACTCCATCGACAACAAGGTGCTGAC
CAGAAGCGACAAGAACCGGGGCAAGAGCGACAACGTGCCCTCCGAAGAGGT
CGTGAAGAAGATGAAGAATACTGGCGGCAGCTGCTGAACGCCAAGCTGATT
ACCCAGAGAAAAGTTCGACAATCTGACCAAGGCCGAGAGAGGGCGGCCTGAGC
GAACTGGATAAGGCCGGCTTCATCAAGAGACAGCTGGTGGAAACCCGGCAG
ATCACAAAGCACGTGGCACAGATCCTGGACTCCCGGATGAACACTAAGTACG
ACGAGAATGACAAGCTGATCCGGGAAGTGAAAGTGATCACCTGAAGTCCA
AGCTGGTGTCCGATTTCCGGAAGGATTTCCAGTTTTACAAAGTGCGCGAGATC
AACTACTACCACCGCCACGACGCCTACCTGAACGCCGTCTGTTGGAAACCG
CCCTGATCAAAAAGTACCCTAAGCTGGAAAGCGAGTTCGTGTACGGCGACTA

CAAGGTGTACGACGTGCGGAAGATGATCGCCAAGAGCGAGCAGGAAATCGG
CAAGGCTACCGCCAAGTACTTCTTCTACAGCAACATCATGAACTTTTTCAAGA
CCGAGATTACCCTGGCCAACGGCGAGATCCGGAAGCGGCCTCTGATCGAGAC
AAACGGCGAAACCGGGGAGATCGTGTGGGATAAGGGCCGGGATTTTGCCAC
CGTGCGGAAAGTGCTGAGCATGCCCAAGTGAATATCGTGAAAAAGACCGA
GGTGCAGACAGGCGGCTTCAGCAAAGAGTCTATCCTGCCCAAGAGGAACAG
CGATAAGCTGATCGCCAGAAAGAAGGACTGGGACCCTAAGAAGTACGGCGG
CTTCGACAGCCCCACCGTGGCCTATTCTGTGCTGGTGGTGGCCAAAGTGGA
AAGGGCAAGTCCAAGAACTGAAGAGTGTGAAAGAGCTGCTGGGGATCACC
ATCATGGAAAGAAGCAGCTTCGAGAAGAATCCCATCGACTTTCTGGAAGCCA
AGGGCTACAAAGAAGTGAAAAAGGACCTGATCATCAAGCTGCCTAAGTACTC
CCTGTTTCGAGCTGGAAAACGGCCGGAAGAGAATGCTGGCCTCTGCCGGCGAA
CTGCAGAAGGGAAACGAACTGGCCCTGCCCTCCAAATATGTGAACTTCTGT
ACCTGGCCAGCCACTATGAGAAGCTGAAGGGCTCCCCGAGGATAATGAGCA
GAAACAGCTGTTTGTGGAACAGCACAAGCACTACCTGGACGAGATCATCGAG
CAGATCAGCGAGTTCTCCAAGAGAGTGATCCTGGCCGACGCTAATCTGGACA
AAGTGCTGTCCGCCTACAACAAGCACCGGGATAAGCCCATCAGAGAGCAGG
CCGAGAATATCATCCACCTGTTTACCCTGACCAATCTGGGAGCCCCTGCCGCC
TTCAAGTACTTTGACACCACCATCGACCCGGAAGAGGTACACCAGCACCAAAG
AGGTGCTGGACGCCACCCTGATCCACCAGAGCATCACCGGCCTGTACGAGAC
ACGGATCGACCTGTCTCAGCTGGGAGGCGACAAAAGGCCGGCGGCCACGAA
AAAGGCCGGCCAGGCAA AAAAGAAAAAGTAAG

Cas9-β2

ATGGACTATAAGGACCACGACGGAGACTACAAGGATCATGATATTGATTACA
AAGACGATGACGATAAGATGGCCCCAAAGAAGAAGCGGAAGGTCCGGTATCC
ACGGAGTCCCAGCAGCCGACAAGAAGTACAGCATCGGCCTGGACATCGGCA
CCA ACTCTGTGGGCTGGGCCGTGATCACCGACGAGTACAAGGTGCCAGCAA
GAAATTCAAGGTGCTGGGCAACACCGACCGGCACAGCATCAAGAAGAACCT
GATCGGAGCCCTGCTGTTTCGACAGCGCGAAACAGCCGAGGCCACCCGGCTG
AAGAGAACCGCCAGAAGAAGATACACCAGACGGAAGAACCGGATCTGCTAT
CTGCAAGAGATCTTCAGCAACGAGATGGCCAAGGTGGACGACAGCTTCTTCC
ACAGACTGGAAGAGTCCCTCCTGGTGGAAAGAGGATAAGAAGCACGAGCGGC
ACCCCATCTTCGGCAACATCGTGGACGAGGTGGCCTACCACGAGAAGTACCC
CACCATCTACCACCTGAGAAAGAACTGGTGGACAGCACCGACAAGGCCGA
CCTGCGGCTGATCTATCTGGCCCTGGCCACATGATCAAGTTCGGGGCCACT
TCCTGATCGAGGGCGACCTGAACCCCGACAACAGCGACGTGGACAAGCTGTT
CATCCAGCTGGTGCAGACCTACAACCAGCTGTTTCGAGGAAAACCCCATCAAC
GCCAGCGGCGTGGACGCCAAGGCCATCCTGTCTGCCAGACTGAGCAAGAGCA
GACGGCTGGAAAATCTGATCGCCAGCTGCCCGGCGAGAAGAAGAATGGCC
TGTTTCGGAAACCTTATTGCCCTGAGCCTGGGCCTGACCCCAACTTCAAGAGC
AACTTCGACCTGGCCGAGGATGCCAACTGCAGCTGAGCAAGGACACCTACG
ACGACGACCTGGACAACCTGCTGGCCAGATCGGCGACCAGTACGCCGACCT
GTTTCTGGCCGCCAAGAACCTGTCCGACGCCATCCTGCTGAGCGACATCCTG
AGAGTGAACACCGAGATACCAAGGCCCCCTGAGCGCCTCTATGATCAAGA

GATACGACGAGCACCACCAGGACCTGACCCTGCTGAAAGCTCTCGTGCGGCA
GCAGCTGCCTGAGAAGTACAAAGAGATTTTCTTCGACCAGAGCAAGAACGGC
TACGCCGGCTACATTGACGGCGGAGCCAGCCAGGAAGAGTTCTACAAGTTCA
TCAAGCCATCCTGGAAAAGATGGACGGCACCGAGGAACTGCTCGTGAAGCT
GAACAGAGAGGACCTGCTGCGGAAGCAGCGGACCTTCGACAACGGCAGCAT
CCCCACCAGATCCACCTGGGAGAGCTGCACGCCATTCTGCGGCGGCAGGAA
GATTTTTACCCATTCTGAAGGACAACCGGGAAAAGATCGAGAAGATCCTGA
CCTTCCGCATCCCCTACTACGTGGGCCCTCTGGCCAGGGGAAAACAGCAGATT
CGCTGGATGACCAGAAAAGAGCGAGGAAACCATCACCCCCTGGAACCTCGA
GGAAGTGGTGGACAAGGGCGCTTCCGCCAGAGCTTCATCGAGCGGATGACC
AACTTCGATAAGAACCTGCCAACGAGAAGGTGCTGCCAAGCACAGCCTGC
TGTACGAGTACTTCACCGTGTATAACGAGCTGACCAAAGTGAAATACGTGAC
CGAGGGAATGAGAAAGCCCGCCTTCTGAGCGGCGAGCAGAAAAAGGCCAT
CGTGGACCTGCTGTTCAAGACCAACCGGAAAAGTGACCGTGAAGCAGCTGAAA
GAGGACTACTTCAAGAAAATCGAGTGCTTCGACTCCGTGGAAATCTCCGGCG
TGGAAGATCGGTTCAACGCCTCCCTGGGCACATACCACGATCTGCTGAAAAT
TATCAAGGACAAGGACTTCTGGACAATGAGGAAAACGAGGACATTGGTGA
AGATATCGTGCTGACCCTGACACTGTTTGAGGACAGAGAGATGATCGAGGAA
CGGCTGAAAACCTATGCCACCTGTTCGACGACAAAGTGATGAAGCAGCTGA
AGCGGCGGAGATACACCGGCTGGGGCAGGCTGAGCCGGAAGCTGATCAACG
GCATCCGGGACAAGCAGTCCGGCAAGACAATCCTGGATTTCTGAAGTCCGA
CGGCTTCGCCAACAGAACTTCATGCAGCTGATCCACGACGACAGCCTGACC
TTAAAGAGGACATCCAGAAAGCCAGGTGTCCGGCCAGGGCGATAGCCTGC
ACGAGCACATTGCCAATCTGGCCGGCAGCCCCGCCATTAAGAAGGGCATCCT
GCAGACAGTGAAGGTGGTGGACGAGCTCGTGAAAGTGATGGGCCGGCACAA
GCCCCGAGAACATCGTGATCGAAATGGCCAGAGAGAACCAGACCACCAGAA
GGGACAGAAGAACAGCCGCGAGAGAATGAAGCGGATCGAAGAGGGCATCAA
AGAGCTGGGCAGCCAGATCCTGAAAGAACACCCCGTGGAAAACACCCAGCT
GCAGAACGAGAAGCTGTACCTGTACTACCTGCAGAATGGGCGGGATATGTAC
GTGGACCAGGAACTGGACATCAACCGGCTGTCCGACTACGATGTGGACCATA
TCGTGCCTCAGAGCTTTCTGAAGGACGACTCCATCGACAACAAGGTGCTGAC
CAGAAGCGACAAGAACCGGGGCAAGAGCGACAACGTGCCCTCCGAAGAGGT
CGTGAAGAAGATGAAGAATACTGGCGGCAGCTGCTGAACGCCAAGCTGATT
ACCCAGAGAAAAGTTCGACAATCTGACCAAGGCCGAGAGAGGCGGCCTGAGC
GAACTGGATAAGGCCGGCTTCATCAAGAGACAGCTGGTGGAAACCCGGCAG
ATCACAAGCACGTGGCACAGATCCTGGACTCCCGGATGAACACTAAGTACG
ACGAGAATGACAAGCTGATCCGGGAAGTGAAAGTGATCACCTGAAGTCCA
AGCTGGTGTCCGATTTCCGGAAGGATTTCCAGTTTTACAAAGTGCGCGAGAT
CAACAACCTACCACCACGCCACGACGCCTACCTGAACGCCGTCTGTTGGAAAC
GCCCTGATCAAAAAGTACCCTAAGCTGGAAAGCGAGTTCGTGTACGGCGACT
ACAAGGTGTACGACGTGCGGAAGATGATCGCCAAGAGCGAGCAGGAAATCG
GCAAGGCTACCGCCAAGTACTTCTTCTACAGCAACATCATGAACTTTTTCAAG
ACCGAGATTACCCTGGCCAACGGCGAGATCCGGAAGCGGCCTCTGATCGAGA
CAAACGGCGAAACCGGGGAGATCGTGTGGGATAAGGGCCGGGATTTTGCCA
CCGTGCGGAAAGTGCTGAGCATGCCCAAGTGAATATCGTGAAAAGACCGA

GGTGCAGACAGGCGGCTTCAGCAAAGAGTCTATCCTGCCCAAGAGGAACAG
CGATAAGCTGATCGCCAGAAAGAAGGACTGGGACCCTAAGAAGTACGGCGG
CTTCGACAGCCCCACCGTGGCCTATTCTGTGCTGGTGGTGGCCAAAGTGGAA
AAGGGCAAGTCCAAGAACTGAAGAGTGTGAAAGAGCTGCTGGGGATCACC
ATCATGGAAAGAAGCAGCTTCGAGAAGAATCCCATCGACTTTCTGGAAGCCA
AGGGCTACAAAGAAGTGAAAAAGGACCTGATCATCAAGCTGCCTAAGTACTC
CCTGTTTCGAGCTGGAAAACGGCCGGAAGAGAATGCTGGCCTCTGCCGGCGAA
CTGCAGAAGGGAAACGAACTGGCCCTGCCCTCCAAATATGTGAACTTCTGT
ACCTGGCCAGCCACTATGAGAAGCTGAAGGGCTCCCCGAGGATAATGAGCA
GAAACAGCTGTTTGTGGAACAGCACAAGCACTACCTGGACGAGATCATCGAG
CAGATCAGCGAGTTCTCCAAGAGAGTGATCCTGGCCGACGCTAATCTGGACA
AAGTGCTGTCCGCCTACAACAAGCACCGGGATAAGCCCATCAGAGAGCAGG
CCGAGAATATCATCCACCTGTTTACCCTGACCAATCTGGGAGCCCCTGCCGCC
TTCAAGTACTTTGACACCACCATCGACCGGAAGAGGTACACCAGCACCAAAG
AGGTGCTGGACGCCACCCTGATCCACCAGAGCATCACCGGCCTGTACGAGAC
ACGGATCGACCTGTCTCAGCTGGGAGGCGACAAAAGGCCGGCGGCCACGAA
AAAGGCCGGCCAGGCAA AAAAGAAAAAGTAA

Cas9- α 2- β 2

ATGGACTATAAGGACCACGACGGAGACTACAAGGATCATGATATTGATTACA
AAGACGATGACGATAAGATGGCCCCAAAGAAGAAGCGGAAGGTTCGGTATCC
ACGGAGTCCCAGCAGCCGACAAGAAGTACAGCATCGGCCTGGACATCGGCA
CCA ACTCTGTGGGCTGGGCGTGATCACCGACGAGTACAAGGTGCCAGCAA
GAAATTCAAGGTGCTGGGCAACACCGACCGGCACAGCATCAAGAAGAACCT
GATCGGAGCCCTGCTGTTTCGACAGCGGCGAAACAGCCGAGGCCACCCGGCTG
AAGAGAACCGCCAGAAGAAGATACACCAGACGGAAGAACC GGATCTGCTAT
CTGCAAGAGATCTTCAGCAACGAGATGGCCAAGGTGGACGACAGCTTCTTCC
ACAGACTGGAAGAGTCCTTCTGTTGGAAGAGGATAAGAAGCACGAGCGGC
ACCCCATCTTCGGCAACATCGTGGACGAGGTGGCCTACCACGAGAAGTACCC
CACCATCTACCACCTGAGAAAGAACTGGTGGACAGCACCGACAAGGCCGA
CCTGCGGCTGATCTATCTGGCCCTGGCCACATGATCAAGTTCGGGGCCACT
TCCTGATCGAGGGCGACCTGAACCCCGACAACAGCGACGTGGACAAGCTGTT
CATCCAGCTGGTGCAGACCTACAACCAGCTGTTCGAGGAAAACCCCATCAAC
GCCAGCGGCGTGGACGCCAAGGCCATCCTGTCTGCCAGACTGAGCAAGAGCA
GACGGCTGGAAAATCTGATCGCCCAGCTGCCCGGCGAGAAGAAGAATGGCC
TGTTTCGGAAACGGTATTGCCCTGAGCCTGGGCCTGACCCCAACTTCAAGAG
CAACTTCGACCTGGCCGAGGATGCCAACTGCAGCTGAGCAAGGACACCTAC
GACGACGACCTGGACAACCTGCTGGCCAGATCGGCGACCAGTACGCCGACC
TGTTTCTGGCCGCCAAGAACCTGTCCGACGCCATCCTGCTGAGCGACATCCTG
AGAGTGAACACCGAGATCACCAAGGCCCCCTGAGCGCCTCTATGATCAAGA
GATACGACGAGCACACCAGGACCTGACCCTGCTGAAAGCTCTCGTGC GGCA
GCAGCTGCCTGAGAAGTACAAAGAGATTTTCTTCGACCAGAGCAAGAACGGC
TACGCCGGCTACATTGACGGCGGAGCCAGCCAGGAAGAGTTCTACAAGTTCA
TCAAGCCATCCTGAAAAGATGGACGGCACCGAGGAACTGCTCGTGAAGCT
GAACAGAGAGGACCTGCTGCGGAAGCAGCGGACCTTCGACAACGGCAGCAT

CCCCACCAGATCCACCTGGGAGAGCTGCACGCCATTCTGCGGCGGCAGGAA
GATTTTTACCCATTCTGAAGGACAACCGGGAAAAGATCGAGAAGATCCTGA
CCTTCCGCATCCCCTACTACGTGGGCCCTCTGGCCAGGGGAAACAGCAGATT
CGCCTGGATGACCAGAAAGAGCGAGGAAACCATCACCCCCTGGAACCTCGA
GGAAGTGGTGGACAAGGGCGCTTCCGCCCAGAGCTTCATCGAGCGGATGACC
AACTTCGATAAGAACCTGCCAACGAGAAGGTGCTGCCAACGCACAGCCTGC
TGTACGAGTACTTCACCGTGTATAACGAGCTGACCAAAGTGAAATACGTGAC
CGAGGGAATGAGAAAGCCCGCCTTCTGAGCGGCGAGCAGAAAAAGGCCAT
CGTGGACCTGCTGTTCAAGACCAACCGGAAAGTGACCGTGAAGCAGCTGAAA
GAGGACTACTTCAAGAAAATCGAGTGCTTCGACTCCGTGGAAATCTCCGGCG
TGGAAGATCGGTTCAACGCCTCCCTGGGCACATACCACGATCTGCTGAAAAT
TATCAAGGACAAGGACTTCTGGACAATGAGGAAAACGAGGACATTGGTGA
AGATATCGTGCTGACCCTGACACTGTTTGAGGACAGAGAGATGATCGAGGAA
CGGCTGAAAACCTATGCCACCTGTTTCGACGACAAAGTGATGAAGCAGCTGA
AGCGGCGGAGATACACCGGCTGGGGCAGGCTGAGCCGGAAGCTGATCAACG
GCATCCGGGACAAGCAGTCCGGCAAGACAATCCTGGATTTCTGAAGTCCGA
CGGCTTCGCCAACAGAACTTCATGCAGCTGATCCACGACGACAGCCTGACC
TTTAAAGAGGACATCCAGAAAGCCCAGGTGTCCGGCCAGGGCGATAGCCTGC
ACGAGCACATTGCCAATCTGGCCGGCAGCCCCGCCATTAAGAAGGGCCTCCT
GCAGACAGTGAAGGTGGTGGACGAGCTCGTGAAAGTGATGGGCCGGCACAA
GCCCCGAGAACATCGTGATCGAAATGGCCAGAGAGAACCAGACCACCAGAA
GGGACAGAAGAACAGCCGCGAGAGAATGAAGCGGATCGAAGAGGGCATCAA
AGAGCTGGGCAGCCAGATCCTGAAAGAACACCCCGTGGAAAACACCCAGCT
GCAGAACGAGAAGCTGTACCTGTACTACCTGCAGAATGGGCGGGATATGTAC
GTGGACCAGGAACTGGACATCAACCGGCTGTCCGACTACGATGTGGACCATA
TCGTGCCTCAGAGCTTTCTGAAGGACGACTCCATCGACAACAAGGTGCTGAC
CAGAAGCGACAAGAACCAGGGGCAAGAGCGACAACGTGCCCTCCGAAGAGGT
CGTGAAGAAGATGAAGAATACTGGCGGCAGCTGCTGAACGCCAAGCTGATT
ACCCAGAGAAAGTTCGACAATCTGACCAAGGCCGAGAGAGGGCGGCCTGAGC
GAACTGGATAAGGCCGGCTTCATCAAGAGACAGCTGGTGGAAACCCGGCAG
ATCACAAAGCACGTGGCACAGATCCTGGACTCCCGGATGAACACTAAGTACG
ACGAGAATGACAAGCTGATCCGGGAAGTGAAAGTGATCACCTGAAGTCCA
AGCTGGTGTCCGATTTCCGGAAGGATTTCCAGTTTTTACAAAGTGCGCGAGAT
CAACAATAACACCACGCCACGACGCCTACCTGAACGCCGTCGTGGGAACC
GCCCTGATCAAAAAGTACCCTAAGCTGGAAAGCGAGTTCGTGTACGGCGACT
ACAAGGTGTACGACGTGCGGAAGATGATCGCCAAGAGCGAGCAGGAAATCG
GCAAGGCTACCGCCAAGTACTTCTTCTACAGCAACATCATGAACTTTTTCAAG
ACCGAGATTACCTGGCCAACGGCGAGATCCGGAAGCGGCCTCTGATCGAGA
CAAACGGCGAAACCGGGGAGATCGTGTGGGATAAAGGGCCGGGATTTTGCCA
CCGTGCGGAAAGTGCTGAGCATGCCCAAGTGAATATCGTGAAAAAGACCGA
GGTGCAGACAGGCGGCTTCAGCAAAGAGTCTATCCTGCCAAGAGGAACAG
CGATAAGCTGATCGCCAGAAAGAAGGACTGGGACCCTAAGAAGTACGGCGG
CTTCGACAGCCCCACCGTGGCCTATTCTGTGCTGGTGGTGGCCAAAGTGGAA
AAGGGCAAGTCCAAGAAACTGAAGAGTGTGAAAGAGCTGCTGGGGATCACC
ATCATGGAAAGAAGCAGCTTCGAGAAGAATCCCATCGACTTTCTGGAAGCCA

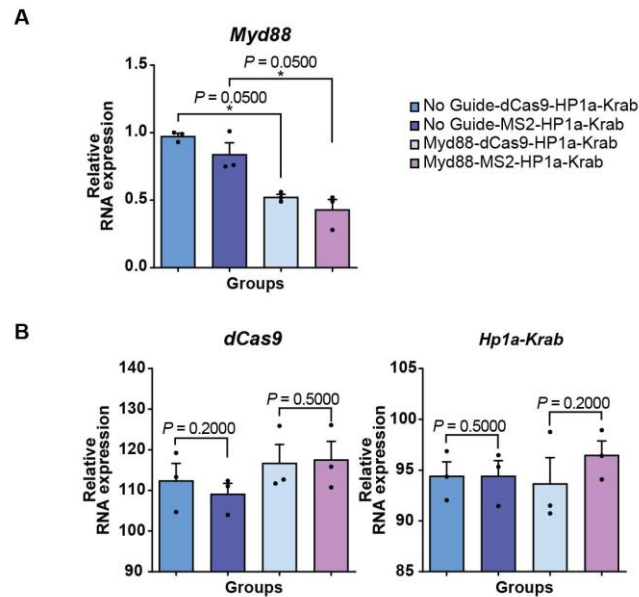
AGGGCTACAAAGAAGTGAAAAAGGACCTGATCATCAAGCTGCCTAAGTACTC
CCTGTTTCGAGCTGGAAAACGGCCGGAAGAGAATGCTGGCCTCTGCCGGCGAA
CTGCAGAAGGGAAACGAACTGGCCCTGCCCTCCAAATATGTGAACTTCCTGT
ACCTGGCCAGCCACTATGAGAAGCTGAAGGGCTCCCCGAGGATAATGAGCA
GAAACAGCTGTTTGTGGAACAGCACAAGCACTACCTGGACGAGATCATCGAG
CAGATCAGCGAGTTCTCCAAGAGAGTGATCCTGGCCGACGCTAATCTGGACA
AAGTGCTGTCCGCCTACAACAAGCACCGGGATAAGCCCATCAGAGAGCAGG
CCGAGAATATCATCCACCTGTTTACCCTGACCAATCTGGGAGCCCCTGCCGCC
TTCAAGTACTTTGACACCACCATCGACCGGAAGAGGTACACCAGCACCAAAG
AGGTGCTGGACGCCACCCTGATCCACCAGAGCATCACCGGCCTGTACGAGAC
ACGGATCGACCTGTCTCAGCTGGGAGGCGACAAAAGGCCGGCGGCCACGAA
AAAGGCCGGCCAGGCAAAAAAGAAAAAGT

APPENDIX B

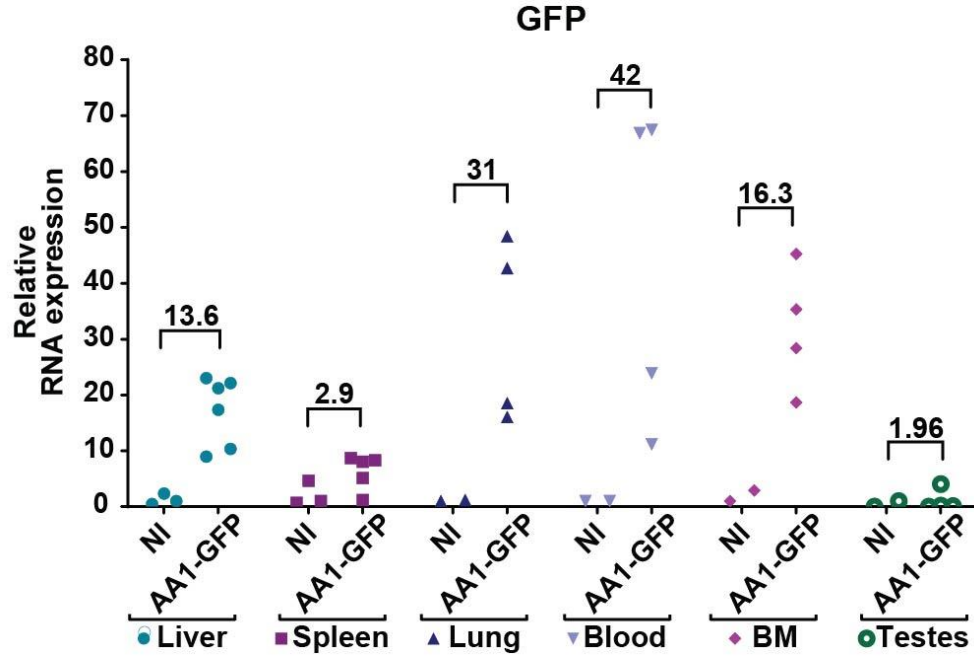
SUPPORTING INFORMATION FOR SYNTHETIC IMMUNOMODULATION WITH

A CRISPR SUPER-REPRESSOR *IN VIVO*

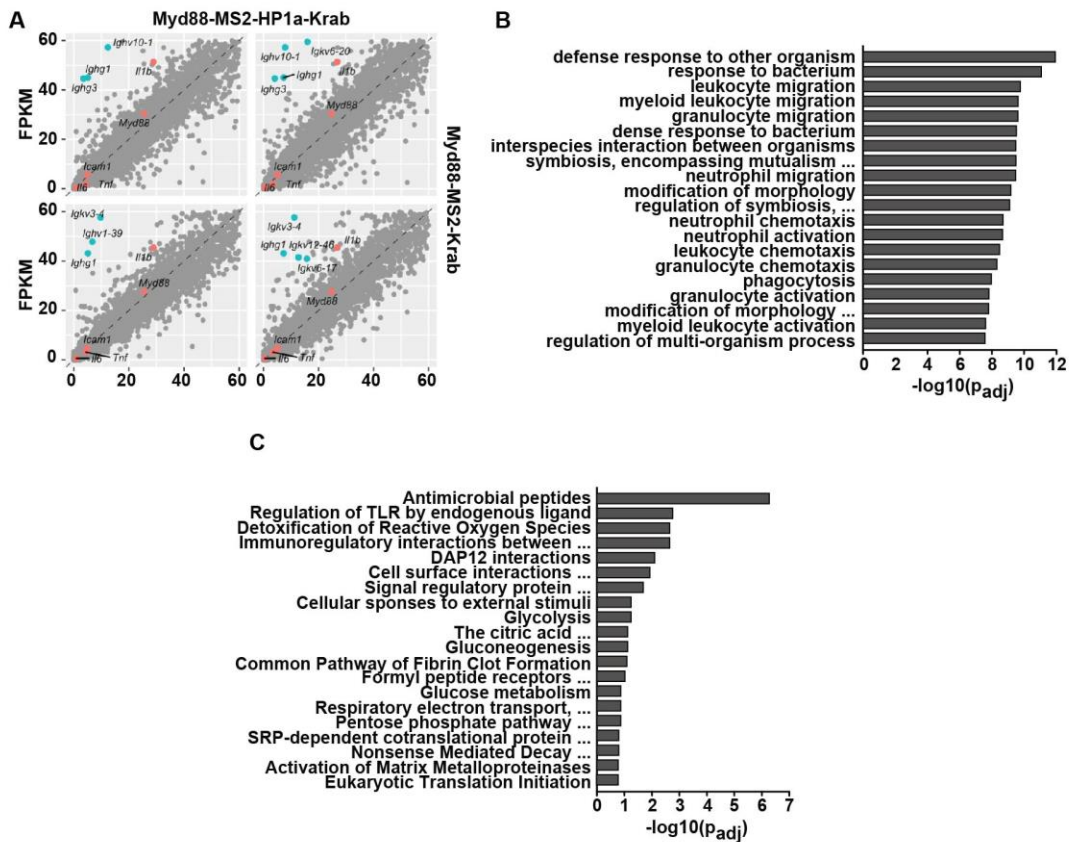
Supplementary Figures



Supplementary figure 3.1. Evaluation of endogenous *Myd88* gene expression using different CRISPR-mediated repressor circuits (A-B) N2A cells were transfected with *Myd88* gRNA pairs along with either dCas9 plasmid fused to HP1aKRAB or dCas9 and MS2-HP1aKRAB on two separate cassettes. Expression levels of (A) *Myd88*, (B) dCas9, and *HP1aKRAB* are quantified relative to No-Guide group (N=3 biologically independent samples) The bars represent the mean + S.E.M. Statistical analysis was performed using the non-parametric one-tailed Mann-Whitney test. A p value ≤ 0.05 was considered significant (* $P \leq 0.05$).

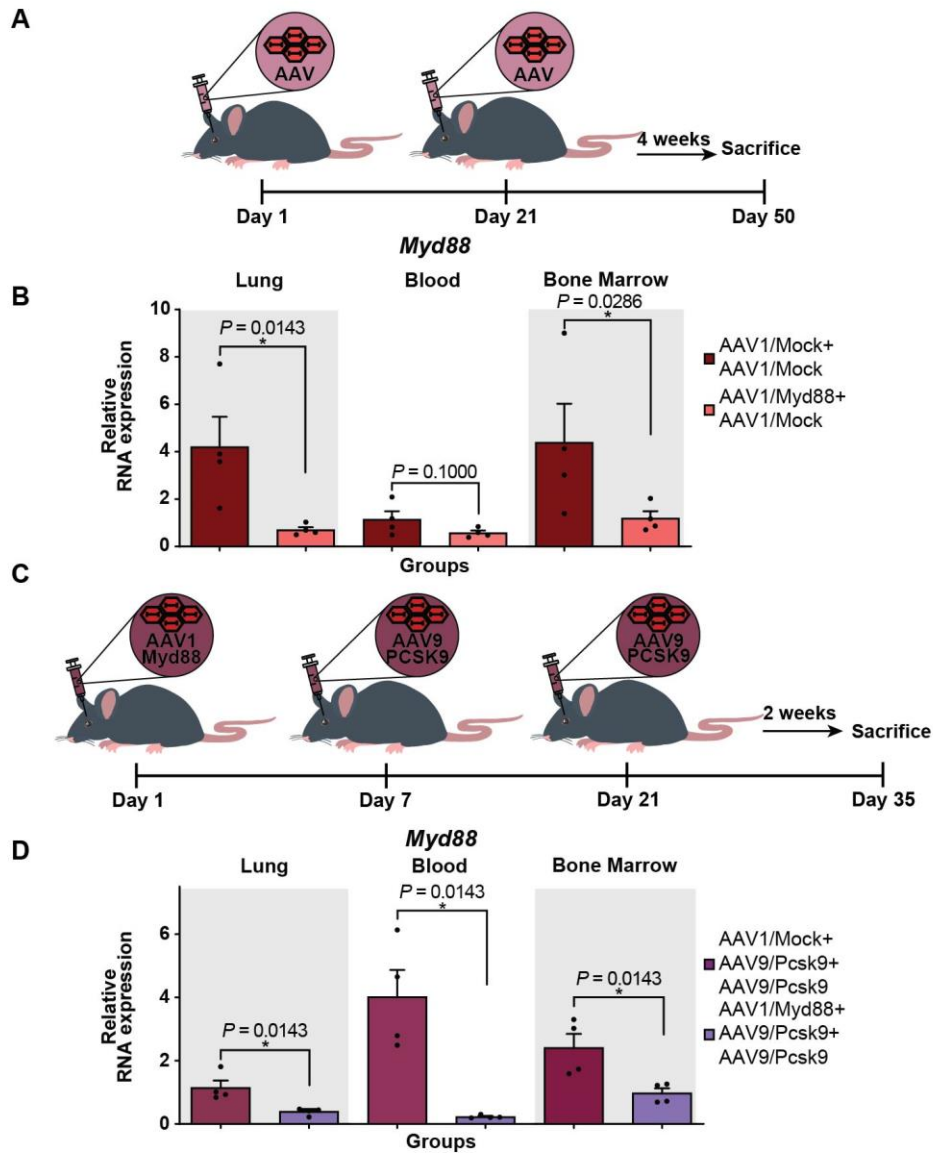


Supplementary figure 3.2. *In vivo* analysis of AAV1 tropism towards different tissues. AAV1-GFP was delivered to C57BL/6 mice via retro-orbital injection. GFP expression was assessed in different tissues by qRT-PCR. Average fold change expression levels are indicated above each group and are quantified relative to not injected mice (N=3 mice for not injected group, N=4 mice for AAV-GFP group, N=5 mice for AAV-GFP group in spleen, and N=6 mice for AAV-GFP group in liver).



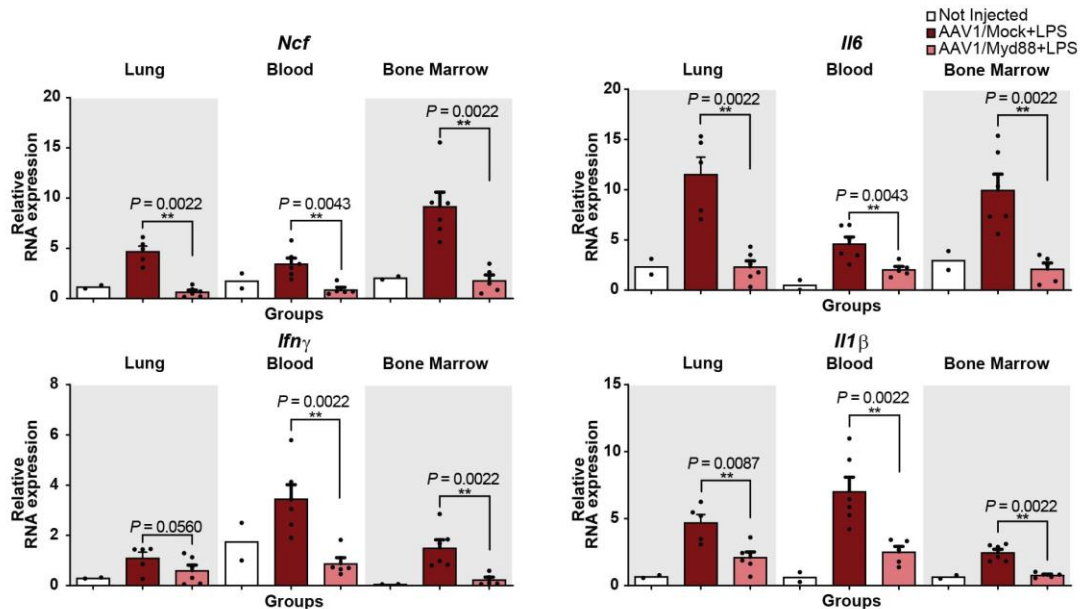
Supplementary figure 3.3. RNA-seq analyses of bone marrow samples collected from mice treated with AAV1/Myd88-MS2-HP1aKrab versus AAV1/Myd88-MS2-Krab. (A) Scatter plot comparing expression of genes (Fragments Per Kilobase of transcript per Million mapped reads FPKM) in two replicates of bone marrow from Myd88-MS2-HP1aKRAB versus Myd88-MS2-KRAB. *Myd88*, *Il1 β* , *Icam1*, *Tnfa* and *Il6* are highlighted in red and the most downregulated genes in Myd88-MS2-HP1a-KRAB groups as compared to MyD88-MS2-KRAB are highlighted in Cyan (N=2 mice). (B) GO enrichment bar graph comparing bone marrow samples collected from mice treated with AAV1/Myd88-MS2-HP1aKrab versus AAV1/Myd88-MS2-Krab. The top 20 significantly enriched terms in the GO enrichment analysis are displayed. Note that

pathways such as defense response to bacteria, which are associated with Myd88 signaling are mostly down regulated when HP1aKRAB was used (N=2 mice). (C) Reactome Enrichment bar graph displaying the top 20 enriched genes in the Reactome database comparing in the BM samples of Myd88-MS2-HP1aKRAB versus Myd88-MS2-KRAB (N=2 mice). Statistical analysis was performed using the two-tailed t test and the method of multiple comparisons adjustments was Benjamini-Hochberg.



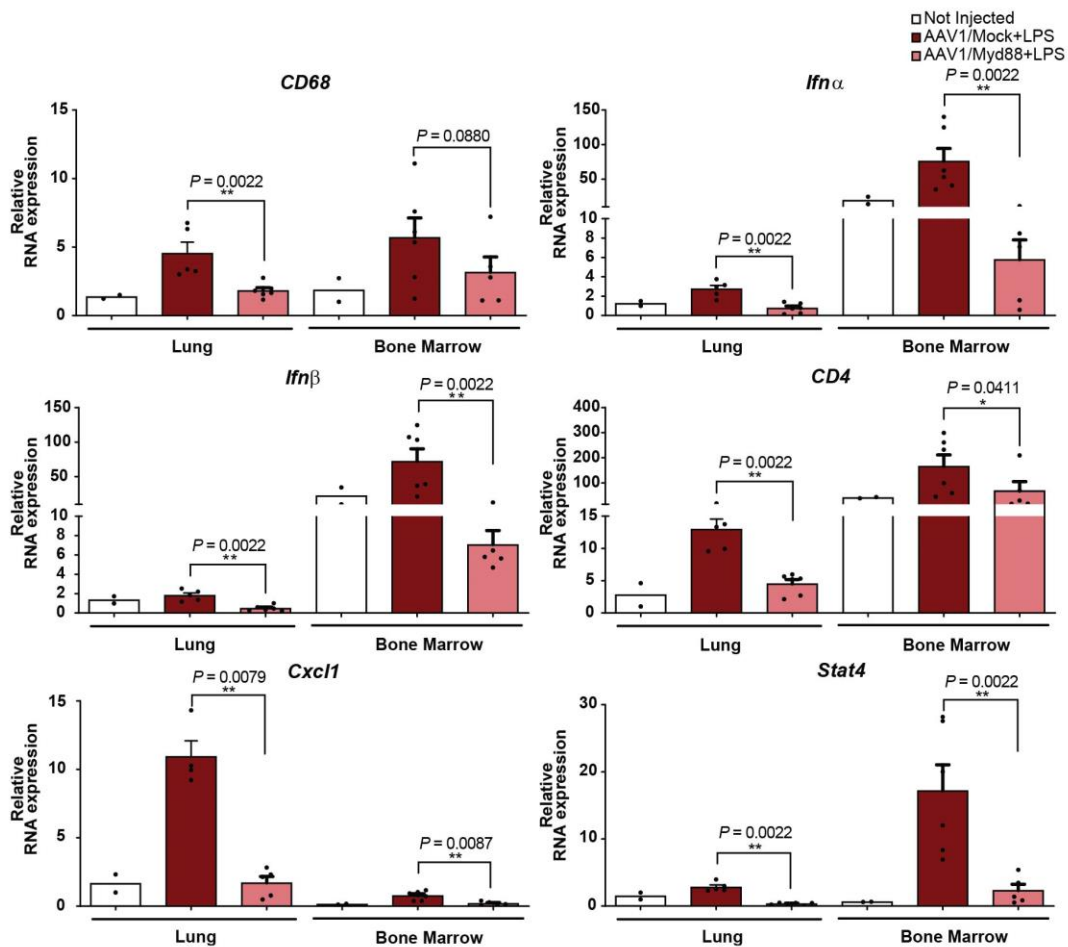
Supplementary figure 3.4. Evaluation of endogenous *Myd88* gene expression following multiple AAV administration. (A) Schematic of experiments demonstrating Cas9 transgenic mice treated with AAV1/*Myd88* or AAV1/Mock at day 1, followed by a second administration of AAV1/Mock on day 21. (B) qRT-PCR analysis of *Myd88* expression level in lung, blood, and bone marrow of Cas9 transgenic mice (N = 4 mice). Fold changes are relative to universal control. The bars represent the mean + S.E.M. (C)

Schematic of the experiment. Cas9 nuclease transgenic mice were treated with AAV1-Myd88 or AAV1-Mock vectors via retro-orbital injection followed by a second and third injection of AAV9-PCSK9 vectors on day 7 and 21. (D) qRT-PCR analysis of *Myd88* expression level in lung, blood, and bone marrow of Cas9 transgenic mice (N = 4 mice). The bars represent the mean + S.E.M. (Mock= Mock-HP1aKRAB, Myd88= Myd88-HP1aKRAB, PCSK9= PCSK9-HP1aKRAB). Fold changes are relative to universal control. Universal control is a blood sample collected from an uninjected Cas9 transgenic mouse. Statistical analysis was performed using the non-parametric one-tailed Mann-Whitney U test. A p value ≤ 0.05 was considered significant (* $P \leq 0.05$).



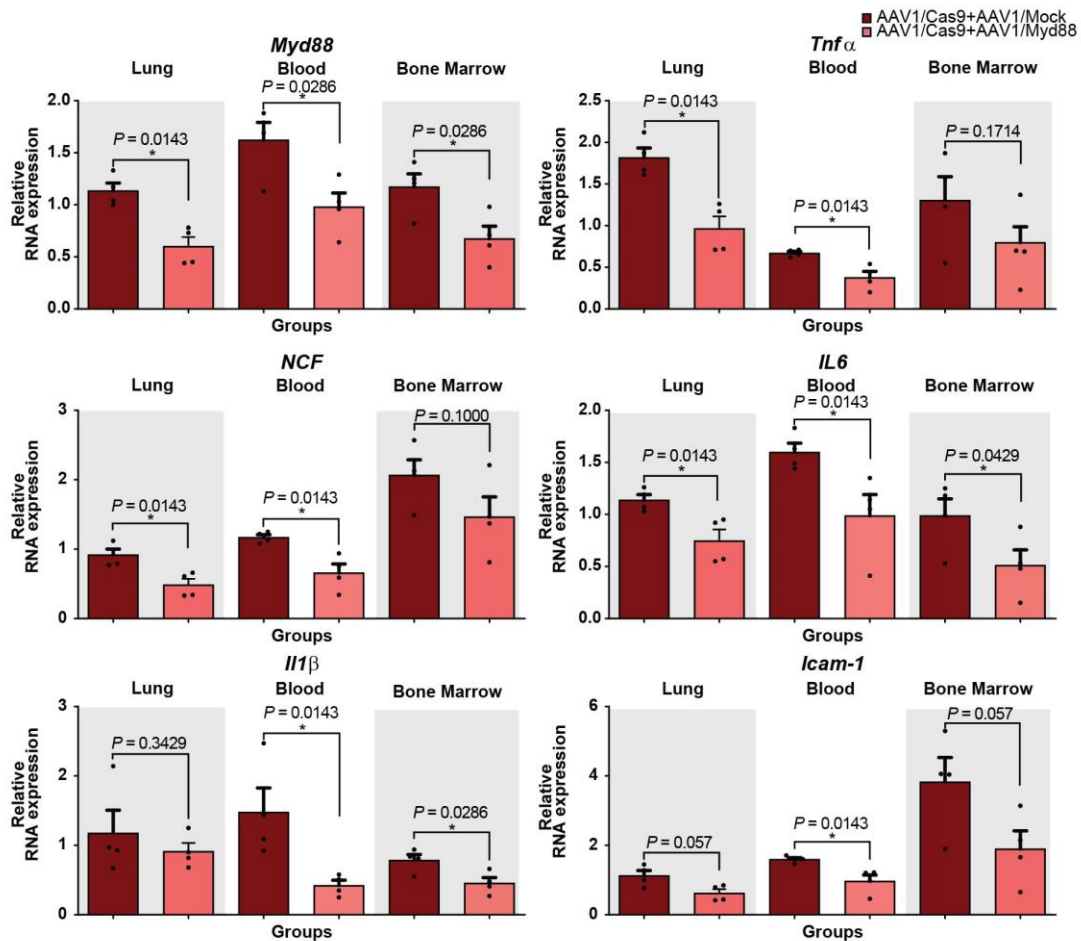
Supplementary figure 3.5. Analysis of a set of immune-related transcripts following LPS injury. qRT-PCR analysis of *Ncf*, *Il6*, *Ifn γ* , and *Il1 β* mRNA expression in lung, blood, and bone marrow quantified relative to the universal control following LPS injection (N = 6

mice for injected groups except for Blood and Bone marrow of Myd88+LPS group which is N=5 mice, and N = 2 mice for Not Injected group). The bars represent the mean + S.E.M. (Mock= Mock-HP1aKRAB, Myd88= Myd88-HP1aKRAB). Universal control is a blood sample collected from an uninjected Cas9 transgenic mouse. Statistical analysis was performed using the non-parametric one-tailed Mann-Whitney U test. A p value ≤ 0.05 was considered significant (* $P \leq 0.05$ and ** $P \leq 0.01$).

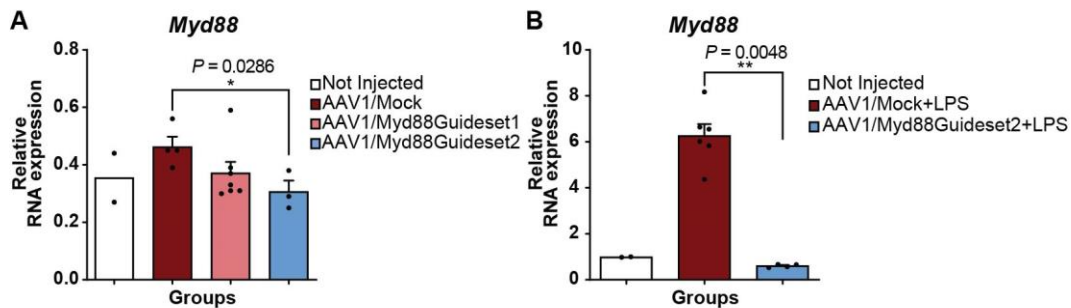


Supplementary figure 3.6. Assessing the level of a panel of immune related genes in lung and bone marrow following LPS injection. qRT-PCR analysis of *in vivo* *CD68*, *Infa*, *Infb*, *CD4*, *Cxcl1*, and *Stat4* relative to the universal control following LPS injection in lung

and bone marrow. (N = 5 mice for Lung of Mock+LPS group except for *Cxcl1* which is N = 4, N = 6 mice for Lung of Myd88+LPS group except *Cxcl1* which is N = 5, N = 6 mice for Bone Marrow of Mock+LPS, N = 5 mice for Bone Marrow of Myd88+LPS, and N = 2 for Not Injected group). The bars represent the mean + S.E.M. (Mock= Mock-HP1aKRAB, Myd88= Myd88-HP1aKRAB). Universal control is a blood sample collected from an uninjected Cas9 transgenic mouse. Statistical analysis was performed using the non-parametric one-tailed Mann-Whitney U test. A p value ≤ 0.05 was considered significant (* $P \leq 0.05$ and ** $P \leq 0.01$).



Supplementary figure 3.7. Targeted gene silencing in wild-type mice using a dual CRISPR/Cas9 system with AAV1/Cas9 and AAV1 carrying gRNA-MS2- HP1aKRAB. AAV1 viruses were delivered to wild-type mice via retro-orbital injection. qRT-PCR analysis was performed to assess *Myd88*, *Icam-1*, *Tnfa*, *Ncf*, *Il6*, and *Il1β* mRNA expression in blood, bone marrow, and lung. Fold change expression levels were quantified relative to the universal control (N = 4 mice). The bars represent the mean + S.E.M. (Mock= Mock-HP1aKRAB, Myd88= Myd88-HP1aKRAB). Universal control is a blood sample collected from an uninjected Cas9 transgenic mouse. Statistical analysis was performed using the non-parametric one-tailed Mann-Whitney U test. A p value ≤ 0.05 was considered significant (* $P \leq 0.05$ and ** $P \leq 0.01$).



Supplementary figure 3.8. Assessing the repression efficiency of AAV1-Myd88 targeting a different region of Myd88 in liver. (A) qRT-PCR analysis of *in vivo* *Myd88* expression in liver samples 3 weeks post retro-orbital injection of AAV1 in Cas9 transgenic animals. Gene expression fold-change was quantified relative to the universal control (N = 2 mice for Not Injected group, N=4 mice for Mock, N=7 mice for Myd88Guideset1, and N=3 mice for Myd88Guideset2). The bars represent the mean + S.E.M. (B) qRT-PCR analysis of *in vivo* *Myd88* expression in liver samples 6 hours post LPS injection. Fold change

expression levels were quantified relative to the universal control (N = 2 mice for Not Injected group, N=6 mice for Mock, and N=4 mice for Myd88Guideset2). The bars represent the mean + S.E.M. Universal control is a blood sample collected from an uninjected Cas9 transgenic mouse. Statistical analysis was performed using the non-parametric one-tailed Mann-Whitney U test. A p value ≤ 0.05 was considered significant (*P ≤ 0.05 and **P ≤ 0.01).

Supplementary table:

No LPS	Lung	Blood	Bone Marrow
	Mean of repression(%) \pm STD	Mean of repression(%) \pm STD	Mean of repression(%) \pm STD
<i>Myd88</i>	75% \pm 0.389	84% \pm 0.124	63% \pm 0.227
<i>Icam-1</i>	74% \pm 0.1	88% \pm 0.05	61% \pm 0.24
<i>Tnfa</i>	63% \pm 0.19	58% \pm 0.09	57% \pm 0.18
Myd88-HP1a-KRAB			
<i>Myd88</i>	52% \pm 0.7	59% \pm 0.185	34% \pm 0.276
<i>Icam-1</i>	NC \pm 0.35	70% \pm 0.29	41% \pm 0.21
<i>Tnfa</i>	37% \pm 0.46	45% \pm 0.57	56% \pm 0.19
Myd88-KRAB			

Supplementary table 3.1. Repression levels of Myd88, Icam-1, and Tnfa assessed by qRT-PCR in lung, blood, and bone marrow 3 weeks post retro-orbital injection of AAV N = 4 for injected groups except for the following: Mock/MS2-KRAB group N=3, Myd88/MS2-HP1aKRAB in bone marrow N=7, Myd88/MS2-HP1aKRAB in blood and lung N=5). Gene expression fold-change was quantified relative to the universal control. The repression levels are reported as percentage of fold change of AAV-Myd88 group divided by the fold change of AAV-Mock group for each gene. NC=No Change

Supplementary table 3.2.1.		
14nt gRNAs- 5' to 3'		
Mouse	Myd88-1	GCATCCACCTTGAT
Mouse	Myd88-2	GCCACCGATCAAGG
Mouse	Myd88-3	GCGAGCGTACTGGA

Mouse	Myd88-4	GTGGACGGCACCGG
Mouse	Mock	AGCTTAGGGATAAC
Human	CXCR4	GCAAAGTGACGCCGA
Mouse	PCSK9	GAACGGGAGCCCAC
Mouse	PCSK9	GGCAGGCTGCCGGT
Supplementary table 3.2.2.		
20nt gRNAs- 5' to 3'		
Human	SEL1L-1	GGCAGGAAGAGCAGCGGCGAGG
Human	SEL1L-5	GGGGGGCGGATACTGACCCG
Human	SEL1L-7	GGATACTGACCCGAGGACGCCG
Human	SYVN1-10	GGGCGCTGGGTTCCTGGTGAGT
Human	SYVN1-4	GGTTGCGGGCGTCGCAGGCA
Human	SYVN1-3	GGCACCGGCGTCTGAGGTCTC
Human	NEAT1-1	GGCGACAGGGAGGGATGCGCGCC
Human	NEAT1-2	GGCGCGCCTGGGTGTAGTTGT
Human	NEAT1-3	GGAAGTGGCTAGCTCAGGGCTTC
Human	XIST-1	GGCAGCGCTTTAAGAACTGAA
Human	XIST-2	GGACTGAAGATCTCTCTGCACTT
Human	XIST-3	GGCCATATTTCTTACTCTCTCG
Human	CXCR4	GCAGGTAGCAAAGTGACGCCGA
Mouse	Myd88	GAGATCGCCTAGTCCATCCA
Mouse	Myd88	CTTGGCCCACCGATCAAGGT

Supplementary table 3.3.1.	
Mouse qPCR primers- 5' to 3'	
GFP-FW1:	CAACCACTACCTGAGCACCC
GFP-RV1:	GTCCATGCCGAGAGTGATCC
Myd88 primer FW	GTGAGGATATACTGAAGGAGCTG
Myd88 primer RV	CTGTAAAGGCTTCTCGGACTC
Stat4-FW	CCTGACATTCCCAAAGACAAAGC
Stat4-RV	TCTCTCAGCACAGCATATGCAC
Cxcl1-FW	GACCATGGCTGGGATTCACC
Cxcl1-RV	CCAAGGGAGCTTCAGGGTCA
IFN α -fw	GGACT T TGGAT TCCCGCAGGAGA AG
IFN α -RV	GCTGCATCAGACAGCCT TGCAGGTC
IFN- γ -PRIMETIME	IDT:MM.PT.58.41769240
IFN- β -PRIMETIME	IDT:MM.PT.58.30132453.G
Icam-1-FW	CAATTTCTCATGCCGCACAG

Icam-1-RV	AGCTGGAAGATCGAAAGTCCG
TNF α -FW	AGGCTGCCCCGACTACGT
TNF α -RV	GACTTTCTCCTGGTATGAGATAGCAA
NCF-FW	GCTGCGTGAACACTATCCTGG
NCF-RV	AGGTCGTACTTCTCCATTCTGTA
18S-FW	GGCCGTTCTTAGTTGGTGGAGCG
18S-RV	CTGAACGCCACTTGTCCCTC
CD68-FW	TGCGGCTCCCTGTGTGT
CD68-RV	TCTTCCTCTGTTCCCTGGGCTAT
CD8-FW	GCTCAGTCATCAGCAACTCG
CD8-RV	TCACAGGCGAAGTCCATC
CD4-FW	GAGAGTCAGCGGAGTTCTC
CD4-RV	CTCACAGGTCAAAGTATTGTTG
IL6-PRIMETIME	IDT: Mm.PT.58.100
IL1B-FW	TCGCTCAGGGTCACAAGAAA
IL1B-RV	CATCAGAGGCAAGGAGGAAAAC
PCSK9	IDT: Mm.PT.58.5401743
LacZ-FW	TTGAAAATGGTCTGCTGCTG 3
LacZ-RV	TATTGGCTTCATCCACCACA 3
dCas9-FW	TCGGAAGCGACCACTTATCG
dCas9-RV	TCCGGTCTGTACTTCGGTCT
HP1a-Krab-FW	TAAGAGCTCGGGAGGTGGTT
HP1a-Krab-RV	GCCGTAAGTGATTTCGCGTC

Supplementary table 3.3.2.	
Human qPCR primers- 5' to 3'	
SEL1L-FW	GTGGCTGTTGGAGTCGGTAT
SEL1L-RV	ATTCACTCCCCACCCTCTCT
NEAT1-FW	AGGTCAGGCAGAGGAAGTCA
NEAT1-RV	CTGCCTCCCGATAACAACAT
XIST-1-FW	AGGTCAGGCAGAGGAAGTCA
XIST-1-RV	CTGCCTCCCGATAACAACAT
SYVN1-FW	ACCAGCATCCCTAGCTCAGA
SYVN1-RV	TCCTCAGGCATCTCCTCTGT
CXCR4-FW	ACTACACCGAGGAAATGGGCT
CXCR4-RV	CCCACAATGCCAGTTAAGAAGA

APPENDIX C

AUTHORSHIP AND CONTRIBUTIONS TO CHAPTERS 1 AND 2

Chapter 1: Engineered CRISPR systems for next generation gene therapies

Authors of the published manuscript: Michael Pineda (M.P.), Farzaneh Moghadam (F.M.), Mo R Ebrahimkhani (M.R.E.), Samira Kiani (S.K.)

M.P. and F.M. designed and wrote the manuscript and initial sketch of figures. S.K. and M.R.E. edited and wrote the manuscript and figures.

Authors would like to thank Garret G. Gosse for his input on the initial version of manuscript. This work was supported by D16AP00047-DARPA Young Faculty Award.

I grant Farzaneh Moghadam permission to use our published manuscript titled, *Engineered CRISPR Systems for Next Generation Gene Therapies* as a chapter in her thesis.

Signature



Name Michael Pineda

Date 07/18/2020

I grant Farzaneh Moghadam permission to use our published manuscript titled, *Engineered CRISPR Systems for Next Generation Gene Therapies* as a chapter in her thesis.

Signature



Name Mo R Ebrahimkhani

Date 07/18/2020

I grant Farzaneh Moghadam permission to use our published manuscript titled, *Engineered CRISPR Systems for Next Generation Gene Therapies* as a chapter in her thesis.

Signature



Name Samira Kiani

Date 07/18/2020

Chapter 2: Multifunctional CRISPR-Cas9 with engineered immunosilenced human T cell epitopes

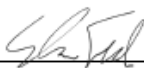
Authors of the published manuscript: Shayesteh R Ferdosi (S.R.F.), Radwa Ewaisha (R.E.), Farzaneh Moghadam (F.M.), Sri Krishna (S.Kr.), Jin G Park (J.G.P.), Mo R Ebrahimkhani (M.R.E.), Samira Kiani (S.K.), Karen S Anderson (K.S.A.)

S.R.F. and R.E. designed experiments, performed experiments, and analyzed data. F.M. generated Cas9 variant constructs, performed Cas9 functional analysis experiments, and analyzed data. S. Kr. generated predicted Cas9 epitopes and designed and assisted with the T cell experiments. F.M. and S. Kr. contributed equally. J.G.P. analyzed RNA seq data. M.R.E. helped with the design of experiments and interpretation of data. S.K. and K.S.A. supervised this study. R.E. took the lead in writing the manuscript with input from S.R.F., S.K. and K.S.A. and support of all the other authors.

Authors thank Dr. Erich Sturgis for providing the serum samples, Dr. Diego Chowell for support with the computational prediction model, and Padhmavathy Yuvaraj for technical assistance. Authors thank all the other members of the Anderson, Kiani, and Ebrahimkhani labs for their assistance and insightful discussions. This work was supported by ASU institutional funds, the startup fund by the School of Biological and Health Systems Engineering of ASU, National Institute of Biomedical Imaging and Bioengineering R01 grant (1R01EB024562-01A1), and DARPA Young Faculty Award (D16AP00047) to S.K. We thank the Center for Computational and Integrative Biology (CCIB) DNA core facility at Massachusetts General Hospital and Genomics and Bioinformatics (TCGB) core at UCLA for the DNA and RNA sequencing services.

I grant Farzaneh Moghadam permission to use our published manuscript titled, *Multifunctional CRISPR-Cas9 with engineered immunosilenced human T cell epitopes* as a chapter in her thesis.

Signature



Name Shayesteh R Ferdosi

Date 07/18/2020

I grant Farzaneh Moghadam permission to use our published manuscript titled, *Multifunctional CRISPR-Cas9 with engineered immunosilenced human T cell epitopes* as a chapter in her thesis.

Signature



Name Radwa Ewaisha

Date 07/18/2020

I grant Farzaneh Moghadam permission to use our published manuscript titled, *Multifunctional CRISPR-Cas9 with engineered immunosilenced human T cell epitopes* as a chapter in her thesis.

Signature



Name Sri Krishna

Date 07/18/2020

I grant Farzaneh Moghadam permission to use our published manuscript titled, *Multifunctional CRISPR-Cas9 with engineered immunosilenced human T cell epitopes* as a chapter in her thesis.

Signature



Name Jin G Park

Date 07/18/2020

I grant Farzaneh Moghadam permission to use our published manuscript titled, *Multifunctional CRISPR-Cas9 with engineered immunosilenced human T cell epitopes* as a chapter in her thesis.

Signature




Name Mo R Ebrahimkhani

Date 07/18/2020

I grant Farzaneh Moghadam permission to use our published manuscript titled, *Multifunctional CRISPR-Cas9 with engineered immunosilenced human T cell epitopes* as a chapter in her thesis.

Signature



Name Samira Kiani

Date 07/18/2020

I grant Farzaneh Moghadam permission to use our published manuscript titled, *Engineered CRISPR Systems for Next Generation Gene Therapies* as a chapter in her thesis.

Signature



Name Karen S Anderson

Date 07/18/2020

BIOGRAPHICAL SKETCH

Farzaneh Moghadam was born in Tehran, Iran, on September 19, 1989. She graduated from the University of Tehran with a B.S. degree in biology and then worked as a research assistant at Oklahoma State University for two years focusing on protein structure-function relationships using molecular science. In August 2016, she entered the Graduate College at Arizona State University in Tempe, Arizona, to pursue her doctorate in the Biological Design program. Her doctoral research was on the applications of the CRISPR-Cas9 technology in genome engineering; mainly on genetic circuit design, cloning, and generation of enhanced CRISPR based gene therapy candidates. So far, she has published 6 peer-reviewed journal articles and 1 book chapter in respected journals of the field and her work has been referred to in over 70 publications.